Antagomir-134 as a Novel Therapeutic for Angelman Syndrome

AUTHOR(S)

Aoife Campbell

CITATION

Campbell, Aoife (2022): Antagomir-134 as a Novel Therapeutic for Angelman Syndrome. Royal College of Surgeons in Ireland. Thesis. https://doi.org/10.25419/rcsi.13071986.v1

DOI

10.25419/rcsi.13071986.v1

Antagomir-134 as a novel therapeutic for Angelman syndrome

Aoife Campbell, BSc (Hons), MSc

Dissertation submitted to the Royal College of Surgeons in Ireland in accordance with the requirements for the degree of Doctor of Philosophy

Supervised by
Professor David C. Henshall
&
Dr. Cristina R. Reschke
2020

I declare that this thesis, which I submit to RCSI for examination in consideration of the award of a higher degree Doctor of Philosophy is my own personal effort. Where any of the content presented is the result of input or data from a related collaborative research programme this is duly acknowledged in the text such that it is possible to ascertain how much of the work is my own. I have not already obtained a degree in RCSI or elsewhere on the basis of this work. Furthermore, I took reasonable care to ensure that the work is original, and, to the best of my knowledge, does not breach copyright law, and has not been taken from other sources except where such work has been cited and acknowledged within the text.

Signed

Scholar Number 16169891

Date 3/07/2020

Table of Contents

Acknowledgments

I would first like to express my gratitude to my supervisor, David Henshall, for the continuous guidance and support over the last four years. I would especially like to thank you for having confidence in me to be part of the Roche project. This has given me significant experience with which I feel I have benefited massively from. At first I thought I would struggle to make a decision about which PhD project to pick from my three rotations, but within the first week of being a part of your group, the decision was made. Thank you for always being so enthusiastic when I got an exciting result – for instance *finally* getting the audiogenic seizure model to work!

I would also like to thank my co-supervisor and good friend, Cristina Reschke, who has been an absolute rock throughout my PhD. Firstly, thank you for taking the time to train me in all of the *in-vivo* procedures. Thank you for always being there for me when I needed advice. From helping me with calculations to taking me out for cocktails when I was stressed while writing my thesis, I appreciate you so much.

Thanks to Gareth for all of your help with me a lot over the past year. I promise I will take my newfound statistical knowledge to the US and never forget. Thank you to Amaya and Elena for being amazing throughout the four years. Amaya, you were so patient with me when you were teaching me qPCRS and RNA extractions during my rotation. Thank you for all of your help with my mouse colonies and all of time we spent figuring out the breeding schemes and generations! Elena, thank you for always taking the time to teach me new techniques, always being available if I needed advice (even on the weekends!) and for being so supportive towards the end. Special thanks to Jimmy for teaching me how to do western blots during lockdown, and for making sure I didn't cry when my antibodies did not work. I know I was an absolute nightmare towards the last few months, and I am so grateful for all the laughs and walks around the park. Thanks for Gary and Ngoc for all of your help sequencing and analysing my samples. Ngoc, thanks for explaining all of the bioinformatics to me (even if it took a while!). Mona, you have

been amazingly supportive over the last few months and I am really going to miss sitting next to you. Thank you for always being available to take a call or to listen to my rambling voice notes, especially since lockdown! Massive thanks to Joana for taking care of my mouse colonies, from daily welfare checks absolutely amazing since the with you. I would also like to thank the FutureNeuro team, Karina, Linda, Lisa and Bridget. It has been amazing being part of the group and I am really going to miss our lunchtime walks around the park. Also, a special thanks to Janosch for also helping me with western blots (it took a while!) and thank you for continuous advice on anything immunohistological related. Special thanks to Halima for all the help with my EEG analysis and for always sharing your cookies with me. Rogerio, thanks for making me leave the office by 7pm every night by taking your shoes and socks off, and of course for helping me with behaviour software. Thank you to the rest of the FutureNeuro /epilepsy group, Jon, Mariana, Karen, Kelvin, Aileen, Justine, Marc, especially those who helped with the welfare checks of my mouse colonies over the Christmas period and holidays.

A special thank you to Professor Ronan Conroy for all of the statistical analysis and advice over the last few months. You have been very patient with my confusing data and experimental designs!

To Aasia, we only got to share about two years of PhD life together, but you've still been there for me since you left RCSI. I miss our pancake and coffee dates so much and I cannot wait to visit you in Longford when I'm finished. You have been so supportive over the last few months and I'm so thankful I can ring you whenever I'm stressed. You're the best. To all of the girls; Laura, Aoife, Sinead and Heather, thank you for all the times you came over to socially distance with ice cream and sweets when I was in the final few weeks of writing. To my housemate Orla, you moved in the week before I started in PhD so you've witnessed all of the stress over my presentations over and over again, you probably know a lot more about Angelman syndrome and miR-134 than I do! You've been the absolute dream to live with and I'm

going to miss you so much when I leave. Also, thanks to Triona, for all of the walks and coffee when I was writing up.

Most importantly, to my family, Mam, Dad, Ian and Ronan. Thank you for all of the support over the last few years of college. To Mam and Dad, I am so grateful for all of the encouragement throughout my life, especially during the last few months. I cannot wait to be able to come to Doolin and finally relax and not worry about my angels (mice!).

Publications

Peer reviewed publications:

Antagomir-mediated suppression of microRNA-134 reduces kainic acid-induced seizures in immature mice.
Campbell A, Morris G, Brindley E, Worm J, Jensen M A, Miller, M T, Henshall D C, Reschke C R. Scientific Reports, 2020. In review.

A systems approach delivers a functional microRNA catalog and expanded targets for seizure suppression in temporal lobe epilepsy.
Venø M T, Reschke C R, Morris G, Connolly N M C, Su J, Yan Y, Engel T, Jimenez-Mateos E M, Harder L M, Pultz D, Haunsberger S J, Pal A, Heller J P, **Campbell A**, Langa E, Brennan G P, Conboy K, Richardson M, Norwood B A, Costard L S, Neubert V, Del Gallo F, B Salvetti, Vangoor V R, Sanz-Rodriguez A, Muilu J, Fabene P F, Pasterkamp R J, Prehn J H M, Schorge S, Andersen J S, Rosenow F, Bauer S, Kjems J, Henshall D C. PNAS 2020.

Spatiotemporal progression of ubiquitin-proteasome system inhibition after status epilepticus suggests protective adaptation against hippocampal injury.
Engel T, Martinez-Villarreal J, Henke C, Jimenez-Mateos E M, Sanz-Rodriguez A, Breenan G P, Kenny A, **Campbell A**, Lucas J J, Henshall D C. Mol Neurodegener. 2017

Manuscripts in preparation:

Antagomir-134 as a novel therapeutic for Angelman syndrome.
Campbell A, Reschke C R, Morris G, Augusto J, Sanz-Rodriguez A, Langa E, Henshall D C, manuscript in preparation.

List of abbreviations:

ADHD: attention deficit hyperactive disorder
AEDs: Anti-epileptic drugs
Ago: Argonaute
AMPA: alpha-amino-3-hydroxy-5-methylisoxazole-4-propionic acid
AMO: antisense miRNA oligonucleotides
Arc: Activity-regulated cytoskeleton-associated protein
AS: Angelman syndrome
ASD: Autism spectrum disorder
BDNF: Brain derived neurotrophic factor
BDZ: Benzodiazepine
CBZ: carbamazepine
CGI-I: Clinical Global Impressions-Improvement
CHD8: Chromodomain-helicase-DNA-binding protein
CNS: Central nervous system
CNTN: Contactin
DS: Dravet syndrome
DS: Down syndrome
EEG: Electroencephalography
EME: early myoclonic encephalopathy
E1: ubiquitin-activating enzyme
FMR1: Fragile X mental retardation gene
Fragile X mental retardation protein
FXS: Fragile X syndrome
GABA: Gamma-aminobutyric acid
GCSE: Generalized convulsive status epilepticus
ID: Intellectual disability
KA: Kainic acid
KCNA1: Potassium voltage-gated channel subfamily A member 1
KCNA2: Potassium voltage-gated channel subfamily A member 2
KD: Ketogenic diet
Limk1: LIM kinase 1
LGIT: low glycemic index treatment
LGS: Lennox Gastaut syndrome
LTD: Long-term synaptic depression
LNA: locked nucleic acids
MAP1b: Microtubule associated protein 1b
MECP2: Methyl CpG binding protein 2
mGlu: metabotropic glutamate receptors
mTOR: Mammalian target of prapamycin
MSNE: myoclonic status in non-progressive encephalophay (MSNE)
NCSE: Non-convulsive status epilepticus
NMDA: N-methyl-D-aspartate receptor
Ngn1 neurogenin 1
OCD: obsessive compulsive disorder
PMBCs peripheral blood mononuclear cells
PMOs: phosphorodiamidate morpholino oligonucleotides
PNAs: peptide nuclei acids
Pum2: pumilo 2
PWS: Prader Willi syndrome
POGZ: Pogo transposable element derived with ZNF domain
PSD-95: Postsynaptic density protein 95kDa

PTZ: pentylenetetrazol
REEL-2: Receptive-Expressive Emergent Language Scale 2
RISC: RNA-induced silencing complex
RGCs: radial glial cells
RTT: Rett Syndrome
SCN1A: Sodium voltage-gated channel alpha subunit 1
SE: Status epilepticus
siRNA: small interfering RNA
SUDEP: Sudden unexpected death in epilepsy
SVZ:subventricular zone
SZ: Schizophrenia
TD: Typically developing
THIP: tetrahydroisothiazolo-[5,4-c]pyridin-3-ol
TLE: Temporal lobe epilepsy
TSC: Tuberous sclerosis complex
Ube3a: ubiquitin protein ligase E3A
UPD: Uniparental disomy
VGSC: voltage-gated sodium channel

List of figures

List of tables:

Abstract

Angelman syndrome is characterised by cognitive impairment with profound speech delay, motor impairments and ataxic-like symptoms, EEG abnormalities and drug-resistant epilepsy. It is caused by the loss of function of the ubiquitin ligase 3A (UBE3A) gene. UBE3A contains three transcripts, two of which are translated to protein, and the third transcript, *Ube3a1* is untranslated and contains 3' *Ube3a1* contains a binding site for a large microRNA (miRNA) cluster, miR-379~410 cluster. The miR-379~410 cluster contains multiple miRNAs that are involved in neuronal morphology and brain development, including miR-134, thus miRNA dysregulation could be involved in the pathophysiology of AS. We have hypothesised that loss of UBE3A in AS, results in loss of the miRNA sponge, which leads to an increase of miR-134 and a downregulation of its targets.

Here, we sought for the first time functionally assess miR-134 role in a model of paediatric *status epilepticus* (SE) by using antagomir-134 (Ant-134). Then, we characterised a mouse model of AS using the *Ube3a* $^{(m-/p+)}$ model. Finally, we attempted to use Ant-134 to treat the most relevant AS-like phenotypes.

The first results chapter investigates the role of miR-134 in a paediatric model of SE. Seizures were induced in 21 day old mice (P21) using a systemic injection of kainic acid. We then demonstrate that Ant-134 has seizure suppressive effects in this model. In addition, Ant-134 blocked the initiation of SE in a number of mice, in comparison to SE induced in all mice that received the scramble-control compound. We also found neuroprotective effects of Ant-134 in the CA3 region of the hippocampus.

In results chapter two, we characterised a mouse model of AS using the *Ube3a* $^{(m-/p+)}$ model. This model recapitulated multiple symptoms associated with AS including an abnormal EEG, motor impairments in the open field and rotarod, deficits in marble burying and increased seizure susceptibility using chemoconvulsant agents and the induction of audiogenic seizures. This was done using two generations of mice, F1 for EEG analysis and behaviour and N4 for the induction of audiogenic seizures.

The final results chapter aimed to use Ant-134 to treat the above phenotypes. Ant-134 significantly reduced audiogenic seizures in both P21 and in adult mice. Furthermore, Ant-134 restored motor phenotypes in the open field. Due to the complexity of the syndrome, we believe a disease-modifying therapy would highly benefit from a "combined approach". Thus, small RNA sequencing and identified a number of miRNAs from the miR-379~410 cluster that were differentially expressed in these mice, and potentially could be used as an adjuvant to Ant-134.

In summary, these data provide strong evidence for miRNA dysregulation in AS. Ant-134 can be used to treat multiple symptoms of AS.

1 Chapter 1

Introduction

1.1 Paediatric epilepsy and *status epilepticus*

Paediatric epilepsy affects 0.5%-1% of children (3-13 years old) and a significant proportion of those are of a genetic basis (Aaberg et al., 2017). A seizure is the clinical manifestation of excessive, synchronized neuronal discharges in the brain. Seizures can be classified into three main types, focal, generalised and unknown onset (Martin et al., 2018). Seizures in infants and children are one of the most common medical emergencies. It has been reported that 5% of children will have a seizure before the age of five (Hauser, 1994). Paediatric epilepsy presenting before the age of three can result in a number of comorbidities such as developmental delay, behavioural issues and drug resistance (Symonds et al., 2019). Furthermore, there is an increase in behavioural issues and cognitive decline in children affected with epilepsy before the age of three (Berg et al., 2008) . There is a correlation between epilepsy and age, with epilepsy being most prevalent in children under the age of five, and an incidence of >60 per 100,000 and similar estimates in those over the age of 65 years, suggesting a bimodal distribution with age (Hauser et al., 1993). Some studies have reported an even greater incidence in infants under the age of 36 months, with one cohort estimating 1 in 613 births (Wirrell et al., 2012) and another estimating 1 per 495 births (Symonds et al., 2019).

Paediatric *status epilepticus* (SE) is a neurological emergency, which is thought to have a prevalence of 17-23 episodes per 100,000 children (Vasquez et al., 2019, Chin et al., 2006, Raspall-Chaure et al., 2007). SE is defined as a prolonged, non-terminating seizure episode, which lasts longer than five minutes (Vasquez et al., 2019, Smith et al., 2016). The incidence of SE declines with age, with the neonatal period being the most vulnerable age, followed by a decline in occurrence, with the lowest incidence between the ages of 5 and 40 years (DeLorenzo et al., 1996) . Patients can also go into refractory SE (RSE), defined as SE that has failed to respond to anti-epileptic drugs (AEDs) and has a mortality rate of roughly 40% (Vasquez et al., 2019, Sahin et al., 2001, Gilbert et al., 1999). Generalized convulsive SE (GCSE) is the most common form of SE observed in paediatric patients (Gross-Tsur and Shinnar, 1993, Treiman, 2008). The most common

etiology for paediatric SE is an episode of a prolonged febrile seizure. Other causes can be traumatic brain injury, hypoxic-ischemic encephalopathy and central nervous system (CNS) infection (Vasquez et al., 2019, Chin et al., 2006, Hussain et al., 2007).

The mechanism by which a single generalized tonic-clonic seizure can transition into GCSE has been well-documented (Alford et al., 2015, Wasterlain and Chen, 2008). Under normal circumstances, following a single seizure, the seizure threshold is increased and the brain's terminating mechanisms come into place (Alford et al., 2015). These include a rise in extracellular adenosine and depolarisation block (Alford et al., 2015, Boison, 2013). However, in SE, these mechanisms appear to fail. Brain tissue studies have detected changes in inhibitory and excitatory neurotransmitters, with a loss of efficacy of GABA (Gamma-aminobutyric acid) and an enhancement of glutamate. For example, prolonged seizures cause swift alterations in GABA receptors to occur (Goodkin et al., 2007a). This includes internalization of GABA receptors whereby they move into the cytoplasm and become functionally inactive (Goodkin et al., 2007a, Alford et al., 2015). These receptors also decrease in number (Goodkin et al., 2007a, Goodkin et al., 2007b, Naylor, 2010). Notably, this reduces surface expression of the γ_2 subunit which is the binding site for benzodiazepines (BDZ), the frontline treatment for SE. This potentially explains the development of pharmaco-resistance to BDZ (Alford et al., 2015, Naylor, 2010). Indeed, there is a 20-fold decrease in the potency of benzodiazepines following 20-30 minute episodes of SE (Chen et al., 2007, Mazarati et al., 1998). Opposing alterations have been reported for glutamate transmission during SE. Increased numbers of N-methyl-D-aspartate receptor (NMDA) subunits are recruited to the synaptic membrane after SE which leads to an overall increase in excitation (Alford et al., 2015, Chen et al., 2007). There is also a 22% increase of non-NMDA receptors at synaptic sites during SE (Naylor, 2010). This increase in ionotropic glutamate receptor surface expression has been proposed as a mechanism that can promote excitotoxicity after SE and the development of epileptogenesis (Hardingham et al., 2002).

While the incidence of SE is higher in children than in adults, the mortality rate appears to be higher in adults (Dham et al., 2014). The reported mortality rates of paediatric SE

have been variable, however, the average rates appear to range between 14-16%, while some figures as low as 3% have been reported (Singh and Gaillard, 2009, Dham et al., 2014, Smith et al., 2016). In accordance with this, the mortality rate of RSE is much higher, with rates ranging from 16-43% (Sahin et al., 2001). Furthermore, it has been shown that SE in infancy and early childhood potentially leads to sudden unexpected death in epilepsy (SUDEP) (Lacey et al., 2012, Nashef et al., 2012), accounting for approximately one third of the cases (Shmuely et al., 2016) .

1.2 Genetic epilepsy syndromes

Genetic factors are presumed to be causal factors in roughly 40% of the epilepsies (Guerrini and Noebels, 2014). Genetic epilepsies are most commonly caused by mutations in genes or receptors that are important for regulating levels of excitability or inhibition in the brain (Steinlein, 2001). Often, these are also referred to as channelopathies, where a mutation causes gain or loss of channel function (Zhang et al., 2017). Such channelopathies most often result from mutations in genes that encode sodium, potassium and calcium channels. The most frequently mutated gene in epilepsy is the sodium voltage-gated channel alpha subunit 1 (*SCN1A*) gene, which has been reported to have several hundred mutations (Oliva et al., 2012). The severity of types of epilepsy associated with *SCN1A* mutations is dependent on the nature of the mutation. For example, a missense mutation can cause genetic epilepsy with febrile seizures (GEFS+) (Scheffer and Berkovic, 1997) or at the more severe end of the spectrum, *SCN1A* mutations can cause Dravet syndrome (Harkin et al., 2007). Mutations have been identified in other subunits of voltage-gated sodium channels. The *SCN2A* gene is mainly expressed in excitatory neurons and functions to initiate action potentials and back propagation (Hu et al., 2009). Mutations in *SCN2A* have been reported to be involved in severe epileptic encephalopathies including Ohtahara syndrome, West syndrome and Lennox-Gastaut syndrome (LGS) among others (Howell et al., 2015). Mutations in *SCN8A* has also been reported to be involved in encephalopathies with intractable seizures

occurring within the first 18 months of life and developmental delay (Veeramah et al., 2012, Estacion et al., 2014).

As previously mentioned, potassium (K^+) channels can also be mutated in epilepsy. These channels play major roles in the regulation of excitability via the regulation of membrane potential, repolarisation during the action potential and the broad regulation of neurotransmitter release (Zhang et al., 2017, Maljevic and Lerche, 2013). Although not a specific epilepsy syndrome, mutations in potassium voltage-gated channel subfamily A member 1 (*KCNA1*) cause episodic ataxia type 1 and patients are ten times more likely to have a seizure, suggesting a potential link between loss of *KCNA1* function and epilepsy (Rajakulendran et al., 2007). Mutations in potassium voltage-gated channel subfamily A member 2 (*KCNA2*) have been found to be causative in cases of early infantile epileptic encephalopathy (Hundallah et al., 2016).

Many epilepsy syndromes begin in early infancy to childhood, which is a critical point in neurodevelopment, thus potentially leading to developmental issues later in life (Camfield et al., 1996), (Berg et al., 2013). That is, the occurrence of epileptiform activity during brain development interferes with brain development. A number of early-onset epilepsy syndromes have multiple seizure types, ranging from absence seizures, myoclonic seizures to tonic-clonic seizures (Chopra and Isom, 2014). Such disorders with an early onset (< 1 year-old) include early myoclonic encephalopathy (EME) and Dravet syndrome (Akiyama et al., 2012). Rasmussen syndrome and Lennox- Gastaut syndrome also emerge in early childhood (> 2 years) (Bien et al., 2005, Al-Banji et al., 2015). Early onset epileptic encephalopathies occur at a young age and are comprised of recurrent, intractable seizures which can lead to severe neurodevelopmental delay (Zhang et al., 2017). The average age of onset of genetic epilepsy syndromes can be illustrated in figure 1.1.

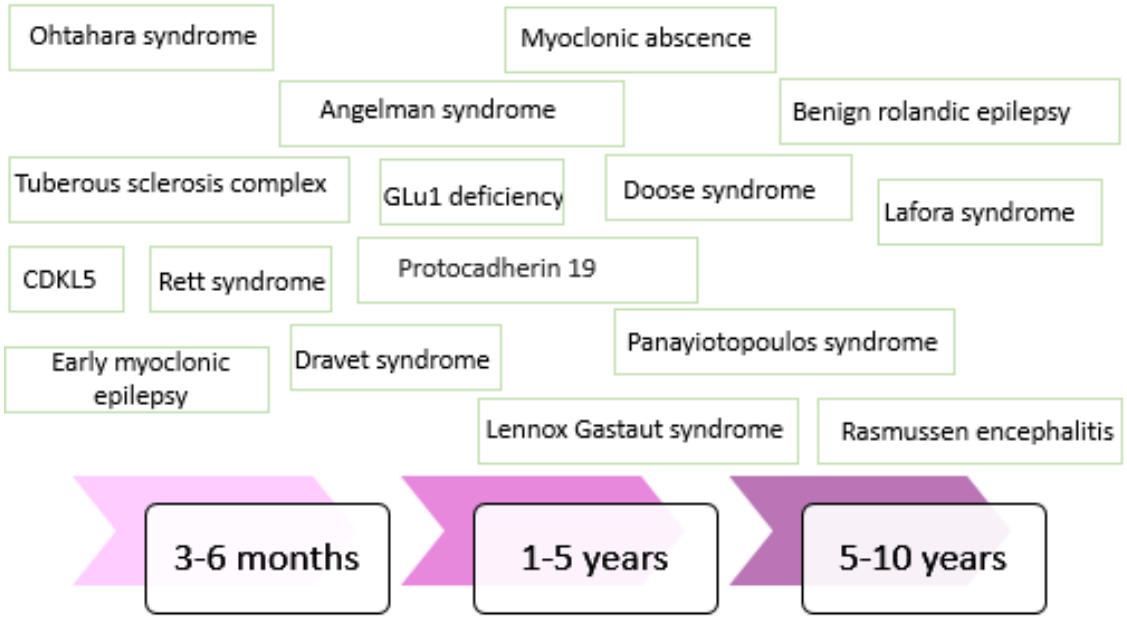

Figure 1.1: Average age of onset of genetic epilepsy disorders

Image represents the average age of onset of childhood genetic epilepsy disorders.

1.3 Neurodevelopmental disorders

Neurodevelopmental disorders are a group of disorders that encompass a range of disabilities that are caused by disruption to the CNS. A number of disorders fall under this terminology. Some can be common disorders such as schizophrenia (SZ) (~1%), autism spectrum disorders (ASD, ~1%) and intellectual disability (ID, ~2%), while others are very rare, such as Rett syndrome (RTT), Angelman syndrome (AS) and Fragile X syndrome (FXS) (Mitchell, 2011). A large proportion of neurodevelopmental disorders have a genetic basis (Mitchell, 2011, Engle, 2010, Millar et al., 2000, Jensen and Girirajan, 2017). With the exception of SZ, many of these disorders emerge during early childhood, suggesting that dysregulation of certain genes can affect a number of processes in the developing brain. A significant number of the genes associated with neurodevelopmental disorders and related phenotypes are involved in cell-to-cell connections, synaptogenesis and axon guidance (Mitchell, 2011, Monteiro and Feng, 2017). This includes members of the contactin (CNTN) family, a group of cell adhesion

molecules involved in axon guidance and synapse formation (Mitchell and Shah, 2002, Nikolaienko et al., 2016). For example, CNTN1 controls the maturation of oligodendrocytes (Lamprianou et al., 2011) and CNTN5 controls the maturation of glutamatergic synapses (Toyoshima et al., 2009). SH3 and multiple ankyrin repeat domains (Shank) proteins are scaffolding proteins that are critical for synaptic development and function (Monteiro and Feng, 2017) and point mutations in these genes can lead to ASD and SZ (Mitchell, 2011). Other important proteins involved in neurodevelopment are the semaphorins proteins. This includes $Sema_3A$ that plays a role in growth cone guidance (Kolodkin et al., 1997), and $Sema_3E$ which is involved in axonal growth regeneration (Steinbach et al., 2002).

1.3.1 Rett syndrome

First described by Dr. Andreas Rett in 1966, RTT is a neurodevelopmental disorder and rare disease that predominantly affects girls (Rett, 1966). RTT is characterised by microcephaly, motor dysfunction, intellectual delay, scoliosis and seizures (Yang et al., 2019). Babies with RTT appear to have a normal development for the first 6-18 months, followed by a decline in development and failure to reach milestones (Yang et al., 2019).

More than 95% cases of RTT are caused by mutations in the methyl-cytosine binding protein (encoded by *MECP2*) which is an X-linked gene (Amir et al., 1999). Mutations which can cause RTT include nonsense, deletions, missense, insertions and duplications of the *MECP2* gene (Yang et al., 2019). MeCP2 is crucial for normal brain development, performing various functions including the regulation of gene expression, chromatin remodelling and RNA splicing (Belichenko et al., 2009). The expression of MeCP2 increases during the postnatal developmental period in rodents, a time during which synapse formation and synaptic pruning occurs, suggesting that MeCP2 is required for the correct inventory of synapses (Fasolino and Zhou, 2017). Similar observations have been reported in humans, with a correlation of MeCP2 expression and increasing age (Balmer et al., 2003). In accordance with this, mice lacking *MeCP2* display fewer dendritic

spines (Belichenko et al., 2009, Armstrong et al., 1995). Comparable results were also found in RTT patients where the decrease in dendritic spine size observed in neurons in the cortex (Belichenko et al., 1994). The mechanism linking the spine phenotype to MeCP2 is thought to be due to reduced levels of brain derived neurotrophic (BDNF), one of its targets (Chang et al., 2006). BDNF is an important neurotrophic factor that stimulates spine formation. Lower levels of BDNF have been detected in *MeCP2* mutant mice and RTT-like symptoms are accelerated in mice in which *Bdnf* is deleted (Li and Pozzo-Miller, 2014, Chang et al., 2006). Furthermore, increasing Bdnf levels has been shown to improve the phenotype in MeCP2 mutant mice (Chang et al., 2006).

1.3.2 Fragile X syndrome

FXS is another neurodevelopmental disorder that was first described in 1943 by Martin and Bell (Martin and Bell, 1943). It is characterised by ID, cognitive impairment and ASD-like features such as impairments in social interaction and repetitive behaviours (Saldarriaga et al., 2014). Seizures occur in roughly 15% of males and 5% of females (Saldarriaga et al., 2014). Physical characteristics have been reported in ~80% of patients. This includes large and prominent ears, macrocephaly and mandibular prognathism (Saldarriaga et al., 2014). FXS is caused by a mutation in the Fragile X mental retardation gene (*FMR1)* gene. The gene contains a DNA segment known as the CGG triplet repeat. This is usually only repeated between 10-40 times but in FXS it can be repeated between over 200 times. Similar to Huntington's disease and trinucleotide repeat disorders, the severity of the FXS phenotype is dependent on the number of repeats (Saldarriaga et al., 2014). Individuals with an expansion between 55 to 200 are classified as 'premutation' and to psychiatric disorders (Tassone et al., 2014). In cases where the CGG repeat increases over 200 repeats, the FMR1 gene undergoes hypermethylation and transcriptional silencing, resulting in loss of the Fragile X mental retardation protein (FMRP) (Pietrobono et al., 2004, Pfeiffer and Huber, 2009). This is mutation is full

Like RTT, FXS is associated with abnormal synaptic function (Pfeiffer and Huber, 2009, Bassell and Warren, 2008). A number of targets of FMRP are expressed in dendrites and have known functions in synaptic development (Bassell and Warren, 2008). These include Arc, microtubule associated protein 1b (MAP1b) and postsynaptic density protein 95kDa (PSD-95). The importance of synapse pruning during development has been known for some time, with links to neurological disorders if this is interrupted (Boksa, 2012, Kim et al., 2017). Notably, there is an abundance of long, immature dendritic spines present in mouse models and patients with FXS (Irwin et al., 2000, Grossman et al., 2006). In particular, it has been reported that this increase in spines was found in the neocortex in adults and this result was echoed in FXS mouse models with the addition of an abundance in the hippocampus (Hinton et al., 1991, Galvez and Greenough, 2005).

1.3.3 Autism spectrum disorder

ASD is a disorder or a group of disorders that are associated with impairments in social interaction, communication and ID. It was first described by Leo Kanner in 1943 (Kanner, 1943). The prevalence of ASD is thought to be roughly 1 in 59 children, with reports of higher rates in males (Loomes et al., 2017) and is usually evident in the first 3 years of life. ASD syndromes include Asperger syndrome, atypical autisms and non-specified pervasive developmental disorders (Sheldrick-Michel et al., 2017). Unlike other neurodevelopmental disorders such as FXS, RTT or AS, there is rarely a single gene known to cause ASD, although some of these neurodevelopmental disorders can be categorized as forms of ASD (Chelini et al., 2019). Instead, it is usually considered a combination of environmental and polygenetic risk factors (Parellada et al., 2014).

In accordance with other neurodevelopmental disorders and the reports of synaptic abnormalities, there has also been reports of defects in synaptic pathways in ASD (Jamain et al., 2003). For instance, some patients with ASD have mutations in neuroligins, NLGN3 and NLGN4. These are genes that code for cell adhesion molecules which are

located postsynaptically and are involved in the remodelling of synapses (Scheiffele et al., 2000, Jamain et al., 2003). Furthermore, long-term synaptic depression (LTD) is dysregulated in mouse models of ASD and in neuroligin-3 knockout mice (Baudouin et al., 2012). There is also evidence of impairments in synaptic pruning in ASD (Hutsler and Zhang, 2009). Mutations in the engrailed homeobox protein 2 (EN-2) have been linked to ASD (Carratala-Marco et al., 2018). Engrailed 2 knockout (En2-/-) mice contributed to identify pathogenic mechanisms common to FXS (Chelini et al., 2019). Furthermore, there is a significant downregulation of Fmr1 in the brain of En2 -/- mice (Provenzano et al., 2015). Dysregulation of chromatin remodelling has also been emerging as a potential causative factor for ASD, with mutations in chromodomain helicase DNA binding protein 8 (*CHD8*) being associated with ASD (State and Šestan, 2012). Moreover, pogo Sanders transposable element derived with ZNF domain (POGZ) has been reported to be mutated in ASD (Matsumura et al., 2020). The group found that POGZ was involved in neuronal development and in a CRISPR generated mouse model with a Q1038R mutation, they found impairments in behavioural tests used for cognition such as novel object recognition and fear-conditioning (Matsumura et al., 2020). The authors concluded that POGZ may play a role in neuronal development through chromatin remodelling (Matsumura et al., 2020). Finally, the amygdala has been proposed as a potential region where dysfunction could result in autistic autism' was speculated (Amaral et al., 2003, Baron-Cohen et al., 2000' 2000). The amygdala was found to be enlarged in children with ASD and reports of it being hyper-functioning and hypo-functioning (Schumann et al., 2004, Baron-Cohen et al., 2000).

There is evidence that ASD and epilepsy co-exist (Bozzi et al., 2018). While it is unclear which disease precedes the other, a co-occurrence is present. For instance, studies have reported the risk of developing epilepsy in individuals with ASD ranges from 6-27% (Amiet et al., 2008, Jeste and Tuchman, 2015). Moreover, in a correlation study of patients with ID, there was a decrease in IQ and an increase in epilepsy rates (Jeste and Tuchman, 2015). Although the connection between ASD and epilepsy has not yet been

elucidated, attempts have been made in this area. A number of common pathologies that are known to give rise to epilepsy have also found to be associated with ASD. For example, studies have shown that there may be a basis for GABAergic dysfunction in ASD (Bozzi et al., 2018, Rubenstein and Merzenich, 2003). Indeed, there have been reports of $GABA_A$ receptor downregulated in patients in brain regions that are associated with ASD (Fatemi et al., 2009). Such brain regions include the superior frontal cortex and the parietal cortex, the latter is thought to govern social behaviours (Ha et al., 2015, Fatemi et al., 2009, Fatemi et al., 2010). Several mouse models of ASD show reduced GABAergic interneurons (Bozzi et al., 2018) as for example En2-null mice (Provenzano et al., 2015, Sgadò et al., 2013). Moreover, altered glutamate expression has also been suggestive of a causative link to epilepsy. Studies have shown that the metabotropic glutamate receptor 5 (MGluR5) is increased in patients with ASD (Fatemi et al., 2011). In addition, 50-70% of ASD children have abnormalities in EEG and magnetoencephalographic recordings during sleep studies (Lewine et al., 1999). While the basis for association between ASD and epilepsy is not yet fully understood, there is a strong association between the two disorders.

1.3.4 Dup15q syndrome

Duplication of chromosome 15q11.2-q13.1, also known as Dup15q syndrome, is one of the most common chromosomal abnormalities to be associated with ASD (DiStefano et al., 2016). It is the same region containing the genes mutated in Prader-Willi (PWS) and Angelman syndrome. Dup15q syndrome has been classified as a form of ASD/ID, however, due to its distinct phenotype it is classified as its own syndrome. Other duplications in this region are strongly associated with ASD (Cook et al., 1997). Dup15q is characterised by ID, ranging from mild to profound, movement dysfunction/ataxia like movements, speech impairments, behavioural difficulties and seizures. Seizures are common in roughly 50% of cases and they usually begin in early life infancy (Conant et al., 2014). Dup15q arises by two genetic mechanisms: isodicentric duplications, two

extra copies of 15q.11.2-q13.1, resulting in tetrasomy, which accounts for roughly 80% of cases, and intersitital duplications, which includes one extra copy of 15q.11.2-q13.1, resulting in trisomy, and accounting for 20% of cases (Frohlich et al., 2019b). It has been postulated that some of the phenotypes present in dup15q may be due to the imprinting of *UBE3A*, the gene associated with AS, which results in the loss of a number of $GABA_A$R subtypes, $GABA_A$ß3, α5 and γ3, possibly contributing (Frohlich et al., 2019b). An EEG phenotype is also seen in dup15q patients. This is characterised by an increase in peak beta power in dup15q children in comparison to typically developing children and could act as a biomarker in future studies (Frohlich et al., 2019b, Frohlich et al., 2016). Moreover, this EEG finding was recapitulated using the $GABA_A$ agonist midazolam, supporting the evidence that GABAergic transmission is affected in dup15q patients (Frohlich et al., 2019b).

1.3.5 Tuberous sclerosis complex

Tuberous sclerosis complex (TSC) is a rare genetic disorder associated with non-cancerous growths in multiple parts of the body, cognitive and psychiatric issues, and epilepsy (Vignoli et al., 2015). It is estimated to have a prevalence of 1:5800 (O'Callaghan et al., 1998). ASD is very common in TSC, with its prevalence ranging from 26-61%, with other reports estimating 43-86% (Gipson et al., 2013, Hunt and Shepherd, 1993, Bolton et al., 2002). Mental retardation has been reported in up to 60% of TSC patients (Harrison and Bolton, 1997). Epilepsy is prevalent in up to 90% of patients, with infantile spasms being the most common form of seizures (Staley et al., 2011, Thiele, 2004, Webb et al., 1996). Seizures generally occur in the first year of life, with an average onset between 3-6 months (Webb et al., 1996). A range of seizure types have been reported in patients with TSC, including, tonic, tonic-clonic, myoclonic, atypical absence, partial and complex partial (Thiele, 2004). The two main genes involved in TSC are *TSC1* and *TSC2*, encoding hamartin and tuberin, respectively (Gipson et al., 2013). Under normal conditions, both proteins are negative regulators of the mammalian target of rapamycin

(mTOR) pathway, which promotes cell proliferation and growth. Mutations in *TSC1* and *TSC2* result in hyperactivation of the mTOR pathway (Curatolo and Moavero, 2012) and the resulting cellular disorganisation is thought to promote hyperexcitable brain tissue.

1.3.6 Angelman syndrome

AS is a rare neurodevelopmental disorder that was first described as a syndrome by Harry Angelman in 1965 (Angelman, 1965). It affects roughly 1:15000-1:20000 births. It is characterized by severe intellectual disability, speech impairment, motor dysfunction, EEG abnormalities and abnormal sleep patterns and epilepsy (Buiting et al., 2016). AS is caused by the loss of function of the maternal copy of ubiquitin protein ligase E3A (*UBE3A*) gene in the brain (Matsuura et al., 1997, Kishino et al., 1997). There are four known mechanisms by which UBE3A is lost in AS; Chromosome deletion (70%), *UBE3A* mutation (10%), paternal uniparental disomy (UPD; 2%) and imprinting defect (3%) (Buiting et al., 2016). Currently, there is no effective treatment for AS, however, some individuals respond to anti-epileptic drugs used to treat generalized seizures (Clayton-Smith, 1993, Boyd et al., 1988).

1.4 Mechanisms of Angelman syndrome

1.4.1 Genomic Imprinting

AS is the result of the loss of function of a gene that is paternally imprinted in the brain. Genomic imprinting is an epigenetic process that involves DNA methylation, resulting in a monoallelic, parental-specific expression of certain genes (Barlow and Bartolomei, Peters, 2014, Clayton-Smith, 2003). Modification of these genes occurs during gametogenesis and can alter the expression of certain genes, rendering them active or inactive (Clayton-Smith, 2003). Genomic imprinting is a rare phenomenon, with as few as 60 genes being identified to date (Clayton-Smith, 2003).

In the brain, *UBE3A* is inactivated on the paternal allele and active on the maternal allele. Accordingly, any loss of function expression and AS. Silencing of the paternal allele is caused by the expression of an antisense RNA transcript (UBE3A-ATS) on chromosome 15q11-q13. UBE3A-ATS is a large (>600 kb) cis-acting antisense transcript that initiates at the PWS-imprinting center (PWS-IC) (Meng et al., 2012). It is currently unclear how UBE3A-ATS silences UBE3A, but a number of mechanisms have been suggested. One hypothesis suggests UBE3A is silenced through transcriptional interference whereby the annealing of UBE3A to UBE3A-ATS could form a double strand and this would decrease the stability of Ube3a. Others have postulated that it is silenced via epigenetic mechanisms by chromatin conformational changes and (Lalande and Calciano, 2007, Landers et al., 2005, Meng et al., 2012). PWS is also caused by imprinting errors on chromosome 15q11-q13. Although occurring at the same region of chromosome 15, PWS results in a different disorder to AS due to altered paternal expression of genes within this region (Clayton-Smith, 2003). PWS is associated with obesity, mental retardation and hyperphagia (Nicholls et al., 1998, Angulo et al., 2015). Genomic imprinting has also been reported in cancer (Steenman et al., 1994).

The region spanning UBE3A is located next to a cluster of imprinted genes which are either maternally or paternally expressed, and are regulated by the PWS imprinting Centre (PWS-IC) (Lalande and Calciano, 2007). This region overlaps with the paternally expressed Snurf-snrpn gene. Other paternally expressed genes in this area include *MKRN3*, *MAGEL2* and *NDN* (Rougeulle et al., 1997, Vu and Hoffman, 1997). These genes differ from UBE3A in the way they are imprinted. For example, *MKRN3*, *MAGEL2*, *NDN*, *SNURF-SNRPN* are silenced by promoter methylation, whereas, UBE3A is silenced by UBE3A-ATS (Runte et al., 2004).

1.4.2 Genetic mechanisms

The severity of AS is usually dependent on the genetic basis for the disruption of UBE3A gene function. Chromosome deletion, which accounts for the majority of cases, results in the most severe phenotype. Affected individuals present with developmental delay, including the inability to walk or speak, microcephaly, hypopigmentation, EEG abnormalities, sleep disturbances and seizures affecting 95% of patients (Minassian et al., 1998, Clayton-Smith, 1993, Andersen et al., 2001, Peters et al., 2004). Paternal uniparental disomy and imprinting defects occur in 2-3% of cases and have a milder phenotype (Lossie et al., 2001). These patients have better motor and cognitive skills and only 20% of patients have seizures (Lossie et al., 2001). Lastly, mutations in the UBE3A gene account for roughly 10% of individuals with AS and have a milder phenotype in comparison to chromosome deletion; with less ataxia, improved speech and seizures affect 50% of these patients.

1.4.3 Ube3a and its function

The protein encoded by *UBE3A* is a member of the ubiquitin protein ligases. Ubiquitylation is a process that leads to changes to protein function via a number of different mechanisms including promoting protein degradation, endocytosis and transporting transmembrane proteins (Rotin and Kumar, 2009). The ubiquitylation process involves the transfer of ubiquitin between an ubiquitin-activating enzyme (E1), a ubiquitin-conjugating enzyme (E2) and a ubiquitin-protein ligase (E3) (Rotin and Kumar, 2009). Two types of ubiquitin-protein ligases exist; RING type and HECT type. RING E3's facilitate the transfer of ubiqu the specificity of ubiquitylation (Rotin and Kumar, 2009). UBE3A is a HECT E3 ligase and thus its targets can be dysregulated in AS when there is loss of function in the *UBE3A* gene.

The tumor suppressor gene, p53 (also known as tumor protein p53), was the first identified substrate of the Ube3a protein (Huibregtse et al., 1991, Scheffner et al., 1993). Changes to p53 levels may contribute to the hyperexcitability features of AS because it has been shown that levels of p53 are higher in human temporal lobe epilepsy (TLE) patients and in mouse models of SE (Engel et al., 2007, Engel et al., 2010). Notably, increased p53 was found in the brain of maternal deficient AS mice (Jiang et al., 1998). Arc (activity-regulated cytoskeleton-associated protein) has been identified as another key substrate for UBE3A (Greer et al., 2010). Studies have shown that Arc levels are increased after neuronal activity, including after a seizure (Chowdhury et al., 2006, Waung et al., 2008). As with p53, Ube3a controls levels of Arc by ubiquitylation and degradation. This may affect excitability states because elevated levels of Arc results in the activation of the glutamate receptor, AMPA (alpha-amino-3-hydroxy-5-methylisoxazole-4-propionic acid) (Greer et al., 2010). Thus, the increased levels of Arc may promote AMPA receptor signaling which in turn leads to excessive neuronal activation in AS (Greer et al., 2010). Dysregulation of AMPA receptors has also been reported in FXS, although there, the elevation of Arc translation was associated with a decrease in AMPA receptor expression at synapses (Dolen and Bear, 2008). Ephexin5 (E5), a RhoA guanine nucleotide exchange factor is another identified substrate of Ube3a (Mabb et al., 2011). Ephexin5 acts as a negative regulator of excitatory synapse development via activating RhoA and suppressing synapse development. The degradation of E5 is mediated by Ube3a, which in turn allows synapse formation to take place (Margolis et al., 2010). In the absence of Ube3a, there are elevated levels of E5 and this can lead to the suppression of synapse development, which may be associated with the cognitive deficits seen in AS (Margolis et al., 2010).

1.5 Characteristic symptoms of Angelman syndrome

1.5.1 Abnormal electroencephalography

Patients with AS display unique features on EEG recordings, which is observed in the first few months of life and usually begins before seizures emerge (Clayton-Smith, 1993). These EEG abnormalities were first described by Boyd and colleagues (Boyd et al., 1988). The three distinct EEG patterns include: a) a persistent generalized rhythmic 4- to 6- Hz activity which was not influenced by eye closure, b) rhythmic delta activity which was found to be more evident in the anterior brain regions, intermittent spikes and sharp waves and c) high amplitude theta slowing mainly found in the posterior regions (Boyd et al., 1988, Vendrame et al., 2012). Recently, a decrease in beta power has also been reported in children with AS (Frohlich et al., 2019a).

Delta waves are a prominent feature of non-rapid eye movement (NREM) sleep and are the slowest brain waves in humans (Olbrich et al., 2017). Delta power is most commonly found during sleep in infants and children, a key time in which brain maturation occurs (Ringli and Huber, 2011). The presence of oscillatory events such as slow waves have been suggested to be biomarkers of brain plasticity during development in early childhood (Olbrich et al., 2017, Kurth et al., 2013). One study in particular found that with an increase in age, there was a decrease in spectral power and delta/theta event ratios, and an increase in sigma frequency in a cohort of neuro-typical children aged 2-5 years (Olbrich et al., 2017). The benefits of sleep for development and cognition have been widely investigated (Kurth et al., 2012, Timofeev, 2011, Kurth et al., 2013). Delta oscillations have also been reported in a number of diseases such as schizophrenia, attention deficit hyperactive disorder (ADHD) and brain injuries (Abhang et al., 2016a, Abhang et al., 2016b, Alfimova and Uvarova, 2007).

Intermittent rhythmic delta (1-4 Hz) waves were found in 83.5%, interictal epileptiform discharges in 74.2% and intermittent rhythmic theta waves in 43.5% of patients with AS, however, the group did not find any correlation between EEG patterns and genotype (Vendrame et al., 2012). There was a correlation between the size of

deletion and the pattern of theta activity. The size of deletion can be separated into two groups: class-1 (5.9 Mb) and class-2 (5.0 Mb). The larger the deletion, those in group 1, the more abnormal EEG pattern was found. Subjects in the class 1 group presented with epileptiform discharges during wakefulness and less than 50% had intermittent rhythmic theta activity. Group 2 had a normal posterior rhythm during wakefulness but greater than 50% intermittent theta activity (Vendrame et al., 2012). The genetic and EEG differences between these groups may be the result of differential expression of certain genes. It is known that there are a number of genes that are expressed in Class 1 and not in Class 2, however, the function of the majority of the genes are unknown and therefore it's difficult to determine if the presence or absence of these genes could affect the phenotype of AS. One known gene, NIPA1 is exclusively expressed in Class 1 and its expression may be associated with spastic paraplegia (Rainier et al., 2003). However, some of the genes present in Class 1 and not in Class 2 may also be imprinted (Vendrame et al., 2012).

Work by Philpot's group proposed the co frequency as an EEG biomarker for patients with AS. In a parallel study of AS patients and using an AS mouse model, they found an increase in delta power in both subjects in comparison to healthy controls and WT littermates (Sidorov et al., 2017). The increase in delta frequency was not limited to one specific brain region as there was an enhancement across all placements of electrodes and this was not affected by the time of day (i.e. wakefulness and sleep) (Sidorov et al., 2017).

1.5.2 Seizures

As mentioned previously, seizures occur in up to 85% of individuals with AS (Clayton-Smith, 1993). Seizures usually begin in the first three years of life but vary between patients with seizures sometimes occurring as early as one month up to 20 years of age, with a mean age of onset of 13 months (Matsumoto et al., 1992a, Clayton-Smith, 1993, Valente et al., 2006a). The presence of febrile seizures commonly precedes the diagnosis

of AS (Valente et al., 2006a, Viani et al., 1995, Buoni et al., 1999). However, it is important to highlight the fact that 5-20% of patients with AS never develop seizures, though they have other key characteristic symptoms (Thibert et al., 2013). Since cognitive deficits are ubiquitous in AS, this suggests the occurrence of seizures at an early age may not be responsible for the cognitive deficits seen as the individual develops.

The most common type of seizures present in AS patients include atypical absence, generalized tonic-clonic and myoclonic seizures (Clayton-Smith, 1993, Buoni et al., 1999). In a study which analysed 19 patients with chromosome deletion, it was found that febrile seizures occurred in 53% of patients which sometimes lead to status epilepticus (7/19 patients) (Valente et al., 2006b, Valente et al., 2006a). Although the prevalence of SE in AS is not very well characterized, Valente and colleagues found that SE occurred in 84% of patients with chromosome deletion, with 37% of these recurrent SE (Valente et al., 2006a). However, non-convulsive SE (NCSE) has been reported to be more common than convulsive SE in AS (Valente et al., 2006a, Matsumoto et al., 1992a, Ohtsuka et al., 2005). Significantly, one study reported that while 10/11 patients presented with NCSE at an early age, this was not seen after the age of eight years old (Ohtsuka et al., 2005). An investigation of whether the presence of NCSE at a young age was associated with the development of mental retardation was inconclusive, suggesting that the presence of seizures alone does not necessarily lead to developmental delay (Ohtsuka et al., 2005).

It has been reported that chromosome deletion patients have a stronger phenotype including severe refractory seizures and neurodevelopmental delay, although sample sizes in studies of each genetic mechanism of AS tend to be relatively low and therefore this cannot be reported with confidence (Ostergaard and Balslev, 2001). One study found that epilepsy occurred in all patients with chromosome deletion (19 patients), while another study analyzing 160 patients with AS did not find a correlation between seizure type and genotype (Vendrame et al., 2012, Minassian et al., 1998, Valente et al., 2006a). Refractory epilepsy is common in AS and it is more difficult to treat due to the wide range of multiple seizure types present in AS. Revisiting Valent

an improvement in epilepsy, as characterized by seizure frequency and seizure control, however, epilepsy was only fully controlled with the help of anti-epileptic drugs in 37% of patients at the mean age of 8 years (Valente et al., 2006a).

It has been reported that there is an improvement in epilepsy in AS patients as age increases (Viani et al., 1995, Clayton-Smith, 1993, Matsumoto et al., 1992a). This may be due to better management of seizures with anti-epileptic drugs or the number of seizures in adult AS patients may decrease. The exact percentage of adult patients with AS is unknown, mainly due to the fact that AS is most commonly studied in children and many studies do not follow the subjects until adulthood (Laan et al., 1997). Valente's group reported a decrease in the severity of epilepsy as age increased (Valente et al., 2006a). They found that seizures are most common in infancy and early childhood but decrease in late childhood/early adolescence (Valente et al., 2006a). However, work by Laan et al and Matsumoto et al was discordant (Laan et al., 1997, Matsumoto et al., 1992a). For example, 92% of adult patients had epilepsy with atypical absence and myoclonic seizures being most common (Laan et al., 1997). Similarly, another study reported atypical absence seizures in eight patients and atypical absence status in four patients (Matsumoto et al., 1992a). It was also found that EEG abnormalities often persist into adulthood (Matsumoto et al., 1992a). Work by Thilbert's g large adult cohort of patients with AS (16-50 years old with a mean age of 25) and found similar results to Laan et al and Matsumoto. Seizures appear to be at their most severe in the first decade of life, followed by a period of seizure freedom in late adolescence, with reoccurrence in adulthood (Larson et al., 2015). They also found myoclonic status in non-progressive encephalopathy (MSNE) characterized by shaking episodes without loss of consciousness, to be common in this cohort (Larson et al., 2015).

1.5.3 Sleep abnormalities

Distinctive sleep problems have been reported in AS patients. There is a decrease in sleep duration, an increase in latency to sleep onset, a decrease in total time spent in

rapid eye movement (REM) sleep and frequent awakening throughout the night (Spruyt et al., 2018, Pelc et al., 2008b). Moreover, in a study of children with AS, sleep spindles were decreased and there was a reduction in the duration of these spindles (den Bakker et al., 2018). It is unclear if the sleep difficulties are a specific consequence of UBE3A dysregulation or a more general symptom of neurodevelopmental disorders as the prevalence of sleep disturbances in this population have been reported as high as 86% (Robinson-Shelton and Malow, 2015). In typically developing children sleep disturbances tend to be common in early childhood but improve in adolescence, but it appears that individuals with neurodevelopmental disorders, including AS, sleep disturbances occur throughout life (Angriman et al., 2015). Sleep problems are also common in many epilepsy patients, therefore this issue may not be specific to AS (Conant et al., 2009). While some groups have suggested that sleep difficulties subside by late childhood, conflicting reports have emerged (Pelc et al., 2008b, Clayton-Smith, 1993, Spruyt et al., 2018).

1.5.4 Cognition and behaviour

Severe mental impairment is one of the most common characteristics of AS, often preceding the onset of seizures. In some cases, the presence of developmental delay is evident in the first year of life (Peters et al., 2004). The severity of developmental delay is usually dependent on the type of genetic mechanism responsible for AS (Lossie et al., 2001). Specifically, it was found that there was a significant impairment in speech in patients with chromosome deletions in comparison to those with other genetic mechanisms (Bottani et al., 1994, Lossie et al., 2001). Penner et al concluded that all participants were functioning below a range of 0-2 years, which is known as the sensorimotor cognitive period, regardless of age (Penner et al., 1993). They also analysed the vocabulary of these individuals using the Receptive-Expressive Emergent Language Scale 2 (REEL-2) and found that 11 individuals in this study had less than 2 words, seven had 2-3 words and two had up to 5 words (Andersen et al., 2001). Similarly, in a study

analyzing the cognitive ability of patients aged 2.5-15.3 years, they found the highest level of comprehension of language on the REEL scale was 22 months (Jolleff and Ryan, 1993). However, it has been suggested that with an increase in age there may be an improvement in developing a large vocabulary (Jolleff and Ryan, 1993). This group also reported the inability to use sign language or Makaton signing to communicate their needs, which differs from claims made by Clayton-Smith (Clayton-Smith, 1993).

In addition to developmental delay, patients with AS also present with a range of behavioural features including a happy demeanor, short attention span and disruptive behaviours (Bird, 2014, Williams, 2010, Horsler and Oliver, 2006). The happy demeanor is one of the main characteristic features of AS, with it being responsible for the old term 'happy puppet syndrome' and may be the fi persistent smiling occurring as early as 1-3 months old (Williams, 2010). In an extensive review of the behavior of 842 AS patients, researchers found that 77% of patients had a happy demeanor characterized by either laughing or smiling (Horsler and Oliver, 2006). AS patients have been described to have a short attention span and present with behaviours that are excessively active and hypermotoric, features that may decrease with age (Williams, 2010, Clayton-Smith, 2003, Clarke and Marston, 2000).

Anxiety is also present in AS patients with its prevalence increasing with age (Smith, 2001, Larson et al., 2015, Wheeler et al., 2017). It is unclear what the neuroanatomical basis is of the anxiety. In an adult cohort with AS, Smith et al noted that the anxious phenotype in some patients was heightened when there was a disruption to routine (Smith, 2001). Another study in a cohort of 248 age 3-22 years old found similar findings, reporting that a change in routine upset almost 50% of patients, which may also indicate an anxious phenotype (Walz, 2007). In the same cohort, the authors also analysed the prevalence of obsessive compulsive disorder (OCD) and found it was present in 44% of patients (Walz, 2007).

Aggression is another aspect of behavior that is frequently reported in AS (Arron et al., 2011, Smith, 2001, Thibert et al., 2013). In fact, AS was found to have the highest

reported levels in a study analyzing the incidence of aggression in a number of genetic syndromes (Arron et al., 2011). It has been suggested that the aggression arises from the inability to explain ones needs, as it has been reported that patients with better communication skills have lower levels of aggression (Smith, 2001).

1.5.5 Movement impairments

An abnormal-looking gait/movement pattern is a significant (Clayton-Smith, 1993, Clayton-Smith, 2003, Williams et al., 2006). It has been described by Williams as *'wide-based gait with a pronated or valgus-positioned ankles'* (Williams et al., 2006). One study focused on the dysfunctional gait of six patients with AS (6-9 years old) by using an electronic walkway used to analyse spatiotemporal parameters and found a reduction in step length and speed in comparison to typically developing children (Grieco et al., 2018). It has also been noted that adolescents/adults with AS (16-40 years old) present with a decrease in mobility, although this may be secondary to weight gain as a child or the presence of an abnormal gait (Smith, 2001). In the same study, they found an increase in the number of contractures that developed in the limbs due to hypertonicity, which led to a kyphotic posture (Smith, 2001). Scoliosis was also present in the same cohort sometimes requiring surgical intervention (Smith, 2001).

1.5.6 Dysmorphic features

A significant proportion of AS patients have a distinctive appearance which is characterized by microcephaly, brachycephaly, deep set eyes and hypopigmentation (Lossie et al., 2001, Bird, 2014, Clayton-Smith and Laan, 2003, Laan et al., 1999, Clayton-Smith, 1993).These features can arise in the first few years of life (Laan et al., 1999). Studies show that up to 73% of patients have hypopigmentation (Clayton-Smith, 1993, Laan et al., 1999). Other features may include deep-set eyes, mandibular prognathism and strabismus (Laan et al., 1999, Clayton-Smith, 1993). Such dysmorphic features do not appear to be correlated to the genetic

group found microcephaly was more common in chromosome deletion patients (85%) in comparison to 80% in non-deletion cases. Interestingly, patients with UPD and imprinting defects had a higher BMI than chromosome deletion patients and the general population (Tan et al., 2011).

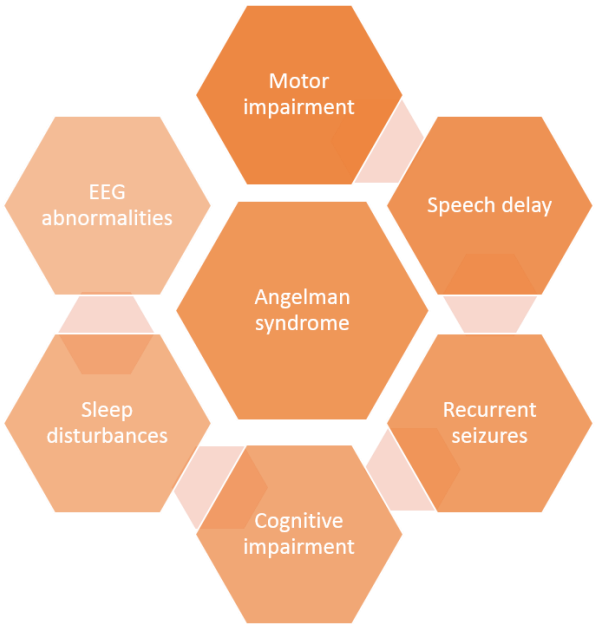

Figure 1.2 Most commonly reported symptoms in AS
AS is characterised by motor impariments, profound speech delay, recurrent seizures, cognitive impairments, sleep disturbances and EEG abnormalities.

1.6 Mouse models of Angelman Syndrome

The first mouse model of AS created and characterized Arthur L Beaudet in 1998, was developed using a targeted mutation (Jiang et al., 1998). This was done using a targeting vector that replaced a 3kb DNA fragment containing exon 2 that deleted all of the isoforms of the protein, yielding heterozygous mice that had a paternally imprinted copy of *Ube3a* and a maternal deletion of *Ube3a (Jiang et al., 1998)*. Since, there have been other models of AS developed, including the generation of a rat model of AS (Dodge et

al., 2020) and a conditional *Ube3a* knockout mouse by Ype Elgersma, to analyse the effect of *Ube3a* reinstatement, (Silva-Santos et al., 2015).

Characterisation of the model by Beaudet was done using two different background strains; a hybrid background which was bred using C57BL/6 with 129/SvEv, and an inbred strain which was bred using only 129/SvEv mice (Jiang et al., 1998). They reported an increase in mortality in homozygous mice on the hybrid background and a further decrease of survival on the inbred background, usually in the first 48 h after birth. Those that survived typically displayed a reduction in locomotor activity, and abnormal hind limb clasping (Jiang et al., 1998). They also found the inbred background to be more susceptible to audiogenic seizures, with seizures in 85% of maternal deficient or homozygous mice, whereas seizures were induced in only 20-30% of homozygous mice on the hybrid background (Jiang et al., 1998). This was done by vigorously scratching the cage lid for 10-20 seconds, which resulted in wild running, followed by generalized tonic-clonic convulsions (Jiang et al., 1998).

When comparing the maternal deficient mice (m-/p+) to WT littermates, the authors reported a reduction in overall brain weight, specifically in the cortex and cerebellum at P18 and this difference was still evident at four months old, although overall bodyweight no longer differed (Jiang et al., 1998). A number of behavioural tests were performed to compare the phenotype of the mouse model to the human symptoms. To analyse the presence of motor incoordination, the step length and step width were analysed and the bar-crossing test was used. The m-/p+ mice displayed shorter step length and they also exhibited a decrease in performance on the bar-crossing test, but the hind-paw footprint analysis was not different to WT littermates (Jiang et al., 1998). Finally, the group found no differences between brain and organ morphology using hematoxylin and eosin staining (Jiang et al., 1998).

A similar study comparing two different background strains of AS mouse models was performed by Greenberg's group. Once again, they used however, the inbred strain was pure B6 (i

model) (Mandel-Brehm et al., 2015). In terms of motor dysfunction and incoordination, they reported a reduction in locomotor activity in the open field test in both strains at P21 and defects were present in the hindlimb-clasp as early as P13 (Mandel-Brehm et al., 2015). In accordance with Beaudet that mice work, G with 129-strain presence in the background were more susceptible to seizures (~60% of WT mice died from seizures). However, this was reported on the hybrid rather than the inbred strain (Mandel-Brehm et al., 2015, Jiang et al., 1998), indicating that pure 129/SvEv or backcrossing with 129/SvEv results in a more severe phenotype. Due to the bimodal seizure curve present in AS, with seizures occurring early in life and presenting again in adulthood (Larson et al., 2015), the group analysed the change in seizure phenotype in older mice. They found that at P42-90, there was no longer a difference in latency to recover from a seizure, suggesting that the mice are less susceptible at an older age. It is well characterized that patients with AS have an abnormal baseline EEG with an increase in delta frequency (1-4 Hz) (Sidorov et al., 2017). To analyse the presence of such phenotype in the mouse model the group performed baseline EEG on the inbred strain and found high amplitude spikes in AS mice, which occurred within theta frequency (4-8 Hz) and is also commonly reported to be increased in AS patients and mouse models (Sidorov et al., 2017, Boyd et al., 1988, Laan et al., 1997, Valente et al., 2006a).

Taken together, these studies conclude that transgenic mouse models recapitulate many of the symptoms seen in AS. It is evident that the presence of 129/SvEv backcrossing or pure background, results in increased phenotype severity, with mice being more susceptible to audiogenic seizures. Both groups also displayed a robust phenotype for motor dysfunction (Jiang et al., 1998, Mandel-Brehm et al., 2015, Laan et al., 1997).

1.7 Current treatment for epilepsy and SE

There is currently no cure for epilepsy and available drugs do not change the underlying pathophysiology responsible for hyperexcitability. They only provide symptomatic relief in some cases. Moreover, roughly 30% of patients remain refractory (Mohanraj and Brodie, 2003) . Current AEDs are ineffective at seizure control in over 20% of children (Wirrell, 2013, Rosati et al., 2015). AEDs generally work by reducing overall excitability in the brain by restoring the balance between excitation and inhibition (Silvestro et al., 2019). This is done either via enhancement of GABA transmission or reduction of glutamate transmission. As previously mentioned, due to the significant role of voltage gated channels in epilepsy such as sodium and calcium, a large proportion of AEDs act by inactivating these channels to reduce hyperexcitability (Catterall, 2017). They can be divided into four main categories: ion channel blockers, drugs that act on GABA neurotransmission, drugs that modulate glutamate neurotransmission and miscellaneous drugs. A brief description of the mechanism of action and types of drugs in the above categories follows.

Phenytoin works via modulation of the voltage-gated sodium channel (VGSC) (Mantegazza et al., 2010) and is therefore a member of the ion channel blockers. Other drugs in this category include carbamazepine (CMZ), lamotrigine, oxcarbazepine and lacosamide (Brodie, 2017). These drugs elicits their anti-convulsant effects by blocking sodium channels that are responsible for the generation of action potentials (Yaari et al., 1986). Phenytoin was discovered in the 1930s in a groundbreaking study by Merritt & Putnum and was the first drug to show anticonvulsant properties without serious effects on cognition. It is still widely used today for the treatment of focal and generalized seizures and SE (Yaari et al., 1986). During seizure activity there is an increase of high-frequency repetitive spiking which is then blocked by phenytoin (Rogawski and Löscher, 2004). Under normal conditions, phenytoin exhibits a weak blockade of sodium channels, however, during a seizure when the channels are open, there is an increase in the channel blockade (Rogawski and Löscher, 2004). This can lead to an indirect

alteration of glutamate transmission which leads to an overall inhibition of glutamate release (Rogawski and Löscher, 2004).

Another class of ion channel blocker with use in the treatment of epilepsy is the calcium channel blockers. There are three subtypes of voltage-gated calcium channels. The Ca_v1 subfamily are involved in muscle contraction, regulation of gene expression and synaptic transmission. Ca_v2 subfamily initiate rapid synaptic transmission (Catterall, 2011, Catterall, 2017) and lastly, the Ca_v3 subfamily conduct T-type Ca^{2+} currents (Catterall, 2011, Catterall, 2017). Voltage-gated calcium channels are activated when there is membrane depolarization and they mediate Ca^{2+} entry into cells (Catterall, 2011, Catterall, 2017). There are also subunits of calcium channels that are structurally homologous but not structurally identical complexes, four ß subunits (Catterall, 2000). Some drugs, for example gabapentin, bind specifically to particular subunits. Gabapentin, originally synthesised to modulate GABA neurotransmission, exerts its anti-convulsant effects by blocking calcium channels, which in turn inhibits neurotransmitter release without direct actions on GABA (Rogawski and Löscher, 2004, Katz, 1986, Rose and Kam, 2002). Another calcium channel blocker, ethosuximide, is used to treat absence seizures and myoclonus (Gören and Onat, 2007). Ethosuximide reduces Ca^{2+} currents in thalamic neurons by blocking T-type (transient) calcium channels which are low threshold channels that open to depolarization (Rossier, 2016, Rogawski and Löscher, 2004). Some of the anti-convulsant effects of phenobarbital are also due to blocking calcium channels although its main effects are to potentiate $GABA_A$ receptor signalling (Rogawski and Löscher, 2004).

The next category of AEDs are drugs that affect GABA activity. As mentioned briefly, GABA is an inhibitory neurotransmitter that acts upon two main classes of receptor. The fast, post-synaptic effects of GABA are mediated by iontotropic (chloride-gating) $GABA_A$ receptors. $GABA_A$ receptors comprise a pentamer of subtypes, α, ß, γ, θ, ρ which contains three subtypes, γ, θ, ρ each having one of α and two ß subunits. Slow, post-synaptic effects of GABA are via metabotropic G-

protein coupled GABA-B receptors. GABA normally exerts an inhibitory tone within the brain as evidenced by the induction of seizures upon blockade of $GABA_A$ receptors, for example by injection of picrotoxin (Sigel and Steinmann, 2012). (Sigel and Steinmann, 2012, Rogawski and Löscher, 2004).

Benzodiazepines, which include diazepam, clobazam, clonazepam and lorazepam, are one of the most widely used drugs to treat seizures. They act as allosteric modulators to $GABA_A$ receptors, targeting γ_1 receptor and prolonging unit opening. (Rogawski and Löscher, 2004). Benzodiazepines are first in line treatment of SE but its effectiveness may be lost with prolonged SE (Ochoa and Kilgo, 2016). They are generally not used for the chronic management of epilepsy due to their addictive properties along with common side effects such as sedation and irritability (Ochoa and Kilgo, 2016, Rogawski and Löscher, 2004). Importantly, clobazam is licensed for children above the age of 2 years with Lennox-Gastaut syndrome (LGS) (Purcarin and Ng, 2014).

Other drugs in this class can modulate GABA transmission by interacting with GABA transporters and enzymes involved in GABA metabolism (Sarup et al., 2003). Vigabatrin, which is used for the treatment of infantile spasms, reduces excitability by blocking GABA metabolism by GABA transaminase. This prevents the breakdown of GABA thus leading to an increased supply of GABA (Sarup et al., 2003, Mitchell and Shah, 2002). Use of viagabatrin is now rare due to a side effect that can result in retinal injury. Tiagabine is licensed as an adjunctive treatment of partial seizures by inhibiting GABA transporter-1, leading to an increased availability of GABA (Bauer and Cooper-Mahkorn, 2008, Sarup et al., 2003).

Another class of AED includes drugs that act on glutamate receptors. As glutamate is the primary excitatory neurotransmitter in the brain, antagonists of glutamate receptors generally produce anti-excitability effects. Released glutamate acts upon ionotropic and metabotropic receptors. Ionotropic receptors can be further divided into subtypes; N-methyl-D-aspartate receptor (NMDA) can be activated by glutamate and glycine, kainate receptor, 2-amino-3-hydroxy-5-methyl-4-isoxazolepropionic acid receptor (AMPA)

facilitate fast synaptic transmission and lastly, delta receptors that do not bind glutamate. The metabotropic glutamate receptors (mGluRs) can be classified into three groups. Group one includes $mGluR_1$ and $mGluR_5$ which are stimulatory receptors that act postsynatptically and are activated by phospholipase C (Shigemoto et al., 1997, Crupi et al., 2019). Group two; $mGluR_2$ and $mGluR_3$ and group three; $mGluR_4$, $mGluR_6$, $mGluR_7$, $mGluR_8$ both inhibit glutamatergic neurotransmission presynaptically (Conn and Pin, 1997). For example, stimulation of $mGluR_2$ has shown to decrease GABAergic inhibition (Crupi et al., 2019).

Felbamate is an AED that exerts its anticonvulsant effects by interacting with a number of targets in the brain. This includes particular subunits (NR1, NR2B) of the NMDA receptor (Kleckner et al., 1999), as well as voltage-gated calcium channels (Taylor et al., 1995), voltage-gated sodium channels (Taglialatela et al., 1996), and acts as a positive modulator of $GABA_A$ receptors (Rho et al., 1994, Kleckner et al., 1999). (Kleckner et al., 1999). Importantly, it has been suggested that the use of Felbamate and its general safety in children with LGS may be accounted for as the NR2B receptor is predominantly expressed in the forebrain and not ubiquitously expressed like other NMDA receptors, thus potentially reducing the neurotoxicity (Rogawski and Löscher, 2004).

Kainate receptors are ionotropic receptors involved in glutamate mediated excitation (Rogawski and Löscher, 2004). This family of receptors can be divided into the following subunits: $GluR_5$, $GluR_6$, $GluR_7$, KA1 and KA2. Kainate receptors act as cation channels whereby they allow sodium and calcium to enter the neuron in response to glutamate, which results in depolarization and an increase in excitation (ROGAWSKI et al., 2003). Topiramate specifically acts on the $GluR_5$ and AMPA receptors and is used in the treatment of generalized and focal seizures in children and adults (Nolan et al., 2016, Mula et al., 2006). Its mechanism of action was elucidated by Gibbs and colleagues whom applied different concentrations of topiramate to cultured hippocampal neurons and found that it blocked kainic acid evoked currents (Gibbs et al., 2000).

The final class of glutamate receptors are the AMPA receptors, which are the most abundantly expressed ionotropic receptors that mediate fast excitatory neurotransmission (Greene and Greenamyre, 1996, Franco et al., 2013). They are localized at the postsynaptic membrane and play major roles in synaptic plasticity and memory processing (Henley and Wilkinson, 2016, Rogawski, 2011). Upon glutamate binding, AMPA receptors open and allow depolarising entry of sodium into the postsynaptic membrane (Rogawski, 2011). Perampanel, a novel drug that directly modulates glutamate transmission and acts as a selective non-competitive antagonist. It does this by blocking AMPA receptor, therefore blocking the influx of calcium and sodium ions, reducing the overstimulation of AMPA receptors. (Franco et al., 2013, Löscher and Schmidt, 2012). It is currently licensed for the treatment of partial-onset seizures and generalised tonic-clonic convulsions (Frampton, 2015, Franco et al., 2013). Interestingly, unlike other AEDs, perampanel does not interact with NMDA or kainate receptors (Franco et al., 2013).

Table 1.1: Most commonly used anti-epileptic drugs and their mechanism

Anti-epileptic drug	**Mechanism of action**
Carbamazepine	Blockage of voltage-gated sodium channel
Clobazam	GABA enhancing
Clonazepam	GABA enhancing
Diazepam	GABA enhancing
Ethosuximde	Calcium channel blocker
Felbamate	Modulation of the NMDA receptor, inhibition of voltage-gated sodium channels
Gabapentin	Blockade of calcium channel
Lorazepam	GABA enhancing
Lacosamide	Blockage of voltage-gated sodium channel
Lamotrigine	Blockage of voltage-gated sodium channel
Perampanel	Antagonist of AMPA receptor
Phenytoin	Blockage of voltage-gated sodium channel
Pregablin	Blockage of calcium channels
Rufinamide	GABA enhancing and blockade of voltage-gated sodium channels
Tiagabine	GABA enhancing
Topirmate	Blockade of calcium and sodium channels, GABA enhancing
Vigabtrin	GABA enhancing
Zonisamide	Blockage of voltage-gated sodium channel

Frontline treatment of SE is usually with administration of a BDZ (Falco-Walter and Bleck, 2016). If the BDZ fails to curtail seizures this leads to refractory and potentially super-refractory SE (Alford et al., 2015). Refractory GCSE is defined as failure to terminate seizures for over an hour (Alford et al., 2015, Lothman, 1990). In the case of RSE, a second anti-epileptic drug (AED), such as valproate, phenytoin or levetiracetam is usually given (Vasquez et al., 2019, Alford et al., 2015). Refractory SE can lead to severe neurological effects and mortality. In one particular cohort of children analysed with refractory GCSE, there was an overall mortality rate of 20% in a cohort of 111 children (Gilbert et al., 1999).

Non-pharmacological treatment options for seizure control in children include the ketogenic diet, hormonal therapy (adrenocorticotropic hormone), immunotherapy, vitamin supplementation with pyridoxine (B_6) and surgical intervention (Nariai et al., 2018, Engel, 2014, McCoy and Benbadis, 2010, Valencia et al., 2001). Therefore, there is a major unmet clinical need for new therapeutic approaches.

1.7.1 Ketogenic diet

The ketogenic diet (KD) is a well-recognized treatment for drug-resistant paediatric epilepsy since 1927 (Bough and Rho, 2007, Hallböök et al., 2007, Dahlin et al., 2005, 1927). The diet entails a diet high in fats, moderately low in protein and low in carbohydrates. It is most commonly used for controlling seizures in paediatric refractory epilepsies. Research has shown that the KD reduces seizures in 50% of children when the diet is strictly adhered to (Vining, 1999). The exact mechanism of the KD is unknown, but it is thought to involve alterations of key neurotransmitters and neuromodulators including adenosine, GABA and glutamate (Vining, 1999). In a study analyzing the levels of amino acids in cerebrospinal fluid (CSF) following initiation of the KD, they saw an increase in GABA levels after four months, and an even greater increase in GABA levels in patients that were considered to be refractory (Dahlin et al., 2005).

There is a growing increase in interest of the KD for the treatment of AS, though there has not been any large-scale trials completed to date. One trial is currently in process and aims to recruit 15 patients aged four to eleven with AS. This trial will test the efficacy of three diets, KD, low glycemic index treatment (LGIT) and a standard American diet (Herber et al., 2020). Thibert and colleagues performed a small-scale trial of a LGIT diet on six children (under five years old) with genetically confirmed AS. They found a reduction in seizure frequency in all patients and five out of six patients had a decrease in seizure frequency by 80%. Furthermore, there was an improvement in baseline EEG and a trend towards an improvement in cognition (Thibert et al., 2012). One particular case study of a 5-year-old girl with refractory epilepsy went from having more than five seizures daily to being seizure free two months after starting the KD (Evangeliou et al., 2010). The KD was also beneficial in improving sleep (average of 5 hours a night to 9 hours upon initiation of the diet). Another interesting key finding in this study was the change in EEG abnormalities. As mentioned previously, an abnormal EEG is present in AS, rhythmic delta activity of 2-3 Hz and persistent generalized rhythmic 4-6 Hz activity was described in this patient. Interestingly, there was no epileptic activity on the EEG following initiation of the KD.

1.8 Pharmacological treatment in AS

The selection of AED's in AS has proven to
types associated with AS. However, there are a number of anticonvulsants that have been shown to be more effective (Fiumara et al., 2010). Valproate appears to be the gold standard treatment for AS used (Valente et al., 2006a, Fiumara et al., 2010, Ostergaard and Balslev, 2001). In one study Valproate was successful in seizure control in 18/19 patients (Valente et al., 2006a). Another study found 4/11 patients were completely seizure free when valproate was used and there was also greater than 50% reduction in seizure severity and frequency in another 4 patients (Ostergaard and Balslev, 2001). The remaining three patients in this study did

not positively respond to valproate, but most importantly, it was noted that their seizures did not worsen (Ostergaard and Balslev, 2001). Topiramate was found to be effective in children and adults with AS and LGX (Franz et al., 2000), with 2/5 patients experiencing prolonged seizure freedom and a further two patients had a 90% reduction in seizure frequency (Franz et al., 2000). A number of AED's have, found to increase the severity and frequency of seizures in AS. Carbamazepine, oxacarbazepine and vigabatrin all worsen seizures in AS (Fiumara et al., 2010, Valente et al., 2006a). Carbamazepine in particular was responsible for seizure aggravation in 5/8 patients and improvements were seen immediately once the drug was stopped (Ostergaard and Balslev, 2001).

1.8.1 Potential therapeutics for Angelman syndrome

As mentioned previously, there is currently no specific therapy or cure for AS and the existing treatments do not treat all of the symptoms. Due to the heterogeneity of AS, it has been challenging to develop a single therapy that could target all of the issues. In addition to the use of AED's to control se for AS. Supplement based trials are also being undertaken, along with dietary changes like the ketogenic diet.

An industry sponsored trial for AS is currently underway using a compound known as OV101 or gaboxadol (tetrahydroisothiazolo-[5,4-c]pyridin-3-ol; THIP). As the name suggests, gaboxadol modulates GABAergic activity by acting as a selective $GABA_A$ receptor agonist (Zanettini et al., 2016). Gaboxadol is not a new compound, nor is it specific to the treatment of AS, as multiple studies have shown its efficacy for anxiety and sleep disorders such as insomnia (Deacon et al., 2007, Hajak et al., 2009, Hoehn-Saric, 1983). As mentioned previously, the $GABA_A$ receptor contains a number of subunits, notably α and δ subunits and hav of depression, insomnia and alcohol abuse (Jin et al., 2011, Klempan et al., 2009). Gaboxadol has been reported to directly en

of the $GABA_A$ receptors in the midbrain, thalamus and forebrain (Krogsgaard-Larsen et al., 2004, Adkins et al., 2001, Wafford and Ebert, 2006, Zanettini et al., 2016). After successfully passing phase 1 and 2 safety and efficacy trails, gaboxadol is currently entering phase 3 and recruiting patients. In phase 2 trials, testing the drug in 78 adults with AS, they found good tolerability to the drug with little adverse events (mild if present) and it was reported to increase the score of the CGI-I (Clinical Global Impressions-Improvement) scale. The CGI scale was developed to assess mental disorders in patients during clinical trials (Busner and Targum, 2007). After 12 weeks of treatment of either gaboxadol once-daily, twice daily or placebo, there was an increase in the CGI-I score in 67% of patients on the once-daily dose, in comparison to 43% and 22% in the twice daily group and placebo group, respectively. The phase 3 trial will move forward to analyse safety, tolerability, and efficacy in a younger cohort, aged 2 to 12 years.

GTX-102 (GeneTX Biotherapeutics) is another compound that is currently entering phase 1/2 trials to study the safety and tolerability in paediatric patients. GTX-102 is an antisense oligonucleotide that has been designed to reactivate the expression of the paternal UBE3A allele by inhibition of the UBE3A-AS. Reinstatement of the paternal allele in mouse models of AS have shown to be encouraging (Gu et al., 2019a, Silva-Santos et al., 2015). Work by Philpot's group identified a which can unsilence the paternal allele of Ube3a (Huang et al., 2011). Topotecan was administered by a unilateral intracerebral (ICV) infusion for 2 weeks in the mouse. They reported that topotecan upregulated Ube3a by downregulating the expression of Ube3a-ATS (Huang et al., 2011). The paternal allele was unsilenced to the highest degree in the infused hemisphere of the brain, most specifically, the hippocampus, striatum and cerebral cortex, however, this effect was not seen to the same degree in the other hemisphere, and no effect was seen in the cerebellum (Huang et al., 2011). Following drug delivery cessation, the concentration dramatically reduced after 5 hours, suggesting that it is rapidly metabolized in the brain. The group found that intra-thecal administration, which is already a FDA approved as a route of administration for this

drug, had lasting effects (up to 12 weeks following drug cessation) on spinal cord neurons (Huang et al., 2011). Further tests are required to determine if unsilencing the paternal allele can rescue the AS mouse model phenotype.

Table 1.2: List of active trials of current drugs being tested for AS

Drug name	Mechanism	Outcome measures	Phase	Sponsor
RO7248824	Unknown	Safety, Tolerability, PK and PD.	1	Hoffmann-La Roche
GTX-102	Antisense oligonucleotide	Phase 1:Safety, Tolerability, PK and PD. Phase 2: Changes in motor function, development, communication, seizure frequency, sleep and adaptive behaviours .	1& 2	GeneTX Biotherapeutics, LLC
OV101/Gaboxadol	GABA activation	Incidence of adverse events and EEG evaulations.	2	Ovid Therapeutics Inc
Levodopa	Dopamine precursor	Bayley Cognitive Age Equivalent and presence of tremors.	2&3	Wen-Hann Tan
Circadin	Melatonin	Baseline profile of saliva melatonin concentrations. Adverse events.	1	Neurim Pharmaceuticals Ltd.
Minocycline	Antibiotic	Increase on the equivalent age of development, improved cognitive, language and communication, motor development, adaptive behaviour, EEG improvement and safety and tolerability.	2	Puertade Hierro University Hospital

https://clinicaltrials.gov/ct2/home.

1.9 MicroRNAs

1.9.1 Overview

MicroRNAs were first discovered in 1993, in *C.elegans* (Lee et al., 1993, Wightman et al., 1993). MiRNAs are small (~22 nt) non-coding RNAs that play a crucial role in the regulation of gene expression by posttranscriptional repression of mRNA targets (Bartel, 2018) (Kosik, 2006) . MiRNA regulation has been described as essential for all developmental processes including cell proliferation, apoptosis and neuronal firing rate (Ardekani and Naeini, 2010, Croce and Calin, 2005). Their function is critical to the development of nearly every organ from the heart to the brain to vasculature to the skeleton (Bartel, 2018). In accordance with this, abnormal levels of miRNAs have been associated with disease, which will be described later in detail (Paul et al., 2018, Ardekani and Naeini, 2010). MiRNAs can be found in a number of extracellular fluids and can therefore hold promise as potential biomarkers in the future (O'Brien et al., 2018).

1.9.2 Biogenesis

MiRNA can be separated into two classes - canonical and non-canonical - depending on the processing of the pri-miRNAs (Graves and Zeng, 2012). MiRNA biogenesis starts with the transcription of a miRNA gene to generate a pri-miRNA transcript. In the canonical pathway, the pri-miRNA is cleaved by the microprocessor complex that contains Drosha, a ribonuclease which cuts the stem of the pri-miRNA hairpin. This generates a pre-miRNA (precursor-miRNA), that is roughly 60-70 nucleotides (overhang and con (Graves and Zeng, 2012). The pre-miRNA is then exported into the cytoplasm by Exportin 5 (Epx5) and RAN-GTP. The pre-miRNA undergoes further processing by Dicer, an endonuclease which cuts both strands to generate a miRNA duplex of roughly 22 base-pairs (Graves and Zeng, 2012). One of the arms (3p or 5p) of the miRNA duplex is then loaded into an Argonaute (Ago) protein (the other, so-called passenger strand, is usually degraded) and a miRNA induced silencing complex (RISC) is formed. Once loaded onto

the RISC, the miRNA pairs with mRNA targets to direct posttranscriptional repression (Bartel, 2018). The processing for non-canonical miRNAs does not include all of the protein factors mentioned above. For example, instead of Drosha cleavage, the pre-miRNA is spliced, it also bypasses Dicer and is directly cleaved by Ago2 (Graves and Zeng, 2012).

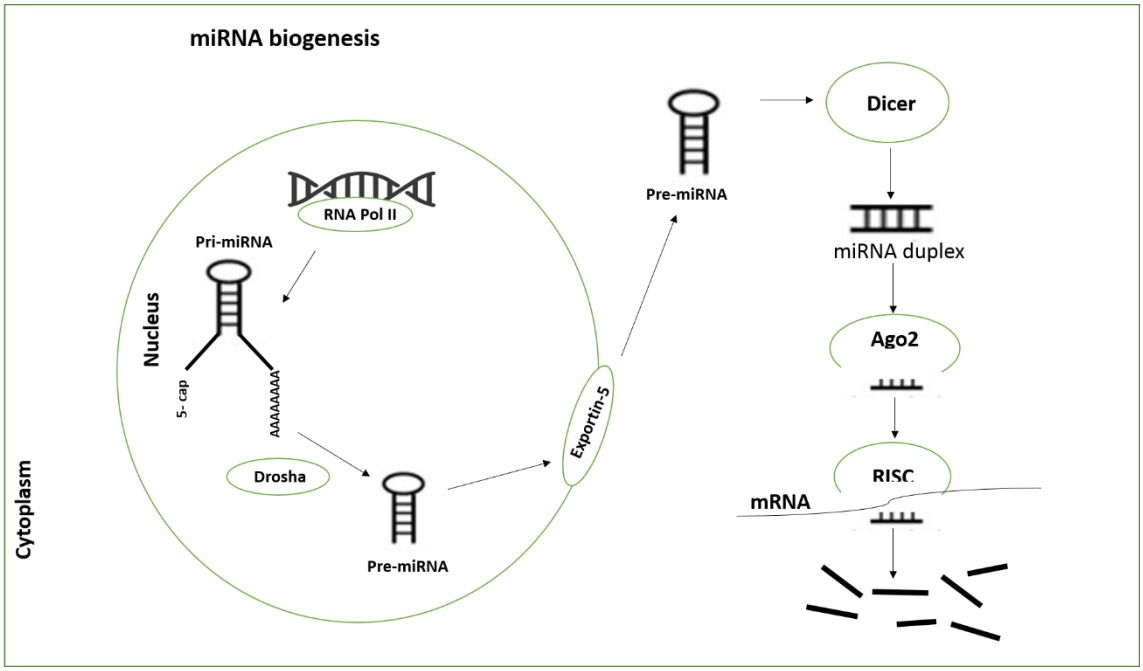

Figure 1.3: MicroRNA biogenesis. Schematic represents the pathway of miRNA biogenesis.

1.9.3 Neuronal miRNAs

The brain is the most miRNA-enriched organ; up to 70% of miRNAs detected thus far have been found to be expressed in the brain (Fineberg et al., 2009) (Kosik, 2006, De Pietri Tonelli et al., 2014). Several are expressed in specific cell types. For example, miR-124, miR-128, miR-9 and miR-134 are neuron-enriched miRNAs (Peng et al., 2013b) (Cho et al., 2019). Numerous studies have demonstrated the extensive role of miRNAs in the developing brain. For example, a study using conditional mice where Dicer was deactivated, found it had a significant impact on neuronal development by affecting

cortical apoptosis, changes in spine morphology, axonal tracts and a reduced lifespan indicating the critical roles played by miRNAs (Davis et al., 2008).

Roles have been demonstrated for specific miRNAs in neuronal development. For instance, miR-9 is required for the normal development of the telencephalon and diencephalon via regulation of genes such as *Foxg1*, *Pax6* and *Meis2*. Notably, miR-9 also targets neurogenin 1 (Ngn1), which suppresses astrogliogensis (Zhao et al., 2015). MiR-124 has also shown to be important in neurogenesis via its targets *sox9* and *DLX2* (Cheng et al., 2009). The authors found that abnormal expression of miR-124 leads to the early development of neuron formation, whereas knockdown of this miR-124 maintains subventricular zone (SVZ) stem cells as dividing precursors (Cheng et al., 2009). This effect appeared to be driven by *Sox9*, as blockade of *Sox9* leads to an increase in the formation of neurons, while the over-expression prevents neuronal differentiation (Cheng et al., 2009). In accordance with this a separate study found that the overexpression of miR-124 causes the early initiation of synaptic plasticity via HDAC1 (Hou et al., 2015).

One of the largest miRNA clusters, the miR-379-410 cluster, contains a number of miRNAs that have critical roles in neurogenesis and neuronal function (Rago et al., 2014, Winter, 2015). For instance, three miRNA of this cluster, miR-369-3p, miR496 and miR-542, were shown to be involved in neurogenesis and neuronal migration by the regulation of N-cadherin (Rago et al., 2014). The authors found that these miRNAs repressed N-cadherin levels, which led to the differentiation of radial glial cells (RGCs) (Rago et al., 2014). Other miRNAs of this cluster have potential roles in neurodevelopmental diseases. Levels of miR-300, miR-299 and miR-154 were all found to be upregulated in a mouse model of RTT suggesting Mecp2 negatively regulates these miRNA (Wu et al., 2010, Winter, 2015). Some miRNAs in this cluster have also been associated with SZ (Winter, 2015). MiR-154, miR-134, miR-544, miR-654-5p, miR-323-30, miR-487b, miR-410, miR-409-3p have all been found to be downregulated in peripheral blood mononuclear cells (PMBCs) of SZ patients, postulating that targets of these miRNA may play a role in SZ (Gardiner et al., 2012, Perkins et al., 2007, Moreau et al., 2011).

1.9.4 Therapeutic targeting of miRNAs

MiRNAs have become attractive drug targets due to their ability to modulate multiple targets. To date, there have been over 20 clinical trials using different forms of miRNA and small interfering RNA (siRNA) based therapies (Chakraborty et al., 2017). MiRNAs can be manipulated in a number of different ways, by either inhibition or miRNA gain-of-function. This includes the use of miRNA inhibitors, miRNA mimics, miRNA precursors and miRNA biogenesis enhancement. Inhibition of particular miRNAs can be accomplished using antisense miRNA oligonucleotides (AMOs) which have complementary sequences to target miRNAs and bind directly to the single strand to block the function (Zhang et al., 2013). Silencing miRNAs can be accomplished using a number of different miRNA therapeutics including modified AMOs, conjugate RNA analogues that are 22-23 nucleotides long, 2'O-methyl group modified locked nucleic acids (LNAs), phosphorodiamidate morpholino oligonucleotides (PMOs) and peptide nucleic acids (PNAs) (Zhang et al., 2013). Miravirsen was the first miRNA therapy to enter a clinical trial. Miravirsen is LNA based ASO that targets miR-122 and is used in the treatment of Hepatitis C (Lindow and Kauppinen, 2012). In terms of gain-of-function miRNA therapy, miRNA mimics act to overexpress a particular miRNA and can be used to substitute depleted miRNAs (Baumann and Winkler, 2014). This is done by developing a synthetic mimic that has an identical strand sequence to imitate the target miRNA (Jin et al., 2015). MiRNA precursors have been developed to express a specific miRNA by using a vector-based inserting a miRNA precursor sequence downstream of the RNA polymerase II (Zhang et al., 2013, Chung et al., 2006). Lastly, attempts have been made to manipulate the miRNA pathway with the aim of modifying the expression of a particular miRNA (Zhang et al., 2013). A table of current miRNA based therapies can be seen in table 3.1.

Table: 1.3: Current miRNA based therapy drugs in on-going trials

Drug name	Target	miRNA therapy	Disease	Phase	Company
Miravirsen	miR-122	AntimiR	Hepatitis C	2a	Santaris Pharma
MRX34	miR-34a	Mimic	Melanoma	1	MiRNA Therapeutics
RG-012	miR-21	AntimiR	Alport syndrome	1	Sanofi
RG125/AZD4076	miR-103	AntimiR	Nonalcoholic fatty liver disease in Type 2 diabetes	2	AstraZeneca
RGLS4326	miR-17	AntimiR	Autosomal dominant polycystic kidney disease (ADPKD)	1	Regulus Therapeutics
RG-101	miR-122	AntimiR	Hepatitis C	2	Regulus Therapeutics
RGLS5040	miR-27	AntimiR	Cholestasis	Preclinical	Regulus Therapeutics

https://clinicaltrials.gov/ct2/home.

1.9.5 MicroRNAs in epilepsy and related disorders

Multiple studies have profiled the expression of miRNA in experimental and human epilepsy (Gorter et al., 2014, Bot et al., 2013, Hu et al., 2012, Song et al., 2011, Henshall, 2014). For instance, miR-132, a miRNA that has multiple roles in neuronal development, was found to be upregulated in a rat model of electrically induced SE and in a mouse model of kainic acid induced SE (Bot et al., 2013, Jimenez-Mateos et al., 2011, Qian et al., 2017). Moreover, inhibition of miR-132 using an antagomir led to a reduction in seizure-induced neuronal death (Jimenez-Mateos et al., 2011). MiR-146a has also been shown to be increased in models of epilepsy. MiR-146a is an inflammatory-associated miRNA that has been found to be upregulated in a rat model of temporal lobe epilepsy (TLE) and a lithium-pilocarpine induced SE (Aronica et al., 2010, Hu et al., 2012). Among those downregulated in models of epilepsy, miR-33 was detected in the model of

electrically induced SE and in a TLE model (Bot et al., 2013) (Hu et al., 2012). MiR-134 has reported to be increased in TLE patients and in multiple rodent models of epilepsy and SE (Jimenez-Mateos et al., 2012, Reschke et al., 2017a, Gao et al., 2019). MiRNA dysregulation has also been hypothesised to contribute to RTT (Urdinguio et al., 2010, Wu et al., 2010). One study in particular analysed miRNA expression in a mouse model of RTT, in pre-symptomatic and symptomatic mice (Wu et al., 2010). In total, they found fifteen upregulated miRNA and three downregulated miRNA between both sets of mice. Upregulated miRNA included let-7a, miR-137, miR-455 and downregulated included miR-29c and miR-140 (Wu et al., 2010). Similar to other reports the authors found dysregulation of miR-132 in cultured *Mecp2* cortical neurons. This coincides with analysis done by Klein *et al*, who investigated the mechanism by which miR-132 represses *bdnf* and found that *bdnf* levels were increased by using a miR-132 antisense oligonucleotide (Klein et al., 2007). Regulation of miRNAs have also been hypothesised to be involved in *SCNA1*, encoding Nav1.1, the gene commonly mutated in Dravet Syndrome (DS), a severe form of intractable epilepsy that occurs in early childhood (Gross and Tiwari, 2018). For instance, the seizure suppressive effects of valproic acid in DS was shown to be influenced by the expression of miR-155 (Zhang et al., 2018).

1.9.6 MiR-134

One of the best characterised miRNAs from the miR-379-410 cluster with links to epilepsy and schizophrenia is miR-134 (Gardiner et al., 2012, Winter, 2015). MiR-134 was also found to be increased in the amygdala of rats subjected to acute stress, but decreased during chronic stress (Meerson et al., 2010). MiR-134 has a number of essential targets, such as LIM kinase 1 (Limk1), pumilio 2 (Pum2) CREB and DCX, which have shown to be involved in dendritic development and morphology, neuronal migration and neural precursor cell (NPC) proliferation (Jimenez-Mateos et al., 2012, Jimenez-Mateos et al., 2015, Gardiner et al., 2012, Winter, 2015). It has been postulated that SZ is caused by abnormal synaptic pruning, suggesting that the repression of miR-134 targets may

contribute to the pathogenesis (Boksa, 2012, Sellgren et al., 2019). Moreover, a recent study developed an imaging method and using atomic force microscopy, they found that there was a higher abundance of miR-134 in immature spines in comparison to mature spines, supporting the evidence that miR-134 is involved in the regulation of individual spines. Furthermore, they reported that miR-134 was located in the necks of dendritic spines and below dendritic shafts (Park et al., 2019).

The formation of neuronal networks is a critical part of neurodevelopment that involves neuronal migration, axon guidance and neurite outgrowth (Cuberos et al., 2015). The most common type of neuron found in the hippocampus and cortex are pyramidal cells, which contain neuronal dendrites that receive stimulation from excitatory synapses (Jimenez-Mateos et al., 2012, Zampa et al., 2018). Dendritogenesis is a vital process that allows neurons to communicate with each other via the formation of protrusions (spines) that become excitatory synapses. Thus, dendritogenesis is essential for learning and memory formation during development and establishment of correct balance of excitability within neuronal networks (Kulkarni and Firestein, 2012). Dysregulation in dendritogenesis has been implicated in a range of neurodevelopmental disorders such as RTT (Kaufmann and Moser, 2000), FXS and Down syndrome (DS), in neuropsychiatric disorders such as SZ and anxiety/depressive disorders (Eiland and McEwen, 2012, Stephan et al., 2006) and finally in neurological disorders such as Alzheimer's (Müller et al., 1993, Bhattacharyya et al., 2009, Kulkarni and Firestein, 2012).

Compelling work by Schratt *et al* elucidated the functional role of miR-134 in the regulation of dendritic spines (Schratt et al., 2006). They reported that levels of miR-134 peak during postnatal development at P13, an age that coincides with the time of synaptic maturation, hypothesizing a functional role of miR-134 in dendritic and synaptic development (Schratt et al., 2006). Using *in situ* hybridization (ISH), miR-134 expression in dendrites was confirmed. They also identified that it was localized near synaptic sites on dendrites and to compliment this result, they found miR-134 to be increased in synaptoneurosome preparations (Schratt et al., 2006). Schratt et al identified Limk1 as a

key target of miR-134 (Schratt et al., 2006). Limk1 phosphorylates and thereby inhibits cofilin (an actin de-polymerising factor), thus promoting actin polymerisation and spine expansion. Notably, loss of limk1 in a knockout mouse model results in abnormal dendritic spines (Schratt et al., 2006, Jimenez-Mateos et al., 2012) . This indicates that miR-134 acts as a negative regulator of dendritic spines via its target limk1. When miR-134 was blocked, this increased levels of Limk1 and increased spine volume whereas overexpression of miR-134 repressed Limk1 and reduced spine volume and width (Schratt et al., 2006).

Extensive work has linked miR-134 to epilepsy (Morris et al., 2019). For instance, studies have shown that miR-134 is upregulated in the hippocampus of children and adults with TLE (Peng et al., 2013b) (Jimenez-Mateos et al., 2012). Notably, it is also increased in the same brain region following experimentally induced seizure activity in rodents (Jimenez-Mateos et al., 2015, Jimenez-Mateos et al., 2012, Peng et al., 2013a, Morris et al., 2018). Previous work in our lab has shown that blocking miR-134 using a LNA oligonucleotide antagomir (Ant-134) before inducing SE in mice had seizure suppressive effects as analysed by seizure onset, seizure burden and EEG total power (Jimenez-Mateos et al., 2012, Reschke et al., 2017a). This protective effect of Ant-134 has since been shown in multiple models (Jimenez-Mateos et al., 2012, Jimenez-Mateos et al., 2015, Reschke et al., 2017b). The intra-amygdala model is used to replicate TLE as injection of KA into the amygdala results in hippocampal cell death, specifically in the CA3 region. Direct injection of KA into the amygdala induces SE and mice begin to develop spontaneous seizures roughly 14 days after SE. This resulted in an increase of miR-134 levels and a downregulation of Limk1 (Jimenez-Mateos et al., 2012). These results are comparable to analysis done on human samples from TLE patients where an increase in miR-134 and a decrease in Limk1 was found when compared to autopsy control samples (Jimenez-Mateos et al., 2012). Pre-treatment with Ant-134 resulted in seizure suppressive and neuroprotective effects which had lasting effects. In addition, post-treatment with Ant-134 was also successful in reducing the severity of seizures and these results lasted over two months (Jimenez-Mateos et al., 2012). For instance, the

efficacy of Ant-134 was replicated in the pentylenetetrazol (PTZ) model which induces seizures by blocking GABAergic transmission. Here, seizure induction was associated with an increase in miR-134 levels. Seizures in mice treated with Ant-134 were significantly delayed in comparison to those treated with the scramble-control compound and there was a reduction in the ictal seizure severity measured by the EEG total power. Furthermore, there was a reduction in the behavioural seizure severity as analysed by the Racine scale (Reschke et al., 2017a). In the same study, the efficacy of Ant-134 in the perforant pathway stimulation model (PPS), which is a toxin-free model of epilepsy was analysed. The PPS model is a model of acquired epilepsy that is induced by continuous electrical stimulation of the perforant path. This causes seizures that are similar to SE and is associated with the loss of hilar and pyramidal cells in the hippocampus (Kelsey et al., 2000). Interestingly, seizure suppression was only evident in this model with post-treatment of Ant-134 (Reschke et al., 2017a). While this model was not associated with an elevation of miR-134 after SE, Ant-134 was still effective in reducing the developed of spontaneous seizures over eight weeks after SE induction (Reschke et al., 2017a). In addition, Ant-134 was shown to protect against pilocarpine-induced SE (Jimenez-Mateos et al., 2015). Pilocarpine is a cholinergic agonist that is used in conjunction with scopolamine to induce SE. This method of SE differs slightly to other methods described above as pilocarpine can be administered intraperitoneally in one single dose or in multiple doses and SE usually occurs after 60-90 min post injection. The latter is used more frequently to reduce morbidity/mortality. There was a significant increase in miR-134 levels following pilocarpine induced SE and this was evident at 4 h and 24 h (Jimenez-Mateos et al., 2015). As observed in other models, pre-treatment with Ant-134 protected against pilocarpine induced SE and in those that were not protected against SE, there was a delay to the initiation of SE (Jimenez-Mateos et al., 2015). Taken together, the role of miR-134 has been well established in multiple models of epilepsy and SE and provide a basis for the use of Ant-134 in models of paediatric epilepsy.

1.10 Remit of thesis

The treatment of early life seizures is challenging and remains a major unmet need. Seizures at a young age can impact brain development which can have detrimental consequences later on in life. MiRNAs are critical in CNS development and have been shown to be involved in seizure pathology in both mouse models of epilepsy and in patients with epilepsy. Before moving to a genetic model of epilepsy, we first questioned the functional role of miR-134 in the immature brain using a paediatric chemoconvulsant model. The role of miRNAs in AS has not yet been investigated. Thus, our next questions aimed to elucidate whether/how miRNAs are involved in the pathophysiology of AS; how miR-134 would contribute to the hyperexcitable phenotype in AS and if its silencing using antagomir-134 could protect against seizures in this genetic model of epilepsy.

Aim 1:

To develop a paediatric model of SE using systemic kainic acid and to determine if Ant-134 can render seizure protective effects in this model.

Hypothesis 1:

We have hypothesized that the induction of SE by kainic acid will increase the hippocampal and cortical levels of miR-134 in young mice. Accordingly, we expect that a pre-treatment with Ant-134 will prevent the expected severity and occurrence of SE characteristic of the model.

Aim 2:

To comprehensively characterise a mouse model of AS with a maternal mutation in *Ube3a* (Ube3a $^{m-/p+}$) at phenotypic and molecular levels using two generations of mice.

Hypothesis 2:

We have hypothesised that the Ube3a $^{m-/p+}$ mouse model will have an abnormal EEG, with increases in delta and theta frequency, motor impairments in the open field and rotarod and increased seizure susceptibility. In addition, levels of miR-134 are expected to be altered in these mice in comparison to their WT littermates.

Aim 3:

To determine if Ant-134 can reverse AS-like phenotypes. Specifically, we investigate the effect of Ant-134 on resting EEG, audiogenic seizures and behavioural phenotypes.

Hypothesis 3:

We have hypothesised that miR-134 will be elevated in AS mice due to the loss of the Ube3a1 binding site. Furthermore, targets of miR-134 are expected to be repressed. Blocking miR-134 using Ant-134 will correct some of the behavioural and seizure phenotypes.

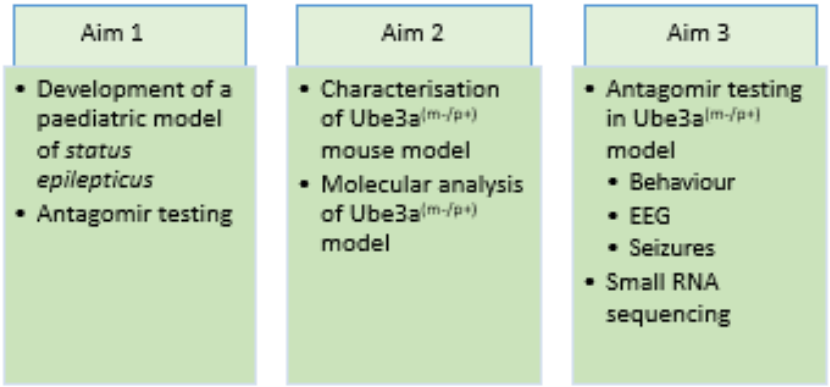

Figure 1.4 Outline of main aims of PhD project

2 Chapter two

Materials and methods

2.1 Animal work

All animal experiments were performed in accordance with the European Communities Council Directive (2010/63/EU), the NIH Guide for the Care and Use of Laboratory Animals (National Research Council Committee for the Update of the Guide for the and Use of Laboratory, 2011), and followed ARRIVE guidelines (Kilkenny et al., 2010). Protocols were reviewed and approved by the Research Ethics Committee of the Royal College of Surgeons in Ireland (REC 1302bbb) under licenses from the Department of Health (AE19127/P013 and AE19127/P064), Dublin, Ireland. Animal work was performed by either Aoife Campbell (AE19127/I178) or by Dr Cristina Reschke (AE19127/I018). Male C57BL/6 mice (P7-42) were obtained from RCSI's Biom stock from Harlan, Oxon, Bicester, U.K.). P7 and P14 mice were housed with littermates and dam until non-recovery experiments. *Ube3a* mutant mice were obtained from Jackson Laboratory, Maine, US (Stock No. 016590) and bred as detailed below. Weaned animals were housed (up to 5 mice per cage) in on-site barrier-controlled facilities with a 12 h light-dark cycle and *ad libitum* access food and water.

2.1.1 Mouse husbandry and breeding

2.1.1.1 *Generation F1*

We initiated a colony using B6.129S7-*Ube3a*^{tm1alb}/J mice carrying a mutation in *Ube3a* were maintained on C57BL/6 (B6) background. A simplified breeding scheme is illustrated in figure 2.1. To generate mice to model the maternal deficiency of *Ube3a*, *Ube3a* $^{(p+/m-)}$ adult males were crossed with wildtype (WT) C57BL/6 females maintenance colony (A). Heterozygous (het) females generated from maintenance colony (A) were crossed with WT 129Sv/Ev males from maintenance colony (B) to generate the experimental colony (C). Maintenance colony (B) was continuously breeding to generate WT 129Sv/Ev males. Mice generated in colony (C) were from the first generation, and will be referred to as 'F1'.

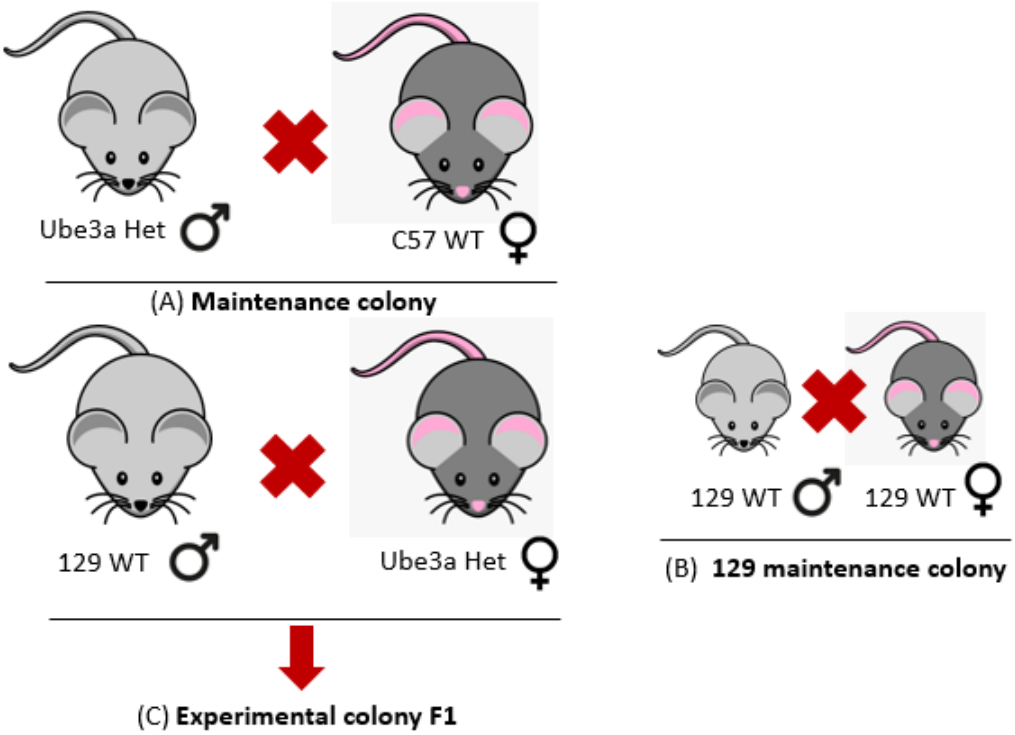

Figure 2.1: Breeding scheme of F1 generation for experimental colony

2.1.1.2 *Generation N4*

To generate mice that were susceptible to audiogenic seizures, F1 mice were backcrossed for four generations and maintained on a 129Sv/Ev background. A simplified breeding scheme is illustrated in Figure 2. Briefly, F1 female het mice from the experimental colony were crossed with male WT 129Sv/Ev mice from the maintenance colony B (Ai). This offspring was conside backcrossing through a generation. Female het mice from N2 colony were then crossed with male WT 129Sv/Ev mice (Aii) to produce N3 mice. Finally, female hets (N3 offspring) were then crossed with male WT 129Sv/Ev mice (Aiii) to reach the fourth generation, which was the experimental colony for audiogenic seizure susceptibility experiments.

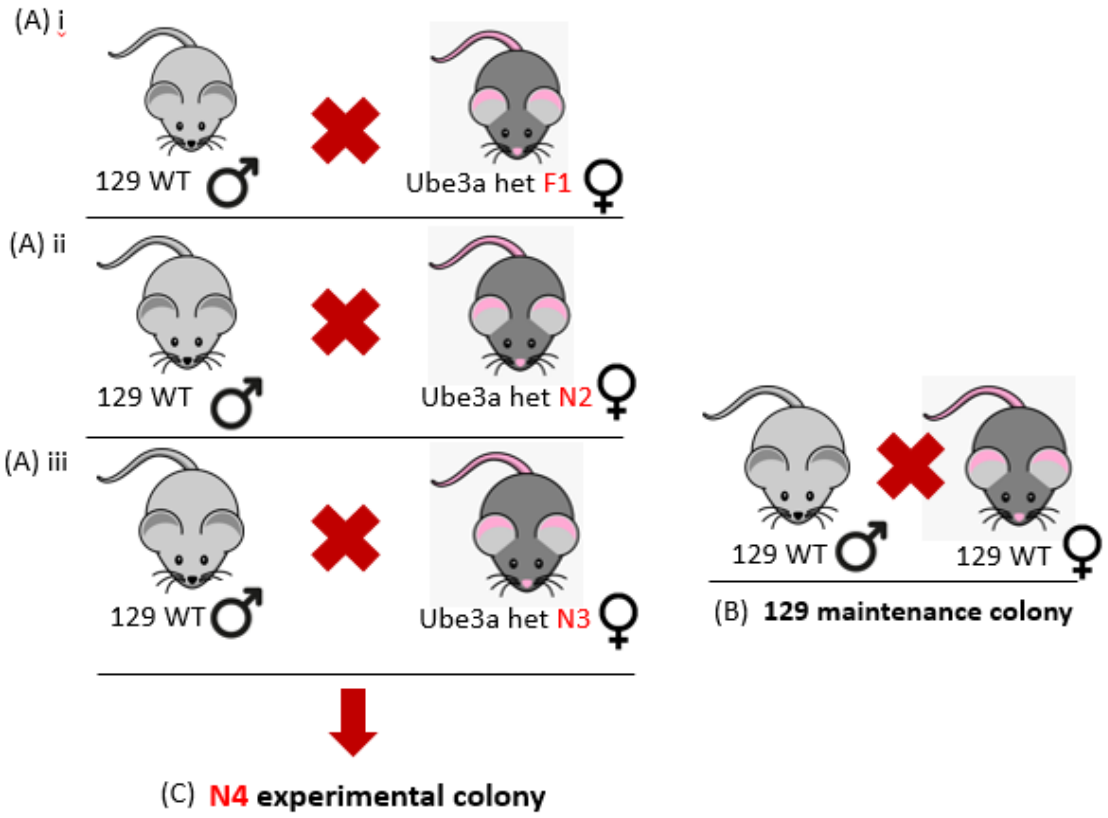

Figure 2.2: Breeding scheme to obtain the N4 generation experimental colony

2.1.2 Genotyping

Ube3a $^{m-/p+}$ mice were identified by either ear punching or by tattooing. Ear or tail samples were used for genotyping. For the experimental colonies, tail snipping was done before P7 to minimize pain. DNA was extracted from samples by adding 150 µl of 50 mM NaOH (Sigma-Aldrich, Ireland) to the samples and placed on a thermomixer shaking at 1400 rpm at 95°C for 2.5-3 hours. When the tissue was fully dissolved, 15 µl of Tris-HCL (pH8, Sigma-Aldrich) was added to the samples and centrifuged at max speed for 10 mins at max speed. Genotyping was performed using KAPA2G Fast Genotyping Mix (KAPA Biosystems, UK). Briefly, 500 ng of DNA was made up to 2 µl of dH_20 and a master mix containing primers (WT, het and common primer) and the KAPA mix were added to strip

tubes. A polymerase chain reaction (PCR) was set up using the following conditions listed in table 2.1. The samples were then separated by electrophoresis on a 2% agarose gel (Sigma-Aldrich, Ireland) and the results were imaged using a Fuji Las 3000 under ultraviolet light.

Table 2.1: Polymerase chain reaction for genotyping F1 and N4 mice.

Step	Temp °C	Time	Note
1	94	2 min	
2	94	20 sec	
3	65	15 sec	-0.5 °C per cycle decrease
4	68	10 sec	
5			Repeat steps 2-4 for 10 cycles
6	94	15 sec	
7	60	15 sec	
8	72	10 sec	
9			Repeat steps 6-8 for 28 cycles
10	72	2 min	
11	10		Hold

Table 2.2: Primer sequences for genotyping F1 and N4 mice

Primer	Catalogue no.	Sequence
Common	25384	5' GAA AAC ACT AAC
Wildtype	25383	5' TCA ATG ATA GGG
Mutant	25385	5' CTT GTG TAG CGC

2.1.3 Behavioural characterization

All behavioural experiments were done between the hours of 1-6 pm. Mice were placed into the behaviour room 30 minutes prior to testing to habituate to the room in their home cages. All behaviour apparatus was cleaned with 30% ethanol before use. Male and female mice were used in all behavioural tests and an even ratio was kept between WT and AS mice.

2.1.3.1 *Open field*

The open field is used to measure locomotor activity and anxiety. The method for open field testing was adopted from Sonzogni et al (Sonzogni et al., 2018). *Ube3a* $^{m-/p+}$ mice (WT and AS) were placed individually in the middle of an open field test chamber (27.3 cm 27.3, Med Associates, Inc, Fairfax, Vermont) and allowed to explore the arena for 10 minutes. The arena was cleaned with 30% ethanol between trials. Mouse movement was recorded on a Logitech HD1080p camera. Data were analysed by manually recording the length of time the mouse was active during the 10-minute trial. Next, using the AnyMaze (6.1) software (Stoelting, Dublin, Ireland), the exact dimensions of the arena were identified on the video by a ruler tool (30 mm). The inner and outer zones of the arena were also identified to track the number of crossings between zones and the total time spent in each area. The mouse's tail and head

tracked throughout the trial. The following parameters were measured: total distance travelled (mm), speed (m/s), entries into inner zone, total time spent in inner zone (s).

Figure 2.3: Open field test chamber from Med Associates, Inc.

2.1.3.2 Accelerating rotarod

The rotarod protocol was adapted from a number of articles and modified to adhere to the guidelines of our approved animal licenses (Deacon, 2013, Shiotsuki et al., 2010, Sonzogni et al., 2018). Motor function was assessed using the accelerating rotarod (Letica scientific instruments, Portugal). A trial period was performed before the testing phase commenced. This consisted of *Ube3a* $^{m-/p+}$ mice (WT and AS) being placed on the rotarod for 3 minutes at a constant speed. Mice were placed back onto the rotarod apparatus if they fell off during the trial (this was noted). During the test phase, mice were placed onto the rotarod at an accelerating speed of 4-40 rpm, for 5 minutes. This trial and testing phase were repeated on two consecutive days at the same time of the day, with two trials per day with at least 40 minutes between each test. The latency to fall (s) per mouse was recorded and the average of two trials was taken.

Figure 2.4: Rotarod apparatus from Letica scientific instruments.

2.1.3.3 *Light-dark box*

The light-dark box protocol was adopted from Takao and Miyakawa (Takao and Miyakawa, 2006). *Ube3a* $^{m-/p+}$ mice (WT and AS) were individually placed in the open field chamber (Med Associates, Inc.) for 10 minutes. A dark box insert (Med Associates, Inc.) was placed into the chamber and represented the dark section of the arena. A light (60 W/600 lux) was used to illuminate the light section of the arena. Upon trial initiation, the mouse was placed into the light compartment of the arena. The time spent in each compartment was analysed manually and using AnyMaze software, as before. For the software analysis, the dark compartment therefore, the length of time the mouse was not visible, i.e. in the dark compartment, was recorded. A full transition was identified and recorded when all four paws were in the given arena.

Figure 2.5: Light-dark box chamber (Med Associates, Inc).

2.1.3.4 Marble burying

The marble burying protocol was adopted from Sonzogni *et al* and Deacon (Deacon, 2006b, Sonzogni et al., 2018). Polycarbonate cages (365 x 207 x 140 mm h) were filled with 5 cm of bedding. Twenty marbles were placed on top of the bedding and arranged in 5 x 4 grid at equal distance. *Ube3a* $^{m-/p+}$ mice (WT and AS) were individually placed into the middle of the cage for a 30-minute period. After the trial, the amount of marbles with 50% or more of their surface buried in the bedding were counted. The cage and marbles were cleaned with 30% ethanol after use. Fresh bedding was used for each mouse.

Figure 2.6: Marble burying set-up.

2.1.3.5 Nest building

The nest building method was adopted from Sonzogni *et al* (Sonzogni et al., 2018). Before commencing the nest building test, *Ube3a* $^{m-/p+}$ mice (WT and AS) were single housed for a week. Twenty-four hours prior to testing, environmental enrichment was removed from each cage. On the first day of testing, 10 g of blotting filter paper (Bio-rad) was placed in each cage. The amount of unused nesting material was weighed daily, at the same time of the day, for five consecutive days. For statistical analysis, the average weight of blotting paper from WT and AS mice was graphed.

Figure 2.7: Day 1 of nest building test.

2.1.4 Surgical procedures

All surgical procedures were performed by the researcher, with the exception of surgeries performed on C57 mice in section 1.1.4.1 (intracerebroventricular injections and electrode implantation) which were performed by Cristina R. Reschke. Surgeries were performed on WT C57 P21 male mice for experiments outlined in chapter 3. Surgeries were performed on *Ube3a* $^{m-/p+}$ mice WT and AS P21 and adult (P42-P60) male and female mice for experiments outlined in chapter 4 and 5.

2.1.4.1 Intracerebroventricular (ICV) injections and electrode implantation

ICV injections and electrode implantation were performed in C57 P21 mice and in *Ube3a* $^{m-/p+}$ mice using the same surgical procedures. For electrode implantation, mice were anesthetised with isoflurane (5% induction, 1-2% maintenance) and placed in a mouse-adapted stereotaxic frame. After local analgesia with lidocaine and prilocaine cream (EMLA), a midline scalp incision was made, Bregma was located and three partial craniotomies were performed for the placement of skull-mounted recording screws

(Bilaney Consultants, Kent, UK) for intracranial electroencephalographic (EEG) recordings. For ICV injections, a fourth craniotomy was drilled to allow direct ICV injections (coordinates from Bregma: anterior-posterior (AP) +0.3, lateral (L) = +0.9, ventral (V) = -1.35 mm. Mice received either mmu-miR-34a-3' 5' TGGTCAACCAGTCACA/-3 (Ant-1 inhibitor, 0.5 nmol in 2 µL PBS), a non-targeting scrambled control (Scr; -3' 5' CGTCTAGCCACCTAG/3 Exiqon, 0.5 nmol in 2 µL PBS), or vehicle control (2 µL PBS), injected using a 2 µl Hamilton syringe at a rate of 1 µl/min . The ICV needle was left in the brain for 5 min after injection to ensure even distribution. The electrode assembly was fixed in place using dental cement. For ICV injections alone, the surgical site was closed with surgical glue. After surgery, the mouse was placed in a temperature-controlled open Perspex box and monitored throughout post-op recovery. For ICV injections in *Ube3a* $^{m-/p+}$ mice, ink injections were performed to confirm the coordinates from bregma were the same as C57 mice.

2.1.5 Induction of seizures

2.1.5.1 EEG recording during *status epilepticus* (SE) in C57 mice

Following full recovery from surgery, C57 P21 male mice were connected to the lead socket of a swivel commutator, which was connected to a brain monitor (Xltec, 32 channels, Natus Neurology) amplifier for acute tethered EEG recordings. After a 15 minutes EEG baseline recording, mice were lightly restrained while KA (Sigma-Aldrich, 5mg/kg or 7.5mg/kg IP) was injected to induce SE. After 30 minutes, mice received lorazepam (LZ; 8 mg/kg, IP) to terminate seizures and reduce morbidity/mortality. Mice were disconnected from the EEG system and placed in a warmed recovery chamber.

2.1.5.2 Induction of seizures using chemoconvulsants in *Ube3a*$^{m-/p+}$ *mice*

Subconvulsant doses of PTZ or KA were used to assess whether F1 AS *Ube3a* $^{p+/m-}$ mice would be more susceptible to seizures than WT littermates. Adult male and female mice (P42-P60) were implanted with three electrodes (as per section 1.1.4.1) and allowed to recover. Baseline EEG recordings were obtained for 15 minutes per mouse. Kainic acid (Sigma Aldrich Ireland Limited, Cat. No: K0250) was intraperitoneally injected per bodyweight (10 mg/kg dose with a maximum injection volume of 10 mL/kg). In a second set of mice, 40 mg/kg of PTZ (Sigma Aldrich Life Science, Cat. No: P6500) was intraperitoneally injected per bodyweight. After seizure induction, the onset to the first electrographic seizure was recorded manually with a timer and later confirmed electrographically on LabChart software. The onset to SE (if present, as defined above) was also recorded in the same manner. Using LabChart, the total power, amplitude and frequency of ictal activity was analysed. The seizure burden, defined as the total time spent in ictal activity, was also analysed. Mice were transcardially perfused 30 minutes post injection and whole brains were removed, snap frozen in 2-methylbutane and stored at -80°.

2.1.5.3 Audiogenic seizure model in *Ube3a*$^{m-/p+}$ *mice*

To induce audiogenic seizures in *Ube3a* $^{m-/p+}$ mice different methods were adapted and trialed in F1 *Ube3a* $^{m-/p+}$ mice (Born et al., 2017). WT and AS mice (P21, P28 and adult mice aged P42-P60) were implanted with electrodes (as described in section 1.1.4.1) and allowed to recover for at least two hours post-surgery. Mice were individually placed in a soundproof chamber, shown in figure 8 (SR-Lab, Startle response system, San Diego instruments) and tethered swivel cables were wired through the back of the chamber for EEG recordings. A Logitech HD 1080p camera was placed inside of the chamber. An alarm (Screaming Meanie 220, Pacific Conrnetta, Oregon, USA) was set to desired time and decibel (110-140 dB) and also placed inside the chamber. Mice were left for 15 minutes to habituate to the chamber and to record baseline EEG. During the model

characterisation, under EEG recording, the alarm went off at the desired time from 30 seconds to 2 minutes, depending on experimental design. In most cases the alarm was repeated at least twice, with 10 minutes between each audiogenic stimulus. EEG was also recorded for 15 min after each stimulus. At the completion of the experiment, mice were removed from the chamber and returned to their home cage.

Induction of audiogenic seizures in the F1 generation did not induce behavioural or electrographic seizures, thus, mice from the fourth generation were tested. As per literature, increasing the background percentage of 129 yielded mice that were more sensitive to audiogenic seizures (Mandel-Brehm et al., 2015, Sonzogni et al., 2018, Jiang et al., 1998). The same protocol used above was repeated in N4 mice, however, again, this was unsuccessful in inducing seizures. We therefore adopted a second audiogenic protocol (Sonzogni et al., 2018). P21 and adult mice were placed in a polycarbonate cage (365 x 207 mm x 140 mm) and the lid of the cage was vigorously scratched for 30 seconds (generating approximately 110 Db). This method was adapted from Sonzogni et al and Mandel-Brehm *et al* (Sonzogni et al., 2018, Mandel-Brehm et al., 2015). The seizures were recorded by a Logitech HD 1080p camera and analysed using an adapted audiogenic seizure scale [original scoring scale from Dailey et al. (1989) and Muñoz De La Pascua and López (2005)]. The maximum score per seizure type was noted per mouse. The latency to wild running (type 1), generalized tonic-clonic convulsions (type 2), and tonic hyperextension of the hindlimbs and tail (type 3) was identified by video analysis. This method of seizure induction was unsuccessful in F1 mice.

Table 2.3: Modified Racine scoring scale for audiogenic seizures.

Score	Seizure type
0	No seizure
1	Wild running
2	Tonic-clonic convulsions
3	Hyper-extension of hindlimbs
4	Death

Figure 2.8: Soundproof chamber for audiogenic seizures in F1 Ube3a m-/p+ mice.

2.1.6 EEG analysis

EEG data were analysed and quantified manually using LabChart 8 software (AD instruments, Oxford, UK) by an observer blind to the experimental groups. Seizures induced by KA were defined as high-amplitude (> 2 x baseline) high-frequency (> 5 Hz) polyspike discharges lasting > 5 seconds. SE was defined as at least 5 minutes of continuous seizure activity without a return to baseline. The presence of SE, the onset to first electrographic seizure or SE, the total time spent in seizure/SE (seizure burden) and the total EEG power (0-40 Hz, measured by fast Fourier transform) between KA and LZ injections were recorded for each mouse. Mice that did not present electrographic seizures during the recording period were assigned cut-off time as onset (1800 seconds) for statistical purposes.

Frequency band analysis was performed by Dr. Gareth Morris using custom MATLAB scripts. Briefly, a 30-minute artefact-free epoch was selected for each trace and converted to the frequency domain by fast Fourier transform. Data were subdivided into delta (2-4 Hz), theta (4-8 Hz), alpha (8-12 Hz) and beta (12-30 Hz). The relative power of each frequency band was calculated in order to adjust for differences in total power caused by electrode placement and other experimental factors.

2.1.7 Transcardial perfusion

All mice were euthanized by overdose using 200 µl phenobarbital (Dolethal, Vetoquinol, UK Ltd). With the abdomen facing upwards, a small lateral incision was made down the centre of the stomach. Another incision was made at the diaphragm and cut laterally through the ribs until the heart was exposed. The lungs and any connective tissue were moved until the heart was fully exposed. A needle (22 gauge) was placed into the left ventricle and the right atrium was snipped. 10-15 ml of ice-cold PBS was slowly and consistently pumped through the heart. Whole brains were removed and flash frozen

for Fluro-Jade b (FJB) or immunofluorescence staining or microdissected for molecular work (as detailed in 2.9) and frozen at -80 °C.

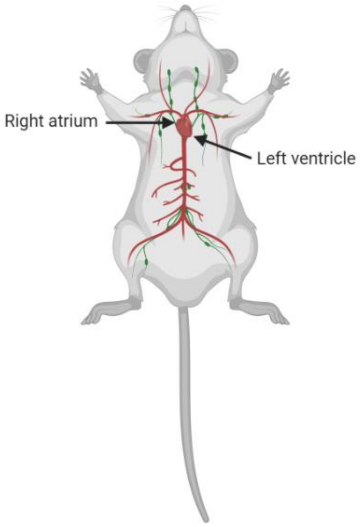

Figure 2.9 : Cardiac perfusion of mouse before whole brains were dissected.

2.1.8 Microdissection of the brain

Brains were microdissected for molecular analyses. Following a cardiac perfusion, whole brains were placed on a small petri dish mounted on an ice block. The cerebellum was removed and immediately placed in an eppendorf in dry ice. Next, the brain was hemisected. The midbrain was gently removed using forceps until the hippocampus was exposed. Gently, the hippocampus was rolled out and placed in an eppendorf. Finally, the cortex was cleared of remaining striatum and placed in an eppendorf. Tubes were immediately placed in a bed of dry ice and stored at -80°C.

2.2 Molecular work

2.2.1 Synaptosome extraction

Method was adapted from Nagy and Delgado-Escueta (Nagy and Delgado-Escueta, 1984). Two hippocampi were pooled per mouse. Hippocampi were homogenised on ice in 2 mL of cold homogenising buffer with added protease and phosphate inhibitors. Samples were centrifuged and the supernatant was recovered. The pellet was re-suspended in 200 µL of Krebs-Ringer buffer, followed by 90 µL of Percol (45% v/v) and centrifuged. The enriched synaptosomes were recovered and re-suspended in 1 mL of Krebs-Ringer buffer. The samples were centrifuged and the supernatant was discarded. Finally, the pelleted synaptosomes were re-suspended in Trizol and a standard RNA extraction for low input was carried out.

2.2.2 Argonaute-2 Immunoprecipitation

Hippocampi were homogenised by hand in 500 µL immunoprecipitation buffer (150 mM NaCl, 20 mM Tris-HCL (pH 7.5), 5 mM MgCl2, and 1% NP-40) and centrifuged. 500 µL of lysate was added to agarose beads and incubated for 2-6 hours on a rotator at 4 °C. Samples were incubated overnight at 4 °C with 10 µg of Ago antibody (1:10, C34C6, Cell Signalling Technology). The lysate bound antibody solution was added to agarose beads and left on the rotator for 2 hours. The supernatant was removed and the pellet was suspended in 200 µL Trizol and an RNA extraction was performed.

2.2.3 Standard mRNA extraction

Hippocampi and cortices were homogenised in 750 µL of Trizol (re-suspended in 200 µL for synaptosomes and AgoIP) and centrifuged at 12000g for 10 min at 4 °C. Phase separation was performed by adding 200 µL of chloroform to each sample (75 µL for synaptosomes and AgoIP) and vigorously mixing for 15 seconds before incubating at room temperature. Samples were centrifuged at 15600 g for 15 min at 4°C. The upper

phase was removed and 450 µL of isopropanol (125 µL for synaptosomes) was added and samples were stored at -20 °C overnight. Samples were centrifuged at 15600 g for 15 min at 4 °C and 750 µL (200 µL for synaptosomes and AgoIP) of 75% cold ethanol was used to wash the pellet. Samples were centrifuged at 13300 g for 5 min and the ethanol was removed. The pellets were left to dry for 1h and resuspended in 25 µL (8 µL for synaptosomes and AgoIP) of RNase free H_20. Samples were incubated for 10 min at 60°C with 60 g of agitation.

2.2.4 DNA degradation and reverse transcription

RNA (500 ng) was diluted in RNase free dH_20 and made up to 8 µl. The sample was degraded using 1 µl DNase 10X buffer and 1 µl DNase 1. The samples were incubated at room temperature for 15 min. The reaction was stopped using 1 µl EDTA (25 mM) and the samples were heated in a thermocycler at 65°C for 10 min. 1 µl of random hexamer primers were added to each sample. The samples were incubated at 65°C for 5 min, followed by cooling to 4°C for 1 min. The reaction was paused and a master mix was added (reagents listed in table 4). The samples were returned to the thermocycler and heated to 25°C for 10 mins, 42°C for 50 min, 72°C for 15 min and then cooled to 4°C.

Table 2.4 Master mix for PCR reaction

5X RT buffer	4 µl
0.1 M DTT	2 µl
10 µM dNTPs	1 µl
RNase Out	0.5 µl
Superscript III	0.5 µl

2.2.5 Quantitative Real-Time Polymerase Chain Reaction (RT-PCR) of mRNA levels

RNA (500 ng) was used to generate cDNA by reverse transcription using Superscript II Reverse Transcriptase enzyme (Invitrogen). Quantitative RT-PCR was performed using LightCycler 1.5 (Roche, Burgess Hill, West Sussex, UK) and QuantiTech SYBR green PCR kit (Qiagen, Crawley, West Sussex, UK). Two µl of cDNA product was added to each LightCycler glass capillary followed by 18 µl of the master mix per sample (10 µl SYBR green master mix 1 µl primer (gene-specific) and 7 µl dH_20). The PCR reaction was ran as outlined in table 5.

Table 2.5: PCR reaction for qPCR

Cycle	Target temp.	Incubation time	Temp. trans. rate
Pre-incubation	95	15 min	20 °C/sec
Amplification (40 cycles)	94	15 sec	20 °C/sec
	55	20 sec	20 °C/sec
	72	40 sec	20 °C/sec
Melting curve	94	0	20 °C/sec
	65	15 sec	20 °C/sec
	95	0	0.01 °C/sec
Cooling	40	30 sec	20 °C/sec

Table 2.6: Primers and sequences used for mRNA qPCR.

Gene name	Forward sequence	Reverse sequence
Arc	5 -'AGCAGCAGACCTGACATCCT	5 -'GTGATGCCCTTTCCAGACAT
ß-actin	5 -'AGGTGTGATGGTGGGAATGG	5 -'GGTTGGCCTTAGGGTTCAGG
c-Fos	5 -'GGAATTAACCTGGTGCTGGA	5 -'CATTCAGACCACCTCGACAA
Doublecortin	5 -'GGAGTGGGTTACATTTACACCAT	5 -'GTCTGAGGAACAGACATAGCTT
Lim Kinase 1	5 -'TTATCGGGCGTGTGAATGCA	5 -'ACCAGACAAGTGCATGGGAA
Pumilo 2	5 -'AGTCTGGCCATGTTTCACCA	5 -'AATTCAACCCAGGGCCAAGA
Serpine1	5 -'AAGCAAGCTGTGTCAAGGGA	5 -'TGGAGGGCACAACACTTCA
Creb1	5 -'TGGGGACTGGCATTTTGTA	5 -'GCAGGAGAAAGCACAGCAAA

2.2.6 Quantitative Real-Time Polymerase Chain Reaction (RT-PCR) of miRNA levels

500 ng of RNA was reverse transcribed using stem-loop Multiplex primer pools (Applied Biosystems, Dublin, Ireland). We used reverse-transcriptase-specific primers for the miRNAs of interest. 8 µl of the reaction mix described in table 7 was added to 500 ng of extracted RNA sample in a 200 µL PCR tube. Samples were incubated in the conditions listed in table 8.

Table 2.7: Master mix for miRNA reverse transcriptase reaction.

Reagent	Volume
dNTP	0.15
Multiscribe RT	1.00
10X RT buffer	1.50
RNase Inhibitior	0.19
dH20	5.16

Table 2.8: Reverse transcription incubation conditions.

RT	Time	Temperature
1	30 min	16 °C
2	30 min	42 °C
3	5 min	85 °C
4	∞	4 °C

Real-time quantitative PCR was carried out on a 7900HT Fast Realtime System (Applied Biosystems) using TaqMan miRNA assays (Applied Biosystems). 135 µl of dH_20 was added to cDNA product. Specific miRNA primer (0.5 µl) was added to cDNA product along with Taqman master mix (5 µl) and dH_20 (3.5 µl). Samples were incubated under PCR conditions listed in table 9. All samples were performed in triplicate in a 96-well plate. Ct values were measured on the 12K-Flex. U6B (Applied Biosystems miRNA assay ID 001093), U19 (Applied Biosystems miRNA assay ID 001003) and miR-124 (Applied Biosystems miRNA assay ID 480902) were used for normalisation. A relative fold change in expression of the target gene transcript was determined using the comparative cycle threshold method (2-Δ Δ C. T)

Table 2.9: Incubation conditions for PCR reaction.

PCR	Time	Temperature
1	20 s	95 °C
2	1 s	95 °C
3	20 s	60 °C
4		2-3 for 46 cycles
5	∞	4 °C

Table 2.10: Primers and sequences for miRNA targets used.

miRNA name	Sequence	Assay ID
miR-134	UGUGACUGGUUGACCAGAGGGG	001186
miR-132	UAACAGUCUACAGCCAUGGUCG	000457
U6B	CGCAAGGATGACACGCAAATTCGTGAAGCGTTCCATATTTTT	001093
RNU19	TTGCACCTCTGAGAGTGGAATGACTCCTGTGGAGTTGATCCTAGTCTGGGTGCAAACAATT	001003
miR-410	AAUAUAACACAGAUGGCCUGU	001274
miR-411	UAUGUAACACGGUCCACUAACC	002238
miR-300	UAUGCAAGGGCAAGCUCUCUUC	000191
miR-135a-5p	UAUGGCUUUUUAUUCCUAUGUGA	478581

miR-21-5p	UAGCUUAUCAGACUGAUGUUGA	482709

2.3 Protein analysis by Western blotting

2.3.1 Protein extraction

Western blotting was used to determine the levels of specific proteins in hippocampi and cortices from WT and *Ube3a* $^{(m-/p+)}$ mice. Samples for protein analysis were homogenised in lysis buffer (0.1 M NaCl, 20 nM Tris-HCL pH7.6, 1 mM EDTA pH 8.0, 1% NP-40, and protease inhibitors [Phosphatase (Vanadate, 1:1000) and protease (Aprotinin, 1:1000; Leupeptin, 1:1000; PMSF, 1:500]). 300 µL hippocampus or 600 µL cortex was added to tissue and homogenised with a plastic dounce. The protein concentration of the samples was determined using a Bicinchoninic acid assay (BCA) as described in section 2.3.2.

2.3.2 Bicinchoninic acid assay

A BCA Protein Determination Kit (life Technologies, Ireland) was used to determine the concentration of protein in hippocampi and cortices from *Ube3a* $^{m-/p+}$ mice. Protein standards of 0-14 mg/mL from a 2 mg/µL stock of bovine serum albumin (BSA) were added in triplicate to a 96 well plate. 2 µL of samples were added in triplicate. 150 µL of 0.9% NaCl (Sigma-Aldrich) was added to wells. Reagents A, B and C were made up in a 25:25:1 ratio and added to wells. The plate was incubated in a dark area for 30 minutes at room temperature. The plate was analysed at 570 nm on a microplate reader (Victor C5 Perkin Elmer 2030 Multi Label Reader, Ireland). The concentration of each sample was calculated from the protein standards. This was done by plotting the protein standards on the X-axis and the absorbance on the Y-axis. From this, linear regression was used to calculate the concentration of each sample using Y=a + bX, with X being the explanatory value and Y being the unknown concentration.

2.3.3 Gel electrophoresis

Proteins were separated by size using SDS-PAGE. Polyacrylamide stacking (4%) and resolving gels (10%) were prepared. The resolving gel was made up using dH_20; 1M Tris-HCL pH 8.8; 40% Acrlyamide; 10% SDS; 10% APS, tetramethylethylenediamine (TEMED). A layer of isopropanol was added to the surface of the resolving gel. The stacking gel was made up of dH_20; 1M Tris-HCL, pH 6.8%; 40% Acrylamide; 10% SDS; 10% APS and TEMED. Polymerized gels were placed in an electrophoresis system container (BioRad) and the tank was filled with 1X electrophoresis buffer (250 mM glycine; 25 Mm Tris-HCL, pH 8.3; 0.1% SDS). Samples of known concentrations were denatured by heating at 95°C for 5 minutes. Samples were loaded into the gel and 120 V was applied to the system for roughly 1.5 h until the samples reached the end of the glass.

2.3.4 Protein transfer and immunoblotting

Proteins were transferred to a polyvinylidene difluoride (PVDF) membrane (following activation by methanol) or to a nitrocellulose membrane, using the TurboBlot semi-dry transfer system in 1 X semidry transfer buffer [25 mM Tris-Base, 192 mM glycine, 20% methanol (Sigma-Aldrich)]. Membranes were blocked in 5% milk in TBS with 0.5% Tween-20 (TBS-T) for 1 h at room temperature. Membranes were incubated in primary antibodies made up in 5% milk in TBST overnight at 4°C or for two hours at room temperature. Membranes were washed in TBS-T 5 times for 5 minutes. Then, membranes were incubate with appropriate secondary antibodies in 5% milk in TBS-T for 2 h at room temperature. Membranes were washed in TBS-T 5 times for 5 minutes. Membranes were immersed in a chemoluminescence substrate (Millipore, Ireland) mixed in a 1:1 ratio. Proteins were visualized using the Fujifilm LAS-4000. Finally, to determine equal loading of samples, blots were washed and re-incubated as described above in a loading control antibody.

Table 2.11: Table of antibodies used for western blotting.

Antibody	Type	Dilution	Manufacturer	Catalog no.
ß-Actin	Mouse	1:1000	Sigma	A5441
GapDH	Mouse	1:1000	ThermoFisher Diagnostics, UK	AM4300
E6AP/UBE3A	Rabbit	1:500	Bethyl Laboratories	A300-352A
Limk1	Rabbit	1:500	Cell signalling	38425
Creb1	Mouse	1:500	Santa Cruz	SC-271
DCX	Goat	1:500	Cell signalling	4604S

2.4 Fluoro-Jade B staining

C57 P21 mice were perfused with ice-cold PBS and the brains were fresh frozen in 2-methylbutane (at −80°C), and 30 µm in the coronal plane (CM1900 cryostat, at 12 Leica) and placed on a glass slide. Frozen tissue was fixed, dehydrated and transferred to a 0.06% potassium permanganate solution for 15 minutes. Sections were placed into a 0.001% FJB staining solution (in 0.1% acetic acid) for 30 minutes and rinsed in distilled water followed by histoclear solution. Slides were mounted using DPX mounting medium (Sigma Aldrich, Poole, UK) and examined using a Leica DM4000 microscope. FjB positive cells were counted for individual hippocampal sub-fields (CA1, CA2, CA3 and DG) for each section and an average was taken from three sections per mouse.

2.5 Small RNA sequencing

All of the sequencing was done by Dr. Gary Brennan. This included extraction of RNA from samples, library preparation and sequencing.

2.5.1 Preparation of small RNA libraries

P21 naïve AS F1 or N4 mice were perfused with PBS and brains were micro-dissected. The right hippocampus was used for sequencing. Twenty mice from each generation were used (n=40), including an even distribution of genotype and gender, including an even distribution of genotype and gender (n=5/experimental group), as per table 5.1. Small RNA libraries were prepared using the Illumina TruSeq small RNA Library Prep Kit according to the manufacturer's protocol. Reagents and samples were kept on ice at all times.

Table 2.12: List of samples from both generations of mice used for small RNA sequencing

Generation	Genotype	Gender
F1	WT	Male n=5
	WT	Female n=5
	AS	Male n=5
	AS	Female n=5
N4	WT	Male n=5
	WT	Female n=5
	AS	Male n=5
	AS	Female n=5

2.5.2 Adapter Ligation

1 µL of RNA 3' Adapter was added to 5 µL RNA, centrifuged and incubated at 70°C for 2 min. 2 µL of Ligation Buffer, 1 µL of RNase Inhibitior, 1 µL of truncated T4 RNA Ligase 2 (NEB, UK) were mixed and briefly centrifuged. 4 µL of this was added to the samples and incubated for 28°C for 1 h. 1 µL of Stop Solution was added to the samples and incubated for 15 min at 28°C. 1.1 µL of RNA 5' Adapter was added and incubated at 70°C for 2 min. Finally, 1.1 µL of ATP and 1.1 µL of T4 RNA ligase were added. 3 µL of this mix was added to the samples and incubated at 28°C for 1 h.

2.5.3 Reverse Transcription

25 mM dNTPs were diluated to 12.5 mM by mixing in a 1:1 ration in water. 1 µL of RNA RT primer was added to 3' adapt-ligated RNA and incubated at 70°C for 2 min. A mastermix was prepared by mixing 2 µL of 5X First Strand Buffer, 0.5 µL of 12.5 mM dNTP mix, 1 µL 100 mM DTT, 1 µL RNase Inhibitor and 1 µL of SuperScript II Reverse Transcriptase (Invitrogen, Ireland). 5.5 µL of this mix was added and samples were incubated at 50°C for 1 h.

2.5.4 Polymerase Chain Reaction

In the amplification step, the following mix was prepared: 8.5 µL dH_20, 25 µL of PCR Mix, 2 µL of RNA PCR primer, 2 µL of RNA PCR Primer Index. 37.5 µL of this was added to the RT sample. The index added to each sample was noted. Samples were incubated under the listed PCR conditions.

2.5.5 Size selection

For purification, small RNA libraries were separated by electrophoresis on Pipping Prep (Sage Science, US) using a 3% agarose gel cassette (Lab Tech, UK), selecting for RNA in the size range of 90-250 bp (adapted-ligated miRNA). Loading solution was added and samples were vortexed. 40 µL of buffer from the sample well was removed and replaced with 40 µL of the sample. Samples were then electrophoresed through the gel and eluted. 40 µL of size-selected samples were removed from the well and concentrated using sodium acetate (Invitrogen, Ireland) and resuspended in 9 µL of 10 mM Tris-HC pH8.5 (Sigma-Aldrich, Ireland).

2.5.6 Small RNA sequencing

To obtain an accurate reading of concentration, 2 µL of concentrated library was loaded into a Qubit (Thermo Fisher Scientific, Ireland). The High sensitivity dsDNA kit was used (Thermo Fisher Scientific, Ireland). According to the concentration values, 2 nM library stocks were prepared and 5 µL of each were pooled together. 0.2 M NaOH was added to the pooled and concentrated cDNA library. These samples were

incubated for 5 min. Then, HT1 buffer (Illumina, UK) was added to the samples. 20 pM PhiX (Illumina, UK) library was diluted in HT1 buffer. The diluted library was then added to the PhiX solution. Samples were loaded onto the MiSeq 50 cycle cartridge and run on the Illumina MiSeq. The total number of reads for the 40 samples was 52.6 million reads for 37 samples as three samples failed for sequencing. 84 miRNAs were detected for each of the four groups of samples.

2.6 Data analysis

Statistical analysis was performed using GraphPad Prism (version 5). A probability of $p<0.05$ was considered significant. Data were tested for normality using Shapiro-Wilk test. Data that passed the normality test were analysed with either two-tailed Student *t*-test or one-way ANOVA with Bonferroni *post-hoc* test, as appropriate, and presented as mean ± S.E.M. Data with multiple testing phases was tested using a two-way repeated measures ANOVA. Data with non-Gaussian distribution were tested with Mann-Whitney U test or Kruskal-Wallis test with Dunn's *post-hoc* test and presented as median ± interquartile range. Grubbs test was used to identify significant outliers. Analysis of the Racine scale was performed by Prof. Ronan Conroy using Stata 16.1

Table 2.13: List of materials

Reagent	Manufacturer	Catalog number

2-methylbutane	Sigma-Aldrich	M32631
40% Acrylamide	Sigma-Aldrich	A7168
Agarose	Sigma-Aldrich, UK	A2576-25G
Bovine serum albumin (BSA)	Fisher Scientific	BP9700-100
Chloroform	Sigma-Aldrich	372978
DPX mounting medium	Sigma-Aldrich	6522
EDTA	Sigma-Aldrich, UK	3660
Ethanol	Sigma-Aldrich, UK	51976
Fluoro-jade B	Chemicon	AG310
Glyco-blue Coprecipitant	Invitrogen	AM9516
Histoclear solution	National diagnostics	HS-202
Isoflurane	Isoflurin	-
Isopropanol	Sigma-Aldrich	19-076-4
Kainic acid (KA)	Sigma-Aldrich	K0250
KAPA2G Fast genotyping mix	Kapa Biosystems	KR0385
Lorazepam	Ativan	
Multiscribe RT buffer	Thermo Fisher Scientific	4311235
NP-40	FLuka	74385
Paraformaldehyde	Thermo Fisher Scientific	AAJ19943K2
Percoll	Sigma-Aldrich	EO414
Phenobarbitol	Pharma	-
Phosphate buffered saline (PBS)	Sigma-Aldrich	SLBV2666
Pierce BCA Protein Assay Kit	Thermo Fisher Scientific	23225
Ponceau S solution	Sigma-Aldrich	P7170
Potassium permanganate	Fluka	60459
Pentylenetetrazol	Thermo Fisher Scientific	P6500
RNase out inhibitor	Thermo Fisher Scientific	10777019
Sodium chloride	Sigma-Aldrich	7647-14-5
Sodium dodecyl sulphase (SDS)	Sigma-Aldrich	L3771
SuperScript ™ II Reverse Transcriptase	Thermo Fisher Scientific	18064014
T4 RNA Ligase 2	New England Biolabs	M0242S
TaqMan MicroRNA Reverse Transcription Kit	Thermo Fisher Scientific	4366597
TaqMan[a] Fast Advanced Master Mix	Thermo Fisher Scientific	4444963
Tetramethylethylenediamine (TEMED)	Sigma Aldrich	T9281
Trizol reagent	Ambion	15596018
Tween-20	Sigma	9005-64-5
ß-mercaptoethanol	Sigma Aldrich	M6250

3 Chapter three

Results I

3.1 Introduction

Seizures in infants and children are one of the most common neurological emergencies and around 5% of children will have a seizure (Hauser, 1994). Status epilepticus (SE) is a prolonged seizure that has an incidence of 17-23 per 100,000 children (Chin et al., 2006, Raspall-Chaure et al., 2007), and a 16% mortality rate (Singh and Gaillard, 2009). Seizures at an early age may trigger significant developmental impairment and can result in an increased risk of developing epilepsy later in life (Maytal et al., 1989, Raspall-Chaure et al., 2006). Frontline seizure control is with anti-epileptic drugs (AEDs) and acute administration of anticonvulsants. Despite the availability of more than 20 different AEDs, over 20% of children remain refractory (Wirrell, 2013, Rosati et al., 2015). Furthermore, benzodiazepines are ineffective in controlling SE in almost 50% of cases (Lewena et al., 2009, Abend et al., 2014). Thus, there is a major unmet clinical need for new therapeutic approaches to treat paediatric seizures and protect the immature brain.

Various miRNAs have been identified to have a role in normal brain development and function (Kosik, 2006). Dysregulation of miRNAs has been implicated in the pathogenesis of a number of neurological diseases, including epilepsy (Henshall et al., 2016). Accordingly, miRNAs have emerged as important new treatment targets (Saugstad, 2010, Eacker et al., 2009, Henshall et al., 2016). Among these, miR-134, a brain-enriched miRNA, has been found to be upregulated in the hippocampus of children (Peng et al., 2013b) and adults (Jimenez-Mateos et al., 2012) with mesial temporal lobe epilepsy (MTLE), and increased in the same brain structures following experimentally-induced seizures in rodent models (Jimenez-Mateos et al., 2015, Jimenez-Mateos et al., 2012, Peng et al., 2013b, Morris et al., 2018, Reschke et al., 2017a). The potent *in vivo* anti-seizure effects of Ant-134 have only been demonstrated in adult models of epilepsy (Jimenez-Mateos et al., 2012, Jimenez-Mateos et al., 2015) (Reschke et al., 2019, Reschke et al., 2017a). Given that miR-134 is also dysregulated in children with epilepsy (Peng et al., 2013b), we hypothesized that targeting miR-134 using Ant-134 could protect against seizures in the immature brain.

3.1.1 Hypothesis:

Levels of miR-134 will be increased after induction of SE and pre-treatment with Ant-134 in P21 mice will have seizure suppressive effects in a model of SE.

3.1.2 Aim:

The first part of this project was to develop a mouse model of paediatric SE using systemic kainic acid. Next, we sought to find a suitable dose of Ant-134 that would have seizure protective effects in this model.

3.1.3 Methods

Seizure induction: SE was induced in 21 day-old C57 male mice by systemic injection of 5 mg/kg kainic acid. Intracerebroventricular injection of an antisense oligonucleotide (antagomir) was injected in P21 mice and SE was induced 24 h later. **EEG analysis:** The severity of seizures was analysed by total power of ictal activity. **Cell death**: Fluoro Jade B (FJB) staining was used to analyse cell death in the hippocampus. **Molecular analysis**: RT-qPCR was used to analyse the expression of miR-134 over the developmental period and in P21 mice are SE. Ago2 immunoprecipitation was used to determine the levels of functional miR-134.

3.2 Results

3.2.1 miR-134 expression in mouse brain during postnatal development

We first sought to establish the expression of miR-134 during normal postnatal brain development in mice (P7, P14, P21, P28) compared to the levels in the P42 brain. Analysis of mature miR-134 expression over the postnatal period, using total RNA extracted from tissue homogenates, found a miR-134 levels varied the most in the youngest brain samples, becoming more consistent thereafter (Fig 3.1). A slight decrease in hippocampal miR-134 levels occurred during development (Fig 3.1 A, $p<0.05$). Cortical miR-134 expression varied over development (Fig 3.1 A, $p<0.05$) with a significant decrease between P14 and P21. Again, inter-animal variability tended to be greater in younger mice. Due to the known enrichment of miR-134 in dendrites (Schratt et al., 2006) we also explored whether any developmental differences were evident in this compartment by analysing synaptically-enriched fractions from pooled hippocampi of mice. As expected, miR-134 levels were increased in the synaptoneurosomes in comparison to whole cell readouts. However, synaptic miR-134 expression did not vary significantly over development (Fig 3.1 B, $p>0.05$). These findings suggest that miR-134 expression in the mouse brain can vary during the post-natal period in certain subcellular compartments.

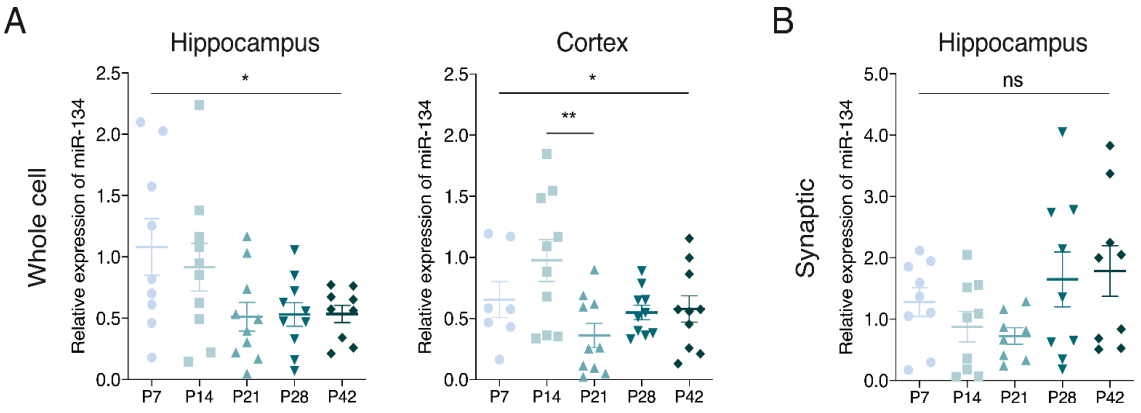

Figure 3.1: Expression of miR-134 in naïve brain over the developmental period P7-P42
The relative expression of miR-134 was analysed over the developmental period in whole hippocampi and cortices, and in hippocampi following a synaptoneurosome extraction. **(A)** Overall miR-134 levels in naïve hippocampus and neocortex and following standard RNA extraction n=10/group. One-way ANOVA with Bonferroni *post hoc* shows an overall change of levels of miR-134 over developmental period following standard RNA extraction (p=0.03 and p=0.013, for hippocampus and cortex, respectively) with a significant decrease in cortex between P14 and P21 (p=0.0063). **(B)** Synaptic miR-134 levels in hippocampus. Two hippocampi were pooled to make up each experimental number (n=9 per group, p=0.11). U6b was used as a normaliser.

3.2.2 Characterisation of kainic acid-induced seizures in P21 mice

To model seizures in the developing brain, P21 mice were implanted with electrodes and given a systemic (IP) injection of kainic acid (KA), 5 mg/kg and 7.5 mg/kg, based on previous studies (Kukko-Lukjanov et al., 2012),(Ravizza et al., 2005). An illustration of the electrode placing can be seen in Fig 3.2 A. A representative trace of electrographic activity from each dose is presented inFig 3.2 B. During preliminary dose range-finding studies, 7.5 mg/kg KA caused robust and reproducible seizures (Fig 3.2 C&D), but also mortality within 24 h (3 of 3 mice tested). This dose was therefore discontinued. The median seizure onset after 7.5 mg/kg KA was 239 seconds (Interquartile range [IQR]: 112.9-331.6 seconds; Fig 3.2, C) and total EEG power was increased to 613% (median; IQR: 59.3-851.9%) from the baseline recordings (Fig 3.2 D). A reduced dose of KA (5 mg/kg) resulted in reliable induction of SE (Figure 3.2 C&D) with low mortality (in 1 of 4 mice tested). Mice that received 5 mg/kg KA developed the first electrographic seizure after 325 seconds (IQR: 256.3-369.6; Fig 3.2 C), and had total EEG power of 306% (IQR: 185.3-402.2%) baseline (Fig 3.2 D). We did not see any significant differences between electrographic activity elicited by 5 mg/kg or 7.5 mg/kg KA (Fig 3.2 D, $p<0.05$).

We next assessed whether the seizures in this model induced brain damage. Fluoro-Jade B (FJB) staining of brain tissue sections obtained 24 hours after SE induced by 5 mg/kg KA revealed typical patterns of KA-induced neuronal death in the hippocampus, primarily in the CA3 subfield (Fig 3.2 E). While always present, the extent and distribution of damage varied between hippocampal hemispheres, as expected after a systemic administration of KA (McCord et al., 2008). Taken together, these results support the induction of SE in P21 mice by 5 mg/kg IP KA as a reliable model to functionally study seizures in the immature brain.

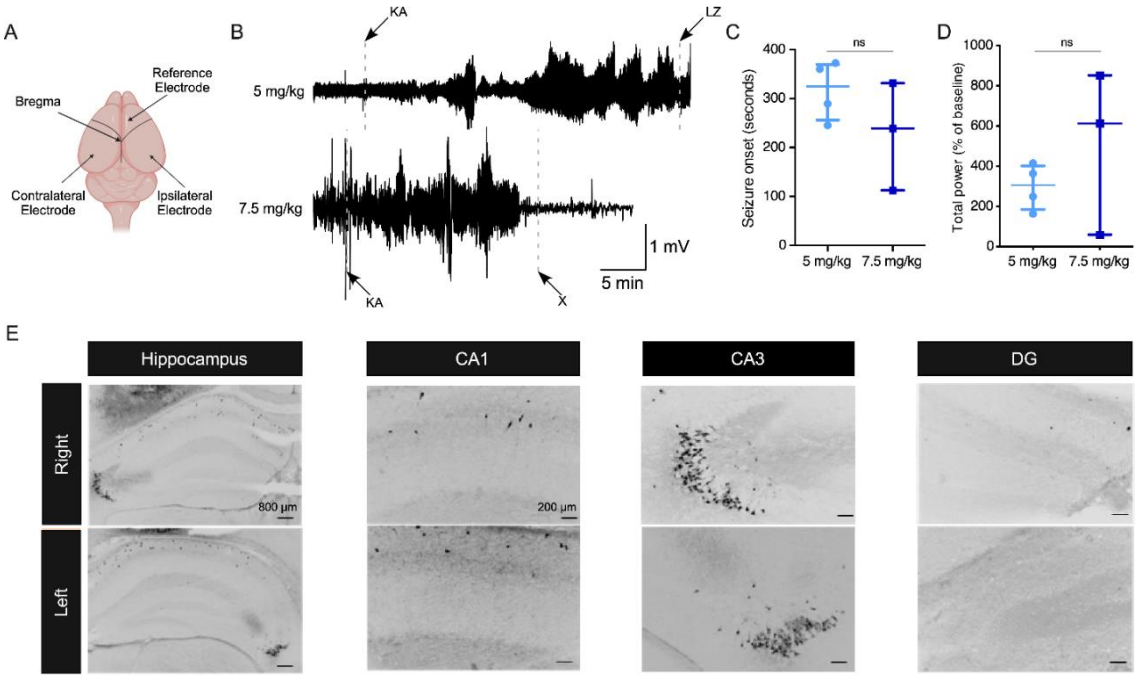

Figure 3.2: KA dose selection for the induction of SE in P21 mice.
P21 mice were injected with 5 mg/kg or 7.5 mg/kg of KA to determine a suitable dose to induce reproducible SE. **(A)** Schematic of electrode placement in P21 mouse brain. **(B)** Representative EEG traces for mice injected with 5 or 7.5 mg/kg KA (KA - KA injection, LZ - lorazepam injection, X - mouse died). **(C)** Graph shows no difference in onset to first electrographic seizure after the IP injection of 5 mg/kg or 7.5 mg/kg of KA n=3-4/group, p=0.23). **(D)** Graph shows no difference in % of increase in EEG total power, relative to baseline, recorded over the 30 minutes after KA injection n=3-4/group, p=0.63). **(E)** Representative images of FJB staining show neuronal death at 24h post SE (5 mg/kg KA) in the right and left hippocampi of a P21 mouse.

3.2.3 miRNA levels following kainic acid-induced seizures in P21 mice

We next explored whether SE induced by systemic KA altered the expression of miR-134 in P21 mice. RT-qPCR analysis of hippocampal and cortical samples obtained 4, 24 or 72 h after SE revealed no significant changes in mature miR-134 levels at any time point (Fig 3.3 A, B & D $p>0.05$). To confirm that subtle changes in the functional miRNA pool were not missed in the total miRNA analyses, we measured levels of miR-134 at 24 h after SE associated with Ago2, which guides the miRNA silencing complex to target mRNAs (Flores et al., 2014). Ago2 was immunoprecipitated from mouse hippocampus after seizures and bound miRNA was eluted and quantified. Again, no changes were observed in the level of Ago2-bound miR-134 in samples 24 h after SE (Figure 3.3 C, $p>0.05$). Together, these findings suggest that systemic KA-induced seizures in P21 mice do not change overall levels or the functional pool of miR-134 within affected brain structures.

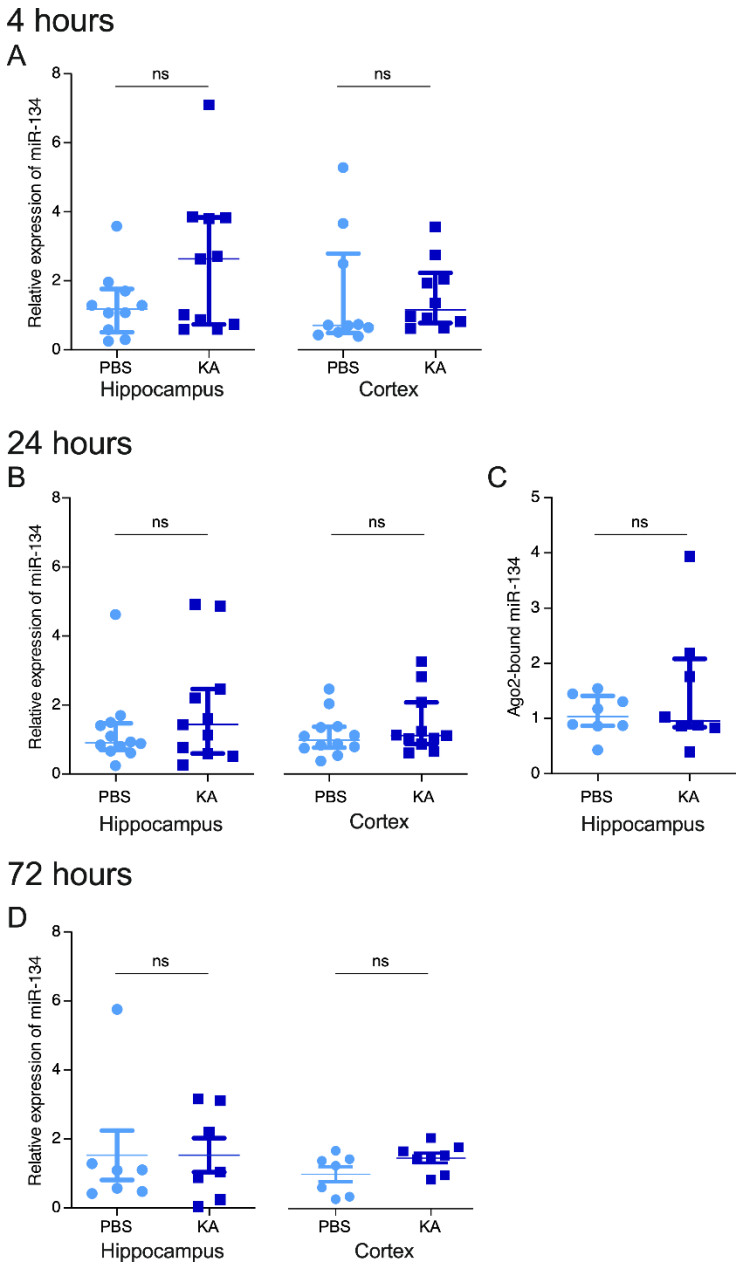

Figure 3.3: Systemic KA does not alter miR-134 expression in P21 mice.
Graphs show RT-qPCR analysis of miR-134 expression in hippocampal and cortical lysates at different time points after systemic KA injection, with counts normalised to U6B. **(A)** Overall miR-134 expression at 4 hours, n=10-11/group; hippocampus p=0.22; cortex P = 0.32. **(B)** Overall miR-134 expression at 24 hours, n=11-12/group; hippocampus p=0.45; cortex P=0.45. **(C)** Ago2-bound miR-134 in hippocampus at 24 hours n=8/group; p=0.88. **(D)** miR-134 expression at 72 hours, n=7/group; hippocampus p=0.99, cortex p=0.088 [*t*-test]). Data did not pass normality. A Mann-Whitney U test was used for analysis between PBS and KA injected mice. Data are expressed as median and interquartile range.

3.2.4 Ant-134 has dose-dependent protective effects against kainic acid-induced seizures in P21 mice

Since upregulation of miR-134 is not a pre-requisite for Ant-134 to have anti-seizure effects (Reschke et al., 2017a), we proceeded to test whether reducing levels of miR-134 could protect against seizures in the model. We first sought to establish an appropriate effective dose of Ant-134 to lower miR-134 levels in P21 mice. Previous work in adult mice found that ICV injection of 0.1 nmol Ant-134 reduced miR-134 levels by approximately 90% within 24 h and resulted in mice being strongly refractory to seizures induced by intra-amygdala KA (Jimenez-Mateos et al., 2012). Here, we ICV injected P21 naïve mice with 0.05, 0.1 or 0.5 nmol Ant-134 and assessed miR-134 silencing 24 h later (Figure 3.4 A, $p<0.01$). Ant-134 caused a dose-dependent knockdown of miR-134 (Fig 3.4 A, $p<0.01$). Injection of 0.05 nmol Ant-134 produced only variable and non-significant knockdown of miR-134 (Fig 3.4 A, $p>0.05$). In contrast, 0.1 nmol Ant-134 significantly reduced miR-134 levels to ~65% of scramble (Fig 3.4 A, $p<0.05$). Injection of 0.5 nmol Ant-134 produced a near-complete reduction in miR-134 levels in the hippocampus of P21 mice (Fig 3.4 A, $p<0.01$).

We next assessed the effects of inhibiting miR-134 levels on seizures induced by systemic KA in P21 mice. Mice received ICV injections of Ant-134 and were then subject to KA-induced SE 24 h later. As expected, mice injected with 0.05 nmol Ant-134 experienced similar seizures to control animals injected with a scrambled (Fig 3.4 B&C). In contrast, mice pre-treated with 0.1 nmol Ant-134 displayed a significant delay to the first electrographic seizure (Fig 3.4 Ci, $p<0.05$). Moreover, four out of five mice that received 0.1 nmol Ant-134 did not develop full SE during the 30-minute recording period (Fig 3.4 Cii). There was also a strong trend for a decrease in seizure burden time in 0.1 nmol Ant-134 mice in comparison to Scr mice (Fig 3.4 Ciii, $p>0.05$). Mice also presented reduced severity, as assessed by total EEG power (Fig 3.4 Civ, $p>0.05$), though this was not significant. At the highest tested dose, 0.5 nmol Ant-134, mice were not protected against KA-induced seizures (Fig 3.4 B&C) and high mortality (100%) was observed. These

results suggest a narrow tolerance for miR-134 inhibition when KA seizures are induced in P21 mice.

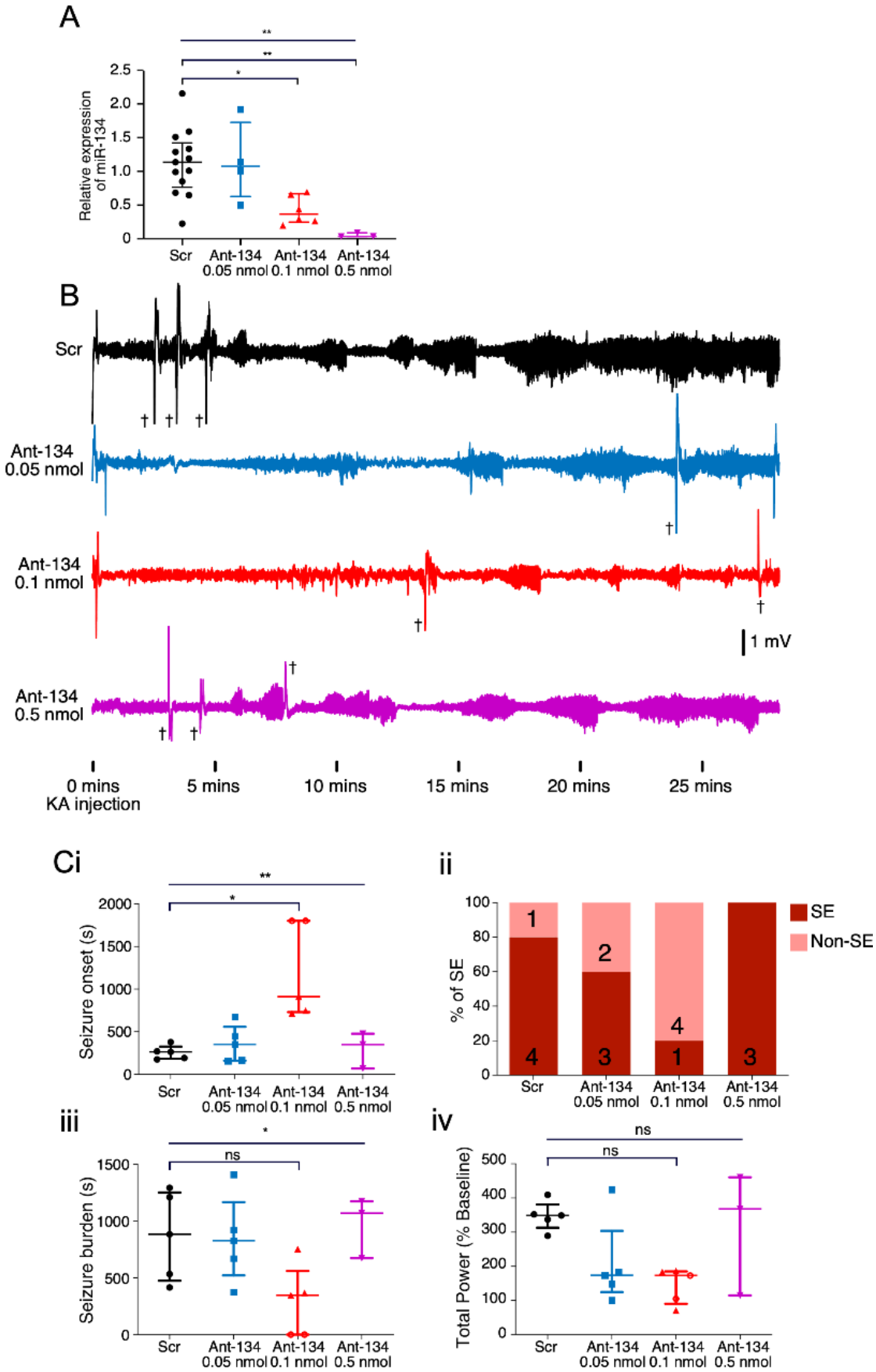
A
Relative expression of miR-134
Scr
Ant-134 0.05 nmol
Ant-134 0.1 nmol
Ant-134 0.5 nmol
B
Scr
Ant-134 0.05 nmol
Ant-134 0.1 nmol
Ant-134 0.5 nmol
1 mV
0 mins KA injection
5 mins
10 mins
15 mins
20 mins
25 mins
Ci
Seizure onset (s)
ii
% of SE
SE
Non-SE
iii
Seizure burden (s)
iv
Total Power (% Baseline)

Figure 3.4: Protective effects of Ant-134 on SE severity in P21 mice

A dose ranging study was performed in P21 mice to determine which dose had seizure suppressive effects. **(A)** Dose-dependent knockdown of miR-134 24 hours after Ant-134 injection, Scr n=13, 0.05 nmol Ant-134 n=4, 0.1 nmol Ant-134 n=6 and 0.5 nmol Ant-134 n=3, p=0.002. **(B)** Representative EEG traces from mice pre-treated with 0.05, 0.1 or 0.5 nmol Ant-134 in 2 µL PBS, or scramble control. Traces shown begin at the time of KA injection. **(Ci)** Dose-dependent effects of Ant-134 on seizure onset, n=5 per group [Scr,0.05 nmol,0.1 nmol] or n=3 [0.5 nmol]). 0.1 nmol Ant-134 increased time to seizure onset after KA injection, p=0.013. **(Cii)** % of SE induction in mice pre-treated with Scr/Ant-134. **(Ciii)** Total time spent in seizures as analysed by electrographic seizure, p<0.05. **(Civ)** Seizure severity as analysed by total EEG power % of baseline, p>0.05. † - Artefacts caused by injections in other mice recorded simultaneously. Open circles represent mice which did not experience any seizure activity. Seizure onset was assigned a maximum value of 1800s for statistical purposes. U6b was used as a normaliser.

3.2.5 0.1 nmol Ant-134 reduces seizure severity and protects against the induction of SE

To substantiate the seizure suppressive effects of Ant-134 at the 0.1 nmol dose, we independently validated the initial findings in a second cohort, using a different batch of Ant-134. As before, ICV injection of 0.1 nmol Ant-134 resulted in delayed seizure onset when P21 mice were exposed to KA the next day (Fig 3.5 Bi, $p<0.01$). Similarly to the results obtained above, five out of seven mice did not present full SE during the recording period (Fig 3.5 Bii). Further, we observed significant reductions in seizure burden (Fig 3.5 Biii, $p<0.01$. There was also a reduction in total EEG power after KA injection (Fig 3.5 Biv; $p<0.01$), confirming that the pre-treatment with 0.1 nmol Ant-134 has seizure-suppressive effects in this model of paediatric SE.

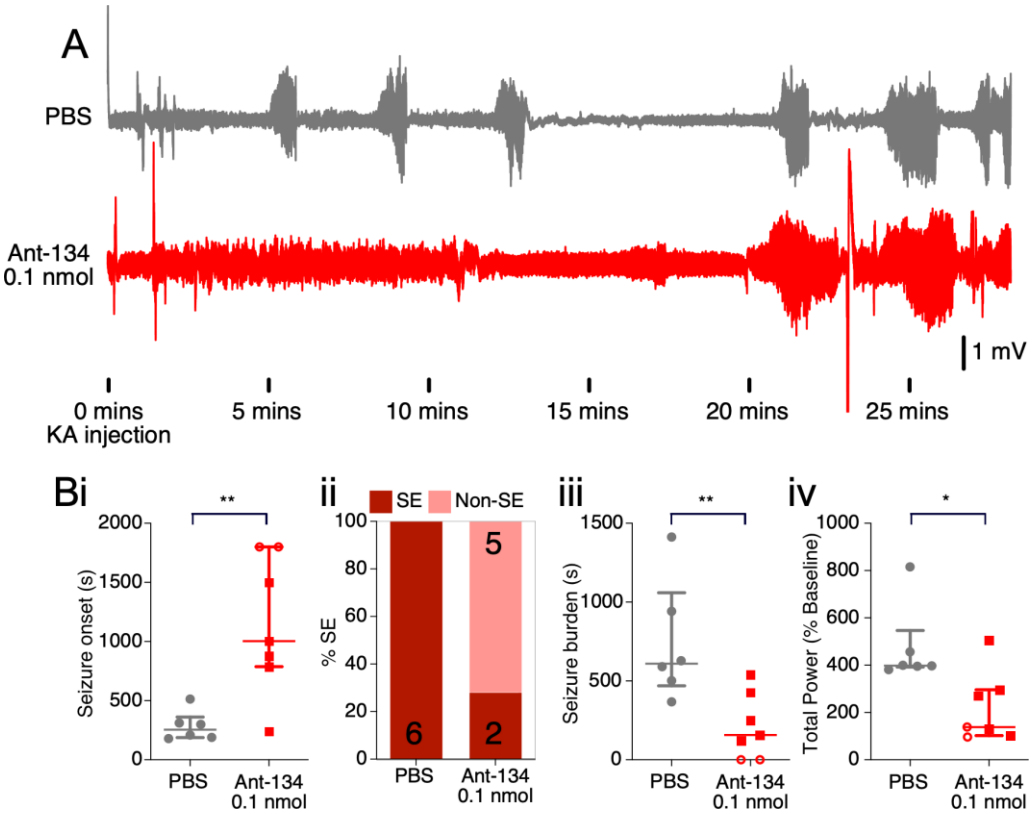

Figure 3.5: Ant-134 reduces severity of seizures and protects against SE
(A) Representative EEG traces following pre-treatment of 0.1 nmol Scr/Ant-134 and 5 mg/kg of KA, EEG trace starts at the time of KA injection **(Bi)** Seizure onset time in mice pre-treated with Scr/Ant-134, 0.1 nmol Ant-134 delayed seizure onset PBS n=6, Ant-134 n = 7, $p<0.01$. **(Bii)** % of mice that went into SE in 30 minute period. **(Biii)** Total seizure burden time, $p<0.01$. **(Biv)** Total power of seizures over 30 minute period, $p<0.05$. Open circles represent mice which did not experience any seizure activity. Seizure onset was assigned a maximum value of 1800s for statistical purposes.

3.2.6 Neuroprotective effects of Ant-134 in P21 mice

Finally, we assessed the effect of 0.1 nmol Ant-134 on neuronal death following SE in P21 mice. SE induced by 5 mg/kg KA caused neuronal death in the ipsilateral and contralateral CA3 region of the hippocampus 24 h later (Fig 3.6 A). P21 mice pre-treated with 0.1 nmol of Ant-134 presented significantly reduced neuronal death in the hippocampus relative to Scr-injected mice (Fig 3.6 A&B, $p<0.01$). The neuroprotective effect was most pronounced in the hippocampus ipsilateral to Ant-134 injection (Fig 3.6 A). Patterns of protection in the hippocampus were variable, however. In some cases, the CA3 subfield was entirely protected by 0.1 nmol Ant-134 pre-treatment. We also confirmed that miR-134 knockdown by 0.1 nmol Ant-134 persisted after SE (Fig 3.6 C $p<0.05$). Taken together, these data show first evidence that a fine-tuned knockdown of miR-134 by Ant-134 can protect against chemoconvulsant-induced SE and subsequent neuronal death in the developing brain.

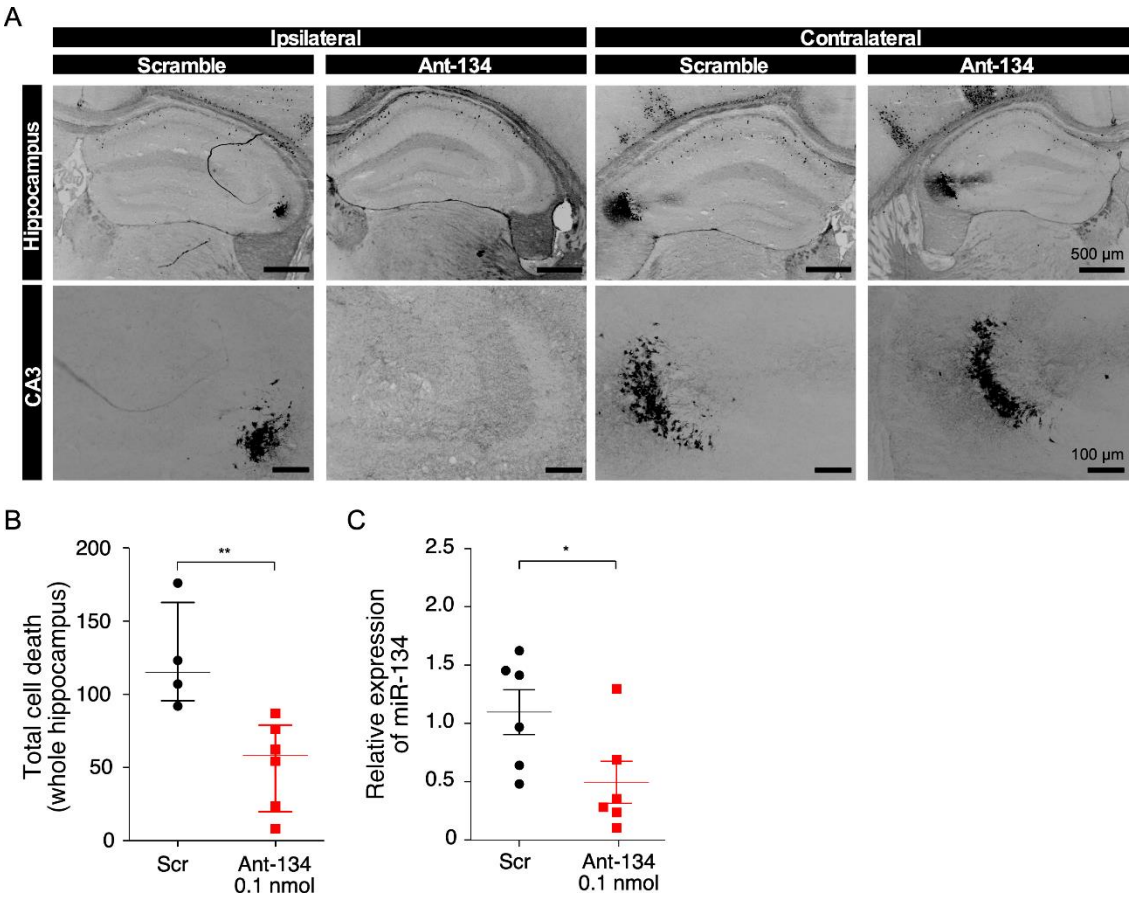

Figure 3.6: Neuroprotective effects of Ant-134 in P21 mice

Pre-treatment with 0.1 nmol Ant-134 had neuroprotective properties in the hippocampus. **(A)** Representative FJB-stained images show neuronal death in the hippocampus 24 h after SE ipsilateral and contralateral to pre-treatment with 0.1 nmol Ant-134 or scramble. **(B)** The number of FJB-stained cells was reduced in mice pre-treated with Ant-134, Scr n=4, Ant-134 n=6, $p<0.01$, data are expressed as median interquartile range. **(C)** Partial knockdown of miR-134 levels was retained 24 h after SE in the hippocampus of mice that were pre-treated with 0.1 nmol Ant-134 Scr n=4, Ant-134 n=6, $p<0.05$, data are expressed as standard error mean.

3.3 Discussion

Targeting miR-134 has been reported to have potent anti-seizure effects in the adult rodent brain (Jimenez-Mateos et al., 2012, Reschke et al., 2017a). The present study shows that inhibition of miR-134 using antisense oligonucleotides can protect against seizures and hippocampal damage in a model of SE in P21 mice. ICV injection of 0.1 nmol Ant-134 delayed the onset of the first seizure, reduced the overall seizure severity and attenuated neuronal death after systemic KA. In addition, we report the hippocampal and cortical expression of miR-134 in mice over the developmental period from birth to adulthood and investigate the effects of seizures on miR-134 levels in the model. Together, these results are proof-of-concept that silencing miR-134 can mediate anti-excitability effects in the immature brain.

There remains a major unmet need for novel approaches to treat seizures and prevent the epileptogenic effects of SE in the brain. MiRNAs have emerged as important regulators of the gene expression landscape underlying brain structure and function and their targeting, particularly using antisense oligonucleotides, has emerged as a promising therapeutic strategy for seizure control and disease modification (Henshall et al., 2016). The main focus to date, however, has been on targeting miRNAs in the adult brain (Jimenez-Mateos et al., 2012, Henshall et al., 2016, Reschke et al., 2017a). Inhibition of miR-134 has been shown to suppress evoked and spontaneous seizures in adult rodents (Jimenez-Mateos et al., 2012, Reschke et al., 2017a). Expression of miR-134 has also been reported to be increased in brain tissue following SE in immature rodents and in resected brain samples from children with MTLE (Peng et al., 2013b). The present study is the first to functionally test whether inhibiting miR-134 *in vivo* can reduce seizures in the immature brain.

Here we show that inhibiting miR-134 using an antisense oligonucleotide, termed Ant-134, reduced seizures induced by systemic KA injection in P21 mice, a model of paediatric SE. While there remain challenges with how to age-match rodent to human brain development, the P21 mouse is likely to correspond to approximately 2.3 human years (Dutta and Sengupta, 2016, Selemon, 2013). This is an important period of brain

maturation, during which time there is significant synaptic pruning and synaptogenesis in both humans (Selemon, 2013) and mice (Koss et al., 2014, Kim et al., 2015). The model we used was adopted from previous work in mice (Kukko-Lukjanov et al., 2012) and rats (Ravizza et al., 2005) and we observed similar electrographic seizure activity during SE, comprising mainly bi-lateral electrographic seizures that started within a few minutes of KA injection and continued thereafter, consistent with SE. We also observed bi-lateral damage to the hippocampus in the model. Together, this provides an age-appropriate model for an initial screen for potential anti-seizure effects of Ant-134.

The most important finding of the present study was that pre-treating P21 mice with an antagomir targeting miR-134 resulted in significant protection against KA-induced seizures. Antagomir-treated mice displayed a delay to first seizure and reduced total EEG power, a measure of seizure severity. This matches the effects of Ant-134 in studies in which seizures were evoked in adult mice using intraamygdala KA (Jimenez-Mateos et al., 2012) , pilocarpine (Jimenez-Mateos et al., 2015) and pentylenetetrazol (Reschke et al., 2017a). Our findings are also consistent with *in vitro* work that showed Ant-134 delays epileptiform activity in brain slices from rats (Jimenez-Mateos et al., 2012). The anti-seizure effects of Ant-134 were most evident at a dose of 0.1 nmol which is within the same range found to have seizure suppressive effects in adult mice (Jimenez-Mateos et al., 2012). Thus, inhibition of Ant-134 produces broad model and age-independent anti-seizure effects. Ant-134 appears to have a superior anti-seizure effect when compared with another microRNA targeting strategy in juvenile rodents, where over-expression of miR-146a in P21-P28 rats only increased the latency to SE by roughly 20% in a lithium-pilocarpine model (Wang et al., 2018).

The anti-seizure effects of Ant-134 were apparent despite the observation that miR-134 was not upregulated following SE in P21 mice. This result was unexpected since increases in miR-134 levels have been reported in several animal models of SE (Jimenez-Mateos et al., 2012) and in children with MTLE (Peng et al., 2013b) . These differences may relate to model, timing or method of tissue or miR-134 analysis. For example, the seizures produced by the dose of systemic KA we used in P21 mice may be more

generalised or lower intensity compared to those generated by either intraamygdala KA (Jimenez-Mateos et al., 2012) or systemic pilocarpine (Peng et al., 2013b, Jimenez-Mateos et al., 2015). Thus, seizures in this model do not appear to elicit transcription or maturational changes to miR-134 levels. Since miRNA processing activity is stimulated by synaptic activity, it is possible that maturation differences in pathways such as those mediated by NMDA receptors (Sambandan et al., 2017) could explain the failure of seizures to elicit changes in mature miR-134 levels. Our findings complement other reports that upregulation of miR-134 is not necessary for anti-epileptogenic actions of Ant-134 (Reschke et al., 2017a). Together, these findings demonstrate that upregulation of miR-134 is not a pre-requisite for the anti-seizure effects of Ant-134 in immature mice, broadening the range of anti-seizure therapeutic applications.

We observed significant neuroprotection in mice given 0.1 nmol Ant-134 before SE. This was mainly within the vulnerable CA3 subfield of the hippocampus and was most evident ipsilateral to the side of Ant-134 injection. Because the anti-seizure effects were observed bi-laterally, this suggests a potential specific effect that might be local dose-dependent. Indeed, while the neuroprotection was likely to be secondary to the reduced severity of SE in the model, direct neuroprotective effects of inhibiting miR-134 have been reported *in vitro* (Jimenez-Mateos et al., 2012), a model for immature brain circuits. Further studies will be needed to separate potential direct from indirect neuroprotective effects of Ant-134 in this model.

A caveat of the approach we took for delivery of Ant-134 was to pre-treat mice 24 h before SE to determine how lowered miR-134 levels affect SE onset and development. This was necessary because antagomirs take at least 12 h to produce noticeable reductions in miRNA levels in the mouse hippocampus and then a further period of time must elapse for any targets to be de-repressed for a phenotype to emerge (Jimenez-Mateos et al., 2012) . While this approach allowed us to demonstrate that a lower level of miR-134 reduces seizures in the immature brain, it does not reflect a clinically-relevant strategy. Future studies, delivering Ant-134 after SE has commenced, or once animals

fail to respond to a frontline anticonvulsant would allow us to explore whether targeting miR-134 has any delayed or late anti-seizure or disease-modifying effects.

In the present study we observed an apparently narrower range of safe and effective doses of Ant-134 for seizure control when compared to the adult. Specifically, injection of a dose of Ant-134 that resulted in near-complete knockdown of miR-134 was associated with seizure-related mortality. Since dose-related toxicity was not reported in adult studies (Jimenez-Mateos et al., 2012), this may be due to loss of a function of miR-134 that is critical in the developing brain. Notably, several miR-134 targets are critical for brain development. These include the neuronal guidance molecule doublecortin (DCX) (Gaughwin et al., 2011, Fiore et al., 2009) and the RNA-binding protein Pumilio2 (Pum2) (Fiore et al., 2014), which is implicated in activity-dependent dendritogenesis. These dose-dependent effects of Ant-134 are consistent with a model in which miR-134 levels require to be modulated to within a certain range (Fiore et al., 2009) and excessive over- or under-expression can be deleterious. Further studies will be required to determine whether this is specific to this KA model, mouse age or genetic background.

The mechanism of action of Ant-134 is currently unknown. The pronounced anti-seizure effects are supportive of an effect on neuronal network synchrony and recent work reported Ant-134 does not alter basic electrophysiological properties of principal neurons in the hippocampus (Morris et al., 2018). LIM kinase 1 is a validated target of miR-134 in the rodent brain and inhibition of miR-134 alters dendritic spine morphology whereas depleting LIM kinase 1 obviates the neuroprotective effects of Ant-134 in *in vitro* models of seizure-induced neuronal death (Jimenez-Mateos et al., 2012). However, miR-134, like other miRNAs, has an extensive repertoire of targets and this will likely change during brain maturation. This might be resolved by sequencing the transcriptional landscape of the brain after treatment with Ant-134 and accompanying functional studies to interrogate other age-relevant targets such as DCX (Gaughwin et al., 2011).

In summary, the present study demonstrates that inhibition of miR-134 can reduce seizures and attendant brain damage in a mouse model of paediatric SE. Seizures in this model did not upregulate miR-134 and dose-ranging experiments may indicate a narrower therapeutic window for the use of this miRNA inhibitor than in adults. In summary, moderate knockdown of miR-134 can reduce seizures in immature mice and may expand the potential applications of this novel approach to the treatment of seizures and epilepsy. Finally, we note that more than a dozen miRNAs have been reported as potential targets for seizure control in the adult brain (Henshall et al., 2016). It is likely, therefore, that miRNAs in addition to miR-134 will provide a rich set of anti-seizure targets for investigation.

4 Chapter four

Results II

4.1 Introduction

4.1.1 Overview

As mentioned previously, AS is characterised by movement dysfunction/ataxia, neurodevelopmental delay, EEG abnormalities and recurrent seizures. In order to elucidate the mechanism of disease and develop new targets for potential drugs, we first sought to characterise a mouse model of AS.

The first AS mouse model was created by Arthur L. Beaudet (Jiang et al., 1998). The *Ube3a* $^{(m-/p+)}$ model was generated using a targeting vector that replaced a 3kb DNA fragment (from *SacI* to *XbaI*) containing exon 2 of *Ube3a*. This region was replaced with a neo-loxP-hprt cassette and resulted in a frame shift that deleted 100 amino acids and inactivated all forms of the protein (Jiang et al., 1998). The resulting mice displayed a number of phenotypes that recapitulate many symptoms in AS patients. These mice presented with motor incoordination when tested on the accelerating rotarod and they had deficits when assessed with the hind-paw footprint analysis. *Ube3a* $^{(m-/p+)}$ mice were susceptible to audiogenic seizures and an abnormal EEG was reported. Due to the severe developmental delay associated with AS, fear conditioning was used to assess hippocampal dependent memory and they found that *Ube3a* $^{(m-/p+)}$ mice did not freeze to the same degree as WT mice when reintroduced to the chamber, confirming a learning impairment in these mice. They also reported that a deficiency of *Ube3a* resulted in the impairment of hippocampal long-term potentiation (LTP). Histology analysis of the model did not detect any abnormalities between *Ube3a* $^{(m-/p+)}$ mice and littermate controls. This included morphologic analysis with hematoxylin and eosin staining, Nissl staining and immunohistochemical analysis of the hippocampus and cerebellum (Jiang et al., 1998).

The majority of behaviour characterisation in AS mouse models is performed in the F1 generation (Sonzogni et al., 2018, Born et al., 2017, Huang et al., 2013). This includes motor dysfunction, cognitive testing, EEG analysis and seizure susceptibility testing. For instance, Ype Elgersma's group performed a

Beaudet's model in F1 hybrid mice. Using the F1 hybrid in 1 mice for behavioural analysis, they found results comparable to those described above. These results included an impairment on the rotarod, decreased locomotor activity in the open field, impairments in cage behavioural tests such as nest building and marble burying. However, F1 mice were not used for seizure susceptibility testing (Sonzogni et al., 2018).

Seizures are present in over 80% of patients with AS, thus in order to elucidate the mechanisms behind hyperexcitability, it is critical that a mouse model can recapitulate these seizure phenotypes (Pelc et al., 2008a). It was immediately apparent that background strain influenced the emergence and severity of seizures in AS mice (Jiang et al., 1998, Sidorov et al., 2017, Mandel-Brehm et al., 2015). Work by Greer group have aimed to characterise phenotypes seen in different strains of AS mouse models. Using mice with the same genetic mutation as described above, they found that juvenile (P25) and adult mice (>P42) AS mice on a pure B6 background were susceptible to audiogenic seizures, while mice bred on a 129 strain resulted in severe seizures, and these seizures were also present in 60% of WT littermates (Mandel-Brehm et al., 2015). It has been reported that AS models purely bred on a 129 background or crossed with 129 mice to at least generation four, yields a model that is susceptible to audiogenic seizures. (Sonzogni et al., 2018, Jiang et al., 1998, Gu et al., 2019b).

Two generations of mice were used to characterise the AS model in our laboratory; F1 and N4. F1 mice were generated using a heterozygous (het) female that was crossed with a stock Wildtype (WT) 129 male and this yielded a mild AS phenotype. N4 mice were generated by backcrossing female het mice from generation 1-3. N3 females were mated with stock WT 129 males to yield N4 mice that had a harmful phenotype.

4.1.2 Hypothesis

We have hypothesised that the Ube3a $^{m-/p+}$ mouse model will have an abnormal EEG, with increases in delta and theta frequency, motor impairments in the open field and rotarod and increased seizure susceptibility. Since AS mice are hyperexcitable and because loss of the miR-379~410 cluster sponge function is expected in mice lacking Ube3a, levels of miR-134 are expected to be increased in these mice in comparison to their WT littermates.

4.1.3 Aim

To comprehensively characterise a mouse model of AS with a maternal mutation in *Ube3a* (Ube3a $^{m-/p+}$) at phenotypic and molecular levels using two generations of mice.

4.1.4 Methods

Behaviour: A battery of behavioural tests were performed on the F1 generation to determine if the AS model could recapitulate a number of phenotypes seen in AS patients. All behavioural tests were performed on WT and AS male and female naïve mice at either P21 or in adult mice. This encompassed tests looking at the locomotor activity, motor coordination, anxiety and naturalistic behaviours. **EEG**: EEG baseline was analysed using Labchart Reader and MATLAB to identify any potential EEG phenotypes present in AS mice. This included analysis of total power, presence of electrographic spontaneous seizures and spectral band analysis. Further analysis into the different frequencies was performed on resting EEG. This included spectral analysis in the following frequencies: delta (1-4 Hz), theta (4-8 Hz), alpha (8-12 Hz) and beta (12-30 Hz). **Molecular analysis**: The expression of miR-134 and some of its known targets were also analysed by qPCR in the hippocampus and cortex. P21 male and female naïve mice from

the N4 generation were used to induce audiogenic seizures. An adapted audiogenic seizure Racine scoring scale was used for the classification of these seizures.

4.2 Results

4.2.1 Loss of Ube3a protein in the brains of *Ube3a*$^{(m-/p+)}$ mice

AS is caused by the loss of function of *Ube3a*. Before characterising *Ube3a* $^{(m-/p+)}$ mice, we first sought to analyse the expression of *Ube3a* protein in WT and AS mice. Here, the hippocampi and cortices of naive P21 mice from both generations was examined. As expected, *Ube3a* expression was almost undetectable in AS mice from both generations. In the F1 mice, there was a significant decrease of *Ube3a* in AS mice in the hippocampi and cortices as represented in the blots shown (Fig 4.1 A&B) and in the protein quantification graphs (Fig 4.1 C&D, $p<0.05$). When comparing both brain regions, overall abundance of Ube3a was similar between the hippocampus and cortex of WT mice (Fig 4.1 C&D). The levels of Ube3a between the hippocampi and cortices in AS mice remained comparable (Fig 4.1 C&D). Similar results were obtained in the N4 generation. Western blots of hippocampi and cortices from naïve P21 mice are depicted in Fig 4.1 E&F, with a significant decrease of Ube3a in AS mice. Quantification of these blots demonstrate comparable levels of Ube3a to F1 mice (Fig 4.1 G&H, $p<0.05$).

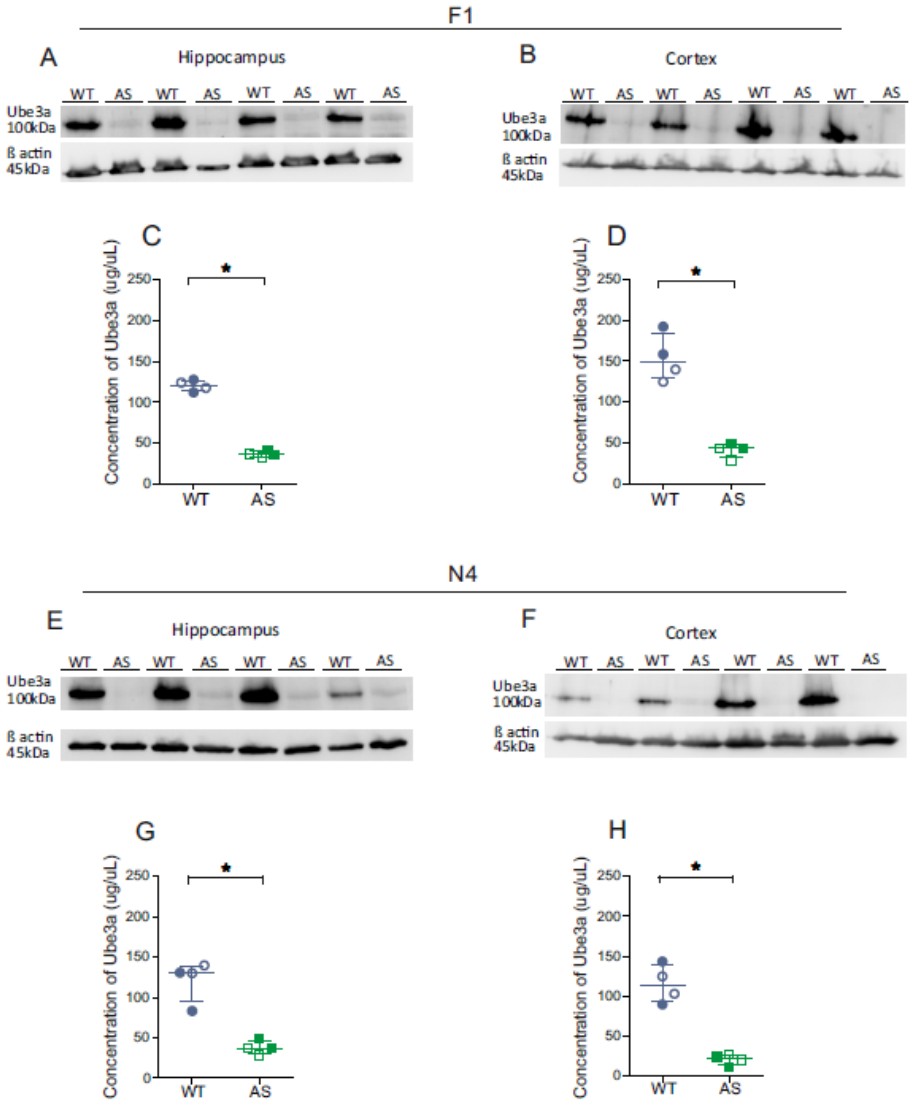

Figure 4.1: P21 Ube3a (m-/p+) mice have significantly lower levels of Ube3a
Western blotting was used to analyse the concentration of E6-AP in *Ube3a* $^{(m-/p+)}$ mouse and littermate WT controls in F1 and N4 P21 mice. **(A)** Western blot showing the expression of Ube3a in the hippocampus of F1 mice. **(B)** Western blot showing the expression of Ube3a in the cortex of F1 mice. **(C)** Relative concentration (µg/µL) of Ube3a in F1 hippocampus, n=4/genotype, p=0.0286. **(D)** Relative concentration (µg/µL) of Ube3a in F1 cortex, n=4/genotype, p=0.0286. **(E)** Western blot showing the expression of Ube3a in the hippocampus of N4 mice. **(F)** Western blot showing the expression of Ube3a in the cortex of N4 mice. **(G)** Relative concentration (µg/µL) of Ube3a in the hippocampus of N4 mice, n=4/genotype, p=0.0286. **(H)** Relative concentration (µg/µL) of Ube3a in the cortex of N4 mice, n=4/genotype, p=0.0286. ß-actin was used as a normaliser. Open circles and squares represents female mice, closed circles and squares represent male mice. A Shapiro-Wilk test was used to check for normality. Data did not pass normality testing due to low n numbers. Data are expressed as median interquartile range. A Mann-Whitney test was used for analysis between WT and AS mice.

4.2.2 Angelman syndrome mouse model has a characteristic EEG phenotype

Angelman syndrome mice were modelled using heterozygous mice expressing a maternal deletion of *Ube3a.* We first sought to determine if the *Ube3a* $^{(m-/p+)}$ mouse model had a characteristic EEG, which is seen in AS patients and is described above (Boyd et al., 1988, Sidorov et al., 2017). We selected mice at P21 to represent early childhood in humans (Laviola et al., 2003, Dutta and Sengupta, 2016). Mice of both sexes were used. We analysed baseline EEG recordings over a period of 4-6 hours in WT and AS mice (Fig 4.2 A). First, we quantified total power and found there was no difference in resting EEG total power in WT vs AS P21 mice (Fig 4.2 B, $p>0.05$). Next, we analysed frequency bands using the same resting EEG recordings because of the characteristic band phenotypes that have been reported in AS patients and mouse models (Sidorov et al., 2017, Frohlich et al., 2019a). In particular, an increase in the amount of delta and theta, and a decrease in beta frequencies have previously been reported in AS models (Frohlich et al., 2019a, Sidorov et al., 2017). Accordingly, analysis focused on four frequency bands that covered a range of 1-30 Hz: delta (1-4 Hz), theta (4-8 Hz), alpha (8-12 Hz) and beta (12-30 Hz).

In WT mice, the relative amounts of each frequency band were within the expected range (Wen et al., 2019, Sidorov et al., 2017). Specifically, the average total power of delta frequency was 29%, theta was 26%, alpha was 15% and beta was 30%. There was no difference in the amount of delta frequency activity between P21 (F1) WT mice and AS mice (Fig 4.2 Ci, $p>0.05$). In contrast, we found an increase in the percentage of the EEG within the theta frequency in AS mice (Fig 4.2 Cii, $p<0.05$). There was no difference in the amount of alpha frequency between genotypes (Fig 4.2 Ciii, $p>0.05$). The percentage of EEG within the beta frequency range was lower in AS mice (Fig 4.2 Civ, $p<0.05$). Thus, these P21 AS model mice (F1) display altered proportions of theta and beta but not delta frequency EEG activity.

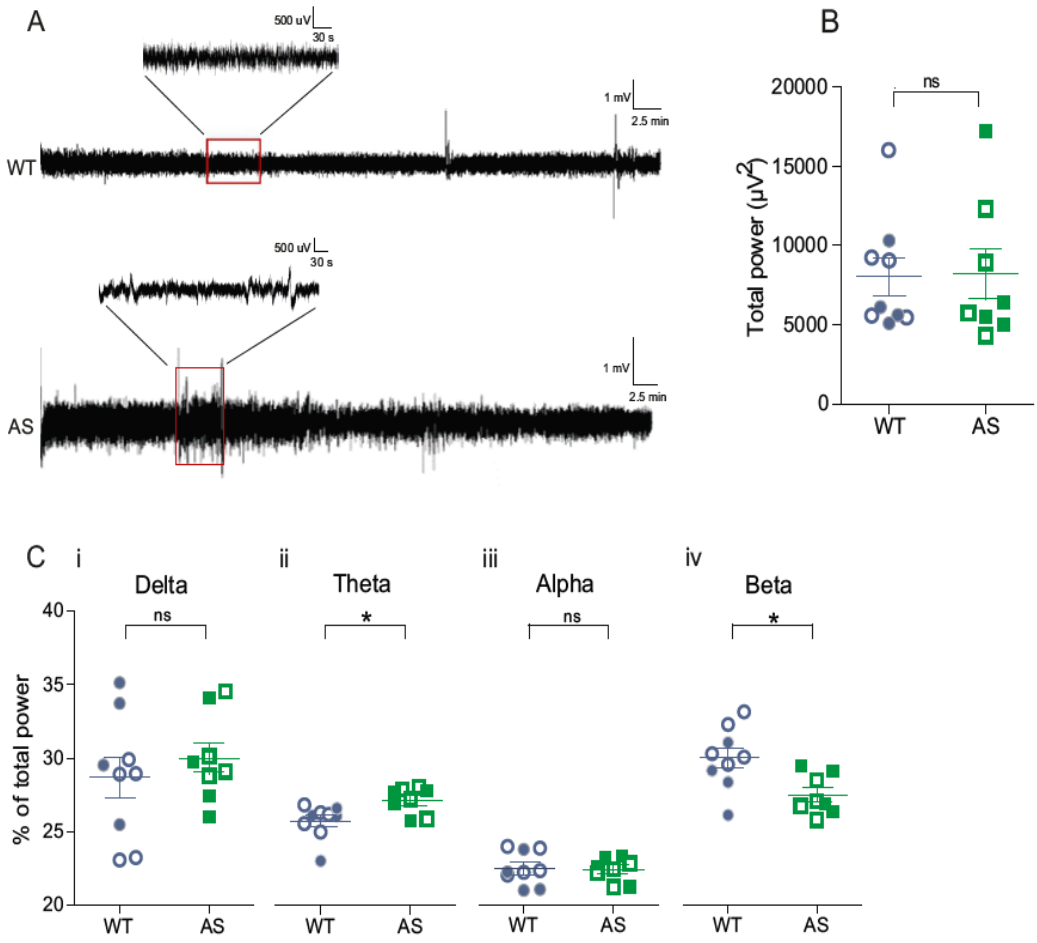

Figure 4.2: AS mice have characteristic EEG phenotypes at P21

Baseline EEG recordings were performed using tethered EEG on P21 F1 male and female, WT and AS mice. **(A)** Representative EEG trace of 1 hour recording from P21 WT and AS mice, Scale bar 1 mV, 2.5 min for full recording, 500 uV, 30 s for zoom. **(B)** Total power of baseline EEG over 4-6 h recordings, WT n=9, AS n=8, p=0.95. **(C)** Spectral analysis of individual band frequencies over baseline recordings, WT n=9, AS n=8. (i) Delta (1-4 Hz) p=0.5. (ii) Theta (4-8 Hz) p=0.015. (iii) Alpha (8-12 Hz) p=0.81. (iv) Beta (12-30 Hz) p=0.011. Open circles and squares represent female mice and closed circles and squares represent male mice. Data are expressed as standard error mean. A Shapiro-Wilk test was used to test for normality. A *t*-test was performed for statistical analysis.

4.2.3 Adult Angelman syndrome mice have a characteristic EEG phenotype

We next investigated the EEG features of adult AS mice (P42-P60). As above, WT and AS mice were equipped with surface-mounted EEG and tethered EEG recordings made for 4-6 hours per mouse. As above, the proportions of the relative frequency bands in adult WT mice was within the expected range. That is, the average total power of delta was 28%, theta was 24%, alpha was 16% and beta was 31%. Analysis of EEG traces of left and right sides of the brain from WT and AS mice revealed an abnormal resting EEG power in AS mice (Fig 4.3 A). Specifically, EEG total power was higher in AS mice in comparison to WT (Fig 4.3 B, $p<0.001$). We also analysed the different band frequencies over the baseline recordings. In accordance with the results obtained in the P21 mice, we did not see any differences in delta frequency (Fig 4.3 Ci, $p>0.05$) but theta frequency was increased in AS mice (Fig 4.3 Cii, $p<0.01$). Alpha frequency remained unchanged between both genotypes (Fig 4.3 Ciii, $p>0.05$. Unlike the results obtained in P21 mice, beta levels were not different between WT and AS mice (Fig 4.3 Civ, $p>0.05$). Thus, AS model mice display age-specific differences in EEG frequency abnormalities.

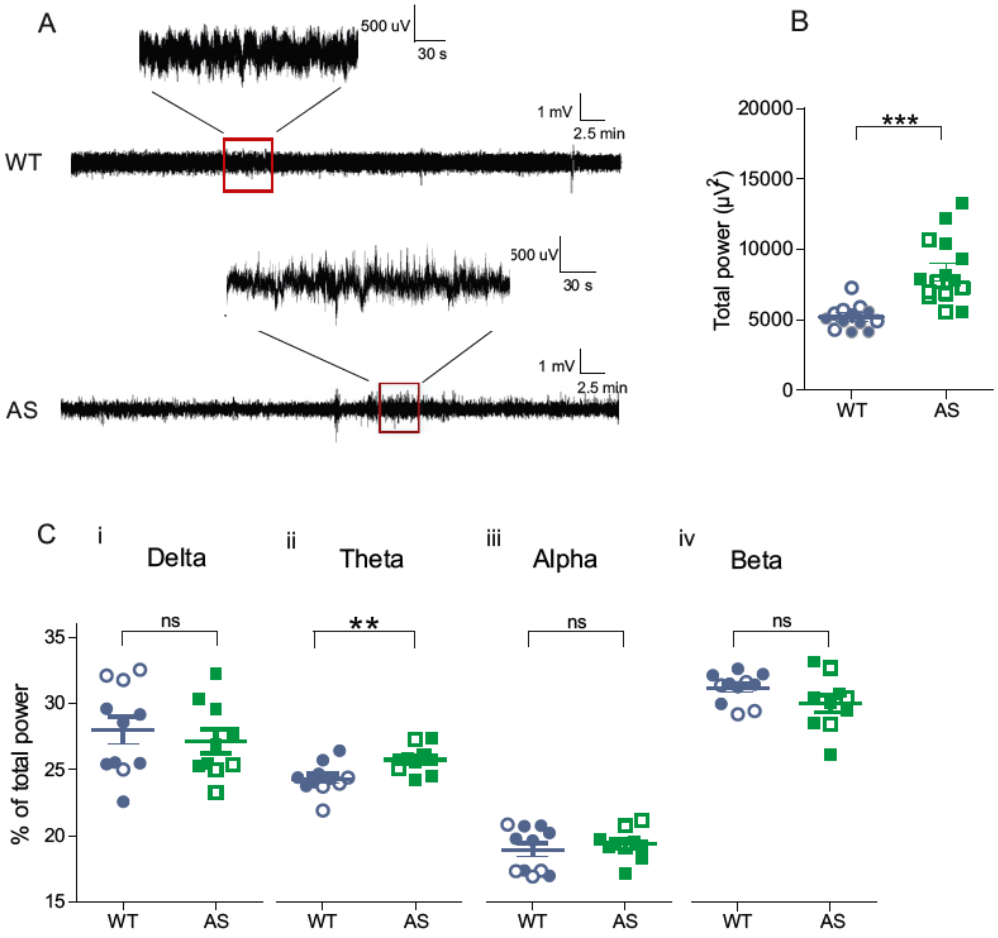

Figure 4.3: AS mice have characteristic EEG phenotypes in adult mice

Baseline EEG recordings were performed using tethered EEG on adult male and female, WT and AS mice. Open circles and squares represent female mice and closed circles and squares represent male mice. **(A)** Representative image EEG trace from one hour recording in adult WT and AS mice. Scale bar 1 mV, 2.5 min for full recording, 500 µV, 30 s for zoom. **(B)** Total power of baseline EEG recording over 4-6 h, WT n=13, AS n=15, $p<0.0001$. **(C)** Spectral analysis of individual band frequencies over baseline recordings, n=11/genotype. (i) Delta (1-4 Hz) $p=0.6$. (ii) Theta (4-8 Hz) $p=0.003$. (iii) Alpha (8-12 Hz) $p=0.7$. (iv) Beta (12-30 Hz) $p=0.14$. Open circles and squares represent female mice and closed circles and squares represent male mice .*t*-test was used for statistical analysis between WT and AS mice. Data are expressed as standard error mean. A Shapiro-Wilk test was used to test for normality.

4.2.4 Analysis of markers of neuronal activity in naïve F1 mice

Immediate early gene expression markers such as Arc and cFos have been reported to be dysregulated in the models of AS (Mandel-Brehm et al., 2015, Mardirossian et al., 2009). They are also associated with seizure induction and spontaneous recurrent seizures (SRS) (Scharfman et al., 2002, Barros et al., 2015). However, changes were not detected between *Arc* or *cFos*mRNA levels in the hippocampus of WT and AS mice (Fig 4.4 A&B, $p>0.05$), and this is in accordance with results presented above, that F1 AS mice do not present with SRS. Next, these markers were analysed in the cortex of naïve mice. *Arc* levels once again remained unchanged between genotypes (Fig 4.4 C, $p>0.05$) while *cFos* levels were increased in the cortex of AS mice (Fig 4.4 D, $p<0.05$). Following on from the analysis of P21 mice, levels of *Arc* and *cFos* were analysed in the hippocampus of adult mice. Similar to results obtained in P21 mice, levels of *Arc* and *cFos* remained similar between genotypes (Fig 4.4 E&F, $p>0.05$).

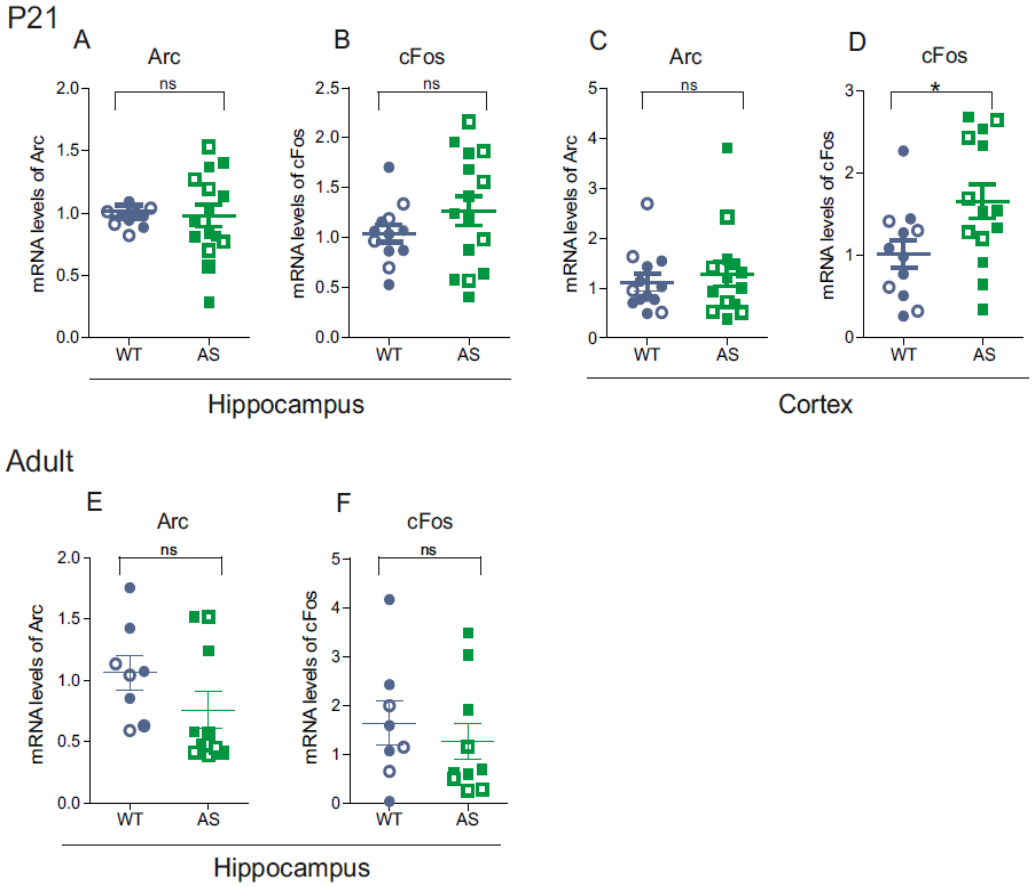

Figure 4.4: Markers of neuronal activity in naive F1 hippocampus and cortex
qPCR was used to analyse levels of neuronal markers in the hippocampus and cortex of naïve P21 mice, and the hippocampus of adult mice. **(A)** mRNA levels of Arc in the hippocampus, WT n=11, AS n=15, p=0.75. **(B)** mRNA levels of cFos in the hippocampus, WT n=12, AS n=15, p=0.23. **(C)** mRNA levels of Arc in cortex, WT n=12, AS n=15, p=0.60. **(D)** mRNA levels of cFos in cortex, WT n=12, AS n=15, p=0.03. **(E)** mRNA levels of Arc in the hippocampus of adult mice, WT n=8, AS n=10, p=0.16. (F) mRNA levels of cFos in the hippocampus of adult mice, WT n=8, AS n=10, p=0.51. ß-actin was used as a normaliser. A Shapiro-Wilk test was used to test for normality. Data are expressed as standard error mean. t-tests were used for statistical analysis.

4.2.5 Induction of seizures using subconvulsant doses of pentylenetetrazol

Following extensive baseline EEG analysis in P21 and adult F1 mice, consisting of in depth examination of frequency bands and total power over 4-6 hour recordings, we did not observe any spontaneous seizures during these periods. We next questioned whether AS mice had lower seizure thresholds or were otherwise more susceptible to convulsants. For this, we elected to test responses to a subconvulsant dose of pentylenetetrazol (PTZ), a $GABA_A$ receptor antagonist that is widely used to induce seizures in experimental models of epilepsy (Shimada and Yamagata, 2018). The aim was to use a PTZ dose that would not cause only limited seizures in WT mice but actual seizures in an animal with greater seizure susceptibility. Since the EEG abnormalities were more pronounced in the adult AS mice, we proceeded to test PTZ thresholds in this age group. A full convulsant dose of PTZ is usually between 60 mg/kg-100 mg/kg, thus we selected a dose of 40 mg/kg (Itoh and Watanabe, 2009). WT and AS mice were equipped with surface EEG as before and then injected with 40 mg/kg (IP). EEG changes and seizure responses were recorded for the subsequent 30 mins.

Low-dose PTZ induced more significant electrographic seizure-like events on EEG in AS mice in comparison to WT mice. A representative EEG trace from both genotypes can be seen in Fig 3. While seizure onset times were similar in both groups (Fig 4.5 B, $p>0.05$), EEG total power, a measure of seizure severity, was greater in AS mice (Fig 4.5 C&D). Further analysis determined that the difference was greatest during recordings from the first 10 minutes after PTZ injection (Fig 4.5 C, $p<0.05$). Over the entire 30 min of recordings, the higher EEG total power did not reach significance (Fig 4.5 D, $P>0.05$). As a molecular read-out of the increase seizure susceptibility we measured transcript levels of *Arc* and *cFos* in the hippocampus 30 min after seizures, however we did not detect any differences in *Arc* or *cFos* between genotypes (Fig 4.5 E&F, $p>0.05$).

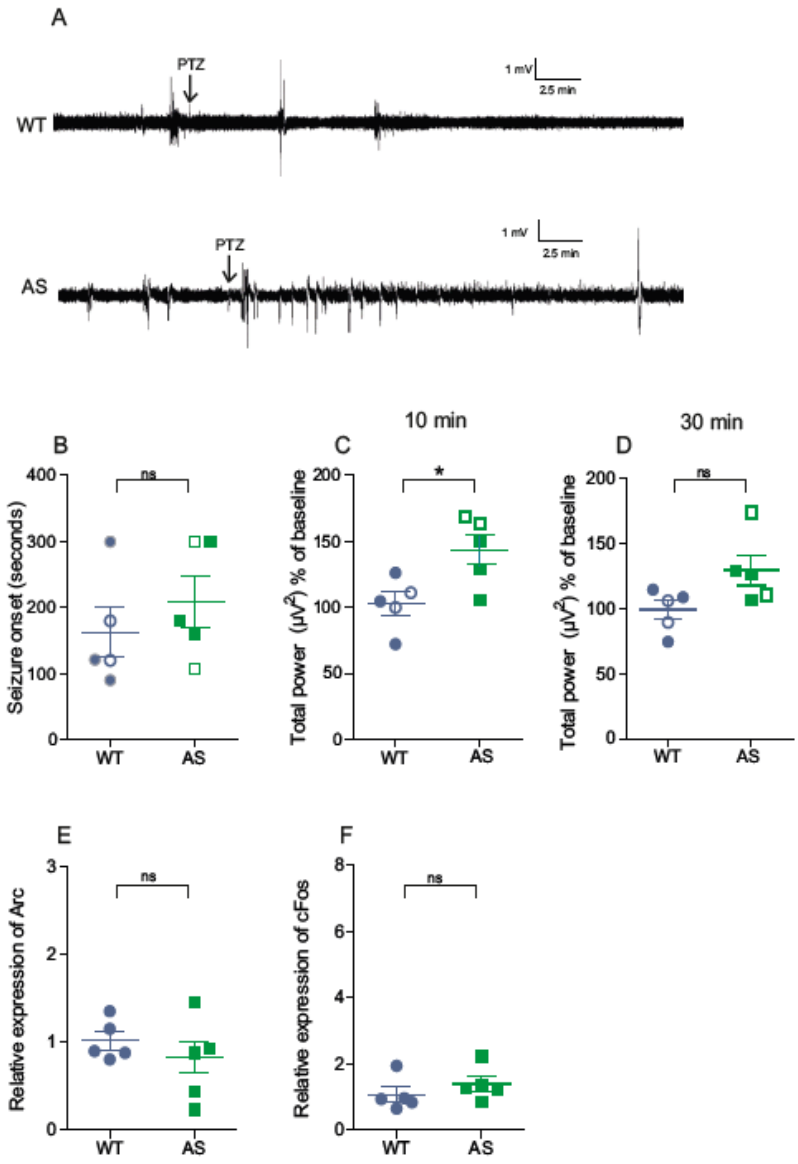

Figure 4.5: AS mice are susceptible to seizures using subconvulsant doses of PTZ
Subconvulsant doses of PTZ were used to induce seizures in AS mice and in WT mice using an IP injection of 40 mg/kg. **(A)** Representative EEG traces for AS and WT mice following 40 mg/kg PTZ, time scale 1 mV, 2.5 min, 30 min scale bar is shown**. (B)** Time (s) to the first electrographic seizure following 40 mg/kg PTZ WT n=5, AS n=5, p=0.41. **(C)** Total power from the first 10 minutes after injection 40 mg/kg PTZ, WT n=5, AS n=5, p=0.024. **(D)** Total power from entire 30 minute recording after injection 40 mg/kg PTZ, WT n=5, AS n=5, p=0.059. **(E)** Relative expression of Arc in the hippocampus, n=5, p=0.37. **(F)** Relative expression of cFos in the hippocampus, n=5, p=0.35. ß-actin was used as a normaliser. Open circles and squares represent female mice and closed circles and squares represent male mice. Data are expressed as standard error mean. A Shapiro-Wilk test was used to test for normality. A *t*-test was performed for statistical analysis.

4.2.6 Induction of seizures using subconvulsant doses of kainic acid

To extend these findings, we investigated the effects of a low dose of kainic acid in P42-P60 AS mice. Again, the intention was to use a dose that produced none to only mild seizure-like activity in WT animals. Having developed a model of SE in P21 WT mice using 5 to 10 mg/kg of KA (see Chapter 3), we tested doses of 10 mg/kg and 20 mg/kg here on the basis that sensitivity to KA declines with age (McCord et al., 2008, Wozniak et al., 1991).

Mice were equipped with EEG and then received 10 mg/kg KA (IP). At this dose, KA injection induced seizures more quickly in AS mice compared to WT mice (Fig 4.6 A, $p<0.05$). The total EEG power over the 30-minute test period was not different between genotypes (Fig 4.6 B, $p>0.05$). A representative EEG trace shows the time from injection with KA in WT and AS mice (Fig 4.6 C). At 20 mg/kg, seizures again began sooner in AS mice compared to their WT littermate (Fig 4.6 D, $p<0.05$). Again, overall seizure severity as measured by EEG total power was not different between genotypes (Fig 4.6 E, $p>0.05$). A representative EEG trace shows time from injection of KA in WT and AS mice (Fig 4.6 F). Consistent with this, levels of *Arc* and *cFos* in the hippocampus, taking 30 min after injection, were similar between AS and WT at the 20 mg/kg dose (Fig 4.6 G&H, $p>0.05$).

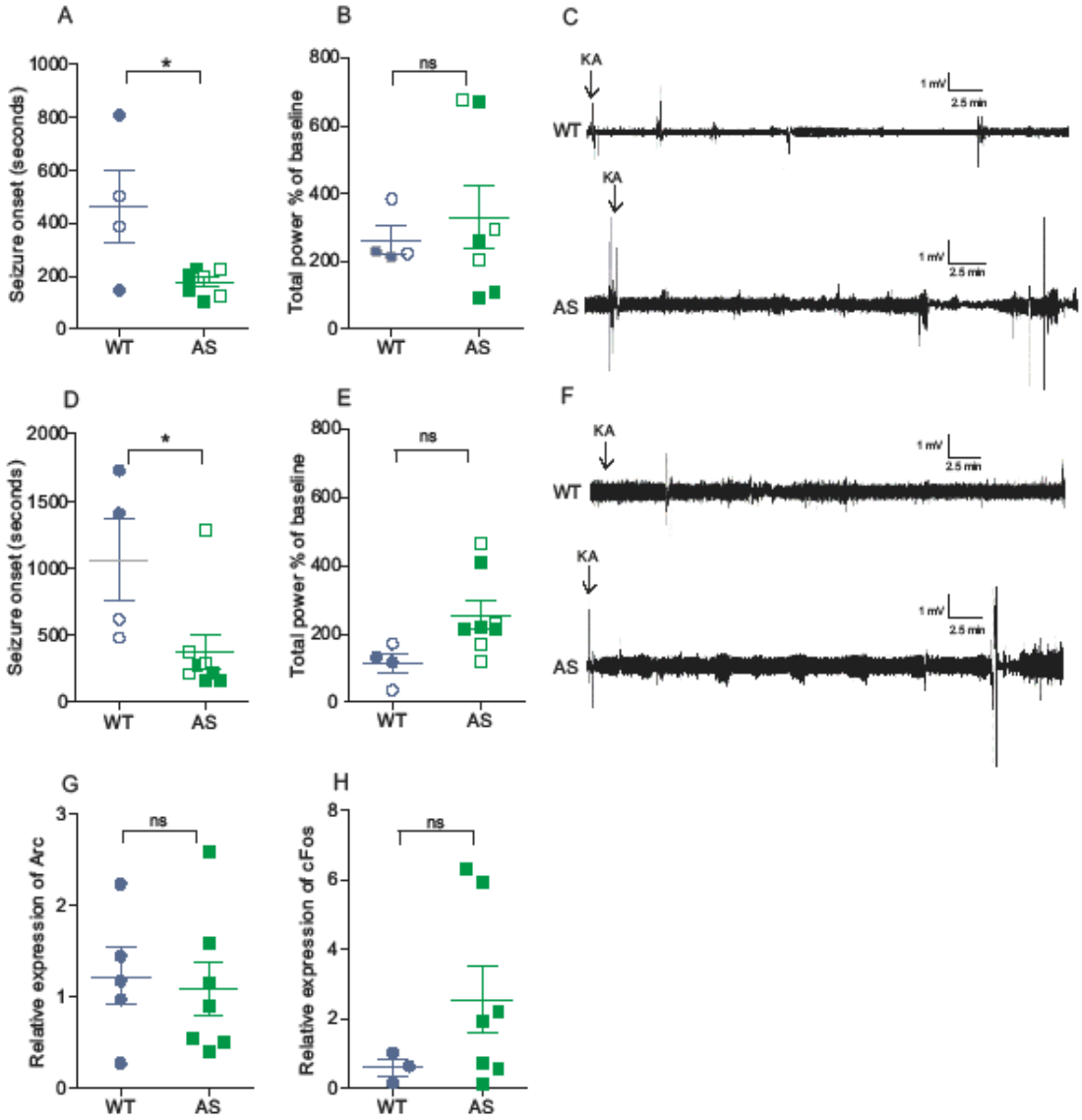

Figure 4.6: AS mice are susceptible to seizures using subconvulsant doses of KA
Subconvulsant doses of KA were used to induce seizures in AS and WT mice. Doses ranged from 10-20 mg/kg. **(A)** Time (s) to the first electrographic seizure following injection of 10 mg/kg, WT *n*=4, AS *n*=7, p=0.023. **(B)** Total power % baseline of ictal activity following injection of 10 mg/kg WT *n*=4, AS *n*=7, p=0.62. **(C)** Representative EEG trace of WT and AS mouse following seizure induction 10 mg/kg, Scale bar 1 mV, 2.5 min. **(D)** Time (s) to the first electrographic seizure following injection of 20 mg/kg, WT *n*=4, AS *n*=8, p=0.033. **(E)** Total power % baseline of ictal activity following injection of 20 mg/kg, WT *n*=4, AS *n*=8, p=0.053. **(F)** Representative EEG trace of WT and AS mouse following seizure induction 20 mg/kg, Scale bar 1 mV, 2.5 min. **(G)** Relative expression of Arc in hippocampus, WT *n*=4, AS *n*=7, p=0.780 (H) Relative expression of cFos in hippocampus, WT *n*=4, AS *n*=7, p=0.241. ß-actin was used as a normaliser. Open circles and squares represent female mice and closed circles and squares represent male mice. Data are expressed as standard error mean. A Shapiro-Wilk test was used to test for normality. A *t*-test was performed for statistical analysis.

4.2.7 Development of an audiogenic seizure model

It has been frequently reported that AS mice are susceptible to sound-induced (audiogenic) seizures (Mandel-Brehm et al., 2015, Born et al., 2017, Gu et al., 2019b). We next sought to determine if the AS mice were susceptible to audiogenic seizures. We first tested P21 mice, by placing in a soundproof container and subjecting to a loud alarm (120 dB) for 60 seconds. The EEG and behaviour was assessed during and after the stimulus. However, this failed to elicit any changes in EEG or clinical seizures (Fig 4.7 A, B). Because audiogenic seizure susceptibility might be age-dependent we next moved to test AS mice at an older age of P28. EEG analysis detected a difference between genotypes and an effect of the stimulus. Specifically, there was a significant difference between total power in WT and AS mice after the first and second stimulus (Fig 4.7 C, $p<0.05$). There was a further increase in EEG power after the last stimulus (Fig 4.7 C, $p<0.01$). However, this increase in EEG power was not correlated with behavioural seizures.

Finally, we attempted to elicit audiogenic seizures in adult AS mice. There was a significant difference between total power caused by each stimulus, with an increase of total power in AS mice in comparison to WT mice (Fig 4.7 E, $p<0.001$). There was a significant difference in total power found after each stimuli (Fig 4.7 E, $p<0.01$). Taken together it is evident that the F1 generation AS mice aged between P28 – P60 are sensitive to loud stimuli over 100dB, but this type of stimulus was not sufficient to induce convulsive seizures.

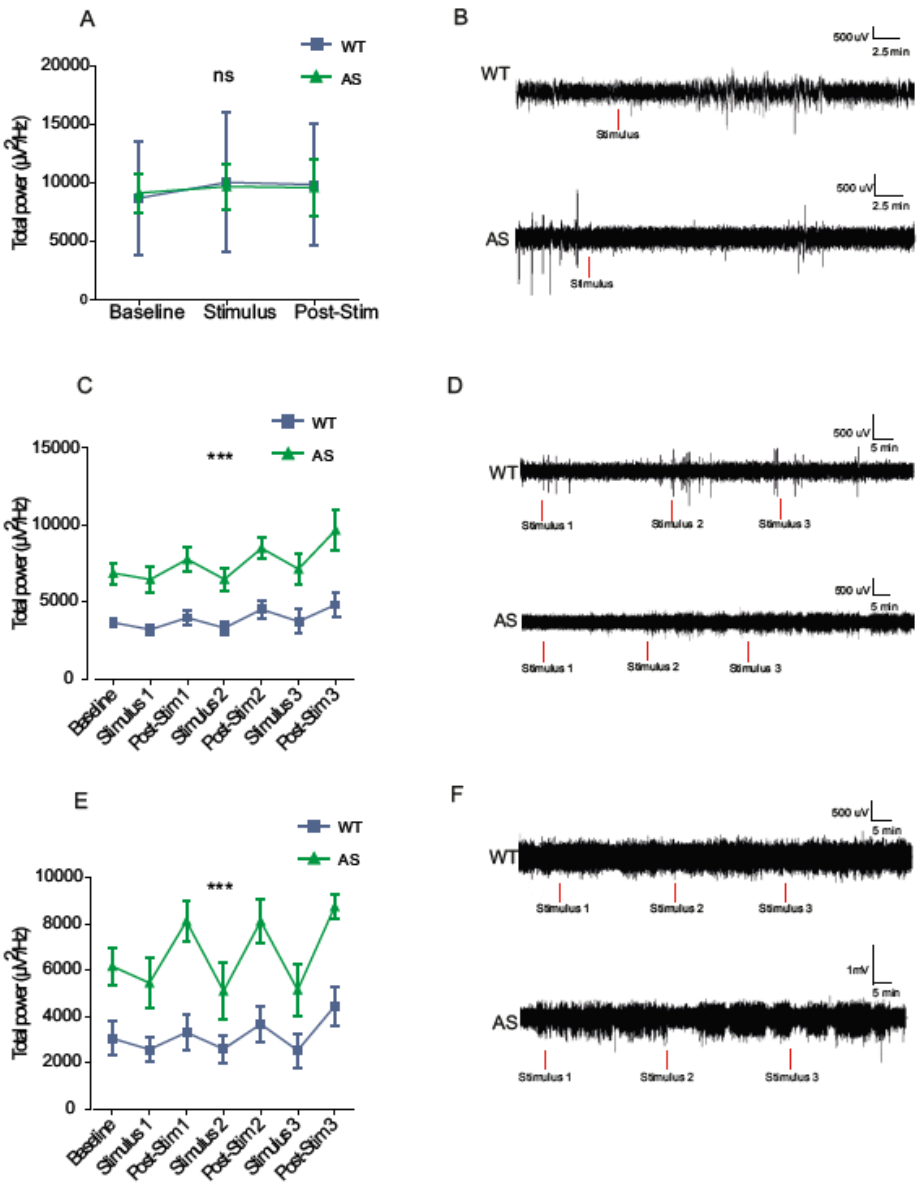

Figure 4.7: F1 AS mice are not susceptible to audiogenic seizures

F1 WT and AS mice were used in attempt to generate an audiogenic seizure model in three different age groups. **(A)** Total power (uV^{2}Hz) at baseline, during stimulus and post-stimulus in P21 mice, n=3/genotype, p=0.99. **(B)** Representative EEG traces of ipsilateral and contralateral recordings from WT and AS mice. **(C)** Total power (µV^{2}Hz) at baseline, during stimuli and after stimuli in P28 mice, WT *n*=4, AS *n*=8, p<0.001. **(D)** Representative EEG traces of ipsilateral and contralateral recordings in WT and AS mice. **(E)** Total power (uV^{2}Hz) at baseline, during and after stimuli in adult mice, n=3/genotype, p<0.001 **(F)** Representative EEG trace of ipsilateral and contralateral recordings in WT and AS mice. Data are represented as standard error mean. A Shapiro-Wilk test was used to check normality of data. A two-way ANOVA was used for statistical analysis.

4.2.8 N4 Angelman syndrome mice are susceptible to audiogenic seizures

On the basis of reports by others (Sonzogni et al., 2018, Mandel-Brehm et al., 2015, Jiang et al., 1998), we next backcrossed the AS line to generation N4 to increase the 129 background strain in the model with the aim of increasing susceptibility to audiogenic seizures. Once again, male and female, P21 and adult mice were placed in a soundproof chamber and we attempted to induce convulsive seizures with an alarm. However, this was not successful. Next, we moved to a different method of inducing seizures as described by Sonzogni and colleagues (Sonzogni et al., 2018), which consisted of vigorously scratching the cage lid. When performed for 30 seconds this induced convulsive seizures in 100% of AS mice (n=10) but only 10% of WT mice (n=10) (Fig 4.8 B). The response to the stimulus followed a stereotyped pattern and this was scored for the purposes of quantification. Following initiation of scratching, mice would begin running around the cage as followed by type 1 wild running (Fig 4.8 Ai). Next, mice would go into tonic-clonic convulsions which were characterised as type 2 (Fig 4.8 Aii), and then to hyperextension of the hind limbs, type 3 (Fig 4.8 Aiii) (Carballosa-Gonzalez et al., 2013). Mice that did not have any seizures or wild running behaviours were given a score of 0, while mice that died during or after the trial were given a score of 4. A table representing the seizure types during the induction of an audiogenic seizure can be seen in table 1. Thus, audiogenic seizures can be elicited in AS mice. This method of inducing seizures was also attempted in the F1 generation but it was unsuccessful in inducing audiogenic seizures.

Table 4.1: Audiogenic seizure scoring scale categorising the severity of seizures.

Type	Seizure type
0	No seizure activity
1	Wild running
2	Generalized tonic-clonic convulsions
3	Tonic hyperextension of the hindlimbs
4	Death

Type 0: No behavioural seizure activity visible. Type 1: Wild running when stimulus is initiated. Type 2: Generalized tonic-clonic convulsions with loss of posture. Type 3: Tonic hyperextension of the hindlimbs and tail. Type 4: Death. Scoring scale was adapted from Munoz De La Pascua and Lopez (2005) (Carballosa-Gonzalez et al., 2013).

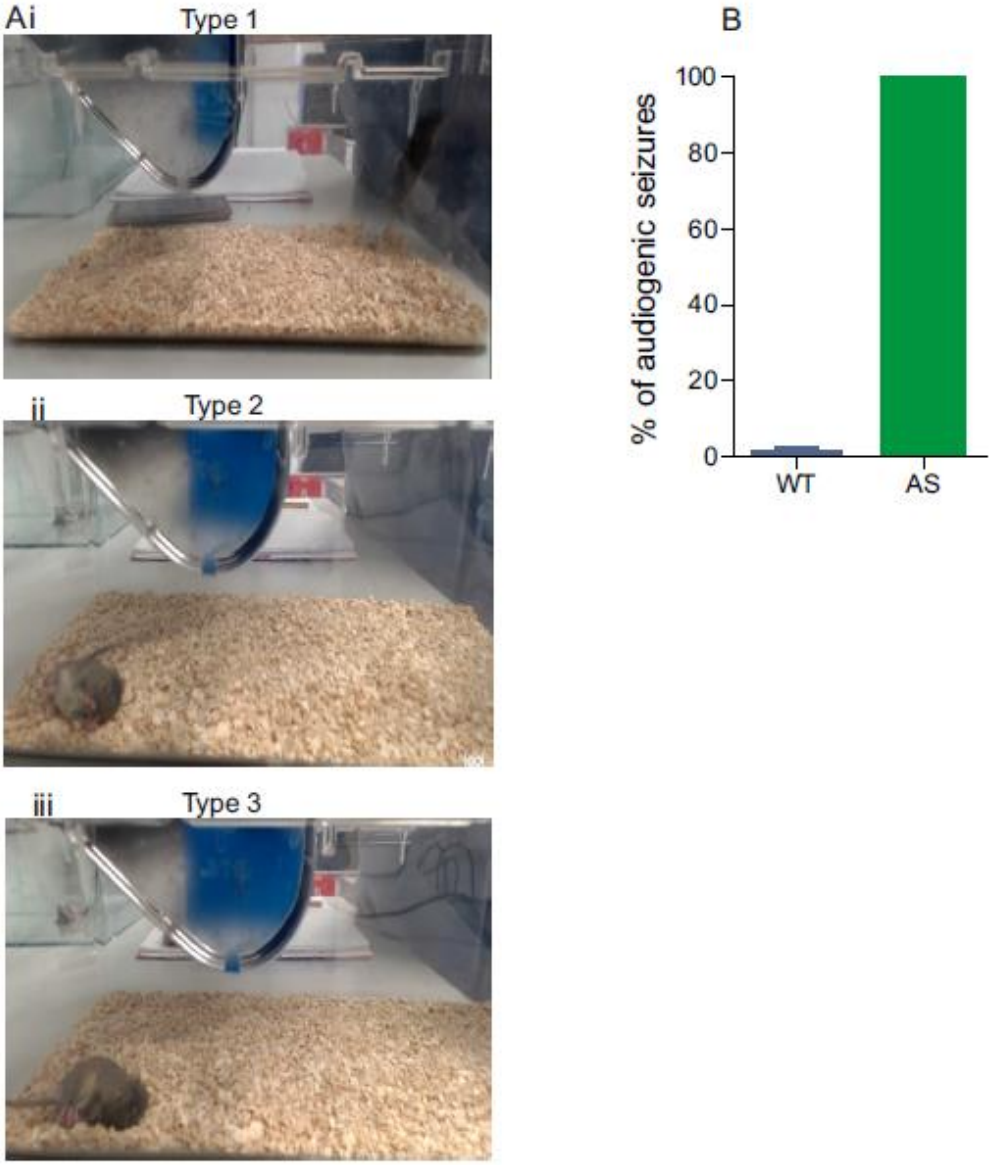

Figure 4.8: N4 P21 mice are susceptible to audiogenic seizures
P21 WT and AS mice from generation N4 were breed specifically to induce audiogenic seizures. **(A)** Screenshots of seizure classification system. (i) Type 1, wild running. (ii) Type 2, tonic-clonic convulsions. (iii) Type 3, tonic hyperextension of the hind limbs. **(B)** Percentage of audiogenic seizure induction in WT and AS mice, n=10/genotype.

4.2.9 Characteristic AS motor phenotype present in adult AS mice

Next, we began to characterise the behavioural aspects of the *Ube3a* $^{(m-/p+)}$ model in the F1 generation. The behavioural characterisation was performed in adult mice due to the abnormal baseline EEG detected in section 1.2.2, suggesting adult AS mice have a more severe phenotype and because several assays require mice to be of a certain size and weight. Once again, this was done in mice aged P42-P60. We first sought to analyse the locomotor activity and general movement ability of the AS mice since motor impairments are commonly seen in AS patients (Clayton-Smith and Laan, 2003, Clayton-Smith, 1993). We used the open field test to analyse locomotor activity (Clayton-Smith, 1993) and anxiety (Larson et al., 2015, Smith, 2001), both common features in AS patients. Similar to other reports using the *Ube3a* $^{(m-/p+)}$ mouse model (Sonzogni et al., 2018), we found a decrease in exploration time in adult AS mice when compared with WT littermates (Fig 4.9 A, $p<0.05$). AS mice generally moved slower than WT mice and could been seen dragging their hindlimbs, possibly contributing to the decrease in locomotor activity. We did not detect a difference in exploration time within genders, as represented by open circles/squares for females and closed circles/squares for males.

The decreased exploration time in the open field could be attributed to an anxious phenotype, thus we proceeded to build on this by using the light/dark box test, which is another measure of anxiety. We saw a trend for less time spent in the light compartment in AS mice when compared to WT mice, however, this result was not statistically significant (Fig 4.9 B, $p>0.05$).

Following on from this, we aimed to further elucidate the nature of the reduction in locomotor activity seen in the open field and analysed the motor coordination of these mice using an adapted method from Sonzogni *et al* 2018 of the accelerating rotarod (Sonzogni et al., 2018). The latency to fall in WT mice was comparable to previous reports in the same mouse model (Sonzogni et al., 2018). We found a significant impairment in AS mice in comparison to WT littermates, as characterised by a reduction in time spent on the rotarod (Fig 4.9 C, $p<0.001$). When separating the graphs by gender, it was evident

that this phenotype was present in both male and female AS mice (Fig 4.9 D&F). However, there was a more significant impairment present between female WT and AS mice (Fig 4.9 D, $p<0.01$). Overall, both WT and AS males performed worse on the rotarod than the female mice (Fig 4.9 E, $p<0.05$).

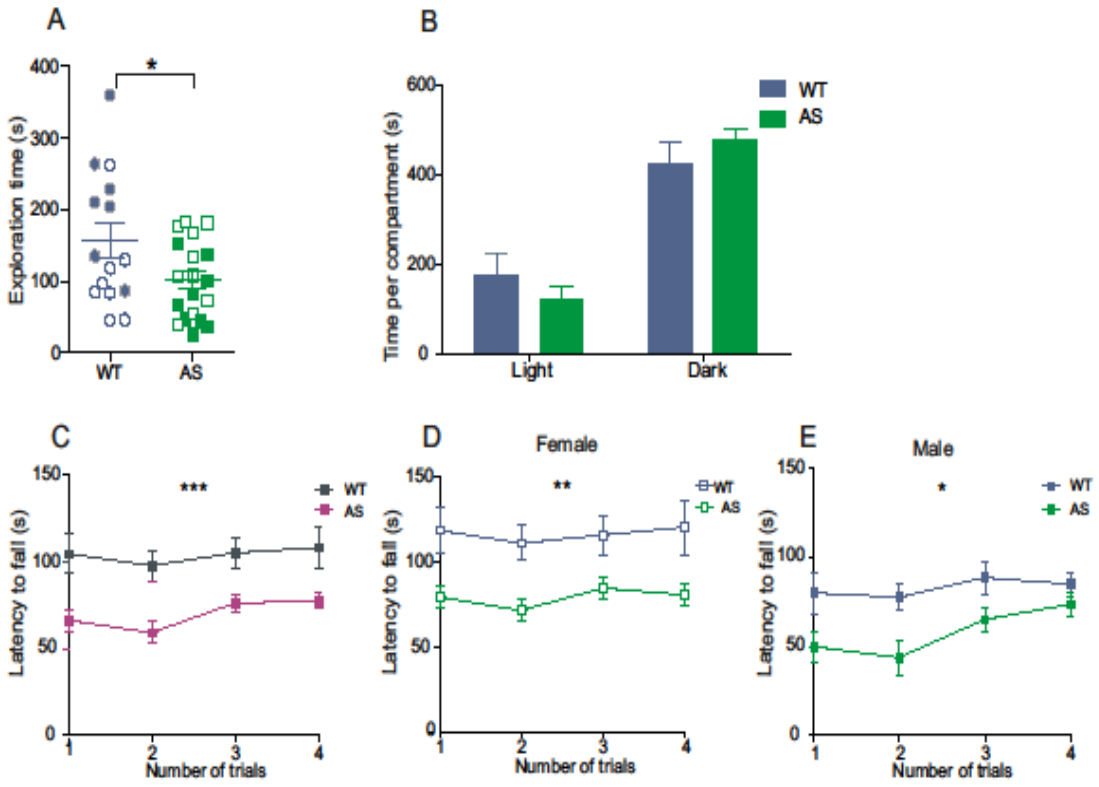

Figure 4.9: AS mice have a characteristic motor deficit

A battery of behaviour tests were performed in F1 adult mice to characterise the behavioural phenotype. **(A)** Total time (s) spent exploring the open field arena over a 10 minute trial, WT n=15, AS n=19, p=0.022. **(B)** Graphs shows the length of time (s) spent in dark and light compartment during the 10 minute trial, WT n=8, AS n=14, p=0.16. **(C)** Graph shows the time spent on the rotarod during four test phases, WT n=12, AS n=18, p=0.0008. **(D)** Graph shows the time spent on the rotarod during four test phases in female mice, WT n=7, AS n=10, p=0.004. **(E)** Graph shows the time spent on the rotarod during four test phases in male mice, WT n=7, AS n=10, p=0.015. Open circles and squares represent female mice and closed circles and squares represent male mice .Data are represented as standard error mean. A Shapiro-Wilk test was used to check normality of data. A t-test was used for comparison between WT and AS mice in the open field. A two-way repeated measures ANOVA was used for analysis of the rotarod. A two-way ANOVA was used for analysis of the light dark box test.

4.2.10 AS mice show impairments in naturalistic behaviours

Next, we sought to characterise naturalistic behaviours like digging and burying in our mice using the marble burying test protocol (Deacon, 2006b). The marble burying test is based on the concept that mice recognise marbles as foreign objects and thus proceed to bury them. Furthermore, this test has also been linked to impairments in hippocampal function in mice (Deacon and Rawlins, 2005), therefore this test could potentially be used to investigate cognitive deficits. AS mice buried significantly fewer marbles in comparison to WT mice during the 30 min test, suggesting a deficit in hippocampal function (Fig 4.10 A, $p<0.05$). A representative image shows the layout of the marbles prior to test initiation and 30 min later (Fig 4.10 B).

Subsequently, we looked at another cage-based behavioural test that assesses nest-building ability. This has been suggested to reflect the innate behaviour of mice, in terms of building a nest for their pups and to maintain body temperature (Sonzogni et al., 2018, Au - Neely et al., 2019). In addition, it has also be used to monitor the health and welfare of mice (Gaskill et al., 2013). Deficits in this paradigm are also suggestive of brain lesions (Deacon, 2006a). While presumably a similar test to marble burying, we did not detect an impairment in AS mice (Fig 4.10 C, $p>0.05$). The amount of unused nesting material was not affected by the genotype (Fig 4.10 C, $p>0.05$). The amount of nesting material buried on the first day was similar between genotypes. There was a slight trend for an increase in nesting material buried in AS mice at day 2, this was not significant. By day 3-5, similar amounts of nesting material were used between genotypes (Fig 4.10 C, $p>0.05$).

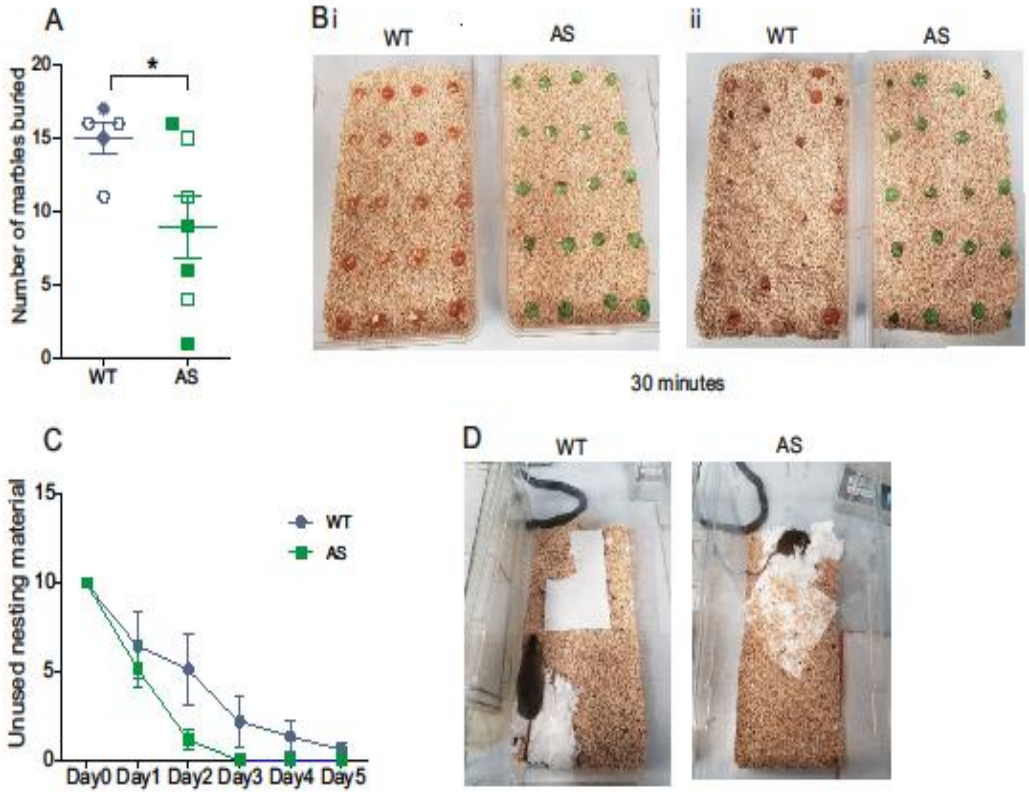

Figure 4.10: AS mice have a characteristic behaviour phenotype
(A) Graph represents the number of marbles buried (50% or less covered counts as one marble buried) over a 30 minute trial , WT n=5, AS n= 7, p=0.045. **(Bi)** Images show the experimental set up for marble burying. **(Bii)** Image shows a representative image of cages 30 minutes after marble burying experiment was completed. **(C)** Graph shows the amount of unused nesting material from day 0- day 5, WT n=3, AS n=4, p=0.16. **(D)** Images show the amount of nesting material used after the first day of the test in representative WT and AS mice.

4.2.11 Analysis of miR-134 and related targets in naïve F1 P21 mice in the hippocampus

Finally, we investigated whether levels of miR-134 or its targets were altered in AS model mice on the basis that AS mice are hyperexcitable and deletion of *Ube3a* results in the loss of the 'miRNA sponge' and cortex samples were obtained from WT and AS mice at P21 mice.

Hippocampal levels of miR-134 were slightly increased, but not significantly, in P21 AS mice comparison to WT (Fig 4.11 A, p=0.0519). Unexpectedly, levels of Limk1 and Pum2, two validated targets of miR-134, were also found to be higher in the hippocampus of P21 AS mice in comparison with age-matching WT controls (Fig 4.11 B&C, p<0.05). . Interestingly, we verified that levels of serpine1 (Klimczak-Bitner et al., 2016), a predicted target of miR-134, were significantly reduced in AS mice in comparison to their WT littermates (Fig 4.11 D, p<0.05). Levels of doublecortin (DCX), another validated target of miR-134 (Gaughwin et al., 2011), were not different between WT and AS mice (Fig 4.11 E, p>0.05). In the cortex, levels of miR-134 were very similar between genotypes (Fig 4.11 F, p>0.05). Accordingly, no differences were observed in the levels of the miR-134 targets, Limk1, Serpine1 and DCX between WT and AS mice (Fig 4.11 G, I, &J, p>0.05). On the other hand, and in accordance with the hippocampal findings, levels of Pum2 were significantly higher in AS mice when compared to the age-matching WT controls (Fig 4.11 H, p<0.01).

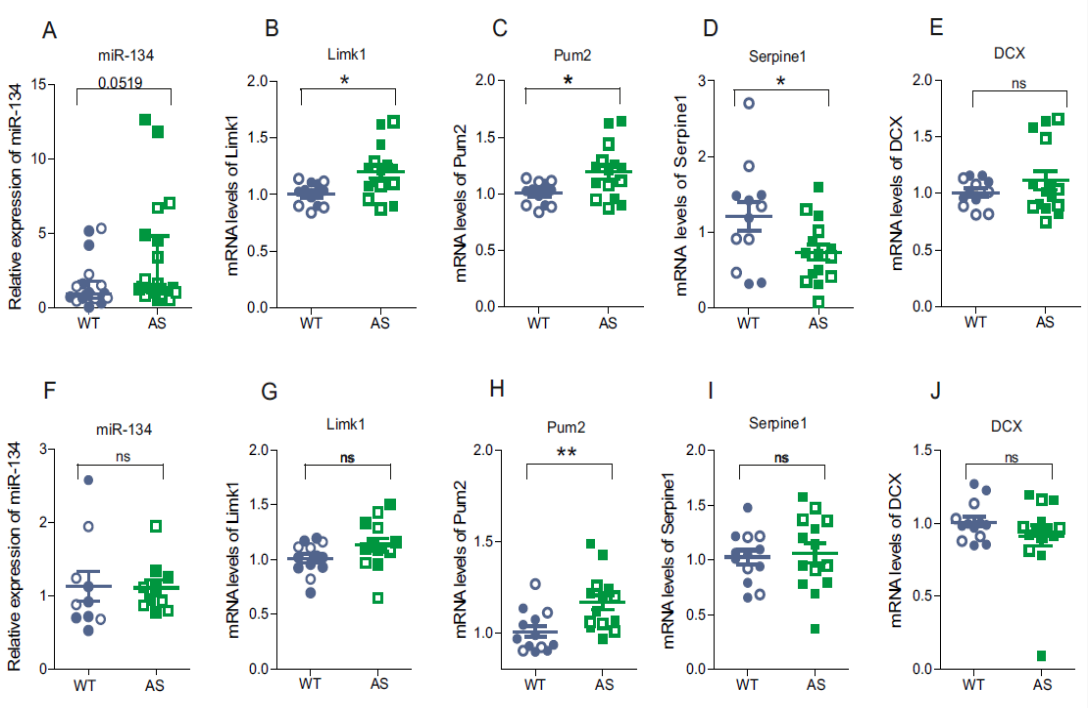

Figure 4.11: Analysis of miR-134 and its targets in P21 F1 naïve mice

qPCR was used to analyse levels of miR-134 and its targets from the hippocampus and cortex of naïve P21 mice. **(A)** Relative expression of miR-134 in the hippocampus, WT n=9, AS n=10, p=0.07. **(B)** mRNA levels of DCX in the hippocampus, WT n=12, AS n=15, p=0.30. **(C)** mRNA levels of limk1 in the hippocampus, WT n=12, AS n=15, p=0.01. **(D)** mRNA levels of pum2 in the hippocampus, WT n=12, AS n=15, p=0.02. **(E)** mRNA levels of serpine1 in the hippocampus WT n=12, AS n=15. **(F)** Relative expression of miR-134 in the cortex, WT n=10, AS n=10, p=0.92. **(G)** mRNA levels of DCX in the cortex, WT n=13, AS n=13, p=0.60. **(H)** mRNA levels of limk1 in the cortex, WT n=13, AS n=14, p=0.09. **(I)** mRNA levels of pum2 in the cortex, WT n=13, AS n=14, p=0.005. **(J)** mRNA levels of serpine1 in the cortex, WT n=13, AS n=14, p=0.80. MiR-124 was used as a normaliser for levels of miR-134 in the hippocampus and cortex. ß-actin was used as a normaliser for analysis of miR-134 targets. Data are expressed as standard error mean. t-tests were used for statistical analysis. A Shapiro-Wilk test was used to test for normality.

4.2.12 Epilepsy regulated miRNAs in P21 mice

Due to the increased susceptibility to the induction of seizures using chemoconvulsant agents and audiogenic seizures, we sought to determine if some of the known epilepsy regulated miRNAs were increased in naive F1 and N4 P21 mice. MiR-21 has been reported to be elevated in models of epilepsy in numerous studies, including in children with MTLE (Henshall, 2014, Peng et al., 2013b). In addition, miR-135a is another epilepsy regulated miRNA (Henshall, 2014) and antagonizing it during the chronic epilepsy phase in an adult mouse models of TLE reduces the development of spontaneous seizures (Vangoor et al., 2019). Expression of miR-135a did not differ between genotypes in F1 mice (Fig 4.12 A, $p>0.05$). Similarly, in N4 mice, the levels of miR-135a were consistent between WT and AS mice, however, the expression of miR-135a was reduced in N4 AS mice in comparison to F1 AS mice (Fig 4.12 B). The expression of miR-135a was combined for both generations and split according to gender. There was no significant differences between miR-135a levels in female or male mice (Fig 4.12 C&D, $p>0.05$). Next, we sought to determine if the expression of miR-21 was altered between genotypes, generation and gender. Levels of miR-21 were similar in WT and AS mice from the F1 generation (Fig 4.12 E, $p>0.05$). In comparison to F1 mice, the expression of miR-21 in N4 mice was decreased but significantly decreased (Fig 4.12 F, $p>0.05$). Finally there were no differences detected in miR-21 between genders (Fig 4.12 G&H, $p>0.05$).

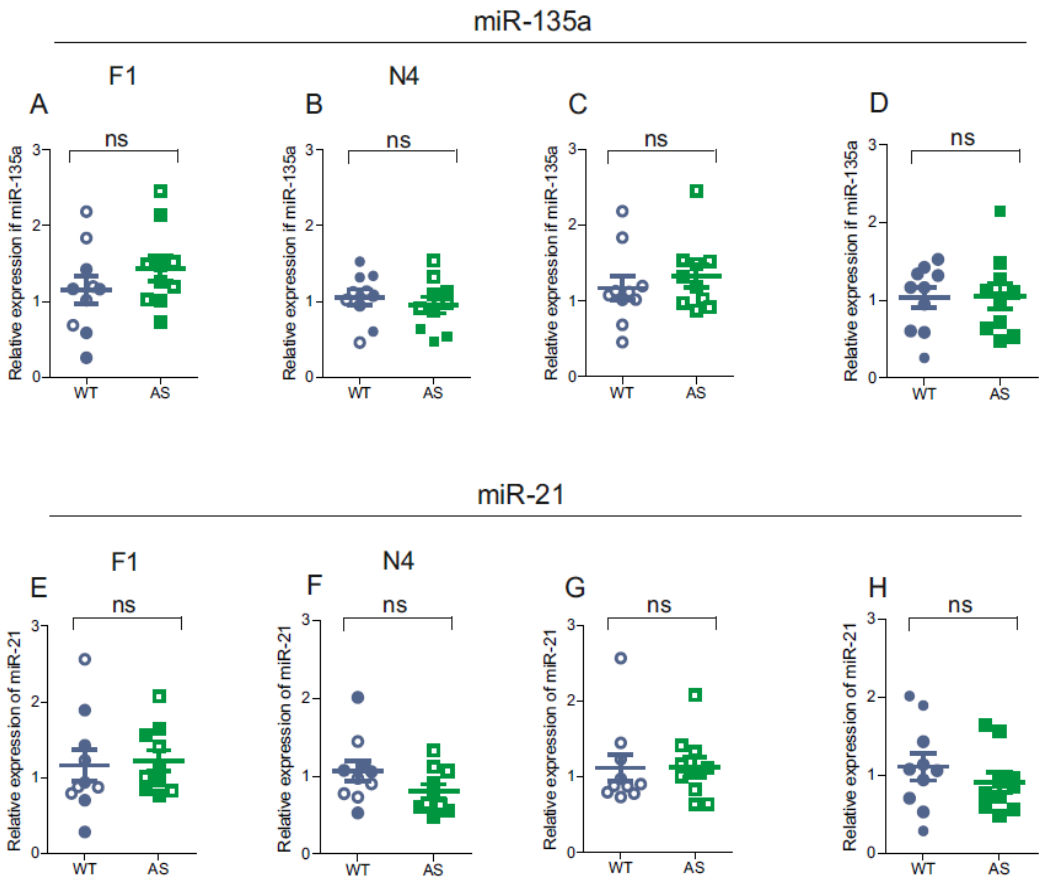

Figure 4.12 Epilepsy regulated miRNAs are not altered in F1 and N4 P21 mice
The expression of epilepsy regulated miRNAs were analysed in naïve F1 and N4 P21 mice. **(A)** Relative expression of miR-135a in F1 male and female mice, WT/AS n=10/group, p=271. **(B)** Relative expression of miR135a in N4 male and female mice, WT/AS n=10/group, p=0.496. **(C)** Relative expression of miR-135a in F1 and N4 female mice combined, WT/AS n=10/group, p=0.476. **(D)** Relative expression of miR-135a in F1 and N4 male mice combined, WT/AS n=10/group, p=0.933. **(E)** Relative expression of miR-21 in F1 mice, WT/AS n=10/group, p=0.793. **(F)** Relative expression of miR-21 in N4 mice, WT/AS n=10/group, p=0.130. **(G)** Relative expression of miR-21 in F1 and N4 female mice combined, WT/AS n=10/group, p=0.962. **(H)** Relative expression of miR-21 in F1 and N4 male mice combined, WT/AS n=10/genotype, p=0.365. U6b was used as a normaliser. Data are expressed as standard error mean. A *t*-test was used for analysis between WT and AS mice.

4.2.13 Analysis of miR-134 and its targets in adult F1 mice

Following on from the molecular characterisation of the P21 model, we analysed the expression of miR-134 and a number of its targets in naïve adult (P42-P60) AS mice and compared with age-matching littermates WT controls. In mature mice, the expression of miR-134 did not differ between genotypes (Fig 4.13 A, $p>0.05$). As regards miR-134 targets, we verified that there was a slight, but not significant, decrease in DCX levels in AS mice in comparison with WT group (Fig 4.13 B, $p>0.05$). Levels of limk1 and pum2, validated targets of miR-134 and previously found to be increased in P21 mice, did not present differences between WT and AS mice (Fig 4.13 C&D, $p>0.05$). Likewise, the expression of serpine1, a predicted target of miR-134, remained unchanged in adult WT and F1 AS mice (Fig 4.13 E, $p>0.05$).

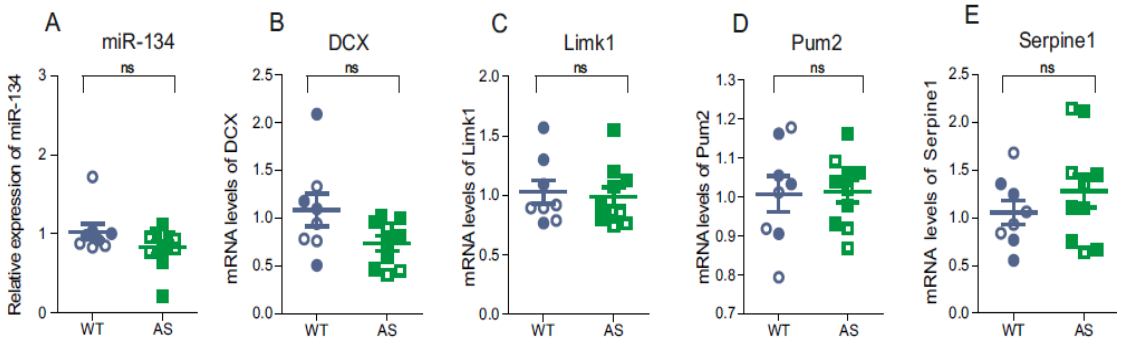

Figure 4.13: miR-134's targets and markers of neuron
qPCR was used to analyse levels of miR-134 and its targets in the hippocampus of adult mice. Levels of neuronal markers were also analysed in these mice. **(A)** Relative expression of miR-134 in the hippocampus, WT n=8, AS n=10, p=0.14. **(B)** mRNA levels of DCX in the hippocampus, WT n=8, AS n=10, p=0.06. **(C)** mRNA levels of limk1 in the hippocampus, WT n=8, AS n=10, p=0.74. **(D)** mRNA levels of pum2 in the hippocampus, WT n=8, AS n=10, p=0.90. **(E)** mRNA levels of serpine1 in the hippocampus, WT n=8, AS n=10, p=0.33. MiR-124 was used as a normaliser of miR-134 levels. ß-actin was used as a normaliser for miR-134 target analysis. Data are expressed as standard error mean. t-tests were used for statistical analysis. A Shapiro-Wilk test was used to test for normality.

4.3 Discussion

The present chapter aimed to establish the behavioural, electrophysiological and molecular phenotypes in AS mice that might be targetable using a miR-134-based therapy. Using the *Ube3a* $^{(m-/p+)}$ mouse, we found AS mice display resting abnormalities in their EEG, seizure susceptibility and motor impairments. We did not detect statistically significant increases in levels of miR-134 or reductions of most of its validated targets. (Reschke et al., 2017b) Together, the results provide a range of phenotypes to study the effects of antagomirs targeting miR-134.

Mouse models of AS have been highly successful in recapitulating multiple features of the human condition and have been useful in evaluating experimental molecular therapies. The objective of the present chapter was to establish which of the reported phenotypes were identifiable in our mice, that might later be evaluated as read-outs of the efficacy of an introduced antimir therapy targeting miR-134. Two main approaches were taken, focusing on two different ages and two generations of the AS mice, achieved by alternate backcrossing. P21 was selected on the basis that miR-134 inhibition can reduce seizures in WT mice at this age and because many symptoms of AS are present in early childhood including motor impairment, developmental delay, abnormal EEG and epilepsy (Clayton-Smith, 1993, Clayton-Smith and Laan, 2003).

The first important finding was that AS model mice display an overt EEG phenotype. EEG phenotypes are well known in AS patients and can be recorded from a young age. In particular, notched delta has been observed in patients as young as 14 months (Korff et al., 2005). They are thought to reflect altered network communication within the brain and may reflect disruption to circuits involved in cognition and sleep (Sidorov et al., 2017, Frohlich et al., 2019a). Here, we detected EEG frequency differences in AS mice at P21, an age equivalent of early childhood in humans (Laviola et al., 2003). The difference was an increase in theta range and lower beta. Increased theta activity has been reported in another epilepsy syndrome known as myoclonic-astatic epilepsy (Doose syndrome), which is also associated with cognitive impairment (Doose, 1992). Theta activity has also

been thought to reflect fear expression, as studies have shown that its increased during fear-conditioning (Stujenske et al., 2014), though its link to AS has not yet been elucidated. Beta activity has been hypothesised to indicate changes in excitatory-inhibitory feedback (Frohlich et al., 2019a, Jensen et al., 2005). A decrease in beta frequency has been described recently in children with AS; however, it is unclear if it is present in mouse models of AS (Frohlich et al., 2019a). A decrease in beta power is suggestive of abnormalities in GABAergic signalling as drugs acting on GABAergic transmission such as benzodiazepines, are known to increase beta power, therefore indicating deletion of Ube3a results in the loss of GABA receptors (Greenblatt et al., 1989). By adulthood, we saw an additional EEG feature emerged, with greater overall total power in the resting EEG of AS mice, though beta frequency remained the same between both genotypes. This result was not entirely unexpected as altered levels of beta power have only been reported thus far in children with AS, suggesting that this abnormality may no longer be present in adults. Moreover, the GABAergic system plays crucial roles in brain development, suggesting that dysfunction of GABAergic transmission may only occur at a young age in AS, thus a beta phenotype may not be present at a later age. Our EEG findings differ somewhat to previous studies which reported increases in delta activity (Sidorov et al., 2017, Frohlich et al., 2019a, Valente et al., 2006a). This could be due to the time of day that EEG was recorded, as delta is most prominent at night. Furthermore, delta abnormalities have been found to be more increased in AS patients with a deletion in comparison to those with other mechanisms of AS (Frohlich et al., 2019a), suggesting the *Ube3a* deletion in our mouse model may not recapitulate the entirety of the abnormal EEG. Lastly, the placement and depth of electrodes could affect the amount of delta signal identified. The EEG phenotype might reflect ongoing changes to neuronal circuits and increased hyperexcitability. Indeed, rates of epilepsy in AS patients show a bimodal distribution, with rates highest at an early age, a decline in late adolescence and a recurrence in seizures in adults (Larson et al., 2015). Consistent with this idea, adult mice responded to chemoconvulsant exposure with earlier onset seizures in the KA model, and increased seizure severity in the PTZ

model, indicating that AS mice may be more susceptible to subconvulsant doses.While the doses of both chemoconvulsants used induced a marked seizure phenotype in AS mice, there were no changes in immediate early gene markers such as *Arc* and *c-fos*. This suggests that the doses used may not have been sufficient enough to induce changes. However, it is more likely that RT-qPCR was not the optimal way to detect *c-fos* and *Arc* expression. In-situ hybridisation or immunohistochemistry could be used in future experiments. This implies a subtle, select defect in inhibition in the AS mice. Indeed, studies have shown that there is a decreased in tonic inhibition in cerebellar granule cells in a mouse model of AS and contributing to this, loss of *Ube3a* causes a reduction in the degradation of GABA transporter 1 (GAT1), thus resulting in lower levels of GABA (Egawa et al., 2012).

We did not observe spontaneous seizures (ie epilepsy) in the AS mouse model. This indicates that any defects in inhibition fall below the level where synchronous discharges of neurons is possible. We did, however, find that sound-induced seizures could be evoked in AS mice once backcrossed. The seizures, triggered by short-lasting vigorous cage lid scratching, featured tonic-clonic components and lend themselves to Racine-type quantification. This is consistent with other reports (Jiang et al., 1998, Sonzogni et al., 2018). This is an important phenotype in the model because it allows anti-seizure assessments of the miR-134 inhibition in a genetic rather than chemoconvulsant model, which has not previously been attempted (Morris et al., 2019). AS mice presented with an increase in seizure susceptibility when challenged with KA or PTZ. This was characterised by a shorter onset to the first seizure and an increase in total EEG power. However, this effect between WT and AS mice was modest and therefore it would be challenging to detect anti-seizure effects.

AS mice displayed a number of other phenotypes. This included a strong motor and coordination deficit. Movement and coordination are prominent features of AS in patients and here we observed much-reduced movement in both open field and rotarod performance. The cause of this is uncertain but studies have hypothesised that the loss of tonic inhibition from cerebellar granule cells may be involved in motor dysfunction

(Egawa et al., 2012). Indeed, it was shown that pharmacological targeting of tonic inhibition with THIP, a $GABA_A$ receptor agonist improved ataxic like movements in AS mice (Egawa et al., 2012). It remains possible that the underlying network defects that produce the EEG features are also responsible for disrupting brain functions that coordinate these activities. The phenotype could also be related to the hyperexcitability features. Indeed, epileptic mice perform worse in the open field. However, the reduced movement and rotarod are not common in epileptic mice and are therefore likely related to defects outside the hippocampus. For example, studies have demonstrated that loss of dopaminergic neurons in AS mice in the nigrostriatal pathway and the cerebellum may contribute to the motor dysfunction present in AS (Mulherkar and Jana, 2010). Conversely, results from Elgersma's lab fo with the cerebellum, as *Ube3a* reinstatement in the cerebellum did not rescue these deficits, though it did rescue cerebellar learning deficits (Bruinsma et al., 2015).

There was also an impairment present in AS mice in the marble burying test. This test can be used to analyse the innate behaviours in mice and it is based on the concept that mice will detect marbles as harmful objects and proceed to bury them (Deacon, 2006b). We found a significant reduction in the number of marbles buried in AS mice, suggesting that AS mice do not exhibit naturalistic behaviours. Furthermore, studies have shown that hippocampal lesions lead to a reduction in marble burying performance, indicating that this test could also be used to test hippocampal function, although further work is required to elucidate the underlying mechanisms (Deacon and Rawlins, 2005). Indeed, there have been reports of impaired learning and memory caused by neuronal dysfunction in AS (Jiang et al., 2010, Wallace et al., 2012).

A significant limitation in this chapter was the inability to test cognition in these mice. As our mice had impairments in locomotor activity, we could not test their performance in novel object recognition due to their inability to explore objects. Future work could use fear conditioning to build on the characterisation of this model as previous work has shown AS mice present with deficits in contextual fear conditioning, building on the hypothesis of hippocampal dysfunction in AS (Huang et al., 2013). In accordance, we did

not detect an anxious phenotype in the light-dark box test, this result may be governed by the decrease in locomotor activity and motor impairments, resulting in a reduction in number of transitions into each compartment.

The present study included both sexes for all experiments. Overall, there were few sex differences and this is in agreement with literature as AS affects both genders equally (Sonzogni et al., 2018). However, we did note that AS male mice performed worse on the rotarod than AS females but this was associated with an overall reduction of time spent on the rotarod in male mice as WT males were comparable to AS females. Furthermore, WT females performed significantly better than both genotypes of male mice. The nature of this sex difference is unclear as the exploration time of genders were comparable in both genotypes in the open f work, as they found similar sex differences on the rotarod (Sonzogni et al., 2018). They delved further into this sex phenotype, however the decrease in male performance was not correlated to weight, as male mice are generally heavier than females (Sonzogni et al., 2018).

The hyperexcitable phenotype, particularly in adults where EEG total power was greater, is consistent with our hypothesis that loss of Ube3a would de-repress miR-134 and increase miR-134 levels in the mice. However, measurement of total miR-134 levels in the hippocampus and cortex of P21 and P42 mice did not reveal significant differences. Nor did we detect consistent changes to levels of miR-134 targets. It is possible that the amount of miR-134 buffering that is lost in AS is too small to detect using this approach. An analysis of hippocampal subfields might be more likely to detect site-specific alterations in miR-134 levels. Ago-based analysis or analysis of levels of miR-134 in synaptic fractions, a key site for miR-134 targeting of Limk1, might yield different results. Notably, levels of Serpine1, a recently identified target were lower in AS mice, consistent with our hypothesis. Regardless, previous studies have shown that increased miR-134 levels is not essential for antimir-134 to produce anti-seizure effects in animal models (Reschke et al., 2017b).

The majority of this characterisation focused on the F1 generation of mice. In the future it would be of benefit to characterise the N4 generation to this extent as due to the presence of spontaneous seizures and the ability to induce audiogenic seizures in them, it is quite possible that these mice could be used to model a more severe form of AS. As mentioned previously, the severity of AS is dependent on the genetic mechanism of disease and there are usually two phenotypes of different severity which arise, thus it would be highly beneficial to fully characterise both models to allow to determine the efficacy of new therapeutics on both levels of severity. Furthermore, due to time restraints and breeding issues, we did not analyse plasma in these mice which could have been used to identify a potential miRNA biomarker.

In summary, we have characterised a mouse model of AS that translates to a number of phenotypes present in AS patients. By doing so, this model can be used to determine if some phenotypes can be restored by antagomir testing. It was important to characterise the model at two different ages as AS begins at a young age and is still present in adulthood. The majority of research using this mouse model is focused on adult mice (Sonzogni et al., 2018, Gu et al., 2019b). This may because of the high percentage of mortality associated with audiogenic seizures in young mice (Mandel-Brehm et al., 2015). While we did not detect dysregulation in miR-134 in our model, one of miR-134s targets, serpine1 was downregulated in P21 AS mice, indicating miR-134 could play a pathophysiological role in AS.

4.4 Conclusion:

The present chapter studies have illustrated that by using the *Ube3a* $^{(m-/p+)}$ mouse model we can successfully recapitulate a number of phenotypes that are present in AS patients. In order to develop new therapeutics to treat AS we first sought to characterise our mouse model using two different ages (P21 and adult) and two different generations (F1 and N4). It was found that AS mice had impairments in locomotor activity, motor coordination and naturalistic animal behaviours as analysed by marble burying.

Furthermore, AS mice had a distinctive EEG phenotype that consisted of an increase in total power, an elevation of theta spectral power and diminished beta power. One caveat to the EEG analysis performed here is that we performed cortical recordings and may have missed non-cortical activity. Significantly, audiogenic seizures were successfully induced in N4 P21 mice. One limitation of this study was that we did not identify any significant alterations in the levels of miR-134 or its known targets. This analysis was focused on the hippocampus and cortex and not any other brain regions, suggesting that alterations in miR-134 could be found to be dysregulated elsewhere.

5 Chapter five

Results III

Overview:

5.1 Introduction

Angelman syndrome patients suffer from a range of symptoms including ataxia, cognitive impairment and drug-resistant epilepsy. A number of medicines are used to control these symptoms, including various AEDs for seizure control, but there is limited efficacy and none of the available treatments modify or reverse the established phenotype. The multifaceted nature of AS symptoms is a particular challenge for the development of treatments. Efforts are underway to re-activate the paternally-silenced copy of the *UBE3A* gene (Silva-Santos et al., 2015). The prominence of drug-resistant epilepsy in AS and the recent discovery that the Ube3a1 transcript harbours a miR-134 binding site raised the possibility that targeting miRNA could be an alternative treatment approach (Valluy et al., 2015). Noteworthy, one single miRNA can have several different targets, indicating the potential to treat multiple symptoms (Peter, 2010, Selbach et al., 2008, Lim et al., 2005). AS mice display behavioural phenotypes, abnormal EEG and appear to be susceptible to seizures. As previous work in our lab and research presented in chapter 3 has shown, blocking miR-134 using an antagomir is seizure suppressive and neuroprotective in age-relevant seizure models. In this final chapter, we sought to determine if Ant-134 could be used as a novel therapeutic target for AS.

5.2 Hypothesis

Inhibition of miR-134 will reverse the characteristic AS-like phenotypes including seizure susceptibility, abnormal EEG and motor impairments in the Ube3a $^{(p+/m-)}$ mouse model.

5.3 Aim

To determine if Ant-134 can reverse AS-like phenotypes. Specifically, we investigated the effect of Ant-134 on resting EEG, audiogenic seizures and behavioural phenotypes.

5.4 Methods

EEG: To test the effect of Ant-134 on the abnormal EEG background, F1 AS adult mice were pre-treated with either 0.5 nmol Scr or Ant-134 (ICV) and 24 hours later EEG was recorded for 4-6 hours. Labchart and Matlab were used for analysis. **Behaviour:** To determine if the AS-like behavioural phenotypes could be rescued using Ant-134, F1 AS P21 mice were pre-treated with either Scr or Ant-134. Twenty-four hours later, P21 mice underwent a series of behavioural tests to determine if Ant-134 restored phenotypes seen in AS mice. These behavioural tests were repeated when the mice were 6 weeks old. **Audiogenic seizures:** To test the efficacy of Ant-134 on a genetic epilepsy, we backcrossed mice using the 129 strain to generation N4, which yielded mice that were susceptible to seizures induced by a loud scratching stimulus, as previously described. AS mice were injected ICV with Scr or Ant-134 at P21 and audiogenic seizures were induced at P22, P24 and P26. This experiment was also performed in another cohort of adult mice where seizures were induced every second day. A modified Racine score, as previously described, was used to analyse seizure severity. To analyse the effects of Ant-134 on seizure protection during audiogenic seizures, western blotting was used for protein analysis and qPCR was used for mRNA analysis. **Small RNA sequencing:** Small RNA sequencing was performed on naïve WT and Het P21 mice from generation F1 and N4. MiRNA sequencing data were uploaded to the Chimira webserver (Vitsios and Enright, 2015) where the sequences were adapter trimmed and mapped against miRBase v22 hairpin sequences (Kozomara et al., 2019) to generate count-based miRNA expression data. MiRNA differential expression analyses were performed using R/Bioconductor utilizing EdgeR (Robinson et al., 2010) and Limma packages (Ritchie et al., 2015) following the protocol by Law et al (Law et al., 2016). A miRNA was considered to be differentially expressed if the p value was less than 0.05.

5.5 Results

5.5.1 Inhibition of miR-134 in Ube3a $^{(p+/m-)}$ model

Before commencing any corrective tests with Ant-134, the percentage of knockdown of miR-134 was first analysed. To determine if the ICV coordinates were correct in the Ube3a $^{(p+/m-)}$ model, ink injections were performed in both female and male mice from the N4 generation. An injection presented in Fig 51.Aillustrates the distribution of ink throughout the ventricles and into surrounding areas in both genders. Once the ICV coordinates were confirmed, the percentage of knockdown of miR-134 was analysed. Here, using a dose that had seizure suppressive effects in chapter 3, 0.1 nmol resulted in roughly 55% knockdown in F1 AS mice (Fig 5.1 B, $p<0.05$). Next, the same dose was tested in N4 mice and similar results were obtained. There was a 56% knockdown of miR-134 in Ant-134-injected mice (Fig 5.1 C, $p<0.05$). As a functional readout of miR-134 silencing we measured levels of DCX, a validated target of miR-134 (Gaughwin et al., 2011), in the same samples. There was a trend for an increase in DCX, though this did not reach significance (Fig 5.1 D, $p>0.05$). Next, the levels of Limk1 and Creb1 were analysed as previous work from our group has shown that Ant-134 prevented the expected reduction in their levels induced by SE (Jimenez-Mateos et al., 2012). However, expression of Limk1 and Creb1 did not change between Scr-treated and Ant-134-treated mice (Fig 5.1 E&F, $p>0.05$). Finally, the percentage of knockdown using a higher dose, 0.5 nmol was tested in N4 mice. This resulted in roughly 88% knockdown of miR-134 in Ant-134-injected mice (Fig 5.1 G, $p<0.05$). As above, targets of miR-134 were analysed after the dose was increased. There was a strong trend for an increase in DCX expression in Ant-134 treated mice in comparison to Scr-treated (Fig 5.1 H, $p>0.05$). Similarly to results obtained with the lower dose, levels of Limk1 and Creb1 were not altered in Ant-134-treated mice (Fig 5.1 I&J, $p>0.05$).

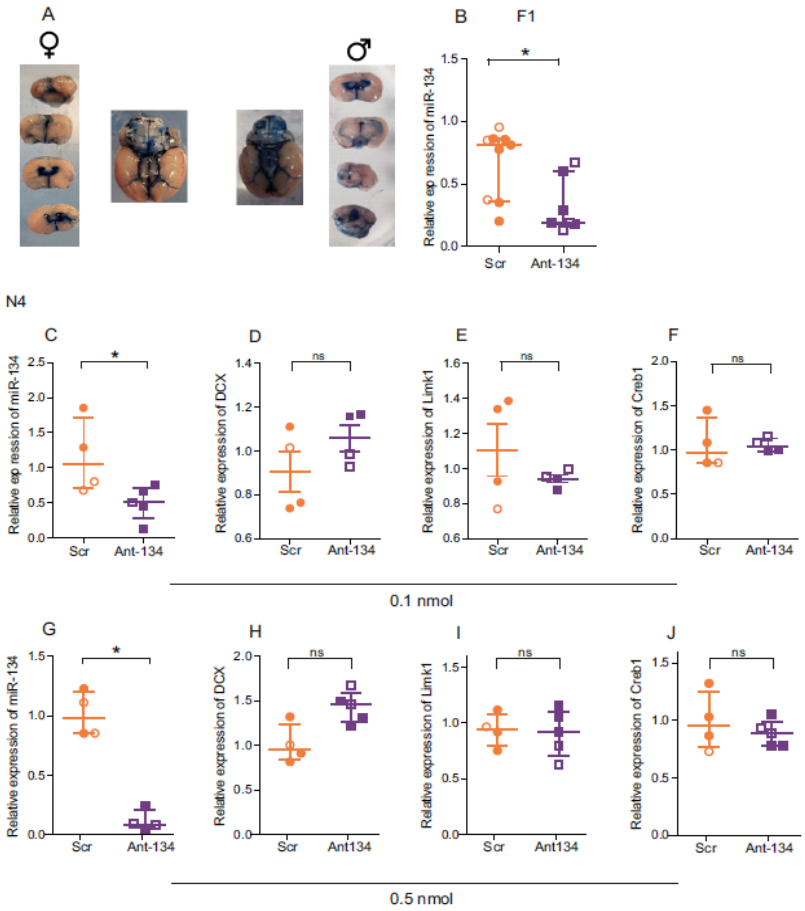

Figure 3: Inhibition of miR-134 in Ube3a (p+/m-) model

The ICV coordinates and percentage of knockdown of miR-134 were tested in F1 and N4 mice using two different doses of Ant-134. **(A)** Ink injection into the ventricles of P21 female and male N4 mice. **(B)** Relative expression of miR-134 in AS mice in Scr-injected or Ant-134-injected mice, AS-Scr n=9, AS-Ant-134 n=7, p=0.017. 55% knockdown of miR-134 in AS mice. **(C)** Relative expression of miR-134 in N4 mice after 0.1 nmol knockdown, Scr n=4, Ant-134 n=5, p=0.032, 56% knockdown of miR-134. **(D)** Relative expression of DCX 24h after ICV injection of Scr/Ant-134, n=4/group, p=0.34. **(E)** Relative expression of Limk1 after ICV injection of Scr/Ant-134, n=4/group, p=0.88. **(F)** Relative expression of Creb1 after ICV injection of Scr/Ant-134, n=4/group, p=0.77**. (G)** Relative expression of miR-134 in N4 mice after 0.5 nmol knockdown, n=4/group, p=0.02. **(H)** Relative expression of DCX following ICV injection of Scr/Ant-134, Scr n=4, Ant-134 n=5, p=0.063 **(I)** Relative expression of Limk1 following ICV injection of Scr/Ant-134, Scr n=4, Ant-134 n=5, p=0.885. **(J)** Relative expression of Creb1 following ICV injection of Scr/Ant-134, Scr n=4, Ant-134 n=5, p=0.90. U6b was used as a normaliser for miRNA analysis following knockdown. ß-actin was used as a normaliser during miR-134 target analyses. A Shapiro-Wilk test was used to check for normality. Data did not pass normality testing. A Mann Whitney test was used for comparison between Scr and Ant-134 groups. Data are expressed as interquartile range. Closed squares and circles represent male mice, open squares and circles represent female mice.

5.5.2 Inhibition of miR-134 improves motor impairment in F1 P21 AS mice

AS mice display a significant motor deficit (see Chapter 4), which may be a model for the impaired movement and ataxia in patients. We next explored whether Ant-134 has any effects on this phenotype. To test the efficacy of Ant-134 on the motor phenotype, AS mice received an ICV injection of Scr or Ant134 (0.1 nmol/2µL). Mice underwent a battery of behavioural tests 24 hours later, including the open field, rotarod and marble burying. AS mice which received the Scr compound displayed reduced exploration time in the open field consistent with the expected motor deficit in AS mice (Fig 5.2 A, $p<0.001$). Remarkably, Ant-134-treated mice exhibited a significant increase in exploration rate, (Fig 5.2 A, $p<0.001$). Ant-134 treatment prevented the expected low exploration phenotype characteristic of the AS mice when compared to AS-Scr group. A number of open field parameters from AnyMaze tracking software were also analysed. This included distance travelled (cm) and entries into inner zone (Fig 5.2 B&C). In these parameters, there was a slight decrease in performance in AS Scr mice in comparison to Ant-134-treated mice, however, this was not significant (Fig 5.2 B, $p>0.05$). In addition to the increase in exploration time, there was also a significant increase in the entries into inner zone, which is also a measure of anxiety (Fig 5.2 C, $p<0.05$). A representative track plot from Scr and Ant-134 mice demonstrates the decrease of overall activity in the Scr mice and a decrease in inner zone crossings (Fig 5.2 D).

Next, we tested whether Ant-134 could correct motor incoordination on the rotarod. There was no difference in latency to fall during the rotarod between Scr-treated and Ant-134-treat, indicating that Ant-134 did not have any significant effect in the rotarod test (Fig. 5.2 E, $p>0.05$). Similarly in marble burying, there was no effect of treatment on marble burying, both groups of mice did not perform well in this paradigm (Fig. 5.2 F, $p>0.05$).

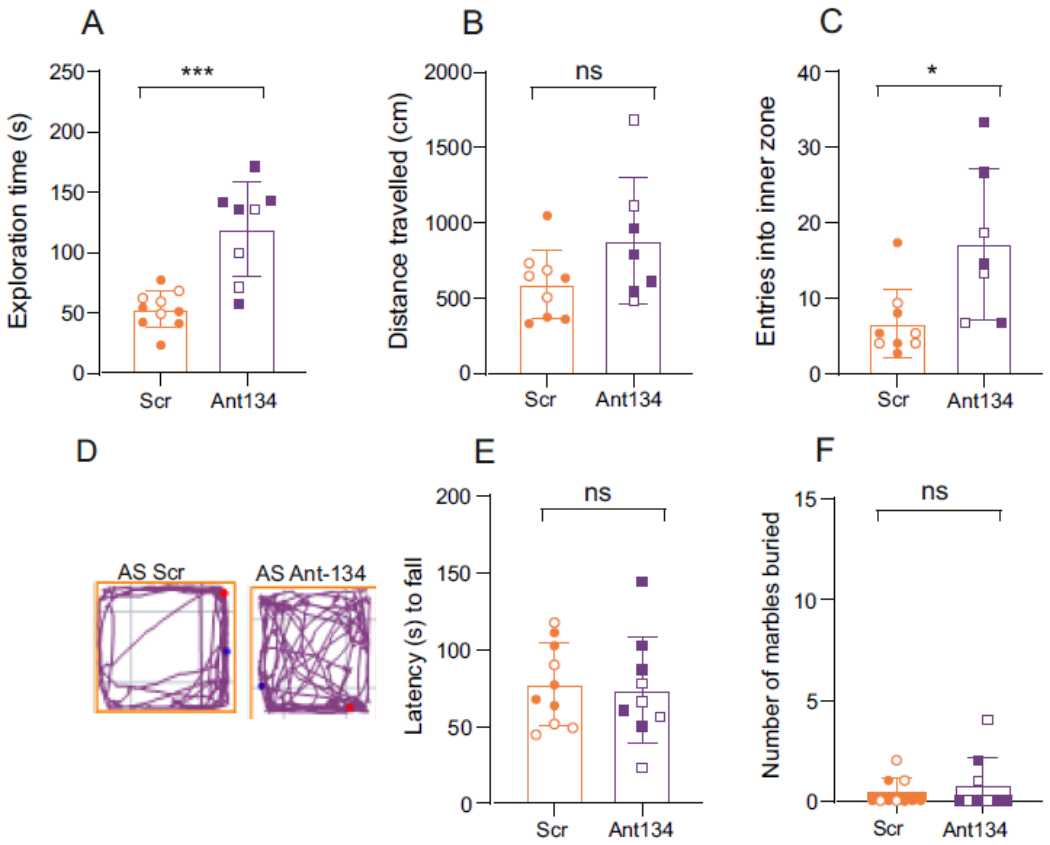

Figure 4: Pre-treatment with Ant-134 partially restores motor impairment in F1 mice. P21 F1 AS mice underwent a series of behavioural tests following pre-treatment with either Scr or Ant-134. **(A)** Exploration time (s) during open field in P21 mice, Scr n=10, Ant-134 n=8, p=0.0002. **(B)** Distance travelled (cm) in open field arena, Scr n=9, Ant-134 n=7, p=0.09. **(C)** Number of entries into inner zone of open field, Scr n=9, Ant-134 n=7, p=0.013. **(D)** Track plot of representative Scr and Ant-134 mouse. **(E)** Latency to fall (s) on accelerating rotarod, Scr n=10, Ant-134 n=9, p=0.81. **(F)** Number of marbles buried during 30 min marble burying test, Scr n=10, Ant-134 n=9. P=0.75. A t-test was used for analysis between Scr and Ant-134-treated mice.

5.5.3 Long-term effects of Ant-134 on motor phenotype

The same cohort of mice was re-tested 3 weeks later in order to assess the presence of any long term effects of Ant-134 on AS phenotypes. This was done to determine the duration of effect of Ant-134 and whether or not effects on motor activity were long-lasting. The mice underwent the same behavioural tests as at P21.

While there was an overall reduction in exploration time in both groups of mice, adult Scr mice still presented with a motor deficit as evident by the decrease in exploration time (Fig 5.3 A, $P>0.05$). Ant-134 prevented the expected low exploration rate in in comparison to Scr-treated mice, though this narrowly missed significance (Fig 5.3 A, $p=0.053$). The effects seen at P22 were not sustained when analysing other parameters such as distance travelled and entries into inner zone. Though there was a slight, but not significant, increase in distance travelled and entries into inner zone in Ant-134-treated mice (Fig 5.3 B&C, $p>0.05$). Track plots of the open field activity in adult mice highlight that Ant-134-treated AS mice display more movement in the open field than Scr-treated AS mice (Fig 5.3 D). Similarly to the results obtained above, Ant-134 did not rescue deficits in the rotarod or marble burying (Fig 5.3 E&F, $p>0.05$).

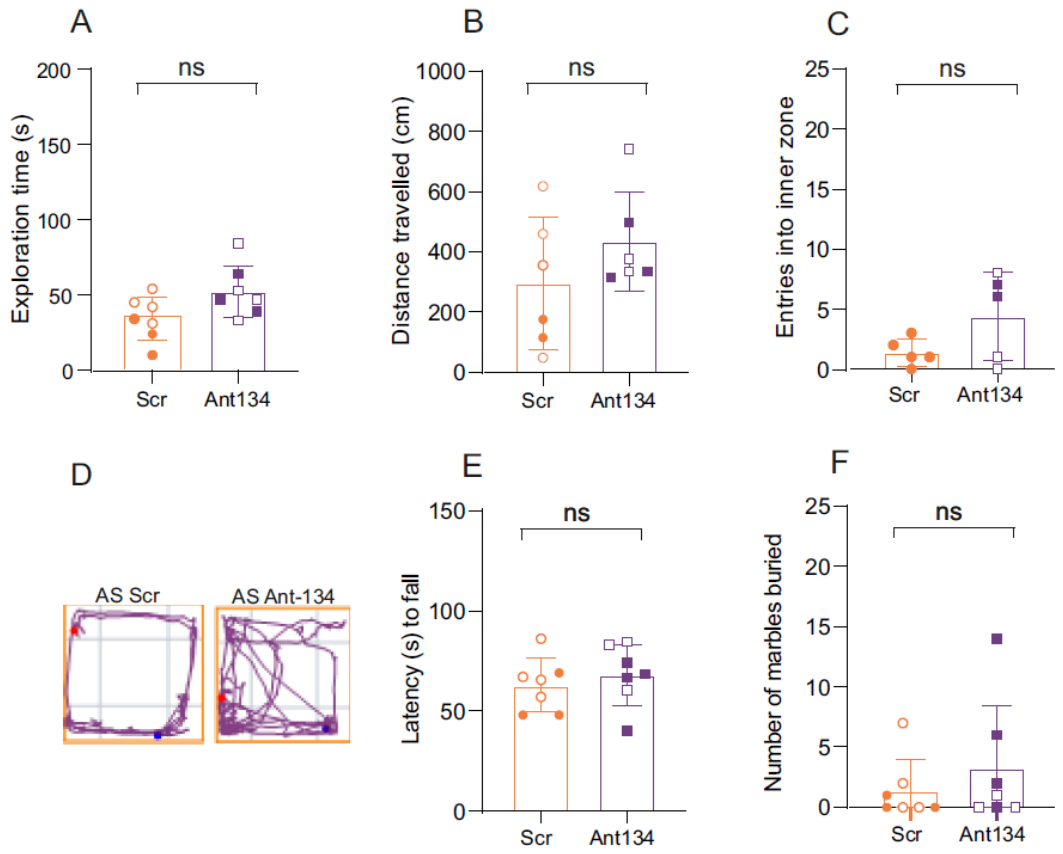

Figure 5: Effects of Ant-134 are not evident during re-testing in adult mice

Mice were re-tested 3 weeks later at P42 and put through the same behavioural tests. **(A)** Exploration time (s) during open field in adult mice, Scr n=7, Ant-134 n=7, p=0.053.**(B)** Distance travelled (cm) in open field arena, Scr n=6, Ant-134, n=6, p=0.245. **(C)** Entries into inner zone of open field arena, Scr n=5, Ant-134 n=5, p=0.117. **(D)** Track plot of representative Scr and Ant-134 mouse in open field arena. **(E)** Latency to fall (s) on rotarod, Scr n=7, Ant-134 n=7, p=0.50. **(F)** Number of marbles buried, Scr n=7, Ant-134 n=7, p=0.60. A *t*-test was used for analysis between Scr and Ant-134-treated mice.

5.5.4 Effect of Ant-134 on resting EEG phenotypes in adult AS mice

Studies in chapter 4 determined there was an abnormal EEG in adult F1 generation AS mice, comprising higher EEG total power and increased theta band activity. We first investigated whether inhibition of miR-134 using Ant-134 had any effects on resting EEG phenotypes in AS model mice. Adult mice were selected due to the more prominent phenotype at this age (see Chapter 4). Under anaesthesia, AS F1 male and female adult mice aged P42-P60 were implanted with electrodes and given an ICV injection of 0.5 nmol Scr or Ant-134. Then, 24 h later, resting EEG was recorded for 4-6 hours. From this, the percentage of total power over this time period was calculated per mouse. The individual frequency bands were also analysed as before.

Resting EEG total power in Scr-injected F1 AS adult mice averaged 6000 μV^2 which was similar to the level in adult AS model mice previously described (see Chapter 4). AS mice injected with Ant-134 had similar resting EEG total power to Scr-injected mice indicating Ant-134 does not correct this phenotype (Fig 5.4 A, $p>0.05$). A representative EEG trace for mice injected with Scr and Ant-134 can be seen in Fig 5.4 B. A zoomed in section of the EEG recording was taken from each mouse (Fig 5.4 B i&ii). Next, as we previously reported an increase in theta frequency, we examined if Ant-134 had an effect on individual frequency bands. There was no effect of Ant-134 on theta frequency (Fig 5.4 D, $p>0.05$). The average percentage of total power of delta treated with Scr was 22.7% and 24.1% for Ant-134 (Fig 5.4 C, $p>0.05$). The average percentage of total power of theta treated with Scr was 26.1% and 26.8% for Ant-134 (Fig 5.4 D, $p>0.05$). The average percentage of total power of beta treated with Scr was 32.9% and 31.9% for Ant-134 (Fig 5.4 E, $p>0.05$). Lastly, the average percentage of total power of alpha treated with Scr was 18.2% and 17.11% for Ant-134 Here, we saw a trend for a decrease of alpha frequency in the Ant-134 group, however this was not significant (Fig 5.4 F, $p>0.05$).

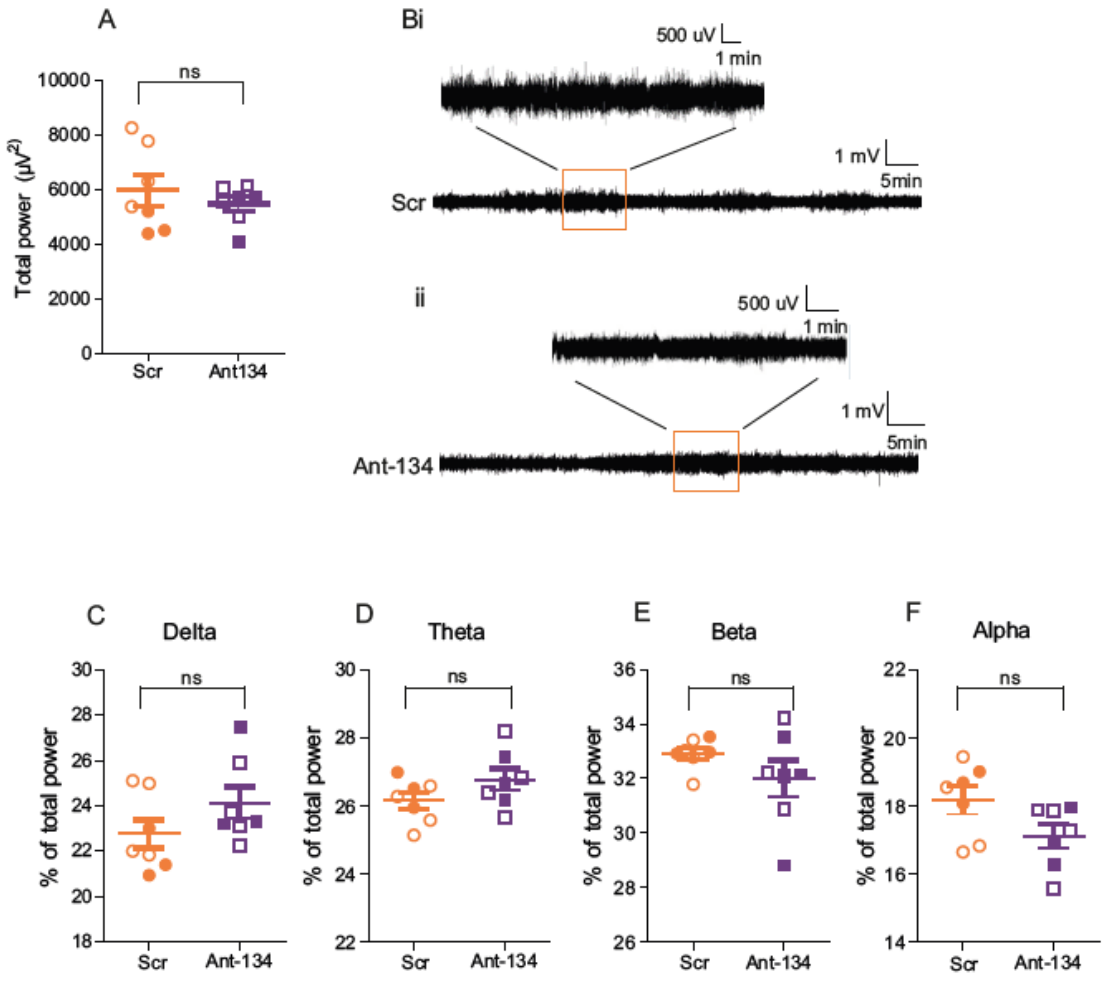

Figure 6: Ant-134 on baseline EEG in adult F1 AS adult mice.
F1 adult mice were pre-treated with Scr/Ant-134 and resting EEG was recorded 24 h later. **(A)** Total power (μV^2) of baseline EEG in Scr and Ant-134 mice, n=7/group, p=0.45. **(B)** Representative EEG traces for Scr and Ant-134 mice of 1 h recordings, scale bar 1 mV, 5 min. Zoom scale bar shows 10 minute recording, 500 uV, 1 min. **(C)** % of total power of delta, n=7/group, p=0.17. **(D)** % of total power of theta, n=7/group, p=0.14. **(E)** % of total power of beta, n=7/group, p=0.21. **(F)** % of total power of alpha, n=7/group, p=0.06. Closed circles and squares represent male mice, open circles and squares represent female mice. *t*-test was used for statistical analysis between WT and AS mice. Data are expressed as standard error mean. A Shapiro-Wilk test was used to test for normality.

5.5.5 0.1 nmol dose of Ant-134 does not protect against audiogenic seizures in young N4 AS mice

Next, we sought to determine if Ant-134 could affect seizure susceptibility of AS mice. Here we used N4 backcrossed mice which were specifically bred for seizure susceptibility as described in Chapter 4. To explore the relationship between miR-134 levels and effects on seizures we first tested the same dose of Ant-134 which was effective in altering the motor deficits in F1 AS mice. AS mice were injected with 0.1 nmol of either Scr or Ant-134 and their response to audiogenic seizures were tested. 24 h later, mice were subjected to the first audiogenic seizure followed, with 48 h intervals, by two further audiogenic seizure challenges at P24 and P26. A modified Racine scale was used to score the severity of audiogenic seizures, ranging from 0-4, with 0= no seizure, 1=wild running, 2=tonic-clonic convulsions, 3=hyperextension of hind limbs and 4=death, as before. At P27, 24 h after the final evoked seizure, the mice were culled (Schematic Fig 5.5. B).

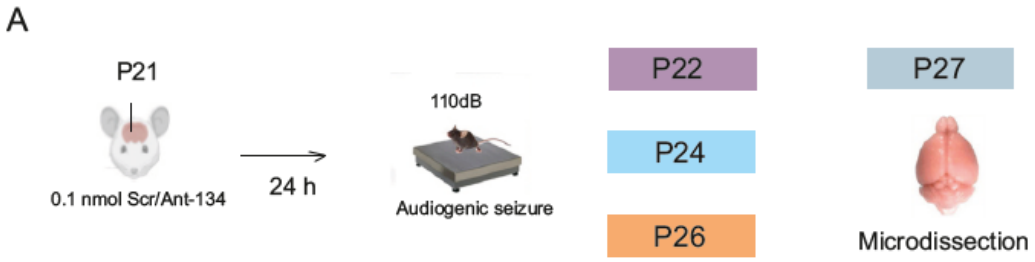

Figure 5.5: Experimental design of Ant-134 (0.1 nmol) in the audiogenic seizure model N4 AS mice were pre-treated with Scr/Ant-134. **(A)** Schematic of experimental design for antagomir testing in the audiogenic seizure model. Mice received an ICV injection of Scr/Ant134 and seizures were induced 24 h later at P22. Seizures were repeated at P24 and P26. Mice were culled and micro dissected 24 h after the final seizure.

The audiogenic stimulus elicited strong tonic-clonic seizures in Scr-treated AS mice on each of the three test days. A tabular representation shows the severity of each mouse during the audiogenic seizure trial (Fig 5.6 A). AS mice injected with 0.1 nmol Ant-134 displayed similar audiogenic seizure severity on the first test day to Scr-injected mice indicating no protective effects of Ant-134 on seizure severity (Fig 5.6 B, $p>0.05$). Seizure severity was also similar in Ant-134 mice during the second (P24) and third seizure (P26) (Fig 5.6 C). Thus, at 0.1 nmol, Ant-134 does not protect against audiogenic seizures in young AS mice.

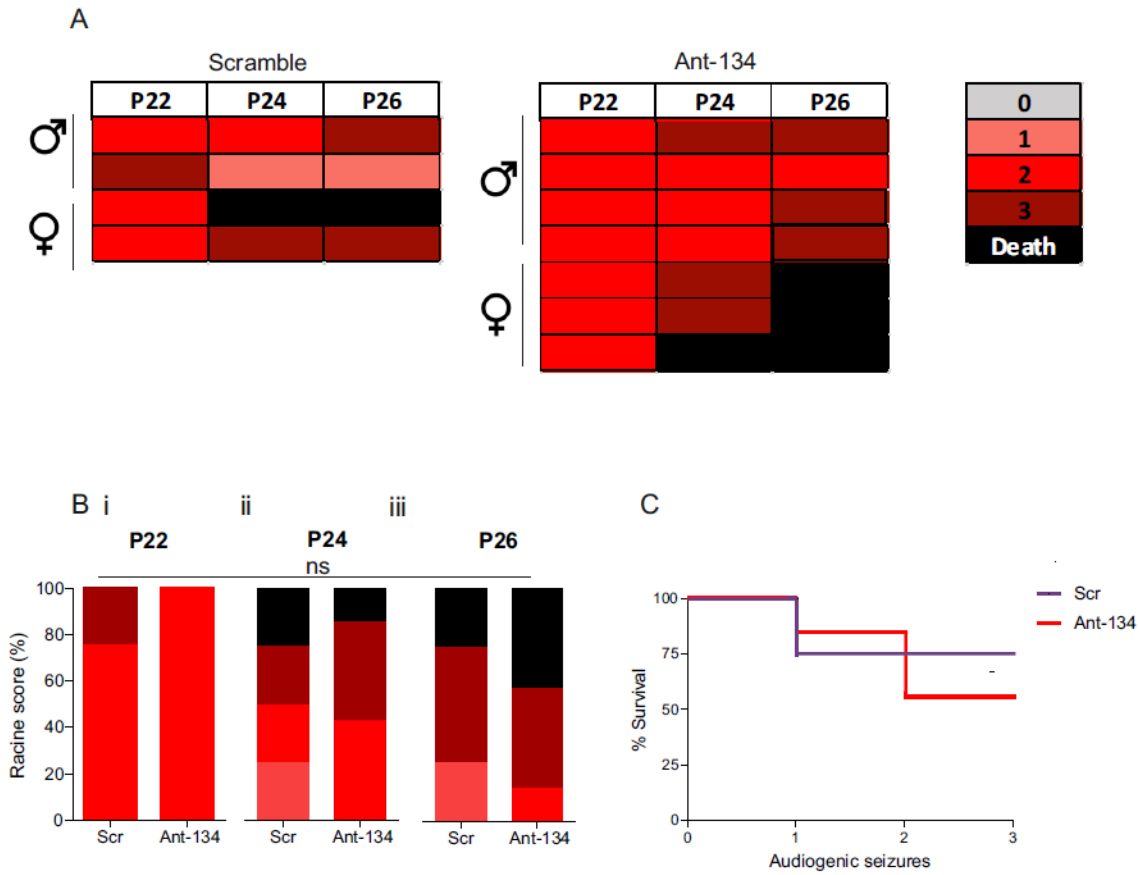

Figure 7: Effect of 0.1 nmol of Scr/Ant-134 on N4 AS P21 mice

P21 N4 mice were pre-treated with Scr/Ant-134 and audiogenic seizures were induced at P22, P24 and P26. 0= No seizure, 1=type 1, wild running, 2=type 2, tonic-clonic convulsions, 3=type 3, hyperextension of hindlimbs and 4= death. **(A)** Tabular representation of the type of seizure each mouse had over three seizures and gender separation of mice. **(B)** Percentage of maximum Racine score per treatment group at P22, P24 and P26, scr n=4, Ant-134 n=7, p=0.61. **(C)** Survival curve in Scr/Ant-134 mice during 3 audiogenic seizures, p=0.73. Audiogenic seizure 1: 100% survival in both groups, audiogenic seizure 2: 75% in Scr and 86% in Ant-134 group and audiogenic seizure 3: 75% survival in Scr and 57.5% survival in Ant-134 group. Data were analysed with Stata Release 16.1. Mortality was compared between treatments using incidence rate ratios and a Poisson model, with number of trials as the exposure variable. Seizure severity was modelled using ordinal logistic regression with robust variance estimation used to adjust for clustering of data with mice. An interaction term was used to test for a change in effectiveness of treatment as a function of trial number.

5.5.6 0.5 nmol Ant-134 reduces audiogenic seizure severity in young N4 P21 AS mice

We next tested a higher dose of Ant-134, reasoning that while 0.1 nmol Ant-134 and the associated reduction in miR-134 activity was sufficient to modify behaviours, it may not have been sufficient to block audiogenic seizures. The experimental design is presented in schematic form in Fig 5.7 A.

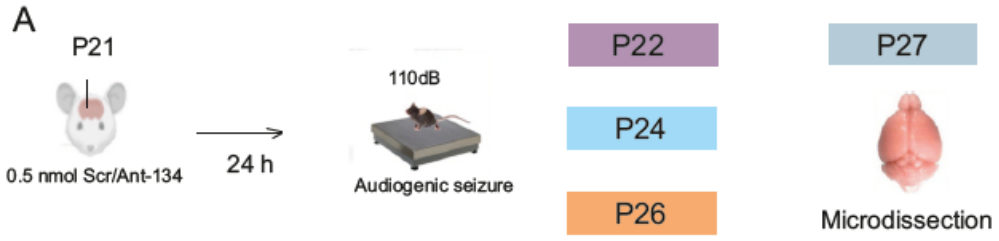

Figure 8: Experimental design of the effect of Ant-134 on audiogenic seizures
N4 P21 mice were pre-treated with Scr/Ant-134 and subjected to three audiogenic seizures. **(A)** Schematic of experimental design for antagomir testing in the audiogenic seizure model. Mice received an ICV injection of Scr/Ant134 and seizures were induced 24 h later at P22. Seizures were repeated at P24 and P26. Mice were culled and micro dissected 24 h after the final seizure.

Next, as described above, P21 N4 mice received ICV injection of Scr/Ant-134 (0.5 nmol) and audiogenic seizures were induced at P22, P24 and P26. A tabular representation of this data can be seen in Fig 5.8 A and can be used to track the gender and the severity of individual mice throughout the seizure trials. As before, audiogenic seizures in Scr-treated AS mice comprised tonic-clonic seizures that increased slightly in severity over the course of the three tests. By the second and third test stimulus, most Scr-treated AS mice displayed seizure score 3 or 4 (death). In contrast, audiogenic seizure severity was significantly lower in Ant-134-treated AS mice compared to Scr-treated AS mice (Fig 5.8 B, $p<0.05$). Over the course of the three test stimuli, Ant-134-treated mice displayed typically score 2 or 3 seizures. Notably, by the time of the second seizure, at P24, there were fewer mice in the Ant-134 group that died during the trial (Fig 5.8 B). However, over the course of the three audiogenic seizures, while survival rate in Ant-134 mice was 81% (9 out of 11 mice survived) compared to 55% (6 out of 11) in Scr mice, this result did not reach significance (Fig 5.8 C, $p>0.05$). There was a higher percentage of survival in female mice pre-treated with Ant-134 in comparison to Scr-treated females. In addition, there was also an increase in female Ant-134-treated mice in comparison to male Ant-134-treated mice, suggesting a potential gender effect.

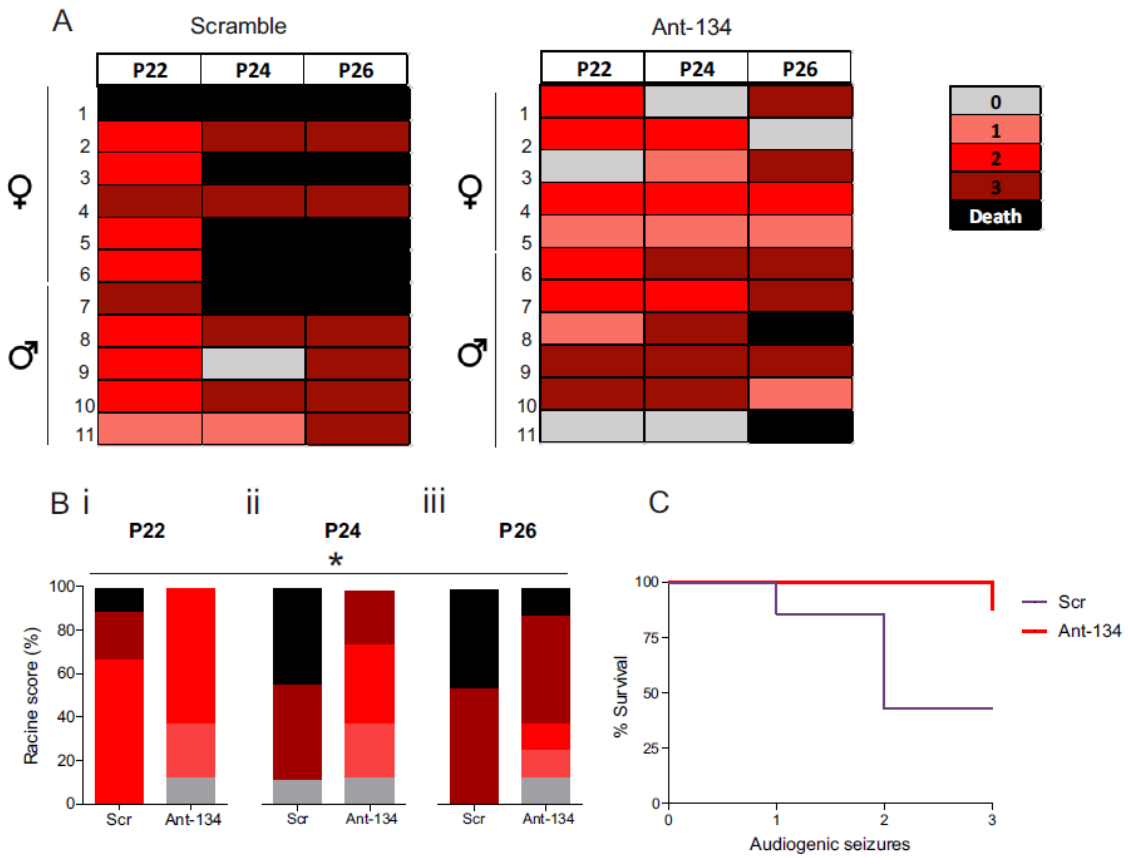

Figure 9: Pre-treatment of 0.5 nmol of Scr/Ant-134 on N4 AS P21 mice
N4 P21 mice received an ICV injection of Scr/Ant-134 and were subjected to audiogenic seizures at P22, P24 and P26. **(A)** Tabular representation of the type of seizure each mouse had over three seizures. **(B)** Percentage of maximum Racine score per treatment group at P22, P24 and P26, scr n=11, Ant-134 n=11, $p<0.05$**. (C)** Kaplan meier curve of survival rates following Scr/Ant-134. 55% survival in Scr group in comparison to 81% survival in Ant-134 group. Data were analysed with Stata Release 16.1. Mortality was compared between treatments using incidence rate ratios and a Poisson model, with number of trials as the exposure variable. Seizure severity was modelled using ordinal logistic regression with robust variance estimation used to adjust for clustering of data with mice. An interaction term was used to test for a change in effectiveness of treatment as a function of trial number.

5.5.7 Analysis of miR-134 targets following pre-treatment with Ant-134

To better investigate the mechanisms of seizure protection by the pre-treatment with 0.5 nmol Ant-134, we next measured protein levels of miR-134 targets in brain tissue samples at the end of audiogenic seizure tests. Brains were obtained at P27, 24 h after the final audiogenic seizure was induced and microdissected to analyse gene expression of miR-134 targets. We analysed expression of Creb1 and Limk1 in the hippocampus and cortex after seizures in our model. The expression of DCX in this cohort of mice could not be analysed due to poor antibodies. Creb1 and Limk1 are both a validated targets of miR-134 (Gao et al., 2010, Schratt et al., 2006) and have been shown to be decreased during SE and in epileptic mice. Moreover, Ant-134 is known to restore these targets levels (Jimenez-Mateos et al., 2012). The severity of seizures in each mouse can be tracked to the levels of Creb1 and Limk1 to determine if any correlations exist. This is presented in Fig 5.11 with each blot using Racine scale data.

We found that Creb1 protein levels were slightly, but not significantly, increased in the cortex of Ant-134-treated AS mice compared to Scr-treated mice (Fig 5.9 A&B, $p>0.05$). Hippocampal protein levels of Creb1 did not differ between Scr and Ant-134 treated mice subject to repeated audiogenic seizures (Fig 5.9 C, $p>0.05$). Each mouse was separated by gender on the quantification graph (Fig 5.9 A&C) and on the blots (Fig 5.9 B&D).

Next, we analysed the protein levels of Limk1 in the same samples. Limk1 contains a seed match for miR-134 in the 3' UTR and has been rep
134 is overexpressed *in vitro* and inhibiting miR-134 has been shown to restore Limk1 in a mouse model of SE (Schratt et al., 2006, Jimenez-Mateos et al., 2012). There were no significant differences in hippocampal or cortical Limk1 levels between Ant-134 and Scr-treated AS mice (Fig 5.9 E&G $p>0.05$). However, levels of limk1 tended to be higher in female mice in the Ant-134 group in comparison to males. Due to mortality in the model, only a sub-set of samples were available for this study and results might be biased because only Scr-treated mice with milder seizures made it to the end.

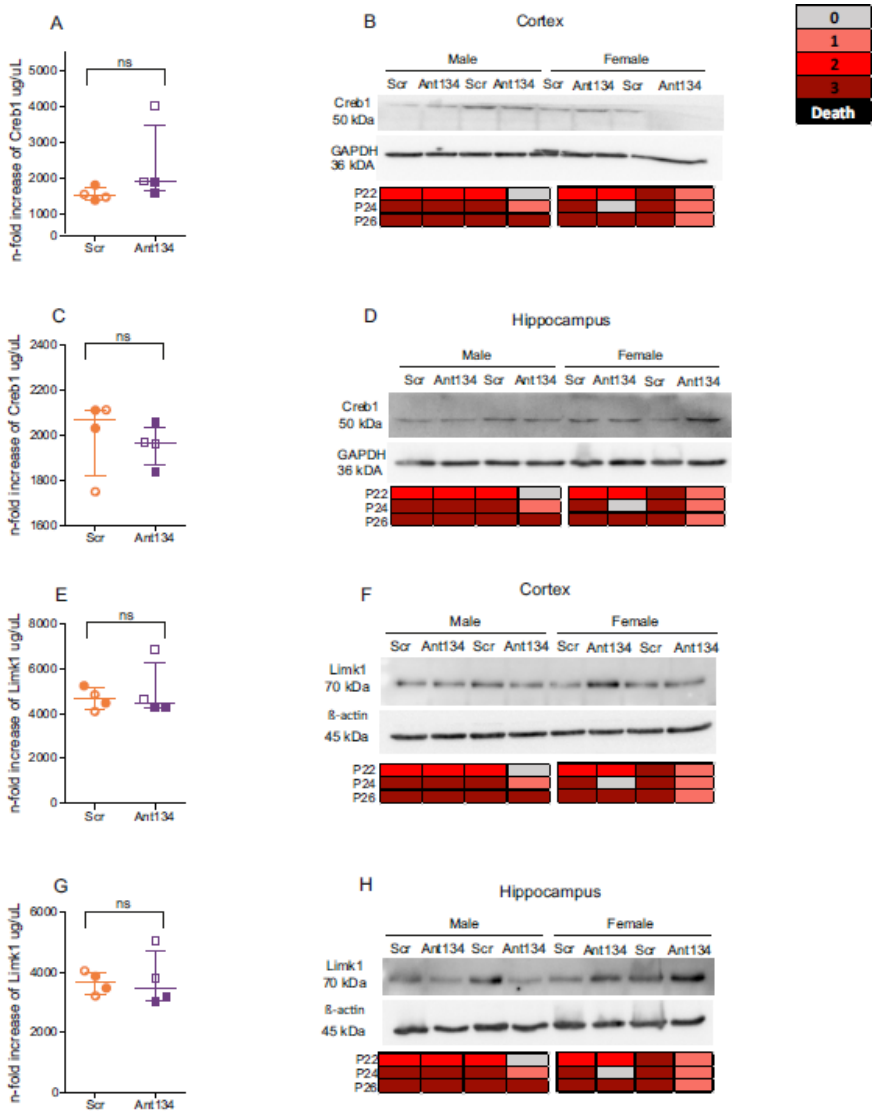

Figure 10: Protein analysis following pre-treatment with Scr/Ant-134

Protein analysis was performed on known targets of miR-134 in hippocampus and cortex following audiogenic seizure induction. **(A)** Concentration of Creb1 in cortex of Scr/Ant-134 mice, n=4/group, p=0.057. **(B)** Western blot showing Creb1 in cortex of Scr/Ant-134 mice. **(C)** Concentration of Creb1 in hippocampus of Scr/Ant-134 mice, Scr n=4, Ant-134 n=3, p=0.485. **(D)** Western blot showing Creb1 in cortex of Scr/Ant-134. **(E)** Concentration of Limk1 in cortex of Scr/Ant-134 mice, n=4/group, p=1. **(F)** Western blot showing Limk1 in cortex of Scr/Ant-134 **(G)** Concentration of Limk1 in hippocampus of Scr/Ant-134 mice, n=4/group, p=0.69. **(H)** Western blot showing Limk1 in hippocampus of Scr/Ant-134 mice. ß-actin was used as a normaliser. A Shapiro-Wilk test was used to check for normality. Data did not pass normality, a Mann-Whitney test was used for analysis. Data are expressed as median with interquartile range.

5.5.8 Ant-134 has seizure suppressive effects in adult mice

Seizures have been reported to re-emerge in adulthood in AS (Larson et al., 2015). To determine if Ant-134 could reduce seizure severity during audiogenic seizures in older mice, we tested the same protocol in a small group of adult N4 AS model mice. Here, P42 AS mice (N4) were pre-treated with 0.5 nmol Scr/Ant-134 and subjected to three seizures repeated at 48 h intervals (Fig 5.10 A).

Overall, audiogenic seizures were less severe in adult N4 mice compared to responses in the P21 mice and all tested animals survived the three evoked seizure. A tabular representation of the data is presented in Fig.10 B to visualise the seizure pattern of each mouse and the sex per treatment group. Treatment of adult AS mice with Ant-134 significantly reduced audiogenic seizure severity (Fig 5.10 C, $p<0.05$). In particular, adult AS mice treated with Ant-134 did not reach type 3 and only experienced wild running and/or tonic-clonic convulsions.

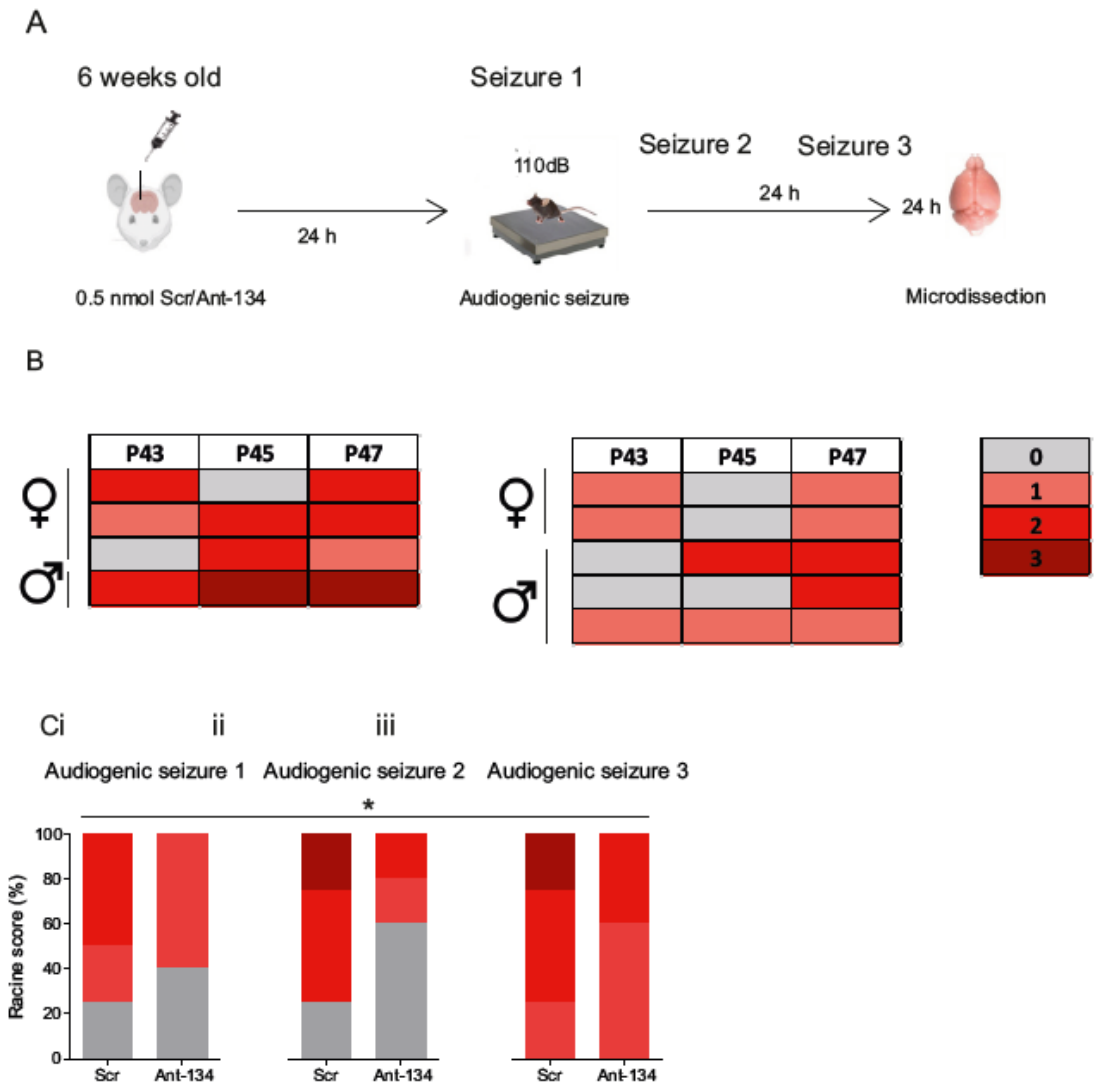

Figure 5.10: 0.5 nmol Ant-134 is protective in an adult mouse model of Angelman syndrome

Pre-treatment with Ant-134 reduces seizure severity during audiogenic seizures in adult mice. **(A)** Schematic illustration of experimental design of antagomir testing in the adult audiogenic seizure model. **(B)** Tabular representation of the type of seizure each mouse had over three seizures. **(C)** Percentage of maximum Racine score per treatment group at P22, P24 and P26, scr n=4, Ant-134 n=5, p=0.04. Data were analysed with Stata Release 16.1. Data were analysed with Stata Release 16.1. Mortality was compared between treatments using incidence rate ratios and a Poisson model, with number of trials as the exposure variable. Seizure severity was modelled using ordinal logistic regression with robust variance estimation used to adjust for clustering of data with mice. An interaction term was used to test for a change in effectiveness of treatment as a function of trial number.

5.5.9 Loss of Ube3a in AS mice elevates microRNAs from the miR-379-410 cluster

To further explore and define the molecular consequences of the loss of Ube3a on miRNA expression in our mouse model, we performed small RNA sequencing on naïve mice from the F1 and N4 generations. The expression of differentially expressed miRNA from both generations were combined onto a volcano plot and the differentially expressed miRNAs from both generation were combined (Fig 5.11). Here, four miRNAs that were found to be differentially expressed in the combined data set; and three of them were from the miR-379-410 cluster. MiR-410-3p and miR-300-3p were among the most significantly differentially expressed ($p<0.01$) miRNA that were found to be upregulated in AS mice. MiR-411-5p, another miRNA part of the cluster was found to be differentially expressed but less significant ($p<0.05$). MiR-488 was also upregulated in AS mice but due to time constraints, this was not validated. A number of neuron-enriched miRNA were also upregulated in AS mice, including miR-204-5p and miR-434-5p. While miR-134 was detected and present in the combined data set, its expression level was not significantly different between genotypes (albeit a small trend to higher levels).

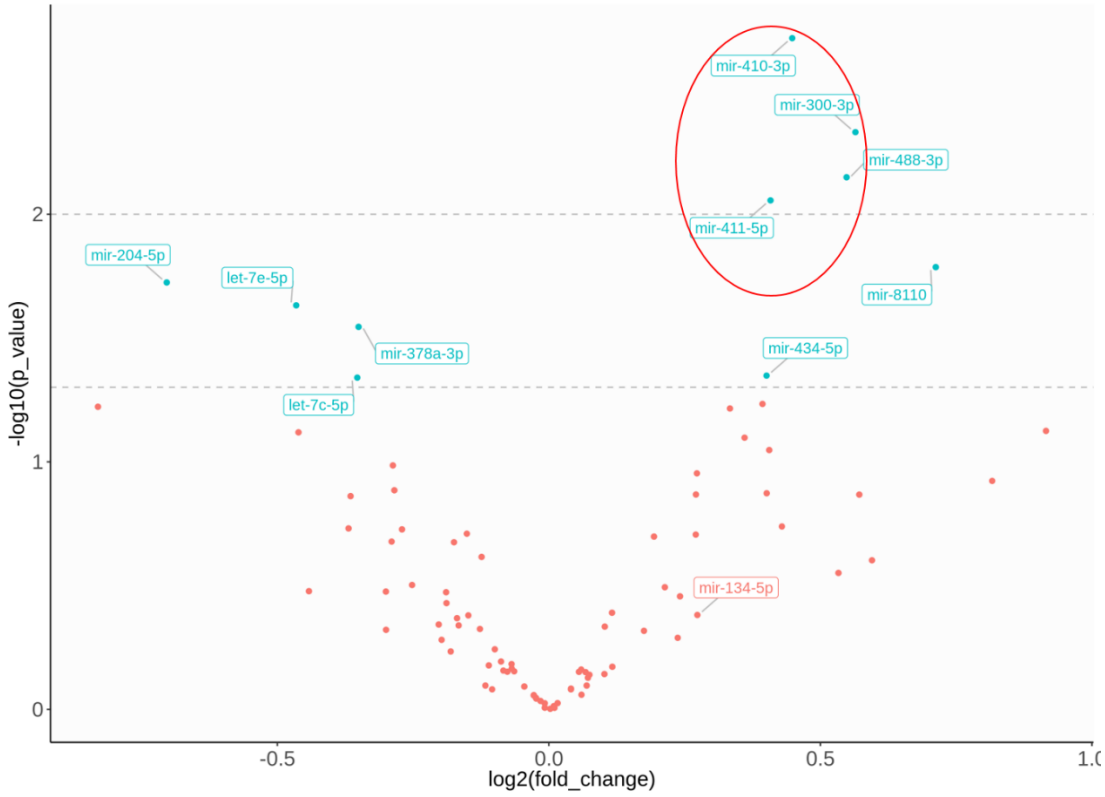

Figure 11: Differentially expressed miRNA in naïve P21 mice from F1 and N4 mice
Volcano plot shows the differentially expressed miRNA of combined data for F1 and N4 hippocampi. Samples in red represent miRNA that were not significantly differentially expressed between genotypes. Samples in blue represent miRNA that were differentially expressed between genotypes. Three miRNAs circled in red are members of the miR-379~410 cluster, miR-411, miR-410 and miR-300 are upregulated. MiR-488, miR-8110, miR-434, miR-204, let-7e, miR-378a and let-7c are also differentially expressed. MiR-134 is present but no differentially upregulated between genotypes.

5.5.10 Validation of differentially expressed miRNA from the miR-379-410 cluster

Next, we selected a number of the differentially-expressed miRNA from the miR-379-410 cluster for validation using RT-qPCR. This included miR-410-3p, miR-300-3p and miR-411-5p. Individual miRNA assays confirmed there was a significant increase in levels of miR-410-3p in AS mice compared to WT mice (Fig 5.12 A i $p<0.05$). As depicted in open squares on the scatter plot, it appeared that this elevation was driven by female mice, thus the data was separated into female and male graphs. Here, we found an increase of miR-410-3p in the female mice (Fig 5.12 A ii $p<0.05$), however there was no difference present in male mice between both genotypes (Fig 5.12 A iii, $p>0.05$). Also in general agreement with the sequencing data displayed in fig 5.12, individual miRNA assays confirmed a trend to higher levels of miR-300-3p in AS mice, although this was not statistically significant (Fig 5.12 B i, $p>0.05$). Separating the data set by sex also showed the increase to be largely driven by levels in female mice although unlike for miR-410-3p this was not significant (Fig 5.13 B ii, $p>0.05$) (Fig 5.12 B ii, $p>0.05$). Levels of miR-300-3p were similar between genotypes in male mice (Fig 5.12 B iii, $p>0.05$). Lastly, expression of miR-411-5p was similar between genotypes (Fig 5.12 Ci, $p>0.05$). While there was a small trend for an increase in female AS mice, this was not significant (Fig 5.12 Cii, $p>0.05$). There was no change in miR-410-5p expression detected in male mice (Fig 5.12 Ciii, $p>0.05$).

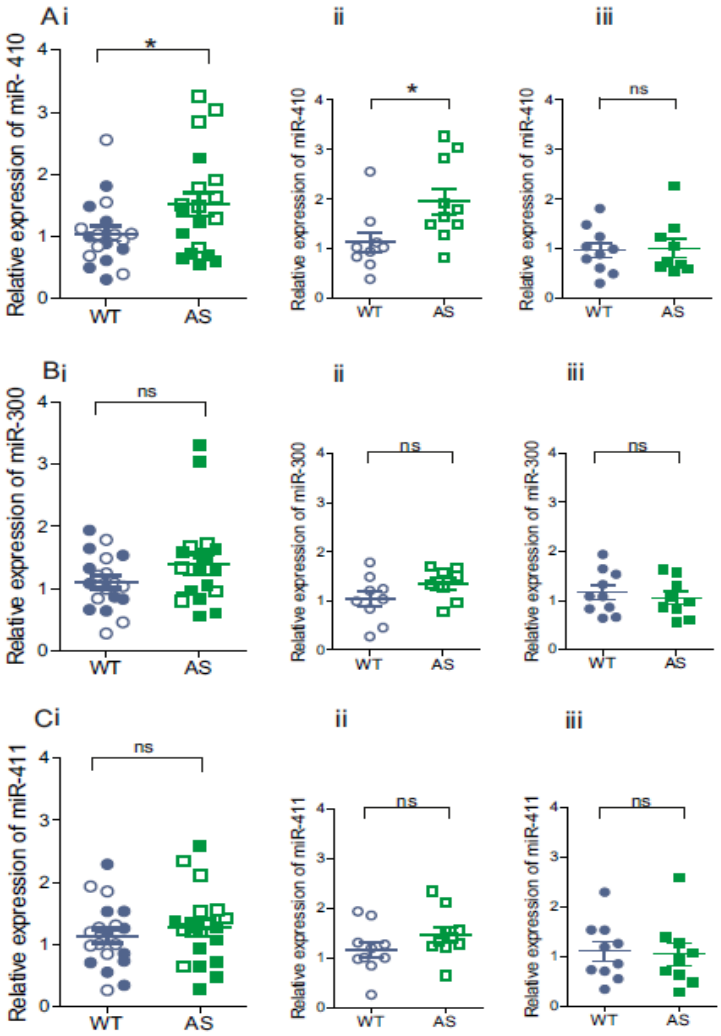

Figure 12: Sequencing validation of differentially expressed miRNA in F1 and N4 mice
Validation was performed on differentially expressed miRNA in WT and AS from both generations at P21. Graphs show miRNA expression of combined genders and the same data further separated by gender. **(Ai)** Relative expression of miR-410 in both genders of WT and AS mice, n=19/genotype, p=0.047. **(Aii)** Relative expression of miR-410 in female mice, WT n=9, AS n=10, p=0.024. **(Aiii)** Relative expression of miR-410 in male mice, WT n=10, AS n=9, p=0.83. **(Bi)** Relative expression if miR-300 in both genders of WT and AS mice, n=20/genotype, p=0.14. **(Bii)** Relative expression of miR-300 in female mice, WT n=9, AS n=8, p=0.13. **(Biii)** Relative expression of miR-300 in male mice, WT n=10, AS n=9, p=0.54. **(Ci)** Relative expression of miR-411 in both genders of WT and AS mice, WT n=20, AS n=19, p=0.5. **(Cii)** Relative expression of miR-411 in female mice, WT n=10, AS n=10, p=0.2. **(Ciii)** Relative expression of miR-411 in male mice, WT n=10, AS n=9, p=0.84. U6b was used as a normaliser. Shapiro-Wilk was used to check for normality of data. Grubbs test was used to statistical outliers. Data are expressed as standard error mean. Closed circles and squares represent male mice, open circles and squares represent female mice.

5.6 Discussion:

The present chapter explored the effects of targeting miR-134 on phenotypes including audiogenic seizures in the *Ube3a* $^{(m-/p+)}$ mouse. Our results demonstrate that inhibition of miR-134 can protect against audiogenic seizures in AS mice and improved locomotor activity in mice. We also identify increased levels of additional members of the miR-379~410 cluster in AS mice. Taken together, these findings suggest targeting miR-134 and/or related miRNAs could have therapeutic uses for multiple symptoms in AS.

Numerous studies have attempted to treat individual symptoms of AS such as movement dysfunction, cognition and epilepsy; however, there have been very few approaches that offer the potential to alleviate multiple symptoms of AS (Sonzogni et al., 2018, Gu et al., 2019b, Bruinsma et al., 2015). Here, we aimed to mitigate the symptoms at different ages using a miRNA based therapy. MiR-134 silencing has been repeatedly shown to reduce seizures in chemoconvulsant models in rodents and elevation in miR-134 levels is not required for anti-seizure effects (Reschke et al., 2017b). This is important since, although loss of Ube3a is predicted to result in a potential elevation in miR-134 levels, we did not detect statistically significant increases in miR-134 in AS mice.

A major finding in this Chapter was that inhibiting miR-134 appeared to restore the movement impairments of AS model mice. Specifically, ICV injection of a low-dose of Ant-134 into P21 F1 mice, which produced only partial knockdown of miR-134, resulted in a significant increase in exploration time in the open field, an increase of the number of entries into the inner zone and a trend for an increase in distance travelled. Notably, this occurred using the lowest test dose of 0.1 nmol indicating only ~50% reduction in miR-134 levels is required. These effects were not present when re-tested three weeks later. This may have been because the mice had already been exposed to the open field and therefore they did not fully explore the arena due to habituation. Taken together, these results indicate that moderate inhibition of miR-134 is able to partly correct the motor impairments in AS model mice. To the best of our knowledge, this is the first

demonstration that inhibiting miR-134 can produce effects on mouse behaviour. How would inhibition of miR-134 result in such changes locomotor activity? One of the best-understood roles for miR-134 is as a negative regulator of spine volume in excitatory neurons via its target, Limk1 (Jimenez-Mateos et al., 2015, Schratt et al., 2006). Introduction of Ant-134 is known to increase hippocampal spine volume. This may result in improvements to neuronal network connectivity in AS mice leading in turn to better performance in the test. However, analysis of Limk1 levels in Ant-134 –treated mice did not show obvious so the mechanism may be unrelated to this.

In contrast to the restorative properties of Ant-134 on locomotor activity and the reduction in anxiety following pre-treatment with Ant-134, work by Schratt found that using a miR-379~410 cluster knockout (KO) mouse model, mice displayed increased sociability behaviours and increased anxiety-like behaviours measured by open field and elevated plus maze (Lackinger et al., 2019). Although social interaction was not tested in this study, an increase in social behaviours in Ube3A KO mice has been reported before (Stoppel and Anderson, 2017). The increase in social behaviour and increase in anxious behaviours in the miR-379~410 cluster KO model is in disagreement with the hypothesis that an upregulation of miR-134 and other miRNAs from this cluster are involved in the pathophysiology of AS. While similar results in marble burying were obtained in the miR-379~410 KO mice and during characterisation of naïve AS mice in chapter 4, our results are in opposition with Schratt's findings (Lackinger et al., 2019). Here, we have shown that silencing miR-134 rescues performance in the open field. We also used parameters from the open field to test if Ant-134 had any anxiolytic effects by analysing the number of entries into the inner zone and we found a significant increase in this parameter in Ant-134-treated mice. The differences obtained between our results and the study from Lackinger *et al.*, can be due to a number of factors (Lackinger et al., 2019). For instance, Schratt's group entire miRNA cluster, whereas we inhibit a single miRNA from this cluster. Furthermore, they use a constitutive KO model which may have mechanisms in place to compensate for deleting the entire cluster. Notably, motor phenotypes such as distance travelled in

the open field or performance on the rotarod of these mice were not tested in this KO model, questioning the source of anxiety in these mice. A potential explanation could be whether the anxious behaviour reported in the open field is caused by a motor impairment, which could prevent the mice from entering the inner zone of the open field and thus, appearing more anxious.

What mechanisms are involved in the restorative properties of Ant-134 in the open field? Analysis of c-fos activation after exposure to the open field has been used to show which brain regions are involved in exploring a novel environment (Nagahara and Handa, 1997). Regions included the prelimbic cortex, prefrontal cortex, caudate and ventral lateral septum (Nagahara and Handa, 1997). In addition, another study found an increase in c-fos mRNA in the CA1 region of the hippocampus (Kerr et al., 1996), and research by our group has shown neuroprotective effects in the hippocampus in Ant-134-treated mice (Jimenez-Mateos et al., 2012). Further investigation into the brain regions associated with motor impairments in AS mice is required.

While characterisation of the motor incoordination in AS mice in Chapter 4 showed robust phenotypes in adult mice on the rotarod, studies have suggested that this test may not be suitable to detect subtle changes in neuromotor deficits and perhaps this parameter is not appropriate to identify changes in young mice (Stroobants et al., 2013). Ant-134 did not correct the marble burying deficit in AS mice, however, at P22, burying marbles that weigh 6g may be challenging. While the average number of marbles buried when retested at P42 increased in both groups of mice, there was still an impairment present in the number of marbles buried in these mice, suggesting that Ant-134 does not improve this phenotype. The exact cognitive basis of the marble burying assay is not fully understood although performance in the marble burying test has previously been linked to hippocampal function (Deacon and Rawlins, 2005). This could indicate that, despite being a hippocampal task, Ant-134 cannot change certain deficits in the AS mouse hippocampus even when delivered early. In agreement with this finding, research has shown that Ant-134 does not affect performance in the novel object location test, which primarily relies on hippocampal functioning (Morris et al., 2018). Perhaps miR-134

targets are more important in the open field or that the behaviours are, for another reason, more plastic and amenable to changes.

The pathways involved in the changes in response to Ant-134 may lie outside the hippocampus. It has been hypothesised that the ataxic like symptoms of AS could be caused by a build-up of toxic substrates due to the loss of *Ube3a* (Mulherkar and Jana, 2010). Using a mouse model of spinocerebellar ataxia (*SCA1*), lacking *Ube3a*, the authors saw an increase of toxic substrates, such as ataxin-1 and elucidated that this increase was accountable for the severe pathological changes present in the cerebellum of *SCA1* mice (Mulherkar and Jana, 2010, Cummings et al., 1999), once again implicating the cerebellum in the motor dysfunction in AS. In relation to studies here, ICV injection may not have caused sufficient miR-134 knockdown in the cerebellum. Further studies on the role of miR-134 in the cerebellum and motor incoordination is required. Another potential mechanism for some of the movement dysfunction in AS can be explained by the α-synuclein. E6-AP, the gene product of *Ube3a*, has been shown to be involved in the degradation of α the protein that aggre (Mulherkar et al., 2009). This may be accountable for Parkins ataxia and cog-wheel rigidity in AS. A number of attempts have been made to rescue the motor phenotype present in AS mice. This has been done using levodopa and minocycline as both drugs are currently in trials for AS patients, however, these drugs had no effect on locomotor activity when tested in the open field and rotarod (Sonzogni et al., 2018). Reinstatement of the paternal copy of UBE3A has shown to be the most promising therapeutic for AS (Silva-Santos et al., 2015). The authors found that when Ube3a was restored during postnatal development, at P21, there was a full rescue of behavioural phenotypes, in comparison to when it was reinstated in adolescent, only motor deficits were rescued (Silva-Santos et al., 2015). While we silenced miR-134 at P21 and followed the same mice to adulthood, these results are in agreement with intervention at a young age. In addition, work by Greenberg' brain activity in AS mice was rescued by reducing levels of arc, but motor phenotypes were not affected (Mandel-Brehm et al., 2015).

The second important finding in this Chapter was the reduction in seizure severity produced by Ant-134 in the audiogenic seizure tests of AS model mice. Epilepsy is present in up to 90% of individuals with AS and these seizures usually begin in the first 6 months of life (Pelc et al., 2008a). Having learned in Chapter 4 that audiogenic seizure susceptibility requires a different genetic backcrossed, we used N4 generation mice that were backcrossed four generations to increase the 129 background and yield AS mice that were susceptible to audio evoked seizures (Jiang et al., 1998). Using a modified Racine scale to determine the severity of seizures, we found an overall reduction of seizure severity in mice treated with 0.5 nmol Ant-134. Several AS mice treated with Ant-134 did not experience any seizures during three trials whereas some only entered type one seizures. Ant-134 treatment was also associated with a reduction in mortality, particularly around the time of the second seizure being given. We did not detect any anti-seizure effects using the 0.1 nmol dose of Ant-134 which had protected WT mice from systemic KA. This suggests model and strain differences in the anti-seizure effects of Ant-134. Also, the anti-seizure effects of Ant-134 in AS require a more substantial reduction in miR-134 levels than that needed to improve movement in the Open field and a higher dose than is needed to affect chemoconvulsant seizures in WT mice. Unexpectedly, we did not observe any signs of the toxicity of the 0.5 nmol dose of Ant-134 detected in WT mice in the KA model.

The present study also tested the age-dependent effects of Ant-134 in the audiogenic seizure model. Inhibition of miR-134 by Ant-134 reduced seizure severity in adult AS mice aged P42-P60. Notably, the model differed somewhat from the P21 version with an overall lower severity of seizure and mortality. These results indicate that Ant-134 could be used to treat or prevent seizures in AS patients across a broad age range. High doses of CBD (100 mg/kg) have shown to reduce the severity of audiogenic seizures using a slightly different Racine scale that did not account for type three seizures, hyperextension of the hindlimbs (Gu et al., 2019b). However, this study was performed in AS mice aged P70-P100, and we have shown that the overall severity of audiogenic seizures decreases as mice get older. In addition, these seizures were induced by an

alarm (125 dB) rather than scratching the cage lid. In general, because of the high percentage of mortality associated with audiogenic seizures in young mice (<P42), the majority of research into anti-seizure drugs in this model is performed in older mice (Sonzogni et al., 2018, Silva-Santos et al., 2015, Gu et al., 2019b). Taken together, these results demonstrate that targeting miR-134 can protect against audiogenic seizures in young mice.

What is the mechanism of the anti-seizure effect of Ant-134 in AS? The majority of research on Ant-134 has used adult models of epilepsy and SE using chemoconvulsants such as PTZ, KA and pilocarpine (Jimenez-Mateos et al., 2012, Reschke et al., 2017b, Reschke et al., 2019), The underlying mechanisms of Ant-134 in a genetic model of epilepsy are currently unknown but a similar mechanism is possible. Previous work has shown that the de-repression of Limk1 with Ant-134 (Jimenez-Mateos et al., 2012). This could interfere with transmission of hyper-synchronous neuronal discharges. Interestingly, studies have linked E6-AP ubiquitin ligase to synaptic function (Dindot et al., 2008, Colledge et al., 2003). One particular study found that E6-AP was detected at synapses, suggestive of regulating spine development (Dindot et al., 2008). Furthermore, they also reported abnormal dendritic spines which were reduced in size and density in a mouse model of AS (Dindot et al., 2008). The abnormal spine functioning in AS could be linked to dysregulation of the CaMKII pathway (Weeber et al., 2003), as regulation of CaMKII by introducing an additional mutation at the inhibitory phosphorylation site of αCaMKII in AS mice has shown to be more (van Woerden et al., 2007). An alternative mechanism would be via an effect on components of the neurogenesis system. Altered hippocampal neurogenesis has been reported in mouse models of AS (Godavarthi et al., 2015, Mardirossian et al., 2009) and in chapter four and we show here that silencing miR-134 increases DCX expression. However, the short time between injection and testing (24 h) makes it somewhat unlikely that Ant-134 is producing effects via neurogenesis. Also, changes to DCX levels were rather inconsistent in the AS model studies. Research has shown that hippocampal neurogenesis is impaired in the dentate gyrus (DG) of the hippocampus in AS (Mardirossian et al., 2009,

Godavarthi et al., 2015), thus perhaps we would have seen more changes in DCX expression in our mice if the hippocampus subfields were microdissected. The protective of effects of Ant-134 may also be mediated by cAMP response element-binding protein 1 (Creb1), another miR-134 target (Friedrich et al., 2020). Work in our lab has shown that Creb1 levels were decreased in epileptic mice with higher miR-134 levels and that Creb1 levels were lower in Scr-treated mice after SE in comparison to those treated with Ant-134 (Jimenez-Mateos et al., 2012). While not significant, levels of Creb1 were slightly increased in the cortex after pre-treatment with Ant-134 when compared to Scr in the audiogenic seizure model. However, since measurement of Creb1 (as well as DCX and Limk1) was performed one week after ICV injections it remains difficult to include or exclude these changes as having causal roles. Future studies could test this, for example by co-injecting a Limk1/Creb1/DCX inhibitor with Ant-134 to see if this obviates the anti-seizure effects

AS patients and several of the mouse models display resting differences in EEG. The present Chapter investigated whether Ant-134 had any effect on the EEG phenotypes we characterised in F1 mice in chapter 4, consisting of an overall increase in total power and theta frequency. Ant-134 did not affect these EEG features, however, we saw a trend for a decrease in alpha frequency in mice treated with Ant-134. While we did not identify alterations between genotypes in alpha during the model characterisation, reductions in alpha levels (albeit moderate) by Ant-134 should be explored further. Alterations in alpha frequency such as increased synchrony have been identified in EEG recordings from patients with major depressive disorder (MDD) and alterations between left and right hemispheres in patients with MDD was indicative of depression (Fingelkurts et al., 2007). Furthermore, transcranial stimulation in patients with ADHD decreased alpha levels (Dallmer-Zerbe et al., 2020, Alexander et al., 2019), suggesting that reducing alpha frequency could restore abnormal connectivity (Alexander et al., 2019). Altered alpha frequency is thought to arise from thalamocortical regions (Alexander et al., 2019). Indeed, abnormal thalamocortical functioning has been linked to AS (Handforth et al., 2005). In one study, the authors demonstrated that abnormal oscillatory thalamocortical

synchrony is causative of the abnormal activity that is seen in AS (Handforth et al., 2005). Future studies are required to determine if Ant-134 reduces alpha frequency and if this effect is specific to AS mice, for example the effect of Ant-134 on alpha frequency could be analysed. Furthermore, the use of telemetry devices could analyse the duration of Ant-134 on alpha frequency.

Mutations in Ube3a may result in de-repression of the miR-379~410 cluster that contains miR-134. In the present study we performed RNA sequencing analysis to profile miRNAs in both the F1 and N4 AS mice. While we did not detect significant alterations in levels of miR-134 in either generation, results obtained from small RNA sequencing corroborates this hypothesis. Three miRNAs from the miR-379-410 cluster were found to be upregulated in the hippocampus of AS mice, supporting the hypothesis that deletion of Ube3a results in the loss of the miRNA sponge function of Ube3a1, and therefore an increase in miRNAs from this cluster. In addition to these differentially upregulated miRNAs, miR-488 was also significantly increased in these mice. Interestingly, target analysis of miR-488 identified a number of genes associated with GABAergic and glutamatergic neurotransmission such as *Gabra1*, *Gabra2*, *Grin2d*, *Gria3*. In addition, miR-448 also regulates potassium channels such as *kcnj2* and *kcnj6*. Due to time constraints, validation only focused on miRNAs from the miR-379~410 cluster, though miR-488 and some of the down-regulated miRNAs will be validated at a later stage.

These findings are in agreement with work by Valluy *et al* who reported that Ube3a1 contains a binding site for the miR-379-420 cluster and Ube3a1 RNA function is dependent on an intact miRNA pathway (Valluy et al., 2015). Interestingly, target analysis of miR-410-3p in mice has shown associations with neuroligins and the regulation of calcium and sodium levels. In addition, miR-410-3p in humans has been linked to MECP2, the gene associated with Rett syndrome. Based on the identification of dysregulated miRNAs in the *Ube3a* $^{(m-/p+)}$ model, this sets the basis for the development of a combined miRNA therapy for AS. Combined antagomir therapies have been used to significantly reduce total EEG power in a mouse model of TLE by

inhibiting miR-21a, miR-142a and miR-10a (Venø et al., 2020). In conjunction with inhibiting miR-134, targeting another miRNA, for example miR-410, could reverse more of the phenotypes not corrected with Ant-134, such as motor coordination on the rotarod. While the role of miR-410 in Rett syndrome is currently unclear, it could be associated with motor phenotypes or seizure susceptibility, as both are common between both disorders. In addition, while not validated in the *Ube3a* $^{(m-/p+)}$ model, targeting miR-488 could have epilepsy-reversing properties due to its multiple links to GABAergic and glutamatergic neurotransmission. Taken together, dysregulation of miRNAs in AS may be caused by loss of Ube3a. Further analysis of the mechanism of these miRNA in AS is required.

5.7 Conclusion:

Here, we have shown that inhibiting miR-134 using Ant-134 can restore motor impairments and attenuate audiogenic seizure severity in young and adult AS mice. This represents an important potential therapeutic approach that could reduce or prevent major clinically-relevant features of the disease. Further work is required to determine the mechanistic pathways of Ant-134 in AS. The increased expression of a number of miRNAs from the miR-379-410 cluster in AS mice is in agreement with our hypothesis and further studies targeting these miRNA using antagomir could alleviate more of the symptoms present in AS.

6 Chapter 6

General discussion

General discussion

AS is a rare neurodevelopmental disorder that affects roughly 1:15000-1:20000 births. It is named after the first person to describe the syndrome, Harry Angelman, and was later found to be caused by mutations or loss of the *UBE3A* gene. The *UBE3A* gene encodes an ubiquitin ligase that functions to regulate protein turnover in cells. It is thought that the accumulation of proteins that would otherwise be degraded results in synaptic dysfunction and interruption in neuronal network behaviour (Sell and Margolis, 2015, Kishino et al., 1997). The main clinical symptoms are cognitive impairment with profound speech delay, motor coordination defects/ataxia and drug-resistant epilepsy. The symptom for which the disease is best known is a happy, often smiling disposition. Currently there is no available treatment that is effective in controlling or improving the symptoms of AS (Clayton-Smith and Laan, 2003). While a number of drugs can be used to treat individual symptoms such as seizures and motor impairments, these have limited efficacy and there is a lack of options to treat the multifaceted nature of AS. Furthermore, current treatments only provide symptomatic relief and do not target the underlying mechanisms of the disorder. A number of therapies are being developed that target the molecular mechanism of the disease. This includes using antisense oligonucleotides to block the non-coding RNA expressed from the UBE3A locus responsible for imprinting (epigenetic shut-down) of the paternal allele. This has been shown to enable expression of the paternal copy of UBE3A (Gu et al., 2019a, Silva-Santos et al., 2015). However, a recent discovery about the transcripts expressed from the UBE3A locus raised an alternative way to treat AS (Valluy et al., 2015).

Seizures are one of the most challenging aspects of AS for patients and carers. In AS, seizures generally occur within the first few years, with an average onset of 18 months (Matsumoto et al., 1992b). Seizures during neurodevelopment can have profound effects on brain development and result in life-long disability (Symonds et al., 2019). Here, we aimed to use a miRNA targeting-based strategy to treat multiple symptoms of AS. MiRNAs have unique advantages as a therapeutic approach for a complex disorder like AS because of the ability of a single miRNA to interact with multiple targets (Peter,

2010). In addition, the importance of miRNAs in neuronal development and neurological disease has been well documented and miRNAs such as miR-134 are potent regulators of seizures (Zhao et al., 2015, Cheng et al., 2009, Rago et al., 2014).

The overarching hypothesis of this project was that miRNA dysregulation is involved in the pathophysiology of AS. Deletion of the *Ube3a* gene results in the loss of *Ube3a1*, a non-protein-coding transcript expressed from the locus which contains a binding site for the large miRNA cluster, miR-379~410 (Valluy et al., 2015). Loss of this miRNA sponge could result in increased total or free levels of miRNAs from this cluster and an increase in the suppression of their targets. MiRNAs from this cluster have been shown to regulate levels of Limk1 and Pum2, which are important regulators of dendritic morphology (Valluy et al., 2015). Thus, we have hypothesised that an increase in a number of miRNAs leads to the repression of such targets and could contribute to hyperexcitability and abnormal EEG patterns in AS. Altogether, the studies performed suggest targeting miR-134 could be suitable for seizure control and other symptom relief for early life seizures as AS. We show that Ant-134, could reduce seizure severity and delay the initiation of SE in a newly developed mouse model of paediatric SE. Next, we characterised a model of AS and identified a number of phenotypes that might be correctable using Ant-134. We then tested the efficacy of Ant-134 to correct a number of phenotypes in this model. The most important finding was that silencing miR-134 reduced audiogenic seizures in AS mice and improved movement and exploration in the Open field test. Finally, we identified a number of other dysregulated miRNAs in the *Ube3a* $^{(m-/p+)}$ mouse model that could be targeted in the future for the treatment of AS.

Chapter 3 of this thesis explored for the first time if antisense oligonucleotides targeting miR-134 could reduce seizures in a model of early-life seizures. While Ant-134 has been repeatedly shown to reduce or prevent evoked and spontaneous seizures, the work has been restricted to testing in adult rodents. Several targets of miR-134 are developmentally regulated (e.g. DCX) and therefore the broad safety and efficacy of targeting miR-134 in young rodents is unknown. We used kainic acid to induce SE in P21 mice. The main aim of this chapter was to determine if Ant-134 was effective in a

paediatric model of SE. Experiments showed that when levels of miR-134 were reduced in mice by prior ICV injection of 0.1 nmol Ant-134 mice experienced reduced-severity seizures in the model [see Fig 3.4]. This is the first demonstration that inhibiting miR-134 has anti-seizure effects in a model of early-life seizures. Levels of miR-134 have been reported to be upregulated in adult seizure models and human brain samples but we did not detect an elevation of levels of miR-134 after SE in P21 mice. This suggests that the transcriptional mechanisms that link seizures to miR-134 levels may not be functional at P21. Alternatively, the seizure intensity or circuitry activated were not sufficient to bring about transcriptional changes. This is less likely, however, since the model featured neuronal death within the hippocampus consistent with prolonged seizures. It also confirms findings in adult rats (Reschke et al., 2017b) that increased miR-134 levels are not required for Ant-134 to have anti-seizure effects in a given model. (Reschke et al., 2017b). Another important finding from these studies was that the hippocampus of mice pre-treated with Ant-134 before KA-induced seizures displayed reduced damage [see Fig 3.5). This is likely secondary to the reduction in seizure severity produced by Ant-134. Taken together, the findings obtained in this chapter build on the evidence that Ant-134 is effective in reducing seizures and show this is also the case in younger rodents. However, a number of important limitations were found. Foremost, at the highest tested dose, seizures appeared to be exacerbated in Ant-134-treated mice, with mortality in all mice prior to end of recordings. This indicates an intolerance for loss of miR-134 at earlier neurodevelopment stages. Why? The higher dose of Ant-134 did not cause any obvious direct toxicity effects; mice used for assessing effects of 0.5 nmol knockdown appeared normal at the time of euthanasia for brain tissue sampling, 24 h after injection. It suggests complexity in how miR-134 targets regulate synaptic structure and function and how this changes when miR-134 is inhibited at this age. 134 achieved using the high dose of Ant-134 may have caused an increase in key targets of miR-134 that then produced proexcitability effects. This may be through interfering with key developmental changes in networks. For example, high amounts of Limk1 may curtail spine function and change network excitability. It remains unclear why this effect

is restricted to this developmental age but may be due to expression of other interactions processes during development. These observations raise important challenges for whether and how Ant-134 could be used for the control of epilepsy in certain age groups. There may need to be a narrow range of doses that can be used or some age groups may just not be suitable candidates for this treatment. The kainic acid model used here lacks some clinical relevance and results may not translate well to patients. Moreover, due to the length of time it takes for delivered ASOs to inhibit their miRNA targets, the studies have not been performed. While treatment in SE is not a translationally realistic approach, it nevertheless serves the purpose of showing that if miR-134 levels are reduced then the brain is less susceptible to seizures. For clinical use, we would imagine either use in patients with long-standing seizure risk or protracted/refractory status.

Chapter 4 moved on to directly address the question of whether Ant-134 could be used for AS, beginning by establishing the various phenotypes that exist in the AS model mice. We selected a model that was developed by Dr. Arthur Beaudet. This model was chosen as it recapitulates many aspects of AS that we are interested in, including EEG phenotypes, seizures and behavioural impairments. In addition, this model has been used in testing new treatments for AS (Sonzogni et al., 2018). Here, we observed a number of phenotypes in the *Ube3a* $^{(m-/p+)}$ mouse model that recapitulated many aspects of AS in humans that could be used for antagomir correction at a later stage. This consisted of an abnormal EEG, motor impairments in the open field and rotarod, a deficit in marble burying and increased susceptibility to seizures induced by chemoconvulsant agents. To induce audiogenic seizures, mice were backcrossed four generations to yield a model that was more susceptible to seizures. While there was a trend for increased expression of miR-134 in AS mice, this narrowly missed significance [see Fig 4.11]. This could mean that our hypothesis is incorrect. That is, loss of Ube3a1 does not result in abundance changes to the miRNAs is the known sponge function instead leaves more miR-134 molecules free to interact with other targets. This would explain why levels of miR-134 were similar to wildtype but that

targeting miR-134 still had important effects in the model. We cannot exclude, however, that abundance of miR-134 is increased but that we missed it using the assays employed. The amounts of the Ube3a1 transcript and changes to miR-134 may be below what is detectable using the techniques we used. For example, RNA was extracted from whole hippocampi so this could obscure differences in specific subtypes or subfields. One approach not tried would be to elute Ago from a sub-population of neurons that express miR-134 or by using a synaptic enrichment step as miR-134 is localized in dendritic spines (Schratt et al., 2006). Levels of miR-134 targets showed variable differences, some of which might be due to miR-134 levels but this was not consistent. Additional investigation is therefore required before we can conclude that miR-134 is not dysregulated in AS.

Chapter 5 consisted of functional studies in the *Ube3a* $^{(m-/p+)}$ model. Here, we questioned whether Ant-134 could alleviate some of the commonly reported symptoms of AS. We focused on correcting the abnormal EEG, motor phenotypes and the marble burying impairment in the F1 generation. Furthermore, in the N4 generation, we tested the efficacy of Ant-134 in reducing the severity of audiogenic seizures. We did not detect any significant effects of Ant-134 on the resting EEG phenotypes [see Fig 5.4]. While Ant-134 did not reduce the total power or change the increased theta frequency, we detected a tendency to reduced alpha frequency by Ant-134, though this narrowly missed significance. This suggests there could still be subtle effects of Ant-134 on resting network activity. This would be a novel observation. Indeed, most prior work found no effects of Ant-134 on various electrophysiological properties of the hippocampus in normal mice (Morris et al., 2018). Prior conclusions were that Ant-134 may block synchronous firing of neurons without changing typical signaling behavior. Accordingly, the present finding is largely in line with that but suggests, if baseline network behavior is altered, targeting miR-134 might have effects to normalize. The presence of abnormal levels of delta and theta frequency have been well documented in AS (Sidorov et al., 2017, Frohlich et al., 2019a), however, we did not detect alterations of delta frequency bands between genotypes in our model. This probably highlights how differences in

breeding and housing as well as backcrossing can result in phenotype drift or disappearance and underscores the importance of picking robust and clinically meaningful phenotypes to target. The reduction in alpha frequency by Ant-134, albeit small, may indicate unexplored aspects of Ant-134 on resting EEG. In addition, alterations in alpha frequency have shown to arise from thalamocortical regions, which have also been reported to be accountable for abnormal ictal activity in AS (Handforth et al., 2005).

A major finding in Chapter 5 was that Ant-134 could reduce the severity of audiogenic-induced seizures in AS mice. This was evident at both P21 [See Fig 5.8] and also in adult AS mice [see Fig 5.10]. The effect depended on sufficient silencing of miR-134. While injection of 0.1 nmol Ant-134 was not effective, 0.5 nmol Ant-134 which reduced levels of miR-134 by roughly 88%, reduced seizures. The reduction in seizure severity was also associated with an increased survival although this did not reach statistical significance. The findings both complement and contrast the earlier tests of Ant-134 in the KA model in P21 mice. Those results, in Chapter 3, indicated only a relatively low and incomplete knockdown of miR-134 was safe and effective to reduce KA seizures in P21 mice. The AS model data indicate that, a-convulsant effect of in that high dose Ant-134. This suggests that Ant-134 could have safe therapeutic use in young and older AS populations because the seizure mechanisms or pathway differ from those activated by KA. Indeed, it is likely audiogenic seizures recruit different structures besides the hippocampus whereas the KA model recruits the hippocampus. During audiogenic seizures, activation begins in the inferior colliculus and leads to the brainstem, medial geniculate, hippocampus and areas of the amygdala (Ross and Coleman, 2000), thus suggestive of some differenences in the pathway of seizure transmission compared to the pathway activated in the KA model. Direct delivery of Ant-134 to these sites might produce even greater effects. Moreover, analysis of miR-134 expression in the areas associated with audiogenic seizures using in-situ hybridization could aid in the mapping of this pathway.

Chapter 5 also included RNA sequencing studies that defined the miRNAome in AS. The use of an unbiased approach meant we were able to identify any miRNA changes we wouldn't have predicted a priori to be of the miR-379~410 cluster. We found increases in some of the miR-379~410 cluster in AS mice besides miR-134 [see Fig 5.11]. This included miR-410 and miR-488. The latter has several predicted targets that are involved in GABA and glutamatergic transmission (Zhao et al., 2012). Seizure susceptibility in AS may therefore also be affected by dysregulation of miR-488. The upregulation of miR-410, miR-411 and miR-300 are consistent with our hypothesis of the lost sponge function whereas miR-488 is not a member of the miR-379~410 cluster. The mechanism by which miR-488 is dysregulated in AS is therefore unknown. Interestingly, loss of the 15q11-q13 region, which occurs in up to 70% of patients with AS is associated with the loss of a number of GABA receptors including GABARB3, GABARA5 and GABRG3 (Frohlich et al., 2019a). The loss of GABA receptors has been hypothesized to be causative of the prevalence of epilepsy in AS, although there is little data to back this up. The loss of GABARB3 could result in the increased expression of miR-488. Future work into the validation of miR-488 and its predicted targets is required.

While we have speculated that protective effects of Ant-134 on seizures and motor impairments could be governed by de-repressing some of miR-134s targets such as limk1, creb1, DCX and pumillio2, we have not fully explored the mechanisms. The inferior colliculus has been reported to be heavily involved in audiogenic seizure propagation (Ross and Coleman, 2000) and studies have shown that GABA and glutamate transmission are involved in seizure activation pathways in this region (Ross and Coleman, 2000, Faingold et al., 1994). For example, injection of the GABAA agonist, muscimol, blocks seizure activity, whereas the $GABA_A$ antagonist, bicuculline, induced audiogenic seizures in non-susceptible rats (Faingold et al., 1994, Browning et al., 1989). This leads us to ask, do the effects of Ant-134 impact on these neurotransmitter systems directly? MiRNAs have been shown to be involved in regulating dopaminergic and GABAergic phenotypes (Dulcis et al., 2017). Furthermore, analysis of the predicted

miRNAs targeting GABA receptors included a number of miRNAs from the miR379~410 cluster, including miR-134, miR-411, miR-410, miR-488, miR-377 and miR-485 and these miRNA have been found to be involved in neurological diseases (Winter, 2015), postulating another mechanism of Ant-134 in this model.

In addition to the effect of Ant-134 on resting EEG and seizure phenotypes, we also found that injection of AS mice with Ant-134 restored motor phenotypes at P21. We found an increase in general locomotor activity in the open field in those treated with Ant-134 in comparison to scramble. The effect did not persist however, and improvement was not evident when re-tested three weeks later. Ant-134 did not correct deficits present in marble burying or rotarod, suggesting that different mechanisms (ie unrelated to miR-134 targets) or brain regions in which Ant-134 did not reach govern these phenotypes. The exact mechanisms underpinning this effect is currently unknown but it may be caused by some of miR-134s targets being de-repressed which would lead to changes to either spine number (Jimenez-Mateos et al., 2015) which may alter the synaptic efficacy of the circuits underlying those behaviors, allowing some deficits to be restored. Indeed, levels of DCX were found to be moderately increased with silencing of miR-134; however, it is unclear if this is the cause of the restoration of the impairment in the open field. Taken together, the results obtained in this thesis provide strong support for the use of a miRNA-based therapy in AS and possible other paediatric seizure disorders. Notably, we demonstrate the effectiveness of Ant-134 to reduce the severity of seizures in two separate models of epilepsy.

The disease modifying effects of Ant-134 were not fully explored in this model. Ant-134 has been shown to have long term disease modifying effects in adult models of epilepsy, when Ant-134 is no longer detectable in the brain (Reschke et al., 2019). When testing the effects of Ant-134 on behaviour, 24 h after injection with Ant-134, we found that partial knockdown had restorative effects on phenotypes in the open field, however, these results were not evident three weeks later when re-tested. This suggests that the effects of Ant-134 on behaviour are not long lasting. Perhaps a higher dose of Ant-134 may have caused disease modifying effects, although this was not explored

during this study. The seizure suppressive effects of Ant-134 were tested over the duration of a week. In order to test the long-term effects of Ant-134 on seizure phenotypes, the experimental design would have to be modified. Reinstatement of UBE3A at P21, has shown to prevent the progression of disease (Gu et al., 2019a), therefore miR-134 inhibition at this age is important. Here, seizures were induced every second day following pre-treatment at P21. This could be adapted by inducing audiogenic seizures once a week, beginning at P21 and lasting until adulthood (P42). This would determine if Ant-134 is disease modifying in this model as Ant-134 would no longer be present in the brain by the end of the study.

6.1.1 Strain and genetic background considerations

Significant strain differences were identified in this thesis. Tests of Ant-134 in wildtype C57BL/6 mice found that a high dose of Ant-134 (0.5 nmol) actually increased seizures in the KA model and there was an increase in mortality. In contrast, the same dose was effective at reducing the severity of audiogenic seizures in N4 AS mice which were backcrossed on the 129 strain. Furthermore, the dose at which initiation of SE was prevented in C57BL/6 mice, 0.1 nmol, was not effective in reducing seizures or preventing seizure induced mortality in N4 AS mice. Strain differences in models of epilepsy are well known, particular for responses to KA (McKhann et al., 2003, Schauwecker, 2002). For example, the genetic background of a mouse can influence the degree of excitotoxic cell death induced following chemoconvulsant induced seizures (Schauwecker, 2002). Interestingly, C57BL/6 mice were found to be one of the most resistant strains to seizures induced by KA (Schauwecker, 2002). These findings are in agreement with reports of strain differences present in mouse models of AS, as seizure susceptibility is dependent on the presence of 129 strain, whether the mice are purely bred on a 129 strain or if they are backcrossed on 129 (Jiang et al., 1998, Mandel-Brehm et al., 2015, Sonzogni et al., 2018). Because C57BL/6 mice appear to be a resistant strain, the difference in the effect of Ant-134 at both doses in the two strains used in this thesis

is suggestive of another mechanism. However, it is important to highlight that knockdown with 0.5 nmol of Ant-134 used alone for analyzing silencing of miR-134 did not result in mortality, therefore, a combination of knockdown and KA induced seizures is responsible for the mortality recorded. While the higher dose was used in both strains at the same age (P21), there may be slight alterations in neurodevelopment in the C57BL/6 strain that underpin this effect. The long-term effects of knocking down miR-134 at P21 is currently unexplored, hence, one might postulate that moderate expression of miR-134 is required for development in C57BL/6 mice.

6.1.2 Sex differences

The gender of mice used in all experiments was tracked throughout this thesis to determine if there were sex differences present. In the final results chapter, we detected some trends that were associated with female mice. In particular, during the validation of differentially expressed miRNA in naïve mice from both generations, the higher levels of miR-410-3p were found to be restricted to female mice. Notably, we previously observed that female mice responded better to Ant-134 treatment during the audiogenic seizure tests with 0.5 nmol Ant-134. Here, we found 100% survival in female mice that received Ant-134, in comparison to a 34% survival rate in female mice treated with the scramble compound. There was also evidence that levels of Limk1 were higher in female mice after Ant-134 treatment. Interestingly, the incidence of epilepsy is thought to be higher in men, while epilepsy in women is associated with more complex and intractable syndromes (Scharfman and MacLusky, 2014, Samba Reddy, 2017, Reddy, 2013). Here, we saw a higher percentage of mortality in female mice treated with the scrambled compound in comparison to male mice; however, this was not significant due to low numbers. In addition, there was a trend for an improved response rate to the Ant-134 treated female mice. While the gender specific response to AEDs has been explored, there has not been any data to suggest gender differences, thus, further work is required in this field (Perucca et al., 2014).

6.1.3 Additional miRNAs relevant to AS

A final segment of this thesis was the identification of differentially expressed miRNA in AS using small RNA sequencing. We identified a number of miRNAs that can be explored further and used for antagomir testing in this mouse model. The elevation of a number of miRNAs from the miR-379~410 cluster is consistent with the hypothesis that *Ube3a1* acts as a miRNA sponge, with the loss or mutation of the Ube3a gene locus leading to an increase of certain miRNAs. While we did not detect much change to overallmiR-134 levels as might have been expected, an increase in a number of miRNAs in Ube3a $^{(m-/p+)}$ mice from the miR-379~410 cluster warrants further investigation. MiR-410 and miR-300 have been found to be upregulated in the cerebellum in Mecp2 knockout mice (Wu et al., 2010). Analysis of the targets of miR-410-3p, miR-411-5p and miR-300-3p should be explored further.

6.2 Challenges and limitations

A number of challenges and limitations were associated with this project. The first, as discussed above, was the unexpected finding of an increase in mortality with the high dose of Ant-134 in P21 mice given KA. This contrasted with the otherwise excellent safety and anti-seizure effect of Ant-134 in previous adult models and the effects of the same dose when used in AS mice of the same age in the audiogenic model (Jimenez-Mateos et al., 2012). Further investigation into the effect of 0.5 nmol Ant-134 on cell death in a naïve brain could determine the cause of the toxicity. Moreover, further analysis of the targets of miR-134 could gain insight into the mechanism of Ant-134 in reducing seizure severity in the audiogenic seizure model.

During the characterisation of Ube3a $^{(m-/p+)}$ mice we were unable to properly characterize some of the phenotypes commonly reported in patients. For instance, several tests of cognition which depend on animal movement were not suitable for testing. Severe developmental delay and learning impairments are a key feature of AS (Micheletti et al., 2016). The significant motor impairment present in the open field

meant that cognitive tests such as novel object recognition and novel object location, which require animals to explore, unimpaired, an arena and objects within it, could not be tested as the deficit in locomotor activity would be a confounding factor. Alternative tests will be needed in the future. While not approved on our HPRA license, fear conditioning has been used to demonstrate hippocampal learning deficits in AS mice (Born et al., 2017, Huang et al., 2013).

Another challenge was the lack of audiogenic seizure susceptibility in F1 mice which necessitated a lengthy process of backcrossing of Ube3a $^{(m-/p+)}$ mice to reach N4 generation. This took roughly 6 months, due to poor breeding performance. Backcrossing required the use of females with a harmful phenotype to breed and the N4 mice bred poorly compared to the F1 mice which limited the number of mice available for studies, particularly in Chapter 5. We also observed a moderately high percentage of mortality of N4 pups within the first seven days of life. This was caused in part by an increase in observed cannibalism in the female breeders from the N3 generation. Second, in some cases the dams may not have been well enough to take care of the pups. Lastly, the pups may have died from SUDEP in the first few days of life. While no spontaneous seizures were observed in pups of this age, mice under P7 were rarely disturbed to avoid cannibalism, therefore seizures may have gone unnoticed.

While the majority of EEG and behaviour characterisation in the literature has been performed in F1 mice (Sonzogni et al., 2018, Huang et al., 2013, Gu et al., 2019b), it would have been beneficial to better characterise the N4 generation. The ability to induce audiogenic seizures in these mice postulates the presence of EEG abnormalities similar to those seen in F1 mice. Further analysis into the presence of spontaneous seizures in N4 mice is required as a small number of spontaneous seizures were recorded when doing welfare checks. Moreover, AS is associated with different levels of severity depending on the type of genetic mechanism. Having two models of different severity could aid in the development of a therapeutic target that could treat severe and milder forms of AS. During the study using Ant-134 to restore impairments in behaviour, we

noticed an anxiogenic phenotype begin to appear in the model that may have resulted in significant variability between litters. This may have been associated with genetic drift, as these mice had been breeding for roughly two years at the time of the study.

As mentioned previously, sequencing was performed on hippocampi from both generations of mice and this was done towards the end of the project due to tissue collection delay. The identification of other miRNAs from the miR-379~410 cluster could have been used as a combined treatment with Ant-134.

6.3 Future work

The present project represents four years of research, including a year of rotations in different labs. While the majority of questions arising from our hypothesis were answered, some areas have not been fully explored:

6.3.1 Antagomir suppression in a paediatric mouse model of epilepsy

Before moving to the AS model, we first sought to test the efficacy of Ant-134 in a paediatric model using WT mice. Previous research using adult models of SE have shown the long-term protective effects of Ant-134 on the emergence of spontaneous seizures two weeks after SE (Jimenez-Mateos et al., 2012, Reschke et al., 2017b). While we present significant seizure suppressive effects of Ant-134 in a model of SE, we did not determine if Ant-134 had any effects on the development of spontaneous seizures at a later stage. This would require extensive long-term video-EEG telemetry studies using the DSI system which cannot be implanted to P21 mice due to their physical size. Further investigation is required to determine if this paediatric model of SE develops spontaneous seizures and if Ant-134 can minimise or prevent this.

6.3.2 Characterisation of the Ube3a $^{(m-/p+)}$ mice

Additional analysis is required to understand the underlying mechanisms of seizure susceptibility in the N4 generation. When analysing levels of miR-134 following small RNA sequencing, there was an increase in expression in the N4 AS mice in comparison to F1 AS mice, postulating that miR-134 may play a role in hyperexcitability in N4 mice. Follow up experiments could analyse miR-134 expression in the synaptosomes in these mice. In addition, analysing the levels of miR-134 by Ago2 immunoprecipitation may identify alterations between genotypes.

Due to time constraints, a number of phenotypes were not explored. Speech impairments in AS are one of the most frequently reported issues in patients and have been extremely challenging to model in mic ultrasonic vocalizations in postnatal Ube3a $^{(m-/p+)}$ mice (Mandel-Brehm et al., 2015). Future experiments could build on determining the underlying mechanism(s) of this phenotype and if it can be restored using a miRNA based therapy. In addition, sleep impairments have also been reported in patients with AS (den Bakker et al., 2018). It is currently unknown if there are sleep disruptions in Ube3a $^{(m-/p+)}$ mice, however, understanding the basis of sleep impairments would be beneficial due to the importance of sleep in brain development. For example, it would be interesting to determine the age at which sleep disturbances occur and if there is any correlation to the initiation of behavioural or seizure phenotypes.

6.3.3 Identification and development of new miRNA based therapies

A number of potential new targets were identified using small RNA sequencing. Further experiments could be done to investigate the role played by these miRNAs in AS and to find out with which phenotypes they are associated. While these miRNAs were validated by RT-qPCR, further work is required to analyse the targets of these miRNA. While we have shown the use of Ant-134 to treat a number of aspects of AS, further optimisation

of dosing is required. Although 0.5 nmol of Ant-134 reduced seizure severity and mortality, higher doses have not yet been tested in this model.

Inhibition of miR-134 improved motor impairments and reduced seizure severity. It did not, however, fully protect against the induction of audiogenic seizures, as some mice still presented with seizures. Perhaps a further increase in the dose of Ant-134 to 1 nmol could rescue seizure susceptibility and seizure induced mortality. In addition, the use of a combined antagomir could aid in this protection. For instance, due to the abundance of predicted targets of genes associated with GABA and glutamatergic transmission, it is quite possible that inhibiting miR-134 and miR-488 could reverse the epilepsy phenotypes. Another potential combination could include miR-134 and miR-410, as the latter has been found to be upregulated in the cerebellum of MECP2 knockout mice. AS and Rett syndrome share a number of symptoms including seizures, movement dysfunction and intellectual disability. While the role of miR-410 in Rett syndrome has yet to be explored, it may be involved in some of the motor phenotypes as both generations sequenced in this study had motor impairments.

6.4 Final conclusions

Taken together, the work presented in this thesis demonstrated the potential use of antisense oligonucleotide inhibition of miR-134 to treat early life seizures and AS. The data in this thesis builds on the hypothesis that disruption of *Ub3a1* results in the loss of a miRNA sponge, which could contribute to the hyper-excitable phenotype present in AS. Antagomir suppression of miR-134 restored a motor phenotype and had seizure suppressive effects in an audiogenic seizure model. These studies have contributed to the AS field and work presented here may be applicable to other forms of genetic epilepsy.

References:

1927. THE TREATMENT OF EPILEPSY. *JAMA,* 88**,** 1638-1638.

AABERG, K. M., GUNNES, N., BAKKEN, I. J., LUND SORAAS, C., BERNTSEN, A., MAGNUS, P., LOSSIUS, M. I., STOLTENBERG, C., CHIN, R. & SUREN, P. 2017. Incidence and Prevalence of Childhood Epilepsy: A Nationwide Cohort Study. *Pediatrics,* 139.

ABEND, N. S., BEARDEN, D., HELBIG, I., MCGUIRE, J., NARULA, S., PANZER, J. A., TOPJIAN, A. & DLUGOS, D. J. 2014. Status epilepticus and refractory status epilepticus management. *Seminars in Pediatric Neurology,* 21**,** 263-274.

ABHANG, P. A., GAWALI, B. W. & MEHROTRA, S. C. 2016a. Chapter 1 - Introduction to Emotion, Electroencephalography, and Speech Processing. *In:* ABHANG, P. A., GAWALI, B. W. & MEHROTRA, S. C. (eds.) *Introduction to EEG- and Speech-Based Emotion Recognition.* Academic Press.

ABHANG, P. A., GAWALI, B. W. & MEHROTRA, S. C. 2016b. Chapter 3 - Technical Aspects of Brain Rhythms and Speech Parameters. *In:* ABHANG, P. A., GAWALI, B. W. & MEHROTRA, S. C. (eds.) *Introduction to EEG- and Speech-Based Emotion Recognition.* Academic Press.

ADKINS, C. E., PILLAI, G. V., KERBY, J., BONNERT, T. P., HALDON, C., MCKERNAN, R. M., GONZALEZ, J. E., OADES, K., WHITING, P. J. & SIMPSON, P. B. 2001. alpha4beta3delta GABA(A) receptors characterized by fluorescence resonance energy transfer-derived measurements of membrane potential. *J Biol Chem,* 276**,** 38934-9.

AKIYAMA, M., KOBAYASHI, K. & OHTSUKA, Y. 2012. Dravet syndrome: a genetic epileptic disorder. *Acta Med Okayama,* 66**,** 369-76.

AL-BANJI, M. H., ZAHR, D. K. & JAN, M. M. 2015. Lennox-Gastaut syndrome: Management update. *Neurosciences,* 20**,** 207-212.

ALEXANDER, M. L., ALAGAPAN, S., LUGO, C. E., MELLIN, J. M., LUSTENBERGER, C., RUBINOW, D. R. & FRÖHLICH, F. 2019. Double-blind, randomized pilot clinical trial targeting alpha oscillations with transcranial alternating current stimulation (tACS) for the treatment of major depressive disorder (MDD). *Transl Psychiatry,* 9**,** 106.

ALFIMOVA, M. V. & UVAROVA, L. G. 2007. [Changes in the EEG spectral power during perception of neutral and emotionally salient words in schizophrenic patients, their relatives and healthy individuals from the general population]. *Zh Vyssh Nerv Deiat Im I P Pavlova,* 57**,** 426-36.

ALFORD, E. L., WHELESS, J. W. & PHELPS, S. J. 2015. Treatment of Generalized Convulsive Status Epilepticus in Pediatric Patients. *The journal of pediatric pharmacology and therapeutics : JPPT : the official journal of PPAG,* 20**,** 260-289.

AMARAL, D. G., BAUMAN, M. D. & SCHUMANN, C. M. 2003. The amygdala and autism: implications from non-human primate studies. *Genes Brain Behav,* 2**,** 295-302.

AMIET, C., GOURFINKEL-AN, I., BOUZAMONDO, A., TORDJMAN, S., BAULAC, M., LECHAT, P., MOTTRON, L. & COHEN, D. 2008. Epilepsy in autism is associated with intellectual disability and gender: evidence from a meta-analysis. *Biol Psychiatry,* 64**,** 577-82.

AMIR, R. E., VAN DEN VEYVER, I. B., WAN, M., TRAN, C. Q., FRANCKE, U. & ZOGHBI, H. Y. 1999. Rett syndrome is caused by mutations in X-linked MECP2, encoding methyl-CpG-binding protein 2. *Nature Genetics,* 23**,** 185-188.

ANDERSEN, W. H., RASMUSSEN, R. K. & STROMME, P. 2001. Levels of cognitive and linguistic development in Angelman syndrome: a study of 20 children. *Logoped Phoniatr Vocol,* 26**,** 2-9.

ANGELMAN, H. 1965. 'Puppet' Report. *Developmental Medicine & Child Neurology,* 7**,** 681-688.
ANGRIMAN, M., CARAVALE, B., NOVELLI, L., FERRI, R. & BRUNI, O. 2015. Sleep in children with neurodevelopmental disabilities. *Neuropediatrics,* 46**,** 199-210.
ANGULO, M. A., BUTLER, M. G. & CATALETTO, M. E. 2015. Prader-Willi syndrome: a review of clinical, genetic, and endocrine findings. *Journal of endocrinological investigation,* 38**,** 1249-1263.
ARDEKANI, A. M. & NAEINI, M. M. 2010. The Role of MicroRNAs in Human Diseases. *Avicenna journal of medical biotechnology,* 2**,** 161-179.
ARMSTRONG, D., DUNN, J. K., ANTALFFY, B. & TRIVEDI, R. 1995. Selective dendritic alterations in the cortex of Rett syndrome. *J Neuropathol Exp Neurol,* 54**,** 195-201.
ARONICA, E., FLUITER, K., IYER, A., ZUROLO, E., VREIJLING, J., VAN VLIET, E. A., BAAYEN, J. C. & GORTER, J. A. 2010. Expression pattern of miR-146a, an inflammation-associated microRNA, in experimental and human temporal lobe epilepsy. *European Journal of Neuroscience,* 31**,** 1100-1107.
ARRON, K., OLIVER, C., MOSS, J., BERG, K. & BURBIDGE, C. 2011. The prevalence and phenomenology of self-injurious and aggressive behaviour in genetic syndromes. *J Intellect Disabil Res,* 55**,** 109-20.
AU - NEELY, C. L. C., AU - PEDEMONTE, K. A., AU - BOGGS, K. N. & AU - FLINN, J. M. 2019. Nest Building Behavior as an Early Indicator of Behavioral Deficits in Mice. *JoVE***,** e60139.
BALMER, D., GOLDSTINE, J., RAO, Y. M. & LASALLE, J. M. 2003. Elevated methyl-CpG-binding protein 2 expression is acquired during postnatal human brain development and is correlated with alternative polyadenylation. *Journal of Molecular Medicine,* 81**,** 61-68.
BARLOW, D. P. & BARTOLOMEI, M. S. Genomic imprinting in mammals. *Cold Spring Harbor perspectives in biology,* 6**,** a018382.
BARON-COHEN, S., RING, H. A., BULLMORE, E. T., WHEELWRIGHT, S., ASHWIN, C. & WILLIAMS, S. C. 2000. The amygdala theory of autism. *Neurosci Biobehav Rev,* 24**,** 355-64.
BARROS, V. N., MUNDIM, M., GALINDO, L. T., BITTENCOURT, S., PORCIONATTO, M. & MELLO, L. E. 2015. The pattern of c-Fos expression and its refractory period in the brain of rats and monkeys. *Frontiers in Cellular Neuroscience,* 9.
BARTEL, D. P. 2018. Metazoan MicroRNAs. *Cell,* 173**,** 20-51.
BASSELL, G. J. & WARREN, S. T. 2008. Fragile X syndrome: loss of local mRNA regulation alters synaptic development and function. *Neuron,* 60**,** 201-14.
BAUDOUIN, S. J., GAUDIAS, J., GERHARZ, S., HATSTATT, L., ZHOU, K., PUNNAKKAL, P., TANAKA, K. F., SPOOREN, W., HEN, R., DE ZEEUW, C. I., VOGT, K. & SCHEIFFELE, P. 2012. Shared synaptic pathophysiology in syndromic and nonsyndromic rodent models of autism. *Science,* 338**,** 128-32.
BAUER, J. & COOPER-MAHKORN, D. 2008. Tiagabine: efficacy and safety in partial seizures - current status. *Neuropsychiatric disease and treatment,* 4**,** 731-736.
BAUMANN, V. & WINKLER, J. 2014. miRNA-based therapies: strategies and delivery platforms for oligonucleotide and non-oligonucleotide agents. *Future medicinal chemistry,* 6**,** 1967-1984.
BELICHENKO, P. V., OLDFORS, A., HAGBERG, B. & DAHLSTROM, A. 1994. Rett syndrome: 3-D confocal microscopy of cortical pyramidal dendrites and afferents. *Neuroreport,* 5**,** 1509-13.
BELICHENKO, P. V., WRIGHT, E. E., BELICHENKO, N. P., MASLIAH, E., LI, H. H., MOBLEY, W. C. & FRANCKE, U. 2009. Widespread changes in dendritic and axonal morphology in Mecp2-

mutant mouse models of rett syndrome: Evidence for disruption of neuronal networks. *Journal of Comparative Neurology,* 514**,** 240-258.

BERG, A. T., BACA, C. B., LODDENKEMPER, T., VICKREY, B. G. & DLUGOS, D. 2013. Priorities in pediatric epilepsy research: Improving children's futures today. *Neurology,* 81**,** 1166-1175.

BERG, A. T., LANGFITT, J. T., TESTA, F. M., LEVY, S. R., DIMARIO, F., WESTERVELD, M. & KULAS, J. 2008. Global cognitive function in children with epilepsy: a community-based study. *Epilepsia,* 49**,** 608-14.

BHATT, D. H., ZHANG, S. & GAN, W. B. 2009. Dendritic spine dynamics. *Annu Rev Physiol,* 71**,** 261-82.

BIEN, C. G., GRANATA, T., ANTOZZI, C., CROSS, J. H., DULAC, O., KURTHEN, M., LASSMANN, H., MANTEGAZZA, R., VILLEMURE, J. G., SPREAFICO, R. & ELGER, C. E. 2005. Pathogenesis, diagnosis and treatment of Rasmussen encephalitisA European consensus statement. *Brain,* 128**,** 454-471.

BIRD, L. M. 2014. Angelman syndrome: review of clinical and molecular aspects. *The application of clinical genetics,* 7**,** 93-104.

BOISON, D. 2013. Adenosine and seizure termination: endogenous mechanisms. *Epilepsy currents,* 13**,** 35-37.

BOKSA, P. 2012. Abnormal synaptic pruning in schizophrenia: Urban myth or reality? *Journal of psychiatry & neuroscience : JPN,* 37**,** 75-77.

BOLTON, P. F., PARK, R. J., HIGGINS, J. N. P., epileptic determinants of autism spectrum disorders in tuberous sclerosis complex. *Brain,* 125**,** 1247-1255.

BORN, H. A., DAO, A. T., LEVINE, A. T., LEE, W. L., MEHTA, N. M., MEHRA, S., WEEBER, E. J. & ANDERSON, A. E. 2017. Strain-dependence of the Angelman Syndrome phenotypes in Ube3a maternal deficiency mice. *Scientific Reports,* 7**,** 8451.

BOT, A. M., DEBSKI, K. J. & LUKASIUK, K. 2013. Alterations in miRNA levels in the dentate gyrus in epileptic rats. *PLoS One,* 8**,** e76051.

BOTTANI, A., ROBINSON, W. P., DELOZIER-BLANCHET, C. D., ENGEL, E., MORRIS, M. A., SCHMITT, B., THUN-HOHENSTEIN, L. & SCHINZEL, A. 1994. Angelman syndrome due to paternal uniparental disomy of chromosome 15: a milder phenotype? *Am J Med Genet,* 51**,** 35-40.

BOUGH, K. J. & RHO, J. M. 2007. Anticonvulsant mechanisms of the ketogenic diet. *Epilepsia,* 48**,** 43-58.

BOYD, S. G., HARDEN, A. & PATTON, M. A. 1988. The EEG in early diagnosis of the Angelman (happy puppet) syndrome. *Eur J Pediatr,* 147**,** 508-13.

BOZZI, Y., PROVENZANO, G. & CASAROSA, S. 2018. Neurobiological bases of autism–epilepsy comorbidity: a focus on excitation/inhibition imbalance. *European Journal of Neuroscience,* 47**,** 534-548.

BRODIE, M. J. 2017. Sodium Channel Blockers in the Treatment of Epilepsy. *CNS Drugs,* 31**,** 527-534.

BROWNING, R. A., LANKER, M. L. & FAINGOLD, C. L. 1989. Injections of noradrenergic and GABAergic agonists into the inferior colliculus: effects on audiogenic seizures in genetically epilepsy-prone rats. *Epilepsy Res,* 4**,** 119-25.

BRUINSMA, C. F., SCHONEWILLE, M., GAO, Z., ARONICA, E. M. A., JUDSON, M. C., PHILPOT, B. D., HOEBEEK, F. E., VAN WOERDEN, G. M., DE ZEEUW, C. I. & ELGERSMA, Y. 2015. Dissociation of locomotor and cerebellar deficits in a murine Angelman syndrome model. *The Journal of Clinical Investigation,* 125**,** 4305-4315.

BUITING, K., WILLIAMS, C. & HORSTHEMKE, B. 2016. Angelman syndrome - insights into a rare neurogenetic disorder. *Nat Rev Neurol,* 12**,** 584-93.

BUONI, S., GROSSO, S., PUCCI, L. & FOIS, A. 1999. Diagnosis of Angelman syndrome: clinical and EEG criteria. *Brain Dev,* 21**,** 296-302.

BUSNER, J. & TARGUM, S. D. 2007. The clinical global impressions scale: applying a research tool in clinical practice. *Psychiatry (Edgmont (Pa. : Township)),* 4**,** 28-37.

CAMFIELD, C. S., CAMFIELD, P. R., GORDON, K., WIRRELL, E. & DOOLEY, J. M. 1996. Incidence of epilepsy in childhood and adolescence: a population-based study in Nova Scotia from 1977 to 1985. *Epilepsia,* 37**,** 19-23.

CARBALLOSA-GONZALEZ, M. M., MUÑOZ, L. J., LÓPEZ-ALBURQUERQUE, T., PARDAL-FERNÁNDEZ, J. M., NAVA, E., DE CABO, C., SANCHO, C. & LÓPEZ, D. E. 2013. EEG characterization of audiogenic seizures in the hamster strain GASH:Sal. *Epilepsy Research,* 106**,** 318-325.

CARRATALA-MARCO, F., ANDREO-LILLO, P., MARTINEZ-MORGA, M., ESCAMEZ-MARTÍNEZ, T., BOTELLA-LÓPEZ, A., BUENO, C. & MARTINEZ, S. 2018. Clinical Phenotypes Associated to Engrailed 2 Gene Alterations in a Series of Neuropediatric Patients. *Frontiers in Neuroanatomy,* 12.

CATTERALL, W. A. 2000. Structure and regulation of voltage-gated Ca2+ channels. *Annu Rev Cell Dev Biol,* 16**,** 521-55.

CATTERALL, W. A. 2011. Voltage-gated calcium channels. *Cold Spring Harbor perspectives in biology,* 3**,** a003947-a003947.

CATTERALL, W. A. 2017. Forty Years of Sodium Channels: Structure, Function, Pharmacology, and Epilepsy. *Neurochem Res,* 42**,** 2495-2504.

CHAKRABORTY, C., SHARMA, A. R., SHARMA, G., DOSS, C. G. P. & LEE, S.-S. 2017. Therapeutic miRNA and siRNA: Moving from Bench to Clinic as Next Generation Medicine. *Molecular Therapy - Nucleic Acids,* 8**,** 132-143.

CHANG, Q., KHARE, G., DANI, V., NELSON, S. & JAENISCH, R. 2006. The disease progression of Mecp2 mutant mice is affected by the level of BDNF expression. *Neuron,* 49**,** 341-8.

CHELINI, G., ZERBI, V., CIMINO, L., GRIGOLI, A., MARKICEVIC, M., LIBERA, F., ROBBIATI, S., GADLER, M., BRONZONI, S., MIORELLI, S., GALBUSERA, A., GOZZI, A., CASAROSA, S., PROVENZANO, G. & BOZZI, Y. 2019. Aberrant Somatosensory Processing and Connectivity in Mice Lacking Engrailed-2. *The Journal of neuroscience : the official journal of the Society for Neuroscience,* 39**,** 1525-1538.

CHEN, J. W., NAYLOR, D. E. & WASTERLAIN, C. G. 2007. Advances in the pathophysiology of status epilepticus. *Acta Neurol Scand,* 115**,** 7-15.

CHENG, L.-C., PASTRANA, E., TAVAZOIE, M. & DOETSCH, F. 2009. miR-124 regulates adult neurogenesis in the subventricular zone stem cell niche. *Nature neuroscience,* 12**,** 399-408.

CHIN, R. F. M., NEVILLE, B. G. R., PECKHAM, C., BEDFORD, H., WADE, A. & SCOTT, R. C. 2006. Incidence, cause, and short-term outcome of convulsive status epilepticus in childhood: prospective population-based study. *The Lancet,* 368**,** 222-229.

CHO, K. H. T., XU, B., BLENKIRON, C. & FRASER, M. 2019. Emerging Roles of miRNAs in Brain Development and Perinatal Brain Injury. *Frontiers in Physiology,* 10.

CHOPRA, R. & ISOM, L. L. 2014. Untangling the Dravet Syndrome Seizure Network: The Changing Face of a Rare Genetic Epilepsy. *Epilepsy Currents,* 14**,** 86-89.

CHOWDHURY, S., SHEPHERD, J. D., OKUNO, H., LYFORD, G., PETRALIA, R. S., PLATH, N., KUHL, D., HUGANIR, R. L. & WORLEY, P. F. 2006. Arc/Arg3.1 Interacts with the Endocytic Machinery to Regulate AMPA Receptor Trafficking. *Neuron,* 52**,** 445-459.

CHUNG, K.-H., HART, C. C., AL-BASSAM, S., AVERY, A., TAYLOR, J., PATEL, P. D., VOJTEK, A. B. & TURNER, D. L. 2006. Polycistronic RNA polymerase II expression vectors for RNA interference based on BIC/miR-155. *Nucleic acids research,* 34**,** e53-e53.

CLARKE, D. J. & MARSTON, G. 2000. Problem behaviors associated with 15q- Angelman syndrome. *Am J Ment Retard,* 105**,** 25-31.

CLAYTON-SMITH, J. 1993. Clinical research on Angelman syndrome in the United Kingdom: observations on 82 affected individuals. *Am J Med Genet,* 46**,** 12-5.

CLAYTON-SMITH, J. 2003. Genomic imprinting as a cause of disease. *BMJ (Clinical research ed.),* 327**,** 1121-1122.

CLAYTON-SMITH, J. & LAAN, L. 2003. Angelman syndrome: a review of the clinical and genetic aspects. *Journal of medical genetics,* 40**,** 87-95.

COLLEDGE, M., SNYDER, E. M., CROZIER, R. A., SODERLING, J. A., JIN, Y., LANGEBERG, L. K., LU, H., BEAR, M. F. & SCOTT, J. D. 2003. Ubiquitination regulates PSD-95 degradation and AMPA receptor surface expression. *Neuron,* 40**,** 595-607.

CONANT, K. D., FINUCANE, B., CLEARY, N., MARTIN, A., MUSS, C., DELANY, M., MURPHY, E. K., RABE, O., LUCHSINGER, K., SPENCE, S. J., SCHANEN, C., DEVINSKY, O., COOK, E. H., LASALLE, J., REITER, L. T. & THIBERT, R. L. 2014. A survey of seizures and current treatments in 15q duplication syndrome. *Epilepsia,* 55**,** 396-402.

CONANT, K. D., THIBERT, R. L. & THIELE, E. A. 2009. Epilepsy and the sleep–wake patterns found in Angelman syndrome. *Epilepsia,* 50**,** 2497-2500.

CONN, P. J. & PIN, J. P. 1997. Pharmacology and functions of metabotropic glutamate receptors. *Annu Rev Pharmacol Toxicol,* 37**,** 205-37.

COOK, E. H., JR., LINDGREN, V., LEVENTHAL, B. L., COURCHESNE, R., LINCOLN, A., SHULMAN, C., LORD, C. & COURCHESNE, E. 1997. Autism or atypical autism in maternally but not paternally derived proximal 15q duplication. *Am J Hum Genet,* 60**,** 928-34.

CROCE, C. M. & CALIN, G. A. 2005. miRNAs, cancer, and stem cell division. *Cell,* 122**,** 6-7.

CRUPI, R., IMPELLIZZERI, D. & CUZZOCREA, S. 2019. Role of Metabotropic Glutamate Receptors in Neurological Disorders. *Frontiers in Molecular Neuroscience,* 12.

CUBEROS, H., VALLEE, B., VOURC'H, P., TASTET, J., ANDRES, C. R. & BENEDETTI, H. 2015. Roles of LIM kinases in central nervous system function and dysfunction. *FEBS Lett,* 589**,** 3795-806.

CUMMINGS, C. J., REINSTEIN, E., SUN, Y., ANTALFFY, B., JIANG, Y.-H., CIECHANOVER, A., ORR, H. T., BEAUDET, A. L. & ZOGHBI, H. Y. 1999. Mutation of the E6-AP Ubiquitin Ligase Reduces Nuclear Inclusion Frequency While Accelerating Polyglutamine-Induced Pathology in SCA1 Mice. *Neuron,* 24**,** 879-892.

CURATOLO, P. & MOAVERO, R. 2012. mTOR Inhibitors in Tuberous Sclerosis Complex. *Current neuropharmacology,* 10**,** 404-415.

DAHLIN, M., ELFVING, A., UNGERSTEDT, U. & AMARK, P. 2005. The ketogenic diet influences the levels of excitatory and inhibitory amino acids in the CSF in children with refractory epilepsy. *Epilepsy Res,* 64**,** 115-25.

DALLMER-ZERBE, I., POPP, F., LAM, A. P., PHILIPSEN, A. & HERRMANN, C. S. 2020. Transcranial Alternating Current Stimulation (tACS) as a Tool to Modulate P300 Amplitude in Attention Deficit Hyperactivity Disorder (ADHD): Preliminary Findings. *Brain Topogr,* 33**,** 191-207.

DAVIS, T. H., CUELLAR, T. L., KOCH, S. M., BARKER, A. J., HARFE, B. D., MCMANUS, M. T. & ULLIAN, E. M. 2008. Conditional Loss of Dicer Disrupts Cellular and Tissue Morphogenesis in the Cortex and Hippocampus. *The Journal of Neuroscience,* 28**,** 4322-4330.

DE PIETRI TONELLI, D., CLOVIS, Y. M. & HUTTNER, W. B. 2014. Detection and monitoring of microRNA expression in developing mouse brain and fixed brain cryosections. *Methods Mol Biol,* 1092**,** 31-42.

DEACON, R. M. J. 2006a. Assessing nest building in mice. *Nature Protocols,* 1**,** 1117-1119.

DEACON, R. M. J. 2006b. Digging and marble burying in mice: simple methods for in vivo identification of biological impacts. *Nature Protocols,* 1**,** 122-124.

DEACON, R. M. J. 2013. Measuring motor coordination in mice. *Journal of visualized experiments : JoVE***,** e2609-e2609.

DEACON, R. M. J. & RAWLINS, J. N. P. 2005. Hippocampal lesions, species-typical behaviours and anxiety in mice. *Behavioural Brain Research,* 156**,** 241-249.

DEACON, S., STANER, L., STANER, C., LEGTERS, A., LOFT, H. & LUNDAHL, J. 2007. Effect of short-term treatment with gaboxadol on sleep maintenance and initiation in patients with primary insomnia. *Sleep,* 30**,** 281-7.

DELORENZO, R. J., HAUSER, W. A., TOWNE, A. R., BOGGS, J. G., PELLOCK, J. M., PENBERTHY, L., GARNETT, L., FORTNER, C. A. & KO, D. 1996. A prospective, population-based epidemiologic study of status epilepticus in Richmond, Virginia. *Neurology,* 46**,** 1029-35.

DEN BAKKER, H., SIDOROV, M. S., FAN, Z., LEE, D. J., BIRD, L. M., CHU, C. J. & PHILPOT, B. D. 2018. Abnormal coherence and sleep composition in children with Angelman syndrome: a retrospective EEG study. *Mol Autism,* 9**,** 32.

DHAM, B. S., HUNTER, K. & RINCON, F. 2014. The epidemiology of status epilepticus in the United States. *Neurocrit Care,* 20**,** 476-83.

DINDOT, S. V., ANTALFFY, B. A., BHATTACHARJEE, M. B. & BEAUDET, A. L. 2008. The Angelman syndrome ubiquitin ligase localizes to the synapse and nucleus, and maternal deficiency results in abnormal dendritic spine morphology. *Hum Mol Genet,* 17**,** 111-8.

DISTEFANO, C., GULSRUD, A., HUBERTY, S., KASARI, C., COOK, E., REITER, L. T., THIBERT, R. & JESTE, S. S. 2016. Identification of a distinct developmental and behavioral profile in children with Dup15q syndrome. *Journal of neurodevelopmental disorders,* 8**,** 19-19.

DODGE, A., PETERS, M. M., GREENE, H. E., DIETRICK, C., BOTELHO, R., CHUNG, D., WILLMAN, J., NENNINGER, A. W., CIARLONE, S., KAMATH, S. G., HOUDEK, P., SUMOVÁ, A., ANDERSON, A. E., DINDOT, S. V., BERG, E. L., O'GEEN, H., SEGAL, D. J., SILVERMAN, J. L., WEEBER, E. J. & NASH, K. R. 2020. Generation of a Novel Rat Model of Angelman Syndrome with a Complete Ube3a Gene Deletion. *Autism Res,* 13**,** 397-409.

DOLEN, G. & BEAR, M. 2008. *Role for metabotropic glutamate receptor 5 (mGluR5) in the pathogenesis of fragile X syndrome*.

DOOSE, H. 1992. Myoclonic-astatic epilepsy. *Epilepsy Res Suppl,* 6**,** 163-8.

DULCIS, D., LIPPI, G., STARK, C. J., DO, L. H., BERG, D. K. & SPITZER, N. C. 2017. Neurotransmitter Switching Regulated by miRNAs Controls Changes in Social Preference. *Neuron,* 95**,** 1319-1333.e5.

DUTTA, S. & SENGUPTA, P. 2016. Men and mice: Relating their ages. *Life Sci,* 152**,** 244-8.

EACKER, S. M., DAWSON, T. M. & DAWSON, V. L. 2009. Understanding microRNAs in neurodegeneration. *Nat Rev Neurosci,* 10**,** 837-41.

EGAWA, K., KITAGAWA, K., INOUE, K., TAKAYAMA, M., TAKAYAMA, C., SAITOH, S., KISHINO, T., KITAGAWA, M. & FUKUDA, A. 2012. Decreased Tonic Inhibition in Cerebellar Granule Cells Causes Motor Dysfunction in a Mouse Model of Angelman Syndrome. *Science Translational Medicine,* 4**,** 163ra157-163ra157.

EILAND, L. & MCEWEN, B. S. 2012. Early life stress followed by subsequent adult chronic stress potentiates anxiety and blunts hippocampal structural remodeling. *Hippocampus,* 22**,** 82-91.

ENGEL, J., JR. 2014. Approaches to refractory epilepsy. *Annals of Indian Academy of Neurology,* 17**,** S12-S17.

ENGEL, T., MURPHY, B. M., SCHINDLER, C. K. & HENSHALL, D. C. 2007. Elevated p53 and lower MDM2 expression in hippocampus from patients with intractable temporal lobe epilepsy. *Epilepsy research,* 77**,** 151-156.

ENGEL, T., TANAKA, K., JIMENEZ-MATEOS, E. M., CABALLERO-CABALLERO, A., PREHN, J. H. M. & HENSHALL, D. C. 2010. Loss of p53 results in protracted electrographic seizures and development of an aggravated epileptic phenotype following status epilepticus. *Cell death & disease,* 1**,** e79-e79.

ENGLE, E. C. 2010. Human genetic disorders of axon guidance. *Cold Spring Harb Perspect Biol,* 2**,** a001784.

ESTACION, M., O'BRIEN, J. E., CONRAVEY, A., HAMMER, M. F., WAXMAN, S. G., DIB-HAJJ, S. D. & MEISLER, M. H. 2014. A novel de novo mutation of SCN8A (Nav1.6) with enhanced channel activation in a child with epileptic encephalopathy. *Neurobiol Dis,* 69**,** 117-23.

EVANGELIOU, A., DOULIOGLOU, V., HAIDOPOULOU, K., APTOURAMANI, M., SPILIOTI, M. & VARLAMIS, G. 2010. Ketogenic diet in a patient with Angelman syndrome. *Pediatr Int,* 52**,** 831-4.

FAINGOLD, C. L., MARCINCZYK, M. J., CASEBEER, D. J., RANDALL, M. E., ARNERIC´, S. P. & BROWNING, R. A. 1994. GABA in the inferior colliculus plays a critical role in control of audiogenic seizures. *Brain Research,* 640**,** 40-47.

FALCO-WALTER, J. J. & BLECK, T. 2016. Treatment of Established Status Epilepticus. *Journal of Clinical Medicine,* 5**,** 49.

FASOLINO, M. & ZHOU, Z. 2017. The Crucial Role of DNA Methylation and MeCP2 in Neuronal Function. *Genes,* 8**,** 141.

FATEMI, S. H., FOLSOM, T. D., KNEELAND, R. E. & LIESCH, S. B. 2011. Metabotropic glutamate receptor 5 upregulation in children with autism is associated with underexpression of both Fragile X mental retardation protein and GABAA receptor beta 3 in adults with autism. *Anatomical record (Hoboken, N.J. : 2007),* 294**,** 1635-1645.

FATEMI, S. H., REUTIMAN, T. J., FOLSOM, T. D., ROONEY, R. J., PATEL, D. H. & THURAS, P. D. 2010. mRNA and protein levels for GABAAalpha4, alpha5, beta1 and GABABR1 receptors are altered in brains from subjects with autism. *J Autism Dev Disord,* 40**,** 743-50.

FATEMI, S. H., REUTIMAN, T. J., FOLSOM, T. D. & THURAS, P. D. 2009. GABA(A) receptor downregulation in brains of subjects with autism. *J Autism Dev Disord,* 39**,** 223-30.

FINEBERG, S. K., KOSIK, K. S. & DAVIDSON, B. L. 2009. MicroRNAs potentiate neural development. *Neuron,* 64**,** 303-9.

FINGELKURTS, A. A., FINGELKURTS, A. A., RYTSÄLÄ, H., SUOMINEN, K., ISOMETSÄ, E. & KÄHKÖNEN, S. 2007. Impaired functional connectivity at EEG alpha and theta frequency bands in major depression. *Hum Brain Mapp,* 28**,** 247-61.

FIORE, R., KHUDAYBERDIEV, S., CHRISTENSEN, M., SIEGEL, G., FLAVELL, S. W., KIM, T. K., GREENBERG, M. E. & SCHRATT, G. 2009. Mef2-mediated transcription of the miR379-410 cluster regulates activity-dependent dendritogenesis by fine-tuning Pumilio2 protein levels. *Embo J,* 28**,** 697-710.

FIORE, R., RAJMAN, M., SCHWALE, C., BICKER, S., ANTONIOU, A., BRUEHL, C., DRAGUHN, A. & SCHRATT, G. 2014. MiR-134-dependent regulation of Pumilio-2 is necessary for homeostatic synaptic depression. *The EMBO journal,* 33**,** 2231-2246.

FIUMARA, A., PITTALÀ, A., COCUZZA, M. & SORGE, G. 2010. Epilepsy in patients with Angelman syndrome. *Italian Journal of Pediatrics,* 36**,** 31.

FLORES, O., KENNEDY, E. M., SKALSKY, R. L. & CULLEN, B. R. 2014. Differential RISC association of endogenous human microRNAs predicts their inhibitory potential. *Nucleic Acids Res,* 42**,** 4629-39.

FRAMPTON, J. E. 2015. Perampanel: A Review in Drug-Resistant Epilepsy. *Drugs,* 75**,** 1657-1668.

FRANCO, V., CREMA, F., IUDICE, A., ZACCARA, G. & GRILLO, E. 2013. Novel treatment options for epilepsy: focus on perampanel. *Pharmacol Res,* 70**,** 35-40.

FRANZ, D. N., GLAUSER, T. A., TUDOR, C. & WILLIAMS, S. 2000. Topiramate therapy of epilepsy associated with Angelman's. *Neurology,* 54**,** 1185-1188.

FRIEDRICH, M., HEIMER, N., STOEHR, C., STEVEN, A., WACH, S., TAUBERT, H., HARTMANN, A. & SELIGER, B. 2020. CREB1 is affected by the microRNAs miR-22-3p, miR-26a-5p, miR-27a-3p, and miR-221-3p and correlates with adverse clinicopathological features in renal cell carcinoma. *Scientific Reports,* 10**,** 6499.

FROHLICH, J., MILLER, M. T., BIRD, L. M., GARCES, P., PURTELL, H., HOENER, M. C., PHILPOT, B. D., SIDOROV, M. S., TAN, W. H., HERNANDEZ, M. C., ROTENBERG, A., JESTE, S. S., KRISHNAN, M., KHWAJA, O. & HIPP, J. F. 2019a. Electrophysiological Phenotype in Angelman Syndrome Differs Between Genotypes. *Biol Psychiatry,* 85**,** 752-759.

FROHLICH, J., REITER, L. T., SARAVANAPANDIAN, V., DISTEFANO, C., HUBERTY, S., HYDE, C., CHAMBERLAIN, S., BEARDEN, C. E., GOLSHANI, P., IRIMIA, A., OLSEN, R. W., HIPP, J. F. & JESTE, S. S. 2019b. Mechanisms underlying the EEG biomarker in Dup15q syndrome. *Molecular autism,* 10**,** 29-29.

FROHLICH, J., SENTURK, D., SARAVANAPANDIAN, V., GOLSHANI, P., REITER, L. T., SANKAR, R., THIBERT, R. L., DISTEFANO, C., HUBERTY, S., COOK, E. H. & JESTE, S. S. 2016. A Quantitative Electrophysiological Biomarker of Duplication 15q11.2-q13.1 Syndrome. *PloS one,* 11**,** e0167179-e0167179.

GALVEZ, R. & GREENOUGH, W. T. 2005. Sequence of abnormal dendritic spine development in primary somatosensory cortex of a mouse model of the fragile X mental retardation syndrome. *American journal of medical genetics. Part A,* 135**,** 155-160.

GAO, J., WANG, W. Y., MAO, Y. W., GRÄFF, J., GUAN, J. S., PAN, L., MAK, G., KIM, D., SU, S. C. & TSAI, L. H. 2010. A novel pathway regulates memory and plasticity via SIRT1 and miR-134. *Nature,* 466**,** 1105-9.

GAO, X., GUO, M., MENG, D., SUN, F., GUAN, L., CUI, Y., ZHAO, Y., WANG, X., GU, X., SUN, J. & QI, S. 2019. Silencing MicroRNA-134 Alleviates Hippocampal Damage and Occurrence of Spontaneous Seizures After Intraventricular Kainic Acid-Induced Status Epilepticus in Rats. *Frontiers in Cellular Neuroscience,* 13.

GARDINER, E., BEVERIDGE, N. J., WU, J. Q., CARR, V., SCOTT, R. J., TOONEY, P. A. & CAIRNS, M. J. 2012. Imprinted DLK1-DIO3 region of 14q32 defines a schizophrenia-associated miRNA signature in peripheral blood mononuclear cells. *Molecular Psychiatry,* 17**,** 827-840.

GASKILL, B. N., KARAS, A. Z., GARNER, J. P. & PRITCHETT-CORNING, K. R. 2013. Nest building as an indicator of health and welfare in laboratory mice. *Journal of visualized experiments : JoVE***,** 51012-51012.

GAUGHWIN, P., CIESLA, M., YANG, H., LIM, B. & BRUNDIN, P. 2011. Stage-specific modulation of cortical neuronal development by Mmu-miR-134. *Cereb Cortex,* 21**,** 1857-69.

GIBBS, J. W., 3RD, SOMBATI, S., DELORENZO, R. J. & COULTER, D. A. 2000. Cellular actions of topiramate: blockade of kainate-evoked inward currents in cultured hippocampal neurons. *Epilepsia,* 41 Suppl 1**,** S10-6.

GILBERT, D. L., GARTSIDE, P. S. & GLAUSER, T. A. 1999. Efficacy and Mortality in Treatment of Refractory Generalized Convulsive Status Epilepticus in Children: A Meta-Analysis. *Journal of Child Neurology,* 14**,** 602-609.

GIPSON, T. T., GERNER, G., WILSON, M. A., BLUE, M. E. & JOHNSTON, M. V. 2013. Potential for treatment of severe autism in tuberous sclerosis complex. *World journal of clinical pediatrics,* 2**,** 16-25.

GODAVARTHI, S. K., DEY, P., SHARMA, A. & JANA, N. R. 2015. Impaired adult hippocampal neurogenesis and its partial reversal by chronic treatment of fluoxetine in a mouse model of Angelman syndrome. *Biochem Biophys Res Commun,* 464**,** 1196-1201.

GOODKIN, H. P., SUN, C., YEH, J. L., MANGAN, P. S. & KAPUR, J. 2007a. GABA(A) receptor internalization during seizures. *Epilepsia,* 48 Suppl 5**,** 109-13.

GOODKIN, H. R., JOSHI, S., KOZHEMYAKIN, M. & KAPUR, J. 2007b. Impact of receptor changes on treatment of status epilepticus. *Epilepsia,* 48 Suppl 8**,** 14-5.

GÖREN, M. Z. & ONAT, F. 2007. Ethosuximide: from bench to bedside. *CNS drug reviews,* 13**,** 224-239.

GORTER, J. A., IYER, A., WHITE, I., COLZI, A., VAN VLIET, E. A., SISODIYA, S. & ARONICA, E. 2014. Hippocampal subregion-specific microRNA expression during epileptogenesis in experimental temporal lobe epilepsy. *Neurobiol Dis,* 62**,** 508-20.

GRAVES, P. & ZENG, Y. 2012. Biogenesis of Mammalian MicroRNAs: A Global View. *Genomics, Proteomics & Bioinformatics,* 10**,** 239-245.

GREENBLATT, D. J., EHRENBERG, B. L., GUNDERMAN, J., LOCNISKAR, A., SCAVONE, J. M., HARMATZ, J. S. & SHADER, R. I. 1989. Pharmacokinetic and electroencephalographic study of intravenous diazepam, midazolam, and placebo. *Clinical Pharmacology & Therapeutics,* 45**,** 356-365.

GREENE, J. G. & GREENAMYRE, J. T. 1996. Bioenergetics and glutamate excitotoxicity. *Prog Neurobiol,* 48**,** 613-34.

GREER, P. L., HANAYAMA, R., BLOODGOOD, B. L., MARDINLY, A. R., LIPTON, D. M., FLAVELL, S. W., KIM, T.-K., GRIFFITH, E. C., WALDON, Z., MAEHR, R., PLOEGH, H. L., CHOWDHURY, S., WORLEY, P. F., STEEN, J. & GREENBERG, M. E. 2010. The Angelman Syndrome Protein Ube3A Regulates Synapse Development by Ubiquitinating Arc. *Cell,* 140**,** 704-716.

GRIECO, J. C., GOUELLE, A. & WEEBER, E. J. 2018. Identification of spatiotemporal gait parameters and pressure-related characteristics in children with Angelman syndrome: A pilot study. *Journal of Applied Research in Intellectual Disabilities,* 31**,** 1219-1224.

GROSS-TSUR, V. & SHINNAR, S. 1993. Convulsive Status Epilepticus in Children. *Epilepsia,* 34**,** S12-S20.

GROSS, C. & TIWARI, D. 2018. Regulation of Ion Channels by MicroRNAs and the Implication for Epilepsy. *Current neurology and neuroscience reports* [Online], 18. Available: http://europepmc.org/abstract/MED/30046905

https://doi.org/10.1007/s11910-018-0870-2

https://europepmc.org/articles/PMC6092942

https://europepmc.org/articles/PMC6092942?pdf=render [Accessed 2018/07//].
GROSSMAN, A. W., ALDRIDGE, G. M., WEILER, I. J. & GREENOUGH, W. T. 2006. Local protein synthesis and spine morphogenesis: Fragile X syndrome and beyond. *The Journal of neuroscience : the official journal of the Society for Neuroscience,* 26**,** 7151-7155.
GU, B., CARSTENS, K. E., JUDSON, M. C., DALTON, K. A., ROUGIÉ, M., CLARK, E. P., DUDEK, S. M. & PHILPOT, B. D. 2019a. Ube3a reinstatement mitigates epileptogenesis in Angelman syndrome model mice. *The Journal of clinical investigation,* 129**,** 163-168.
GU, B., ZHU, M., GLASS, M. R., ROUGIÉ, M., NIKOLOVA, V. D., MOY, S. S., CARNEY, P. R. & PHILPOT, B. D. 2019b. Cannabidiol attenuates seizures and EEG abnormalities in Angelman syndrome model mice. *The Journal of Clinical Investigation,* 129**,** 5462-5467.
GUERRINI, R. & NOEBELS, J. 2014. How can advances in epilepsy genetics lead to better treatments and cures? *Adv Exp Med Biol,* 813**,** 309-17.
HA, S., SOHN, I.-J., KIM, N., SIM, H. J. & CHEON, K.-A. 2015. Characteristics of Brains in Autism Spectrum Disorder: Structure, Function and Connectivity across the Lifespan. *Experimental neurobiology,* 24**,** 273-284.
HAJAK, G., HEDNER, J., EGLIN, M., LOFT, H., STORUSTOVU, S. I., LUTOLF, S. & LUNDAHL, J. 2009. A 2-week efficacy and safety study of gaboxadol and zolpidem using electronic diaries in primary insomnia outpatients. *Sleep Med,* 10**,** 705-12.
HALLBOOK, T., LUNDGREN, J. & ROSEN, I. 2007. Ketogenic diet improves sleep quality in children with therapy-resistant epilepsy. *Epilepsia,* 48**,** 59-65.
HANDFORTH, A., DELOREY, T. M., HOMANICS, G. E. & OLSEN, R. W. 2005. Pharmacologic evidence for abnormal thalamocortical functioning in GABA receptor beta3 subunit-deficient mice, a model of Angelman syndrome. *Epilepsia,* 46**,** 1860-70.
HARDINGHAM, G. E., FUKUNAGA, Y. & BADING, H. 2002. Extrasynaptic NMDARs oppose synaptic NMDARs by triggering CREB shut-off and cell death pathways. *Nat Neurosci,* 5**,** 405-14.
HARKIN, L. A., MCMAHON, J. M., IONA, X., DIBBENS, L., PELEKANOS, J. T., ZUBERI, S. M., SADLEIR, L. G., ANDERMANN, E., GILL, D., FARRELL, K., CONNOLLY, M., STANLEY, T., HARBORD, M., ANDERMANN, F., WANG, J., BATISH, S. D., JONES, J. G., SELTZER, W. K., GARDNER, A., SUTHERLAND, G., BERKOVIC, S. F., MULLEY, J. C. & SCHEFFER, I. E. 2007. The spectrum of SCN1A-related infantile epileptic encephalopathies. *Brain,* 130**,** 843-52.
HARRISON, J. E. & BOLTON, P. F. 1997. Annotation: Tuberous Sclerosis. *Journal of Child Psychology and Psychiatry,* 38**,** 603-614.
HAUSER, W. A. 1994. The prevalence and incidence of convulsive disorders in children. *Epilepsia,* 35 Suppl 2**,** S1-6.
HAUSER, W. A., ANNEGERS, J. F. & KURLAND, L. T. 1993. Incidence of epilepsy and unprovoked seizures in Rochester, Minnesota: 1935-1984. *Epilepsia,* 34**,** 453-68.
HENLEY, J. M. & WILKINSON, K. A. 2016. Synaptic AMPA receptor composition in development, plasticity and disease. *Nat Rev Neurosci,* 17**,** 337-50.
HENSHALL, D. C. 2014. MicroRNA and epilepsy: profiling, functions and potential clinical applications. *Current opinion in neurology,* 27**,** 199-205.
HENSHALL, D. C., HAMER, H. M., PASTERKAMP, R. J., GOLDSTEIN, D. B., KJEMS, J., PREHN, J. H. M., SCHORGE, S., LAMOTTKE, K. & ROSENOW, F. 2016. MicroRNAs in epilepsy: pathophysiology and clinical utility. *Lancet Neurol,* 15**,** 1368-1376.
HERBER, D. L., WEEBER, E. J., D'AGOSTINO, D. P tolerability of a nutritional Formulation in patients with ANgelman Syndrome (FANS): study protocol for a randomized controlled trial. *Trials,* 21**,** 60.

HINTON, V. J., BROWN, W. T., WISNIEWSKI, K. & RUDELLI, R. D. 1991. Analysis of neocortex in three males with the fragile X syndrome. *Am J Med Genet,* 41**,** 289-94.

HOEHN-SARIC, R. 1983. Effects of THIP on chronic anxiety. *Psychopharmacology (Berl),* 80**,** 338-41.

HORSLER, K. & OLIVER, C. 2006. The behavioural phenotype of Angelman syndrome. *J Intellect Disabil Res,* 50**,** 33-53.

HOU, Q., RUAN, H., GILBERT, J., WANG, G., MA, Q., YAO, W.-D. & MAN, H.-Y. 2015. MicroRNA miR124 is required for the expression of homeostatic synaptic plasticity. *Nature Communications,* 6**,** 10045.

HOWELL, K. B., MCMAHON, J. M., CARVILL, G. L., TAMBUNAN, D., MACKAY, M. T., RODRIGUEZ-CASERO, V., WEBSTER, R., CLARK, D., FREEMAN, J. L., CALVERT, S., OLSON, H. E., MANDELSTAM, S., PODURI, A., MEFFORD, H. C., HARVEY, A. S. & SCHEFFER, I. E. 2015. SCN2A encephalopathy: A major cause of epilepsy of infancy with migrating focal seizures. *Neurology,* 85**,** 958-66.

HU, K., XIE, Y. Y., ZHANG, C., OUYANG, D. S., LONG, H. Y., SUN, D. N., LONG, L. L., FENG, L., LI, Y. & XIAO, B. 2012. MicroRNA expression profile of the hippocampus in a rat model of temporal lobe epilepsy and miR-34a-targeted neuroprotection against hippocampal neurone cell apoptosis post-status epilepticus. *BMC Neurosci,* 13**,** 115.

HU, W., TIAN, C., LI, T., YANG, M., HOU, H. & SHU, Y. 2009. Distinct contributions of Na(v)1.6 and Na(v)1.2 in action potential initiation and backpropagation. *Nat Neurosci,* 12**,** 996-1002.

HUANG, H. S., ALLEN, J. A., MABB, A. M., KING, I. F., MIRIYALA, J., TAYLOR-BLAKE, B., SCIAKY, N., DUTTON, J. W., JR., LEE, H. M., CHEN, X., JIN, J., BRIDGES, A. S., ZYLKA, M. J., ROTH, B. L. & PHILPOT, B. D. 2011. Topoisomerase inhibitors unsilence the dormant allele of Ube3a in neurons. *Nature,* 481**,** 185-9.

HUANG, H. S., BURNS, A. J., NONNEMAN, R. J., BAKER, L. K., RIDDICK, N. V., NIKOLOVA, V. D., RIDAY, T. T., YASHIRO, K., PHILPOT, B. D. & MOY, S. S. 2013. Behavioral deficits in an Angelman syndrome model: effects of genetic background and age. *Behav Brain Res,* 243**,** 79-90.

HUIBREGTSE, J. M., SCHEFFNER, M. & HOWLEY, P. M. 1991. A cellular protein mediates association of p53 with the E6 oncoprotein of human papillomavirus types 16 or 18. *Embo j,* 10**,** 4129-35.

HUNDALLAH, K., ALENIZI, A., ALHASHEM, A. & TABARKI, B. 2016. Severe early-onset epileptic encephalopathy due to mutations in the KCNA2 gene: Expansion of the genotypic and phenotypic spectrum. *Eur J Paediatr Neurol,* 20**,** 657-60.

HUNT, A. & SHEPHERD, C. 1993. A prevalence study of autism in tuberous sclerosis. *J Autism Dev Disord,* 23**,** 323-39.

HUSSAIN, N., APPLETON, R. & THORBURN, K. 2007. Aetiology, course and outcome of children admitted to paediatric intensive care with convulsive status epilepticus: A retrospective 5-year review. *Seizure,* 16**,** 305-312.

HUTSLER, J. & ZHANG, H. 2009. Increased dendritic spine densities on cortical projection neurons in autism spectrum disorders. *Brain research,* 1309**,** 83-94.

IRWIN, S. A., GALVEZ, R. & GREENOUGH, W. T. 2000. Dendritic Spine Structural Anomalies in Fragile-X Mental Retardation Syndrome. *Cerebral Cortex,* 10**,** 1038-1044.

ITOH, K. & WATANABE, M. 2009. Paradoxical facilitation of pentylenetetrazole-induced convulsion susceptibility in mice lacking neuronal nitric oxide synthase. *Neuroscience,* 159**,** 735-43.

JAMAIN, S., QUACH, H., BETANCUR, C., RÅSTAM, M., COLINEAUX, C., GILLBERG, I. C., SODERSTROM, H., GIROS, B., LEBOYER, M., GILLBERG, C., BOURGERON, T. & PARIS AUTISM RESEARCH INTERNATIONAL SIBPAIR, S. 2003. Mutations of the X-linked genes encoding neuroligins NLGN3 and NLGN4 are associated with autism. *Nature genetics,* 34**,** 27-29.

JENSEN, M. & GIRIRAJAN, S. 2017. Mapping a shared genetic basis for neurodevelopmental disorders. *Genome medicine,* 9**,** 109-109.

JENSEN, O., GOEL, P., KOPELL, N., POHJA, M., HARI, R. & ERMENTROUT, B. 2005. On the human sensorimotor-cortex beta rhythm: Sources and modeling. *NeuroImage,* 26**,** 347-355.

JESTE, S. S. & TUCHMAN, R. 2015. Autism Spectrum Disorder and Epilepsy: Two Sides of the Same Coin? *Journal of child neurology,* 30**,** 1963-1971.

JIANG, Y.-H., PAN, Y., ZHU, L., LANDA, L., YOO, J., SPENCER, C., LORENZO, I., BRILLIANT, M., NOEBELS, J. & BEAUDET, A. L. 2010. Altered ultrasonic vocalization and impaired learning and memory in Angelman syndrome mouse model with a large maternal deletion from Ube3a to Gabrb3. *PloS one,* 5**,** e12278-e12278.

JIANG, Y. H., ARMSTRONG, D., ALBRECHT, U., ATKINS, C. M., NOEBELS, J. L., EICHELE, G., SWEATT, J. D. & BEAUDET, A. L. 1998. Mutation of the Angelman ubiquitin ligase in mice causes increased cytoplasmic p53 and deficits of contextual learning and long-term potentiation. *Neuron,* 21**,** 799-811.

JIMENEZ-MATEOS, E. M., BRAY, I., SANZ-RODRIGUEZ, A., ENGEL, T., MCKIERNAN, R. C., MOURI, G., TANAKA, K., SANO, T., SAUGSTAD, J. A., SIMON, R. P., STALLINGS, R. L. & HENSHALL, D. C. 2011. miRNA Expression profile after status epilepticus and hippocampal neuroprotection by targeting miR-132. *The American journal of pathology,* 179**,** 2519-2532.

JIMENEZ-MATEOS, E. M., ENGEL, T., MERINO-SERRAIS, P., FERNAUD-ESPINOSA, I., RODRIGUEZ-ALVAREZ, N., REYNOLDS, J., RESCHKE, C. R., CONROY, R. M., MCKIERNAN, R. C., DEFELIPE, J. & HENSHALL, D. C. 2015. Antagomirs targeting microRNA-134 increase hippocampal pyramidal neuron spine volume in vivo and protect against pilocarpine-induced status epilepticus. *Brain Structure and Function,* 220**,** 2387-2399.

JIMENEZ-MATEOS, E. M., ENGEL, T., MERINO-SERRAIS, P., MCKIERNAN, R. C., TANAKA, K., MOURI, G., SANO, T., O'TUATHAIGH, C., WADDINGTON, J. L., PRENTER, S., DELANTY, N., FARRELL, M. A., O'BRIEN, D. F., CONROY, R. M., STALLINGS, R. L., DEFELIPE, J. & HENSHALL, D. C. 2012. Silencing microRNA-134 produces neuroprotective and prolonged seizure-suppressive effects. *Nat Med,* 18**,** 1087-94.

JIN, H. Y., GONZALEZ-MARTIN, A., MILETIC, A. V., LAI, M., KNIGHT, S., SABOURI-GHOMI, M., HEAD, S. R., MACAULEY, M. S., RICKERT, R. C. & XIAO, C. 2015. Transfection of microRNA Mimics Should Be Used with Caution. *Frontiers in Genetics,* 6.

JIN, Z., BAZOV, I., KONONENKO, O., KORPI, E. R., BAKALKIN, G. & BIRNIR, B. 2011. Selective Changes of GABA(A) Channel Subunit mRNAs in the Hippocampus and Orbitofrontal Cortex but not in Prefrontal Cortex of Human Alcoholics. *Front Cell Neurosci,* 5**,** 30.

JOLLEFF, N. & RYAN, M. M. 1993. Communication development in Angelman's syndrome. *Archives of disease in childhood,* 69**,** 148-150.

KANNER, L. 1943. Autistic disturbances of affective contact. *Nervous Child,* 2**,** 217-250.

KATZ, A. M. 1986. Pharmacology and mechanisms of action of calcium-channel blockers. *J Clin Hypertens,* 2**,** 28s-37s.

KAUFMANN, W. E. & MOSER, H. W. 2000. Dendritic anomalies in disorders associated with mental retardation. *Cereb Cortex,* 10**,** 981-91.

KELSEY, J. E., SANDERSON, K. L. & FRYE, C. A. 2000. Perforant path stimulation in rats produces seizures, loss of hippocampal neurons, and a deficit in spatial mapping which are reduced by prior MK-801. *Behav Brain Res,* 107**,** 59-69.

KERR, J. E., BECK, S. G. & HANDA, R. J. 1996. Androgens selectively modulate C-fos messenger RNA induction in the rat hippocampus following novelty. *Neuroscience,* 74**,** 757-66.

KILKENNY, C., BROWNE, W., CUTHILL, I. C., EMERSON, M., ALTMAN, D. G. & GROUP, N. C. R. R. G. W. 2010. Animal research: reporting in vivo experiments: the ARRIVE guidelines. *British journal of pharmacology,* 160**,** 1577-1579.

KIM, H. J., CHO, M. H., SHIM, W. H., KIM, J. K., JEON, E. Y., KIM, D. H. & YOON, S. Y. 2017. Deficient autophagy in microglia impairs synaptic pruning and causes social behavioral defects. *Molecular Psychiatry,* 22**,** 1576-1584.

KIM, I., MLSNA, L. M., YOON, S., LE, B., YU, S., XU, D. & KOH, S. 2015. A postnatal peak in microglial development in the mouse hippocampus is correlated with heightened sensitivity to seizure triggers. *Brain and Behavior,* 5**,** e00403.

KISHINO, T., LALANDE, M. & WAGSTAFF, J. 1997. UBE3A/E6-AP mutations cause Angelman syndrome. *Nat Genet,* 15**,** 70-3.

KLECKNER, N. W., GLAZEWSKI, J. C., CHEN, C. C. & MOSCRIP, T. D. 1999. Subtype-selective antagonism of N-methyl-D-aspartate receptors by felbamate: insights into the mechanism of action. *J Pharmacol Exp Ther,* 289**,** 886-94.

KLEIN, M. E., LIOY, D. T., MA, L., IMPEY, S., MANDEL, G. & GOODMAN, R. H. 2007. Homeostatic regulation of MeCP2 expression by a CREB-induced microRNA. *Nat Neurosci,* 10**,** 1513-4.

KLEMPAN, T. A., SEQUEIRA, A., CANETTI, L., LALOVIC, A., ERNST, C., FFRENCH-MULLEN, J. & TURECKI, G. 2009. Altered expression of genes involved in ATP biosynthesis and GABAergic neurotransmission in the ventral prefrontal cortex of suicides with and without major depression. *Mol Psychiatry,* 14**,** 175-89.

KLIMCZAK-BITNER, A. A., KORDEK, R., BITNER, J., MU MMP9, SERPINE1 and miR-134 as prognostic factors in esophageal cancer. *Oncology letters,* 12**,** 4133-4138.

KOLODKIN, A. L., LEVENGOOD, D. V., ROWE, E. G., TAI, Y.-T., GIGER, R. J. & GINTY, D. D. 1997. Neuropilin Is a Semaphorin III Receptor. *Cell,* 90**,** 753-762.

KORFF, C. M., KELLEY, K. R. & NORDLI, D. R., JR. 2005. Notched delta, phenotype, and Angelman syndrome. *J Clin Neurophysiol,* 22**,** 238-43.

KOSIK, K. S. 2006. The neuronal microRNA system. *Nat Rev Neurosci,* 7**,** 911-20.

KOSS, W. A., BELDEN, C. E., HRISTOV, A. D. & JURASKA, J. M. 2014. Dendritic remodeling in the adolescent medial prefrontal cortex and the basolateral amygdala of male and female rats. *Synapse,* 68**,** 61-72.

KOZOMARA, A., BIRGAOANU, M. & GRIFFITHS-JONES, S. 2019. miRBase: from microRNA sequences to function. *Nucleic Acids Res,* 47**,** D155-d162.

KROGSGAARD-LARSEN, P., FROLUND, B., LILJEFORS, T. & EBERT, B. 2004. GABA(A) agonists and partial agonists: THIP (Gaboxadol) as a non-opioid analgesic and a novel type of hypnotic. *Biochem Pharmacol,* 68**,** 1573-80.

KUKKO-LUKJANOV, T. K., GRONMAN, M., LINTUNEN, M., LAUREN, H. B., MICHELSEN, K. A., PANULA, P. & HOLOPAINEN, I. E. 2012. Histamine 1 receptor knock out mice show age-dependent susceptibility to status epilepticus and consequent neuronal damage. *Epilepsy Res,* 100**,** 80-92.

KULKARNI, V. A. & FIRESTEIN, B. L. 2012. The dendritic tree and brain disorders. *Mol Cell Neurosci,* 50**,** 10-20.

KURTH, S., ACHERMANN, P., RUSTERHOLZ, T. & LEBOURGEOIS, M. K. 2013. Development of Brain EEG Connectivity across Early Childhood: Does Sleep Play a Role? *Brain Sci,* 3**,** 1445-60.

KURTH, S., RINGLI, M., LEBOURGEOIS, M. K., GEIGER, A., BUCHMANN, A., JENNI, O. G. & HUBER, R. 2012. Mapping the electrophysiological marker of sleep depth reveals skill maturation in children and adolescents. *Neuroimage,* 63**,** 959-65.

LAAN, L. A., RENIER, W. O., ARTS, W. F., BUNTINX, I. M., VD BURGT, I. J., STROINK, H., BEUTEN, J., ZWINDERMAN, K. H., VAN DIJK, J. G. & BROUWER, O. F. 1997. Evolution of epilepsy and EEG findings in Angelman syndrome. *Epilepsia,* 38**,** 195-9.

LAAN, L. A., V HAERINGEN, A. & BROUWER, O. F. 1999. Angelman syndrome: a review of clinical and genetic aspects. *Clin Neurol Neurosurg,* 101**,** 161-70.

LACEY, A., SMITH, P., REES, M. & THOMAS, R. 2012. SUDEP (SUDDEN UNEXPECTED DEATH IN EPILEPSY) FOLLOWING STATUS EPILEPTICUS. *Journal of Neurology, Neurosurgery & Psychiatry,* 83**,** A38-A38.

LACKINGER, M., SUNGUR, A., DASWANI, R., SOUTSCHEK, M., BICKER, S., STEMMLER, L., WÜST, T., FIORE, R., DIETERICH, C., SCHWARTING, R. K., WÖHR, M. & SCHRATT, G. 2019. A placental mammal-specific microRNA cluster acts as a natural brake for sociability in mice. *EMBO Rep,* 20.

LALANDE, M. & CALCIANO, M. A. 2007. Molecular epigenetics of Angelman syndrome. *Cellular and Molecular Life Sciences,* 64**,** 947.

LAMPRIANOU, S., CHATZOPOULOU, E., THOMAS, J.-L., BOUYAIN, S. & HARROCH, S. 2011. A complex between contactin-1 and the protein tyrosine phosphatase PTPRZ controls the development of oligodendrocyte precursor cells. *Proceedings of the National Academy of Sciences of the United States of America,* 108**,** 17498-503.

LANDERS, M., CALCIANO, M. A., COLOSI, D., GLATT-DEELEY, H., WAGSTAFF, J. & LALANDE, M. 2005. Maternal disruption of Ube3a leads to increased expression of Ube3a-ATS in trans. *Nucleic acids research,* 33**,** 3976-3984.

LARSON, A. M., SHINNICK, J. E., SHAAYA, E. A., THIELE, E. A. & THIBERT, R. L. 2015. Angelman syndrome in adulthood. *American journal of medical genetics. Part A,* 167A**,** 331-344.

LAVIOLA, G., MACRì, S., MORLEY-FLETCHER, S. & ADRIANI, W. 2003. Risk-taking behavior in adolescent mice: psychobiological determinants and early epigenetic influence. *Neuroscience & Biobehavioral Reviews,* 27**,** 19-31.

LAW, C. W., ALHAMDOOSH, M., SU, S., DONG, X., TIAN, L., SMYTH, G. K. & RITCHIE, M. E. 2016. RNA-seq analysis is easy as 1-2-3 with limma, Glimma and edgeR. *F1000Res,* 5.

LEE, R. C., FEINBAUM, R. L. & AMBROS, V. 1993. The C. elegans heterochronic gene lin-4 encodes small RNAs with antisense complementarity to lin-14. *Cell,* 75**,** 843-54.

LEWENA, S., PENNINGTON, V., ACWORTH, J., THORNTON, S., NGO, P., MCINTYRE, S., KRIESER, D., NEUTZE, J. & SPELDEWINDE, D. 2009. Emergency management of pediatric convulsive status epilepticus: a multicenter study of 542 patients. *Pediatr Emerg Care,* 25**,** 83-7.

LEWINE, J. D., ANDREWS, R., CHEZ, M., PATIL, A. A., DEVINSKY, O., SMITH, M., KANNER, A., DAVIS, J. T., FUNKE, M., JONES, G., CHONG, B., PROVENCAL, S., WEISEND, M., LEE, R. R. & ORRISON, W. W., JR. 1999. Magnetoencephalographic patterns of epileptiform activity in children with regressive autism spectrum disorders. *Pediatrics,* 104**,** 405-18.

LI, W. & POZZO-MILLER, L. 2014. BDNF deregulation in Rett syndrome. *Neuropharmacology,* 76 Pt C**,** 737-46.

LIM, L. P., LAU, N. C., GARRETT-ENGELE, P., GRIMSON, A., SCHELTER, J. M., CASTLE, J., BARTEL, D. P., LINSLEY, P. S. & JOHNSON, J. M. 2005. Microarray analysis shows that some microRNAs downregulate large numbers of target mRNAs. *Nature,* 433**,** 769-73.

LINDOW, M. & KAUPPINEN, S. 2012. Discovering the first microRNA-targeted drug. *Journal of Cell Biology,* 199**,** 407-412.

LOOMES, R., HULL, L. & MANDY, W. P. L. 2017. What Is the Male-to-Female Ratio in Autism Spectrum Disorder? A Systematic Review and Meta-Analysis. *Journal of the American Academy of Child & Adolescent Psychiatry,* 56**,** 466-474.

LÖSCHER, W. & SCHMIDT, D. 2012. Perampanel—new promise for refractory epilepsy? *Nature Reviews Neurology,* 8**,** 661-662.

LOSSIE, A. C., WHITNEY, M. M., AMIDON, D., DONG, H. J., CHEN, P., THERIAQUE, D., HUTSON, A., NICHOLLS, R. D., ZORI, R. T., WILLIAMS, C. A. & DRISCOLL, D. J. 2001. Distinct phenotypes distinguish the molecular classes of Angelman syndrome. *J Med Genet,* 38**,** 834-45.

LOTHMAN, E. 1990. The biochemical basis and pathophysiology of status epilepticus. *Neurology,* 40**,** 13-23.

MABB, A. M., JUDSON, M. C., ZYLKA, M. J. & PHILPOT, B. D. 2011. Angelman syndrome: insights into genomic imprinting and neurodevelopmental phenotypes. *Trends in Neurosciences,* 34**,** 293-303.

MALJEVIC, S. & LERCHE, H. 2013. Potassium channels: a review of broadening therapeutic possibilities for neurological diseases. *J Neurol,* 260**,** 2201-11.

MANDEL-BREHM, C., SALOGIANNIS, J., DHAMNE, S. C., ROTENBERG, A. & GREENBERG, M. E. 2015. Seizure-like activity in a juvenile Angelman syndrome mouse model is attenuated by reducing Arc expression. *Proc Natl Acad Sci U S A,* 112**,** 5129-34.

MANTEGAZZA, M., CURIA, G., BIAGINI, G., RAGSDALE, D. S. & AVOLI, M. 2010. Voltage-gated sodium channels as therapeutic targets in epilepsy and other neurological disorders. *Lancet Neurol,* 9**,** 413-24.

MARDIROSSIAN, S., RAMPON, C., SALVERT, D., FORT, P. & SARDA, N. 2009. Impaired hippocampal plasticity and altered neurogenesis in adult Ube3a maternal deficient mouse model for Angelman syndrome. *Exp Neurol,* 220**,** 341-8.

MARGOLIS, S. S., SALOGIANNIS, J., LIPTON, D. M., MANDEL-BREHM, C., WILLS, Z. P., MARDINLY, A. R., HU, L., GREER, P. L., BIKOFF, J. B., HO, H.-Y. H., SOSKIS, M. J., SAHIN, M. & GREENBERG, M. E. 2010. EphB-Mediated Degradation of the RhoA GEF Ephexin5 Relieves a Developmental Brake on Excitatory Synapse Formation. *Cell,* 143**,** 442-455.

MARTIN, J. B., SAMEER, M. Z., INGRID, E. S. & ROBERT, S. F. 2018. The 2017 ILAE classification of seizure types and the epilepsies: what do people with epilepsy and their caregivers need to know? *Epileptic Disorders,* 20**,** 77-87.

MARTIN, J. P. & BELL, J. 1943. A PEDIGREE OF MENTAL DEFECT SHOWING SEX-LINKAGE. *J Neurol Psychiatry,* 6**,** 154-7.

MATSUMOTO, A., KUMAGAI, T., MIURA, K., MIYAZAKI, S., HAYAKAWA, C. & YAMANAKA, T. 1992a. Epilepsy in Angelman syndrome associated with chromosome 15q deletion. *Epilepsia,* 33**,** 1083-90.

MATSUMOTO, A., KUMAGAI, T., MIURA, K., MIYAZAKI, S., HAYAKAWA, C. & YAMANAKA, T. 1992b. Epilepsy in Angelman Syndrome Associated with Chromosome 15q Deletion. *Epilepsia,* 33**,** 1083-1090.

MATSUMURA, K., SEIRIKI, K., OKADA, S., NAGASE, M., AYABE, S., YAMADA, I., FURUSE, T., SHIBUYA, H., YASUDA, Y., YAMAMORI, H., FUJIMOTO, M., NAGAYASU, K., YAMAMOTO, K., KITAGAWA, K., MIURA, H., GOTODA-NISHIMURA, N., IGARASHI, H., HAYASHIDA, M.,

BABA, M., KONDO, M., HASEBE, S., UESHIMA, K., KASAI, A., AGO, Y., HAYATA-TAKANO, A., SHINTANI, N., IGUCHI, T., SATO, M., YAMAGUCHI, S., TAMURA, M., WAKANA, S., YOSHIKI, A., WATABE, A. M., OKANO, H., TAKUMA, K., HASHIMOTO, R., HASHIMOTO, H. & NAKAZAWA, T. 2020. Pathogenic POGZ mutation causes impaired cortical development and reversible autism-like phenotypes. *Nature Communications,* 11**,** 859.

MATSUURA, T., SUTCLIFFE, J. S., FANG, P., GALJAARD, R. J., JIANG, Y. H., BENTON, C. S., ROMMENS, J. M. & BEAUDET, A. L. 1997. De novo truncating mutations in E6-AP ubiquitin-protein ligase gene (UBE3A) in Angelman syndrome. *Nat Genet,* 15**,** 74-7.

MAYTAL, J., SHINNAR, S., MOSHÉ, S. L. & ALVAREZ, L. A. 1989. Low morbidity and mortality of status epilepticus in children. *Pediatrics,* 83**,** 323-31.

MAZARATI, A. M., BALDWIN, R. A., SANKAR, R. & WASTERLAIN, C. G. 1998. Time-dependent decrease in the effectiveness of antiepileptic drugs during the course of self-sustaining status epilepticus. *Brain Res,* 814**,** 179-85.

MCCORD, M. C., LORENZANA, A., BLOOM, C. S., CHANCER, Z. O. & SCHAUWECKER, P. E. 2008. Effect of age on kainate-induced seizure severity and cell death. *Neuroscience,* 154**,** 1143-1153.

MCCOY, B. & BENBADIS, S. 2010. *Approach to refractory childhood seizures*.

MCKHANN, G. M., 2ND, WENZEL, H. J., ROBBINS, C. A., SOSUNOV, A. A. & SCHWARTZKROIN, P. A. 2003. Mouse strain differences in kainic acid sensitivity, seizure behavior, mortality, and hippocampal pathology. *Neuroscience,* 122**,** 551-61.

MEERSON, A., CACHEAUX, L., GOOSENS, K. A., SAPOLSKY, R. M., SOREQ, H. & KAUFER, D. 2010. Changes in Brain MicroRNAs Contribute to Cholinergic Stress Reactions. *Journal of Molecular Neuroscience,* 40**,** 47-55.

MENG, L., PERSON, R. E. & BEAUDET, A. L. 2012. Ube3a-ATS is an atypical RNA polymerase II transcript that represses the paternal expression of Ube3a. *Human Molecular Genetics,* 21**,** 3001-3012.

MICHELETTI, S., PALESTRA, F., MARTELLI, P., ACCORSI, P., GALLI, J., GIORDANO, L., TREBESCHI, V. & FAZZI, E. 2016. Neurodevelopmental profile in Angelman syndrome: more than low intelligence quotient. *Italian journal of pediatrics,* 42**,** 91-91.

MILLAR, J. K., WILSON-ANNAN, J. C., ANDERSON, S., CHRISTIE, S., TAYLOR, M. S., SEMPLE, C. A., DEVON, R. S., ST CLAIR, D. M., MUIR, W. J., BLACKWOOD, D. H. & PORTEOUS, D. J. 2000. Disruption of two novel genes by a translocation co-segregating with schizophrenia. *Hum Mol Genet,* 9**,** 1415-23.

MINASSIAN, B. A., DELOREY, T. M., OLSEN, R. W., PHILIPPART, M., BRONSTEIN, Y., ZHANG, Q., GUERRINI, R., VAN NESS, P., LIVET, M. O. & DELGADO-ESCUETA, A. V. 1998. Angelman syndrome: correlations between epilepsy phenotypes and genotypes. *Ann Neurol,* 43**,** 485-93.

MITCHELL, K. J. 2011. The genetics of neurodevelopmental disease. *Curr Opin Neurobiol,* 21**,** 197-203.

MITCHELL, W. G. & SHAH, N. S. 2002. Vigabatrin for infantile spasms. *Pediatr Neurol,* 27**,** 161-4.

MOHANRAJ, R. & BRODIE, M. J. 2003. Measuring the efficacy of antiepileptic drugs. *Seizure,* 12**,** 413-43.

MONTEIRO, P. & FENG, G. 2017. SHANK proteins: roles at the synapse and in autism spectrum disorder. *Nature Reviews Neuroscience,* 18**,** 147-157.

MOREAU, M. P., BRUSE, S. E., DAVID-RUS, R., BUYSKE, S. & BRZUSTOWICZ, L. M. 2011. Altered microRNA expression profiles in postmortem brain samples from individuals with schizophrenia and bipolar disorder. *Biol Psychiatry,* 69**,** 188-93.

MORRIS, G., BRENNAN, G. P., RESCHKE, C. R., HENSHALL, D. C. & SCHORGE, S. 2018. Spared CA1 pyramidal neuron function and hippocampal performance following antisense knockdown of microRNA-134. *Epilepsia,* 59**,** 1518-1526.

MORRIS, G., RESCHKE, C. R. & HENSHALL, D. C. 2019. Targeting microRNA-134 for seizure control and disease modification in epilepsy. *EBioMedicine,* 45**,** 646-654.

MULA, M., CAVANNA, A. E. & MONACO, F. 2006. Psychopharmacology of topiramate: from epilepsy to bipolar disorder. *Neuropsychiatric disease and treatment,* 2**,** 475-488.

MULHERKAR, S. A. & JANA, N. R. 2010. Loss of dopaminergic neurons and resulting behavioural deficits in mouse model of Angelman syndrome. *Neurobiology of Disease,* 40**,** 586-592.

MULHERKAR, S. A., SHARMA, J. & JANA, N. R. 2009. The ubiquitin ligase E6-AP promotes degradation of alpha-synuclein. *J Neurochem,* 110**,** 1955-64.

MÜLLER, M., GÄHWILER, B. H., RIETSCHIN, L. & THOMPSON, S. M. 1993. Reversible loss of dendritic spines and altered excitability after chronic epilepsy in hippocampal slice cultures. *Proceedings of the National Academy of Sciences of the United States of America,* 90**,** 257-261.

NAGAHARA, A. H. & HANDA, R. J. 1997. Age-related changes in c-fos mRNA induction after open-field exposure in the rat brain. *Neurobiol Aging,* 18**,** 45-55.

NAGY, A. & DELGADO-ESCUETA, A. V. 1984. Rapid preparation of synaptosomes from mammalian brain using nontoxic isoosmotic gradient material (Percoll). *J Neurochem,* 43**,** 1114-23.

NARIAI, H., DUBERSTEIN, S. & SHINNAR, S. 2018. Treatment of Epileptic Encephalopathies: Current State of the Art. *Journal of child neurology,* 33**,** 41-54.

NASHEF, L., SO, E. L., RYVLIN, P. & TOMSON, T. 2012. Unifying the definitions of sudden unexpected death in epilepsy. *Epilepsia,* 53**,** 227-33.

NATIONAL RESEARCH COUNCIL COMMITTEE FOR THE UPDATE OF THE GUIDE FOR THE, C. & USE OF LABORATORY, A. 2011. The National Academies Collection: Reports funded by National Institutes of Health. *Guide for the Care and Use of Laboratory Animals.* Washington (DC): National Academies Press (US)

NAYLOR, D. E. 2010. Glutamate and GABA in the balance: convergent pathways sustain seizures during status epilepticus. *Epilepsia,* 51 Suppl 3**,** 106-9.

NICHOLLS, R. D., SAITOH, S. & HORSTHEMKE, B. 1998. Imprinting in Prader-Willi and Angelman syndromes. *Trends Genet,* 14**,** 194-200.

NIKOLAIENKO, R. M., HAMMEL, M., DUBREUIL, V., ZALMAI, R., HALL, D. R., MEHZABEEN, N., KARUPPAN, S. J., HARROCH, S., STELLA, S. L. & BOUYAIN, S. 2016. Structural Basis for Interactions Between Contactin Family Members and Protein-tyrosine Phosphatase Receptor Type G in Neural Tissues. *J Biol Chem,* 291**,** 21335-21349.

NOLAN, S. J., SUDELL, M., TUDUR SMITH, C. & MARSON, A. G. 2016. Topiramate versus carbamazepine monotherapy for epilepsy: an individual participant data review. *The Cochrane database of systematic reviews,* 12**,** CD012065-CD012065.

O'BRIEN, J., HAYDER, H., ZAYED, Y. & PENG, C. 2018. Overview of MicroRNA Biogenesis, Mechanisms of Actions, and Circulation. *Frontiers in Endocrinology,* 9.

O'CALLAGHAN, F. J., SHIELL, A. W., OSBORNE, J. P. & MARTYN, C. N. 1998. Prevalence of tuberous sclerosis estimated by capture-recapture analysis. *Lancet,* 351**,** 1490.

OCHOA, J. G. & KILGO, W. A. 2016. The Role of Benzodiazepines in the Treatment of Epilepsy. *Curr Treat Options Neurol,* 18**,** 18.

OHTSUKA, Y., KOBAYASHI, K., YOSHINAGA, H., OGINO, T., OHMORI, I., OGAWA, K. & OKA, E. 2005. Relationship between severity of epilepsy and developmental outcome in Angelman syndrome. *Brain and Development,* 27**,** 95-100.

OLBRICH, E., RUSTERHOLZ, T., LEBOURGEOIS, M. K. & ACHERMANN, P. 2017. Developmental Changes in Sleep Oscillations during Early Childhood. *Neural plasticity,* 2017**,** 6160959-6160959.

OLIVA, M., BERKOVIC, S. F. & PETROU, S. 2012. Sodium channels and the neurobiology of epilepsy. *Epilepsia,* 53**,** 1849-59.

OSTERGAARD, J. R. & BALSLEV, T. 2001. Efficacy of different antiepileptic drugs in children with Angelman syndrome associated with 15q11-13 deletion: the Danish experience. *Dev Med Child Neurol,* 43**,** 718-9.

PARELLADA, M., PENZOL, M. J., PINA, L., MORENO, C., GONZÁLEZ-VIOQUE, E., ZALSMAN, G. & ARANGO, C. 2014. The neurobiology of autism spectrum disorders. *Eur Psychiatry,* 29**,** 11-9.

PARK, I., KIM, H. J., KIM, Y., HWANG, H. S., KASAI, H., KIM, J. H. & PARK, J. W. 2019. Nanoscale imaging reveals miRNA-mediated control of functional states of dendritic spines. *Proc Natl Acad Sci U S A,* 116**,** 9616-9621.

PAUL, P., CHAKRABORTY, A., SARKAR, D., LANGTHASA, M., RAHMAN, M., BARI, M., SINGHA, R. S., MALAKAR, A. K. & CHAKRABORTY, S. 2018. Interplay between miRNAs and human diseases. *J Cell Physiol,* 233**,** 2007-2018.

PELC, K., BOYD, S. G., CHERON, G. & DAN, B. 2008a. Epilepsy in Angelman syndrome. *Seizure,* 17**,** 211-217.

PELC, K., CHERON, G., BOYD, S. G. & DAN, B. 2008b. Are there distinctive sleep problems in Angelman syndrome? *Sleep Med,* 9**,** 434-41.

PENG, J., OMRAN, A., ASHHAB, M. U., KONG, H., GAN, N., HE, F. & YIN, F. 2013a. Expression Patterns of miR-124, miR-134, miR-132, and miR-21 in an Immature Rat Model and Children with Mesial Temporal Lobe Epilepsy. *Journal of Molecular Neuroscience,* 50**,** 291-297.

PENG, J., OMRAN, A., ASHHAB, M. U., KONG, H., GAN, N., HE, F. & YIN, F. 2013b. Expression Patterns of miR-124, miR-134, miR-132, and miR-21 in an Immature Rat Model and Children with Mesial Temporal Lobe Epilepsy. *J Mol Neurosci,* 50**,** 291-7.

PENNER, K. A., JOHNSTON, J., FAIRCLOTH, B. H., IRISH, P. & WILLIAMS, C. A. 1993. Communication, cognition, and social interaction in the Angelman syndrome. *Am J Med Genet,* 46**,** 34-9.

PERKINS, D. O., JEFFRIES, C. D., JARSKOG, L. F., THOMSON, J. M., WOODS, K., NEWMAN, M. A., PARKER, J. S., JIN, J. & HAMMOND, S. M. 2007. microRNA expression in the prefrontal cortex of individuals with schizophrenia and schizoaffective disorder. *Genome Biol,* 8**,** R27.

PERUCCA, E., BATTINO, D. & TOMSON, T. 2014. Gender issues in antiepileptic drug treatment. *Neurobiology of Disease,* 72**,** 217-223.

PETER, M. E. 2010. Targeting of mRNAs by multiple miRNAs: the next step. *Oncogene,* 29**,** 2161-2164.

PETERS, J. 2014. The role of genomic imprinting in biology and disease: an expanding view. *Nat Rev Genet,* 15**,** 517-30.

PETERS, S. U., GODDARD-FINEGOLD, J., BEAUDET, A. L., MADDURI, N., TURCICH, M. & BACINO, C. A. 2004. Cognitive and adaptive behavior profiles of children with Angelman syndrome. *Am J Med Genet A,* 128a**,** 110-3.

PFEIFFER, B. E. & HUBER, K. M. 2009. The state of synapses in fragile X syndrome. *The Neuroscientist : a review journal bringing neurobiology, neurology and psychiatry,* 15**,** 549-567.

PIETROBONO, R., TABOLACCI, E., ZALFA, F., ZITO, I., TERRACCIANO, A., MOSCATO, U., BAGNI, C., OOSTRA, B., CHIURAZZI, P. & NERI, G. 2004. Molecular dissection of the events leading to inactivation of the FMR1 gene. *Human Molecular Genetics,* 14**,** 267-277.

PROVENZANO, G., SGADÒ, P., GENOVESI, S., ZUNINO, G., CASAROSA, S. & BOZZI, Y. 2015. Hippocampal dysregulation of FMRP/mGluR5 signaling in engrailed-2 knockout mice: a model of autism spectrum disorders. *Neuroreport,* 26**,** 1101-5.

PURCARIN, G. & NG, Y.-T. 2014. Experience in the use of clobazam in the treatment of Lennox-Gastaut syndrome. *Therapeutic advances in neurological disorders,* 7**,** 169-176.

QIAN, Y., SONG, J., OUYANG, Y., HAN, Q., CHEN, W., ZHAO, X., XIE, Y., CHEN, Y., YUAN, W. & FAN, C. 2017. Advances in Roles of miR-132 in the Nervous System. *Frontiers in Pharmacology,* 8.

RAGO, L., BEATTIE, R., TAYLOR, V. & WINTER, J. 2014. miR379-410 cluster miRNAs regulate neurogenesis and neuronal migration by fine-tuning N-cadherin. *Embo j,* 33**,** 906-20.

RAINIER, S., CHAI, J. H., TOKARZ, D., NICHOLLS, R. D. & FINK, J. K. 2003. NIPA1 gene mutations cause autosomal dominant hereditary spastic paraplegia (SPG6). *Am J Hum Genet,* 73**,** 967-71.

RAJAKULENDRAN, S., SCHORGE, S., KULLMANN, D. M. & HANNA, M. G. 2007. Episodic ataxia type 1: a neuronal potassium channelopathy. *Neurotherapeutics,* 4**,** 258-66.

RASPALL-CHAURE, M., CHIN, R. F., NEVILLE, B. G. & SCOTT, R. C. 2006. Outcome of paediatric convulsive status epilepticus: a systematic review. *Lancet Neurol,* 5**,** 769-79.

RASPALL-CHAURE, M., CHIN, R. F. M., NEVILLE, B. G., BEDFORD, H. & SCOTT, R. C. 2007. The Epidemiology of Convulsive Status Epilepticus in Children: A Critical Review. *Epilepsia,* 48**,** 1652-1663.

RAVIZZA, T., RIZZI, M., PEREGO, C., RICHICHI, C., VELISKOVA, J., MOSHE, S. L., DE SIMONI, M. G. & VEZZANI, A. 2005. Inflammatory response and glia activation in developing rat hippocampus after status epilepticus. *Epilepsia,* 46 Suppl 5**,** 113-7.

REDDY, D. S. 2013. Neuroendocrine aspects of catamenial epilepsy. *Horm Behav,* 63**,** 254-66.

RESCHKE, C. R., SILVA, L. F., NORWOOD, B. A., SENTHILKUMAR, K., MORRIS, G., SANZ-RODRIGUEZ, A., CONROY, R. M., COSTARD, L., NEUBERT, V., BAUER, S., FARRELL, M. A., O'BRIEN, D. F., DELANTY, N., SCHORGE, S., PASTERKAMP, R. J., ROSENOW, F. & HENSHALL, D. C. 2017a. Potent Anti-seizure Effects of Locked Nucleic Acid Antagomirs Targeting miR-134 in Multiple Mouse and Rat Models of Epilepsy. *Mol Ther Nucleic Acids,* 6**,** 45-56.

RESCHKE, C. R., SILVA, L. F. A., NORWOOD, B. A., SENTHILKUMAR, K., MORRIS, G., SANZ-RODRIGUEZ, A., CONROY, R. M., COSTARD, L., NEUBERT, V., BAUER, S., FARRELL, M. A., O'BRIEN, D. F., DELANTY, N., SCHORGE, S., PASTERKAMP, R. J., ROSENOW, F. & HENSHALL, D. C. 2017b. Potent Anti-seizure Effects of Locked Nucleic Acid Antagomirs Targeting miR-134 in Multiple Mouse and Rat Models of Epilepsy. *Molecular therapy. Nucleic acids,* 6**,** 45-56.

RESCHKE, C. R., SILVA, L. F. A., VANGOOR, V. R., ROSSO, M., DAVID, B., CAVANAGH, B. L., CONNOLLY, N. M. C., BRENNAN, G. P., SANZ-RODRIGUEZ, A., MOONEY, C., BATOOL, A., GREENE, C., BRENNAN, M., CONROY, R. M., RÜBER, T., PREHN, J. H. M., CAMPBELL, M., PASTERKAMP, R. J. & HENSHALL, D. C. 2019. Potent and lasting seizure suppression by systemic delivery of antagomirs targeting miR-134 timed with blood-brain barrier disruption. *bioRxiv***,** 797621.

RETT, A. 1966. [On a unusual brain atrophy syndrome in hyperammonemia in childhood]. *Wien Med Wochenschr,* 116**,** 723-6.

RHO, J. M., DONEVAN, S. D. & ROGAWSKI, M. A. 1994. Mechanism of action of the anticonvulsant felbamate: Opposing effects on N-methyl-D-aspartate and γ aminobutyric acidA receptors. *Annals of Neurology,* 35**,** 229-234.

RINGLI, M. & HUBER, R. 2011. Developmental aspects of sleep slow waves: linking sleep, brain maturation and behavior. *Prog Brain Res,* 193**,** 63-82.

RITCHIE, M. E., PHIPSON, B., WU, D., HU, Y., LAW, C. W., SHI, W. & SMYTH, G. K. 2015. limma powers differential expression analyses for RNA-sequencing and microarray studies. *Nucleic Acids Res,* 43**,** e47.

ROBINSON-SHELTON, A. & MALOW, B. A. 2015. Sleep Disturbances in Neurodevelopmental Disorders. *Current Psychiatry Reports,* 18**,** 6.

ROBINSON, M. D., MCCARTHY, D. J. & SMYTH, G. K. 2010. edgeR: a Bioconductor package for differential expression analysis of digital gene expression data. *Bioinformatics,* 26**,** 139-40.

ROGAWSKI, M. A. 2011. Revisiting AMPA receptors as an antiepileptic drug target. *Epilepsy currents,* 11**,** 56-63.

ROGAWSKI, M. A., GRYDER, D., CASTANEDA, D., YONEKAWA, W., BANKS, M. K. & LI, H. E. 2003. GluR5 Kainate Receptors, Seizures, and the Amygdala. *Annals of the New York Academy of Sciences,* 985**,** 150-162.

ROGAWSKI, M. A. & LÖSCHER, W. 2004. The neurobiology of antiepileptic drugs. *Nature Reviews Neuroscience,* 5**,** 553-564.

ROSATI, A., DE MASI, S. & GUERRINI, R. 2015. Antiepileptic Drug Treatment in Children with Epilepsy. *CNS drugs,* 29**,** 847-863.

ROSE, M. A. & KAM, P. C. A. 2002. Gabapentin: pharmacology and its use in pain management. *Anaesthesia,* 57**,** 451-462.

ROSS, K. C. & COLEMAN, J. R. 2000. Developmental and genetic audiogenic seizure models: behavior and biological substrates. *Neurosci Biobehav Rev,* 24**,** 639-53.

ROSSIER, M. F. 2016. T-Type Calcium Channel: A Privileged Gate for Calcium Entry and Control of Adrenal Steroidogenesis. *Frontiers in Endocrinology,* 7.

ROTIN, D. & KUMAR, S. 2009. Physiological functions of the HECT family of ubiquitin ligases. *Nature Reviews Molecular Cell Biology,* 10**,** 398.

ROUGEULLE, C., GLATT, H. & LALANDE, M. 1997. The Angelman syndrome candidate gene, UBE3A/E6-AP, is imprinted in brain. *Nat Genet,* 17**,** 14-5.

RUBENSTEIN, J. L. & MERZENICH, M. M. 2003. Model of autism: increased ratio of excitation/inhibition in key neural systems. *Genes Brain Behav,* 2**,** 255-67.

RUNTE, M., KROISEL, P. M., GILLESSEN-KAESBACH, G., VARON, R., HORN, D., COHEN, M. Y., WAGSTAFF, J., HORSTHEMKE, B. & BUITING, K. 2004. SNURF-SNRPN and UBE3A transcript levels in patients with Angelman syndrome. *Hum Genet,* 114**,** 553-61.

SAHIN, M., MENACHE, C. C., HOLMES, G. L. & RIVIELLO JR, J. J. 2001. Outcome of severe refractory status epilepticus in children. *Epilepsia,* 42**,** 1461-1467.

SALDARRIAGA, W., TASSONE, F., GONZÁLEZ-TESHIMA, L. Y., FORERO-FORERO, J. V., AYALA-ZAPATA, S. & HAGERMAN, R. 2014. Fragile X syndrome. *Colombia medica (Cali, Colombia),* 45**,** 190-198.

SAMBA REDDY, D. 2017. Sex differences in the anticonvulsant activity of neurosteroids. *Journal of neuroscience research,* 95**,** 661-670.

SAMBANDAN, S., AKBALIK, G., KOCHEN, L., RINNE, J., KAHLSTATT, J., GLOCK, C., TUSHEV, G., ALVAREZ-CASTELAO, B., HECKEL, A. & SCHUMAN, E. M. 2017. Activity-dependent spatially localized miRNA maturation in neuronal dendrites. *Science,* 355**,** 634-637.

SANDERS, S. J., MURTHA, M. T., GUPTA, A. R., MURDOCH, J. D., RAUBESON, M. J., WILLSEY, A. J., ERCAN-SENCICEK, A. G., DILULLO, N. M., PARIKSHAK, N. N., STEIN, J. L., WALKER, M. F., OBER, G. T., TERAN, N. A., SONG, Y., EL-FISHAWY, P., MURTHA, R. C., CHOI, M., OVERTON, J. D., BJORNSON, R. D., CARRIERO, N. J., MEYER, K. A., BILGUVAR, K., MANE, S. M., SESTAN, N., LIFTON, R. P., GÜNEL, M., ROEDER, K., GESCHWIND, D. H., DEVLIN, B. & STATE, M. W. 2012. De novo mutations revealed by whole-exome sequencing are strongly associated with autism. *Nature,* 485**,** 237-241.

SARUP, A., LARSSON, O. M. & SCHOUSBOE, A. 2003. GABA transporters and GABA-transaminase as drug targets. *Curr Drug Targets CNS Neurol Disord,* 2**,** 269-77.

SAUGSTAD, J. A. 2010. MicroRNAs as effectors of brain function with roles in ischemia and injury, neuroprotection, and neurodegeneration. *J Cereb Blood Flow Metab,* 30**,** 1564-76.

SCHARFMAN, H. E. & MACLUSKY, N. J. 2014. Sex differences in the neurobiology of epilepsy: a preclinical perspective. *Neurobiology of disease,* 72 Pt B**,** 180-192.

SCHARFMAN, H. E., SOLLAS, A. L. & GOODMAN, J. H. 2002. Spontaneous recurrent seizures after pilocarpine-induced status epilepticus activate calbindin-immunoreactive hilar cells of the rat dentate gyrus. *Neuroscience,* 111**,** 71-81.

SCHAUWECKER, P. E. 2002. Complications associated with genetic background effects in models of experimental epilepsy. *Prog Brain Res,* 135**,** 139-48.

SCHEFFER, I. E. & BERKOVIC, S. F. 1997. Generalized epilepsy with febrile seizures plus. A genetic disorder with heterogeneous clinical phenotypes. *Brain,* 120 (Pt 3)**,** 479-90.

SCHEFFNER, M., HUIBREGTSE, J. M., VIERSTRA, R. D. & HOWLEY, P. M. 1993. The HPV-16 E6 and E6-AP complex functions as a ubiquitin-protein ligase in the ubiquitination of p53. *Cell,* 75**,** 495-505.

SCHEIFFELE, P., FAN, J., CHOIH, J., FETTER, R. & SERAFINI, T. 2000. Neuroligin expressed in nonneuronal cells triggers presynaptic development in contacting axons. *Cell,* 101**,** 657-69.

SCHRATT, G. M., TUEBING, F., NIGH, E. A., KANE, C. G., SABATINI, M. E., KIEBLER, M. & GREENBERG, M. E. 2006. A brain-specific microRNA regulates dendritic spine development. *Nature,* 439**,** 283-9.

SCHUMANN, C. M., HAMSTRA, J., GOODLIN-JONES, B. L., LOTSPEICH, L. J., KWON, H., BUONOCORE, M. H., LAMMERS, C. R., REISS, A. L. & AMARAL, D. G. 2004. The amygdala is enlarged in children but not adolescents with autism; the hippocampus is enlarged at all ages. *J Neurosci,* 24**,** 6392-401.

SELBACH, M., SCHWANHÄUSSER, B., THIERFELDER, N., FANG, Z., KHANIN, R. & RAJEWSKY, N. 2008. Widespread changes in protein synthesis induced by microRNAs. *Nature,* 455**,** 58-63.

SELEMON, L. D. 2013. A role for synaptic plasticity in the adolescent development of executive function. *Translational Psychiatry,* 3**,** e238.

SELL, G. & MARGOLIS, S. 2015. From UBE3A to Angelman syndrome: a substrate perspective. *Frontiers in Neuroscience,* 9.

SELLGREN, C. M., GRACIAS, J., WATMUFF, B., BIAG, J. D., THANOS, J. M., WHITTREDGE, P. B., FU, T., WORRINGER, K., BROWN, H. E., WANG, J., KAYKAS, A., KARMACHARYA, R., GOOLD, C. P., SHERIDAN, S. D. & PERLIS, R. H. 2019. Increased synapse elimination by

microglia in schizophrenia patient-derived models of synaptic pruning. *Nature Neuroscience,* 22**,** 374-385.

SGADÒ, P., GENOVESI, S., KALINOVSKY, A., ZUNINO, G., MACCHI, F., ALLEGRA, M., MURENU, E., PROVENZANO, G., TRIPATHI, P. P., CASAROSA, S., JOYNER, A. L. & BOZZI, Y. 2013. Loss of GABAergic neurons in the hippocampus and cerebral cortex of Engrailed-2 null mutant mice: implications for autism spectrum disorders. *Exp Neurol,* 247**,** 496-505.

SHELDRICK-MICHEL, T. M., MORTEN, B. T., NIELS, B. & MIROLYUBA, I. 2017. Neurobiology of autism spectrum disorders. *European Psychiatry,* 41**,** S45-S46.

SHIGEMOTO, R., KINOSHITA, A., WADA, E., NOMURA, S., OHISHI, H., TAKADA, M., FLOR, P. J., NEKI, A., ABE, T., NAKANISHI, S. & MIZUNO, N. 1997. Differential presynaptic localization of metabotropic glutamate receptor subtypes in the rat hippocampus. *The Journal of neuroscience : the official journal of the Society for Neuroscience,* 17**,** 7503-7522.

SHIMADA, T. & YAMAGATA, K. 2018. Pentylenetetrazole-Induced Kindling Mouse Model. *J Vis Exp*.

SHIOTSUKI, H., YOSHIMI, K., SHIMO, Y., FUNAYAMA, M., TAKAMATSU, Y., IKEDA, K., TAKAHASHI, R., KITAZAWA, S. & HATTORI, N. 2010. A rotarod test for evaluation of motor skill learning. *J Neurosci Methods,* 189**,** 180-5.

SHMUELY, S., SISODIYA, S. M., GUNNING, W. B., SANDER, J. W. & THIJS, R. D. 2016. Mortality in Dravet syndrome: A review. *Epilepsy & Behavior,* 64**,** 69-74.

SIDOROV, M. S., DECK, G. M., DOLATSHAHI, M., THIBERT, R. L., BIRD, L. M., CHU, C. J. & PHILPOT, B. D. 2017. Delta rhythmicity is a reliable EEG biomarker in Angelman syndrome: a parallel mouse and human analysis. *J Neurodev Disord,* 9**,** 17.

SIGEL, E. & STEINMANN, M. E. 2012. Structure, function, and modulation of GABA(A) receptors. *J Biol Chem,* 287**,** 40224-31.

SILVA-SANTOS, S., VAN WOERDEN, G. M., BRUINSMA, C. F., MIENTJES, E., JOLFAEI, M. A., DISTEL, B., KUSHNER, S. A. & ELGERSMA, Y. 2015. Ube3a reinstatement identifies distinct developmental windows in a murine Angelman syndrome model. *J Clin Invest,* 125**,** 2069-76.

SILVESTRO, S., MAMMANA, S., CAVALLI, E., BRAMANTI, P. & MAZZON, E. 2019. Use of Cannabidiol in the Treatment of Epilepsy: Efficacy and Security in Clinical Trials. *Molecules (Basel, Switzerland),* 24**,** 1459.

SINGH, R. K. & GAILLARD, W. D. 2009. Status epilepticus in children. *Curr Neurol Neurosci Rep,* 9**,** 137-44.

SMITH, D. M., MCGINNIS, E. L., WALLEIGH, D. J. & ABEND, N. S. 2016. Management of Status Epilepticus in Children. *Journal of Clinical Medicine,* 5**,** 47.

SMITH, J. C. 2001. Angelman syndrome: evolution of the phenotype in adolescents and adults. *Dev Med Child Neurol,* 43**,** 476-80.

SONG, Y. J., TIAN, X. B., ZHANG, S., ZHANG, Y. X., LI, X., LI, D., CHENG, Y., ZHANG, J. N., KANG, C. S. & ZHAO, W. 2011. Temporal lobe epilepsy induces differential expression of hippocampal miRNAs including let-7e and miR-23a/b. *Brain Res,* 1387**,** 134-40.

SONZOGNI, M., WALLAARD, I., SANTOS, S. S., KINGMA, J., DU MEE, D., VAN WOERDEN, G. M. & ELGERSMA, Y. 2018. A behavioral test battery for mouse models of Angelman syndrome: a powerful tool for testing drugs and novel Ube3a mutants. *Molecular Autism,* 9**,** 47.

SPRUYT, K., BRAAM, W. & CURFS, L. M. G. 2018. Sleep in Angelman syndrome: A review of evidence. *Sleep Medicine Reviews,* 37**,** 69-84.

STALEY, B. A., VAIL, E. A. & THIELE, E. A. 2011. Tuberous sclerosis complex: diagnostic challenges, presenting symptoms, and commonly missed signs. *Pediatrics,* 127**,** e117-e125.

STATE, M. W. & ŠESTAN, N. 2012. Neuroscience. disorders. *Science,* 337**,** 1301-3.

STEENMAN, M. J., RAINIER, S., DOBRY, C. J., GRUNDY, P., HORON, I. L. & FEINBERG, A. P. 1994. Loss of imprinting of IGF2 is linked to reduced expression and abnormal methylation of H19 in Wilms' tumour. *Nat Genet,* 7**,** 433-9.

STEINBACH, K., VOLKMER, H. & SCHLOSSHAUER, B. 2002. Semaphorin 3E/collapsin-5 inhibits growing retinal axons. *Exp Cell Res,* 279**,** 52-61.

STEINLEIN, O. K. 2001. Genes and mutations in idiopathic epilepsy. *Am J Med Genet,* 106**,** 139-45.

STEPHAN, K. E., BALDEWEG, T. & FRISTON, K. J. 2006. Synaptic plasticity and dysconnection in schizophrenia. *Biol Psychiatry,* 59**,** 929-39.

STOPPEL, D. C. & ANDERSON, M. P. 2017. Hypersociability in the Angelman syndrome mouse model. *Experimental neurology,* 293**,** 137-143.

STROOBANTS, S., GANTOIS, I., POOTERS, T. & D'HOOGE, R. 2013. Increased gait variability in mice with small cerebellar cortex lesions and normal rotarod performance. *Behav Brain Res,* 241**,** 32-7.

STUJENSKE, J. M., LIKHTIK, E., TOPIWALA, M. A. & GORDON, J. A. 2014. Fear and safety engage competing patterns of theta-gamma coupling in the basolateral amygdala. *Neuron,* 83**,** 919-933.

SYMONDS, J. D., ZUBERI, S. M., STEWART, K., MCLELLAN, A., O'REGAN, M., MACLEOD, S., JOLLANDS, A., JOSS, S., KIRKPATRICK, M., BRUNKLAUS, A., PILZ, D. T., SHETTY, J., DORRIS, L., ABU-ARAFEH, I., ANDREW, J., BRINK, P., CALLAGHAN, M., CRUDEN, J., DIVER, L. A., FINDLAY, C., GARDINER, S., GRATTAN, R., LANG, B., MACDONNELL, J., MCKNIGHT, J., MORRISON, C. A., NAIRN, L., SLEAN, M. M., STEPHEN, E., WEBB, A., VINCENT, A. & WILSON, M. 2019. Incidence and phenotypes of childhood-onset genetic epilepsies: a prospective population-based national cohort. *Brain : a journal of neurology,* 142**,** 2303-2318.

TAGLIALATELA, M., ONGINI, E., BROWN, A. M., DI RENZO, G. & ANNUNZIATO, L. 1996. Felbamate inhibits cloned voltage-dependent Na+ channels from human and rat brain. *Eur J Pharmacol,* 316**,** 373-7.

TAKAO, K. & MIYAKAWA, T. 2006. Light/dark transition test for mice. *Journal of visualized experiments : JoVE***,** 104-104.

TAN, W. H., BACINO, C. A., SKINNER, S. A., ANSELM, I., BARBIERI-WELGE, R., BAUER-CARLIN, A., BEAUDET, A. L., BICHELL, T. J., GENTILE, J. K., GLAZE, D. G., HOROWITZ, L. T., KOTHARE, S. V., LEE, H. S., NESPECA, M. P., PETERS, S. U., SAHOO, T., SARCO, D., WAISBREN, S. E. & BIRD, L. M. 2011. Angelman syndrome: Mutations influence features in early childhood. *Am J Med Genet A,* 155a**,** 81-90.

TASSONE, F., HAGERMAN, P. J. & HAGERMAN, R. J. 2014. Fragile x premutation. *Journal of neurodevelopmental disorders,* 6**,** 22-22.

TAYLOR, L. A., MCQUADE, R. D. & TICE, M. A. 1995. Felbamate, a novel antiepileptic drug, reverses N-methyl-D-aspartate/glycine-stimulated increases in intracellular Ca2+ concentration. *Eur J Pharmacol,* 289**,** 229-33.

THIBERT, R. L., LARSON, A. M., HSIEH, D. T., RABY, A. R. & THIELE, E. A. 2013. Neurologic Manifestations of Angelman Syndrome. *Pediatric Neurology,* 48**,** 271-279.

THIBERT, R. L., PFEIFER, H. H., LARSON, A. M., RABY, A. R., REYNOLDS, A. A., MORGAN, A. K. & THIELE, E. A. 2012. Low glycemic index treatment for seizures in Angelman syndrome. *Epilepsia,* 53**,** 1498-1502.

THIELE, E. A. 2004. Managing Epilepsy in Tuberous Sclerosis Complex. *Journal of Child Neurology,* 19**,** 680-686.

TIMOFEEV, I. 2011. Neuronal plasticity and thalamocortical sleep and waking oscillations. *Progress in brain research,* 193**,** 121-144.

TOYOSHIMA, M., SAKURAI, K., SHIMAZAKI, K., TAKEDA, Y., SHIMODA, Y. & WATANABE, K. 2009. Deficiency of neural recognition molecule NB-2 affects the development of glutamatergic auditory pathways from the ventral cochlear nucleus to the superior olivary complex in mouse. *Dev Biol,* 336**,** 192-200.

TREIMAN, D. M. 2008. Generalized convulsive status epilepticus. *Epilepsy - A Comprehensive Textbook***,** 665-676.

URDINGUIO, R. G., FERNANDEZ, A. F., LOPEZ-NIEVA, P., ROSSI, S., HUERTAS, D., KULIS, M., LIU, C.-G., CROCE, C. M., CALIN, G. A. & ESTELLER, M. 2010. Disrupted microRNA expression caused by Mecp2 loss in a mouse model of Rett syndrome. *Epigenetics,* 5**,** 656-663.

VALENCIA, I., HOLDER, D. L., HELMERS, S. L., MADSEN, J. R. & RIVIELLO, J. J., JR. 2001. Vagus nerve stimulation in pediatric epilepsy: a review. *Pediatr Neurol,* 25**,** 368-76.

VALENTE, K. D., KOIFFMANN, C. P., FRIDMAN, C., VARELLA, M., KOK, F., ANDRADE, J. Q., GROSSMANN, R. M. & MARQUES-DIAS, M. J. 2006a. Epilepsy in Patients With Angelman Syndrome Caused by Deletion of the Chromosome 15q11-13. *JAMA Neurology,* 63**,** 122-128.

VALENTE, K. D., KOIFFMANN, C. P., FRIDMAN, C., VARELLA, M., KOK, F., ANDRADE, J. Q., GROSSMANN, R. M. & MARQUES-DIAS, M. J. 2006b. Epilepsy in Patients With Angelman Syndrome Caused by Deletion of the Chromosome 15q11-13. *Archives of Neurology,* 63**,** 122-128.

VALLUY, J., BICKER, S., AKSOY-AKSEL, A., LACKINGER, M., SUMER, S., FIORE, R., WUST, T., SEFFER, D., METGE, F., DIETERICH, C., WOHR, M., SCHWARTING, R. & SCHRATT, G. 2015. A coding-independent function of an alternative Ube3a transcript during neuronal development. *Nat Neurosci,* 18**,** 666-73.

VAN WOERDEN, G. M., HARRIS, K. D., HOJJATI, M. R., GUSTIN, R. M., QIU, S., DE AVILA FREIRE, R., JIANG, Y. H., ELGERSMA, Y. & WEEBER, E. J. 2007. Rescue of neurological deficits in a mouse model for Angelman syndrome by reduction of alphaCaMKII inhibitory phosphorylation. *Nat Neurosci,* 10**,** 280-2.

VANGOOR, V. R., RESCHKE, C. R., SENTHILKUMAR, K., VAN DE HAAR, L. L., DE WIT, M., GIULIANI, G., BROEKHOVEN, M. H., MORRIS, G., ENGEL, T., BRENNAN, G. P., CONROY, R. M., VAN RIJEN, P. C., GOSSELAAR, P. H., SCHORGE, S., SCHAAPVELD, R. Q. J., HENSHALL, D. C., DE GRAAN, P. N. E. & PASTERKAMP, R. J. 2019. Antagonizing Increased miR-135a Levels at the Chronic Stage of Experimental TLE Reduces Spontaneous Recurrent Seizures. *J Neurosci,* 39**,** 5064-5079.

VASQUEZ, A., FARIAS-MOELLER, R. & TATUM, W. 2019. Pediatric refractory and super-refractory status epilepticus. *Seizure,* 68**,** 62-71.

VEERAMAH, K. R., O'BRIEN, J. E., MEISLER, M. H., CHENG, X., DIB-HAJJ, S. D., WAXMAN, S. G., TALWAR, D., GIRIRAJAN, S., EICHLER, E. E., RESTIFO, L. L., ERICKSON, R. P. & HAMMER, M. F. 2012. De novo pathogenic SCN8A mutation identified by whole-genome sequencing of a family quartet affected by infantile epileptic encephalopathy and SUDEP. *Am J Hum Genet,* 90**,** 502-10.

VENDRAME, M., LODDENKEMPER, T., ZAROWSKI, M., GREGAS, M., SHUHAIBER, H., SARCO, D. P., MORALES, A., NESPECA, M., SHARPE, C., HAAS, K., BARNES, G., GLAZE, D. & KOTHARE, S. V. 2012. Analysis of EEG patterns and genotypes in patients with Angelman syndrome. *Epilepsy Behav,* 23**,** 261-5.

VENØ, M. T., RESCHKE, C. R., MORRIS, G., CONNOLLY, N. M. C., SU, J., YAN, Y., ENGEL, T., JIMENEZ-MATEOS, E. M., HARDER, L. M., PULTZ, D., HAUNSBERGER, S. J., PAL, A., HELLER, J. P., CAMPBELL, A., LANGA, E., BRENNAN, G. P., CONBOY, K., RICHARDSON, A., NORWOOD, B. A., COSTARD, L. S., NEUBERT, V., DEL GALLO, F., SALVETTI, B., VANGOOR, V. R., SANZ-RODRIGUEZ, A., MUILU, J., FABENE, P. F., PASTERKAMP, R. J., PREHN, J. H. M., SCHORGE, S., ANDERSEN, J. S., ROSENOW, F., BAUER, S., KJEMS, J. & HENSHALL, D. C. 2020. A systems approach delivers a functional microRNA catalog and expanded targets for seizure suppression in temporal lobe epilepsy. *Proceedings of the National Academy of Sciences***,** 201919313.

VIANI, F., ROMEO, A., VIRI, M., MASTRANGELO, M., LALATTA, F., SELICORNI, A., GOBBI, G., LANZI, G., BETTIO, D., BRISCIOLI, V. & ET AL. 1995. Seizure and EEG patterns in Angelman's syndrome. *J Child Neurol,* 10**,** 467-71.

VIGNOLI, A., LA BRIOLA, F., PERON, A., TURNER, K., VANNICOLA, C., SACCANI, M., MAGNAGHI, E., SCORNAVACCA, G. F. & CANEVINI, M. P. 2015. Autism spectrum disorder in tuberous sclerosis complex: searching for risk markers. *Orphanet journal of rare diseases,* 10**,** 154-154.

VINING, E. P. G. 1999. Clinical efficacy of the ketogenic diet. *Epilepsy Research,* 37**,** 181-190.

VITSIOS, D. M. & ENRIGHT, A. J. 2015. Chimira: analysis of small RNA sequencing data and microRNA modifications. *Bioinformatics,* 31**,** 3365-7.

VU, T. H. & HOFFMAN, A. R. 1997. Imprinting of the Angelman syndrome gene, UBE3A, is restricted to brain. *Nat Genet,* 17**,** 12-3.

WAFFORD, K. A. & EBERT, B. 2006. Gaboxadol — a new awakening in sleep. *Current Opinion in Pharmacology,* 6**,** 30-36.

WALLACE, M. L., BURETTE, A. C., WEINBERG, R. J. & PHILPOT, B. D. 2012. Maternal loss of Ube3a produces an excitatory/inhibitory imbalance through neuron type-specific synaptic defects. *Neuron,* 74**,** 793-800.

WALZ, N. C. 2007. Parent report of stereotyped behaviors, social interaction, and developmental disturbances in individuals with Angelman syndrome. *J Autism Dev Disord,* 37**,** 940-7.

WANG, X., YIN, F., LI, L., KONG, H., YOU, B., ZHANG, W., CHEN, S. & PENG, J. 2018. Intracerebroventricular injection of miR-146a relieves seizures in an immature rat model of lithium-pilocarpine induced status epilepticus. *Epilepsy Res,* 139**,** 14-19.

WASTERLAIN, C. G. & CHEN, J. W. 2008. Mechanistic and pharmacologic aspects of status epilepticus and its treatment with new antiepileptic drugs. *Epilepsia,* 49 Suppl 9**,** 63-73.

WAUNG, M. W., PFEIFFER, B. E., NOSYREVA, E. D., RONESI, J. A. & HUBER, K. M. 2008. Rapid Translation of Arc/Arg3.1 Selectively Mediates mGluR-Dependent LTD through Persistent Increases in AMPAR Endocytosis Rate. *Neuron,* 59**,** 84-97.

WEBB, D. W., FRYER, A. E. & OSBORNE, J. P. 1996. Morbidity associated with tuberous sclerosis: a population study. *Dev Med Child Neurol,* 38**,** 146-55.

WEEBER, E. J., JIANG, Y. H., ELGERSMA, Y., VARGA, A. W., CARRASQUILLO, Y., BROWN, S. E., CHRISTIAN, J. M., MIRNIKJOO, B., SILVA, A., BEAUDET, A. L. & SWEATT, J. D. 2003. Derangements of hippocampal calcium/calmodulin-dependent protein kinase II in a mouse model for Angelman mental retardation syndrome. *J Neurosci,* 23**,** 2634-44.

WEN, T. H., LOVELACE, J. W., ETHELL, I. M., BINDER, D. K. & RAZAK, K. A. 2019. Developmental Changes in EEG Phenotypes in a Mouse Model of Fragile X Syndrome. *Neuroscience,* 398**,** 126-143.

WHEELER, A. C., SACCO, P. & CABO, R. 2017. Unmet clinical needs and burden in Angelman syndrome: a review of the literature. *Orphanet journal of rare diseases,* 12**,** 164-164.

WIGHTMAN, B., HA, I. & RUVKUN, G. 1993. Posttranscriptional regulation of the heterochronic gene lin-14 by lin-4 mediates temporal pattern formation in C. elegans. *Cell,* 75**,** 855-62.

WILLIAMS, C. A. 2010. The behavioral phenotype of the Angelman syndrome. *Am J Med Genet C Semin Med Genet,* 154c**,** 432-7.

WILLIAMS, C. A., BEAUDET, A. L., CLAYTON-SMITH, J., KNOLL, J. H., KYLLERMAN, M., LAAN, L. A., MAGENIS, R. E., MONCLA, A., SCHINZEL, A. A., SUMMERS, J. A. & WAGSTAFF, J. 2006. Angelman syndrome 2005: updated consensus for diagnostic criteria. *Am J Med Genet A,* 140**,** 413-8.

WINTER, J. 2015. MicroRNAs of the miR379-410 cluster: New players in embryonic neurogenesis and regulators of neuronal function. *Neurogenesis (Austin, Tex.),* 2**,** e1004970-e1004970.

WIRRELL, E., WONG-KISIEL, L., MANDREKAR, J. & NICKELS, K. 2012. Predictors and course of medically intractable epilepsy in young children presenting before 36 months of age: A retrospective, population-based study. *Epilepsia,* 53**,** 1563-1569.

WIRRELL, E. C. 2013. Predicting pharmacoresistance in pediatric epilepsy. *Epilepsia,* 54 Suppl 2**,** 19-22.

WOZNIAK, D. F., STEWART, G. R., MILLER, J. P. & OLNEY, J. W. 1991. Age-related sensitivity to kainate neurotoxicity. *Exp Neurol,* 114**,** 250-3.

WU, H., TAO, J., CHEN, P. J., SHAHAB, A., GE, W., HART, R. P., RUAN, X., RUAN, Y. & SUN, Y. E. 2010. Genome-wide analysis reveals methyl-CpG–binding protein 2–dependent regulation of microRNAs in a mouse model of Rett syndrome. *Proceedings of the National Academy of Sciences,* 107**,** 18161-18166.

YAARI, Y., SELZER, M. E. & PINCUS, J. H. 1986. Phenytoin: mechanisms of its anticonvulsant action. *Ann Neurol,* 20**,** 171-84.

YANG, H., LI, K., HAN, S., ZHOU, A. & ZHOU, Z. J. 2019. Leveraging the genetic basis of Rett syndrome to ascertain pathophysiology. *Neurobiol Learn Mem,* 165**,** 106961.

ZAMPA, F., BICKER, S. & SCHRATT, G. 2018. Activity-Dependent Pre-miR-134 Dendritic Localization Is Required for Hippocampal Neuron Dendritogenesis. *Frontiers in Molecular Neuroscience,* 11.

ZANETTINI, C., PRESSLY, J. D., IBARRA, M. H., SMITH, K. R. & GERAK, L. R. 2016. Comparing the discriminative stimulus effects of α5 modulat subunits with those of gaboxadol in rats. *Psychopharmacology,* 233**,** 2005-2013.

ZHANG, D., LIU, X. & DENG, X. 2017. Genetic basis of pediatric epilepsy syndromes. *Experimental and therapeutic medicine,* 13**,** 2129-2133.

ZHANG, H., SHYKIND, B. & SUN, T. 2013. Approaches to manipulating microRNAs in neurogenesis. *Frontiers in neuroscience,* 6**,** 196-196.

ZHANG, Z., WANG, Z., ZHANG, B. & LIU, Y. 2018. Downregulation of microRNA155 by preoperative administration of valproic acid prevents postoperative seizures by upregulating SCN1A. *Mol Med Rep,* 17**,** 1375-1381.

ZHAO, C., HUANG, C., WENG, T., XIAO, X., MA, H. & LIU, L. 2012. Computational prediction of MicroRNAs targeting GABA receptors and experimental verification of miR-181, miR-216 and miR-203 targets in GABA-A receptor. *BMC research notes,* 5**,** 91-91.

ZHAO, J., LIN, Q., KIM, K. J., DARDASHTI, F. D., KIM, J., HE, F. & SUN, Y. 2015. Ngn1 inhibits astrogliogenesis through induction of miR-9 during neuronal fate specification. *eLife,* 4**,** e06885-e06885.